Directing the Assembly of Multicomponent Organic Crystals

Synthesis, characterisation and structural analysis of multicomponent organic
systems formed from dynamic processes

T.S. ALOMAR

PhD

UNIVERSITY OF BRADFORD

2014

Directing the Assembly of Multicomponent Organic Crystals

Synthesis, characterisation and structural analysis of multicomponent organic
systems formed from dynamic processes

BY

TAGHRID SAAD ALOMAR

Submitted for the degree of Doctor of Philosophy

School of Life Sciences

University of Bradford

2014

i

Abstract

Keywords: Multicomponent systems, organic, PXRD, crystal engineering, x-ray crystallography, vibrational spectroscopy, dynamic covalent chemistry.

Directed assembly of molecular solids continues to attract widespread interest with its fundamental application in a wide range of commercial settings where control of the crystalline state of materials corresponds with product performance. These arenas include pharmaceuticals, personal care formulations, foods, paints and pigments and explosives.

In recent times, the assembly of multicomponent organic systems has achieved considerable impetus with the widespread interest in co-crystal systems. However, cogent assembly (or engineering) of multicomponent materials is still in its infancy. Considerable advances in crystal design have been made through consideration of intermolecular 'synthons' – identifiable motifs utilising hydrogen bonds – but the translation of other molecular information (conformation, chirality, etc.) into solid state properties (e.g. long-range (translational) symmetry, crystal chirality) remains poorly understood.

In this study, we have attempted to evaluate the influence of a chiral centre adjacent to molecular synthons to identify potential translation of information into the solid form. We have compared the co-crystallisation of nicotinamide with both the racemic mixture of malic acid against that with an enantiomerically pure form of the acid (L-malic acid). As well as DL-phenyllactic acid and L-phenyllactic acid.

It is apparent that recognition between enantiomeric molecular forms play a significant role in the assembly of these systems. This mechanism can be considered independently from the H-bonding networks supporting the hetero-molecular interactions (e.g. acid-amide recognition). Discrimination and control of such interactions may play a role in transmitting chiral molecular information into solid state multi-component assemblies. In order to develop an understanding of co-crystal formation in chiral and achiral forms with intermolecular interactions, the CSD and crystal structures were obtained to do the analysis of how co-crystals pack.

This study has also investigated the use of boronic acids. The aim of this study was to investigate the modification of the hydrogen bonding environment within the hydrogen bonded multi-component systems of boroxines. The study also attempted to determine how the starting materials drive the systems between the boronic acid co-crystal and the boroxine adduct.

Acknowledgements

This thesis is dedicated to my Mum and Grandad,

Miss you a lot

Table of Contents

List of Figures

List of Tables

List of Symbols and Abbreviation

PXRD   Powder x-ray diffraction

IR   Infrared spectroscopy

NMR   Nuclear magnetic resonance

CCDC   Cambridge Crystallographic Data Centre

CSD   Cambridge Structural Database

API   Active Pharmaceutical Ingredient

List of Appendices

Chapter 1

1.0 Introduction

The directed assembly of molecular solids continues to attract widespread interest because of its fundamental application in a wide range of applications; thus, the control of the crystalline state of materials is important.

In recent times, the assembly of multicomponent organic systems has achieved considerable impetus with the widespread interest in co-crystal systems. However, the cogent assembly (or engineering) of multicomponent materials is still in its infancy[1]. Considerable advances in crystal design have been made through consideration of intermolecular "synthons" – identifiable motifs utilising hydrogen bonds – but the translation of other molecular information (conformation, chirality, etc.) into solid state properties (e.g. long-range [translational] symmetry, crystal chirality) remains poorly understood.

The design and synthesis of stable solid state structures, based on non-covalent interactions, is included in the field of supramolecular chemistry. The construction of a variety of organised frameworks, often with potentially useful chemical and physical properties, is one of the important applications of crystal engineering[2].

1.1 Aims and Objectives

This project aims to investigate the probability of creating new multicomponent crystalline materials, using mixtures of chiral and achiral formers with intermolecular interactions. The relative control over molar ratios of the starting materials will be determined by using different solvents, to illustrate, this research aims to:

- Prepare solid state co-crystal systems from mixtures of chiral and achiral formers.

- Study vibrational modes and hydrogen bonded complexes of acids and amides in the framework of its different polymorphic forms at harmonic levels in order to investigate the hydrogen bonding interactions.

- Select systems based on their known synthons: acid–acid, (homosynthons), acid–amide (hetrosynthon).

- Characterise the system by single crystal analysis.

- Perform a comparative study of selected multicomponent systems by both single crystal and by its powder x-ray diffraction (PXRD) pattern.

- Investigate the systematic changes in molecular features.

- Fully characterise the resultant multicomponent systems using powder x-ray diffraction, nuclear magnetic resonance (NMR) and infrared spectroscopy (IR) analysis.

- Study the effect of the different molar ratios (1:1, 2:1, 1:2) of the starting materials and solvents (acetone, acetonitrile and methanol) on the multicomponent system formation.

1.2   Crystal Engineering

Crystal engineering describes the exploitation of non-covalent bonding to allow control of the arrangement of molecules and ions, in relation to one another in the solid state. Most of the work in this area has focused on the organic molecules and hydrogen bonding. The term "crystal engineering" was first introduced by Schmidt[3] in 1971, in relation to the photo- dimerisation

reactions in cinnamic acid crystallisation. Since then it has been redefined many times and this term now covers many aspects of supramolecular chemistry in the solid state.

The outstanding challenges posed by crystal engineering in the modern day were reviewed by Desiraju[4], who defined it as:

> "The understanding of intermolecular interactions in the context of crystal packing and in the utilisation of such understanding in the design of new solids with desirable physical and chemical properties"[4].

Much focus has more recently been centred on the importance of predicting crystal structures, especially in the pharmaceutical environment whereby the different polymorphs of the same drug have been assessed. Crystal engineering is becoming an increasingly important tool, since many of the bulk properties of materials are dictated by the molecular assembly within the solid state, therefore having control over this assembly affords great control over the properties of the material[5].

1.3   Multicomponent Complexes

Co-crystals have been the topic of investigation for a number of years, even when specific co-crystal titles have not been identified[6]. The first example of co-crystallisation occurred in 1893 with the formation of quinhydrone from the equimolar amount of P-benzoquinone and hydroquinone[7]. The definition of co-crystals is still a matter of debate[8], a simple definition notes that: "multicomponent crystals, in which two or more components that are solids under ambient conditions, coexist through non-covalent interactions". A more precise description was stated by Kitaigorodsky[6] as: "a constituent part of a

system, such that its composition, at least in one state of aggregation does not depend on the concentration of the other parts"[6].

For the purpose of this paper, only compounds that contain two chemically and molecularly distinct functional groups will be used. These are widely studied systems, so it is possible to predict, with a good level of accuracy, how these complexes will form. These assembly types utilise the following three main bonding types: hydrogen bonding, charge transfer interactions and proton transfer interactions[9]. A number of studies have focused predominately on using hydrogen bonding to create a whole new crystal packing system[10,11,12]. The hydrogen bonding approach uses a molecule with two or more hydrogen bonding sites, these can be either accepting or donating, and therefore allow components to bond at these different sites. This approach however requires careful balancing of the hydrogen bond strengths, against the other intermolecular interactions.

1.4   Non-Bonded Interactions between Organic Molecules

Hydrogen bonding, π- π stacking, and N-H--- π and C-H--- π interactions play a considerable role in governing the specific functional structures of important biomolecules[13,14,15]. These non-covalent interactions also form the basis of crystal engineering[16,17,18]. Hydrogen bonding arises from electrostatic interactions, while dispersion forces dominate the stacking and π-hydrogen bonding interactions[13]. Although crystal engineering focuses on understanding the intermolecular interactions and connectivities that lead to the construction of multicomponent complexes, the hydrogen bond remains

an important tool in the formation of co-crystals, because of its strength and directionality.

1.4.1 Dispersive Forces – Van der Waals' Interactions

Van der Waals' forces are simply a specific group of interactions resulting from temporary dipole interactions. These forces are a group of relatively weak intermolecular interactions which generally result when a molecule or group of molecules become polarised into a magnetic dipole. This happens most often as a result of uneven or shifting distributions within the atoms' electron cloud[19] . These attractions are much weaker than a chemical bond, but they can cause molecules to cohere as liquids or solids, and they are therefore responsible for surface tension and capillary actions[19].

1.4.2 Charge Transfer Interactions

Charge transfer interactions are observed between an electron donor (π base) and an electron acceptor (π acid), and an adduct is formed when donation occurs from the base to the acid. Two types of adducts can be formed by these interactions: firstly, if the electron transfer is complete then an ionic solid is formed; and, secondly, if the electron transfer is only partial then the system may delocalise the charge to form a charge transfer complex[20]. In π systems, charge transfer interactions are not fully understood, but it is believed that they comprise of the following three interactions: Van der Waals, hydrophobic and electrostatic interactions[21]. The electrostatic component of the interaction is able to push the π systems into a number of geometries (see also Figure 1.1)[22].

6

1. Edge - Face 2. Offset Stacked

3. Face - Face Stacked
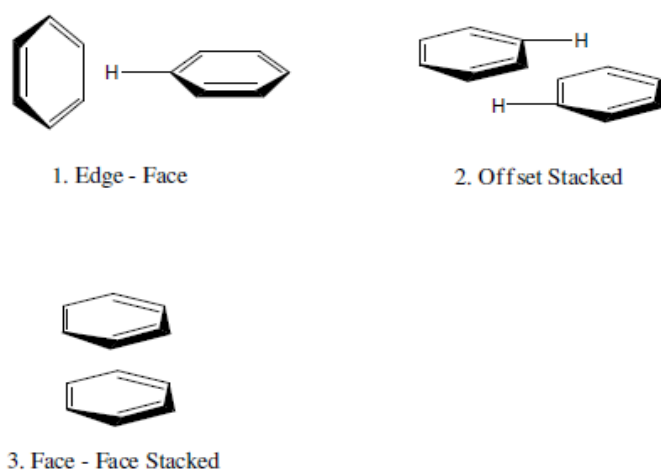
Figure 1.1: Known geometries of aromatic charge transfer systems[22]

1.4.3 Hydrogen Bonding

Hydrogen bonds are bonds between molecules that contain an electronegative atom which possesses lone pairs of electrons (usually O, N or F), these are called acceptors (A); in addition, the molecules containing covalent bonds between a hydrogen and an electronegative atom (usually O-H, N-H, and S-H) are called donors (D). Hence, the polarised nature of the X-H bond (X=O, N) results in a highly electropositive hydrogen which is attracted toward bond formation with electron rich electronegative acceptor atoms[23].

The ideal geometry of the hydrogen bond is linear, with the hydrogen atom positioned along the line connecting the hetero-atoms. The linear geometry is not always obtained, as neighbouring covalent bonds affect the geometry of the hydrogen bonds. It is this property of the hydrogen bond that leads to its directionality. The strength of the individual hydrogen bonds (1-10 kcal/mol) is much weaker than the covalent bonds (70-110 kcal/mol)[24]. It should also

be noted that the hydrogen bond is also sensitive to external environmental factors, such as the polarity of the medium as well as the presence of solvents and water.

1.4.3.1 Etter's Rule for Hydrogen Bonding

Etter, and other co-workers, developed a method of systematising the interactions in the organic solid state through the use of a system of graph sets to describe the motifs observed in the hydrogen bonding patterns[25]. They also set a number of rules, including the following which state:

All good proton donors and acceptors are used in hydrogen bonding;

Six-membered ring intramolecular hydrogen bonds form in preference to intermolecular hydrogen bonds;

The best proton donors and acceptors, remaining after intramolecular hydrogen bond formation, form intermolecular hydrogen bonds[26].

1.4.3.2 Supramolecular Synthons

Hydrogen bonding is one of the most important fundamental interactions that causes association of organic molecules, these form the building block units that are known as supramolecular synthons[26,27,28].

Supramolecular synthons are defined by Schmidt[3] as "structural units within supramolecules, which are formed or assembled by intermolecular interactions". The hydrogen bond is still believed to be the most important intermolecular interaction; the synthons are formed by utilising those hydrogen bonds which can be from the same functional group called

homosynthons, these include: carboxylic acids, oximes, pyridones and amides, and different functional groups known as heterosynthons with examples such as: carboxylic acid···pyridine, acid···amide, and alcohol···pyridine interactions. The concept of supramolecular synthons is employed to construct co-crystals; thus, co-crystals are a consequence of self-assembly between these different molecular species[27,28].

The arrangement of supramolecules is based on the strong hydrogen bonds which include: N-H…O, O-H…O, N-H….N, and O-H….N, as well as weak hydrogen bonds which include: C-H….O-N and C-H…O=C, these are presented, below, in Figure 1.2[29].
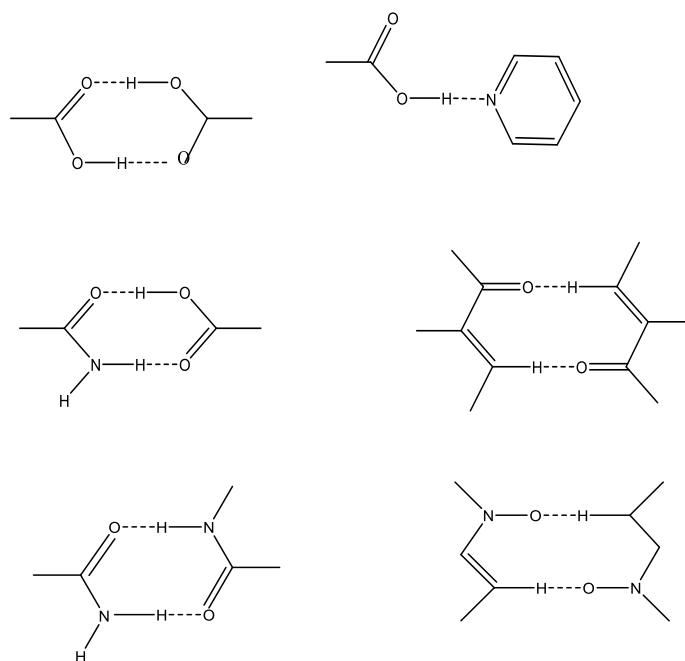
Figure 1.2: Common synthons utilised in the assembly of supramolecules[29]

In the design of co-crystals it is important to recognise synthons that are capable of forming a suitable network structure based on the consequences of selective and directed hydrogen bonds; therefore, functional groups that

are self complementary are able to form homodimers – they are called supramolecular homosynthons. Figure 1.3a shows the formation of carboxylic acid-carboxylic acid or the amide-amide dimers and Figure 1.3b shows that when two complementary functional groups are engaged in the formation of carboxylic-amide dimers then this interaction is called a supramolecular heterosynthon[29].
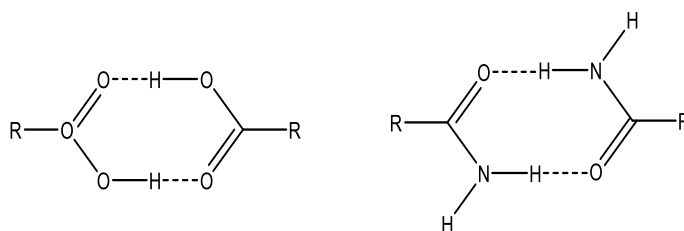
Figure 1.3a: Homosynthons – the formation of homo supramolecular synthons are acid-acid and amide-amide dimers
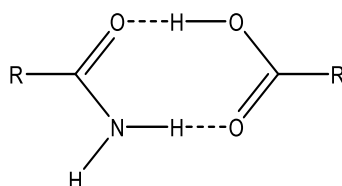
Figure 1.3b: Heterosynthons – the formation of hetero supramolecular synthons in the acid-amide dimer[29]

Numerous papers have reported the synthesis of co-crystals and significant success has been achieved with the interaction of carboxylic acid and N-heterocycle moieties, as with carboxylic acid and pyridines; thus, if the amide is used instead of the carboxylic acid, then a hydrogen bond is not formed between N-H---N and the differences in the behaviour of these functional groups may be related to the differences in the acidity of the protons[30].

Some supramolecular synthons, including carboxylic acid-pyridine, carboxylic acid-amide and alcohol-pyridine, tend to favour co-crystal formation. CSD

studies have shown that a carboxylic acid-pyridine synthon II (Figure 1.4b) is more favoured than a carboxylic acid homosynthon I (Figure 1.4a), whereas calculations show that a carboxylic acid-amide synthon IV (Figure 1.4d) is more stable than an acid (I) or amide homosynthon (III) (Figure 1.4a or 1.4c)[31].

a)

b)

c)

d)
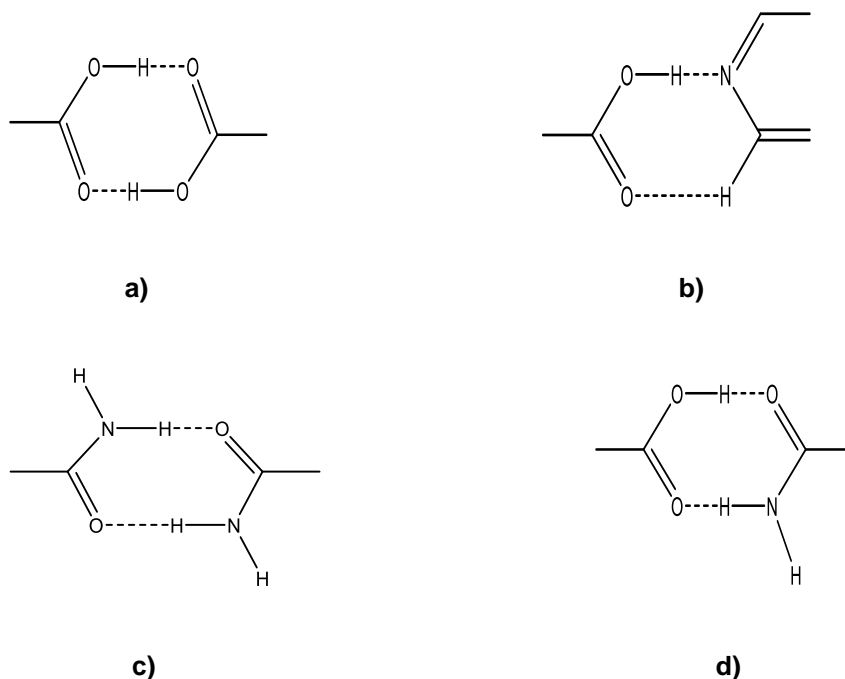
Figure 1.4: Various supramolecular synthons, including: a) carboxylic acid homosynthon; b) carboxylic acid-pyridine synthon; c) acid or amide homosynthon; d) carboxylic acid-amide synthon

1.4.4 Chiral Recognition

The origins of single handed molecules occurring in the natural environment have been of much interest, as all biological molecules adopt single handedness. Pasteur first discovered, in 1848, that tartaric acid existed as a single handed molecule in nature, whereas synthesised tartaric acid existed as an enantiomer[32]. Several theories have been proposed as to how single handedness arose from racemic mixtures in nature[33,34].

Recently McBride proposed that a fundamental physical bias exists, this is what generates a particular molecular handedness[35]. In 1953 Frank, a theoretical physicist , proved mathematically that if an initial random event provided a tiny excess of one hand then this would lead to the exclusive formation of that form[36]. However, in 1990 Kaufman *et al.* demonstrated, by dissolving a concentrated solution of sodium chlorate of no handedness, that after stirring it crystals of a single hand were isolated[37]. In 2005, Viedma illustrated that it was possible to grow single handed crystals of sodium chlorate from a slurry of mixed mirror image crystals, as long as the mixture contained an excess of one hand; furthermore, by stirring the slurry, this resulted in a complete conversion of the crystals of the more dominant form. In addition, grinding has also been shown to work in converting a mixture to one hand[38].

1.4.4.1 Chirality in Nature

Chiral molecules are mirror images that are not superimposable upon one another. Conversely, chiral compounds have superimposable mirror images. The word chirality is derived from the Greek word for hand and it means "handedness" with regards to the reflecting of either the left- or right-handedness of molecules that are chiral in nature. Stereoisomers and enantiomers are types of chiral compounds[39].

Stereoisomers are compounds that have the same atoms connected in the same order, but they differ from each other in the way in which the atoms are orientated in space. The chiral molecules that are structurally different from each other, only in terms of the left- or right-handedness of their orientations,

are called enantiomers. Enantiomers have the same physical properties, but they behave differently under certain conditions; as such, they react at different rates with other chiral compounds and they may also react at different rates in the presence of chiral catalysts and optically active solvents.

When polarised light is passed through a pure sample of each enantiomer, the plane of the polarised light is rotated, in opposite directions and in equal amounts by the two enantiomers. If rotation of the plane of the polarised light occurs, the material is considered to be optically active. An isomer that rotates light to the left is called "levo-" and is indicated with a negative notation (-). However, an isomer that rotates light to the right is called "dextro-" and is notated as being positive (+).

The absolute configuration of a molecule indicates the actual arrangements of the substituents within the chiral compound. The direction of rotation of the plane's polarised light does not indicate the absolute configuration of a chiral molecule. In fact, it is possible for various unrelated compounds, with the same absolute configuration, to rotate light in opposite directions. In the early part of the century there were no empirical methods for determining absolute configuration. But, Rosanoff chose glyceraldehyde to set the standard for configuration by assigning the isomer that rotates plane polarised light to the right as the D isomer, and the isomer that rotates plane polarised light to the left as the L isomer[40]. Only amino acids and carbohydrates, and their derivatives, are still commonly assigned the D and L descriptors.

1.4.4.2 Chiral Separation and Resolution of Enantiomers

The separation of chiral compounds has been of great interest because the majority of bioorganic molecules are chiral[31]. Amino acids, sugars, proteins and nucleic acids are all composed of chiral molecules; for example, amino acids exist in the L form and sugars in the D form.

Chirality is a major concern in the modern pharmaceutical industry[36,37], since the case of thalidomide. The body interacts with each racemic drug differently and metabolises each enantiomer using separate pathways to produce different pharmacological activities. Thus, one isomer may produce the desired therapeutic activities, while the other may be inactive or, in worst cases, produce unwanted effects. Therefore, separation of these is important as different biological responses can be seen as a pair of enantiomers in drugs[35].

Some examples of pharmaceuticals, whereby one isomer has the desired effect and the other has harmful properties, will now be included; to illustrate, in thalidomide[41] the R-enantiomer is a sedative and the S-enantiomer is teratogenic. In addition, there is ethambutol[42], where the S-enantiomer shows antiarthritic properties and the R-enantiomer is extremely toxic. Nonetheless, thalidomide is the best known of these drugs.

The separation of two enantiomers into the two mirror forms is described as resolution. The separation can be carried out using a number of different techniques. Firstly, resolution via diastereomeric salt formation involves forming an acid-base reaction of a racemate with an enantiopure resolving

agent. This gives two diastereomers with different physical properties, a difference in solubility is often used to separate the diastereomers[35].

Secondly, kinetic resolution is another technique where the reaction rate of one enantiomer is different to the reaction rate of the other enantiomer. The difference in rate between the two enantiomers is caused by the use of an enzyme or chiral catalyst. The slower reacting enantiomer will be the dominant form if the reaction is stopped before completion. The two diastereomeric transition states must be different in energy in order for the strategy to be successful[43].

Thirdly, Dutch resolution is a term given to the use of mixtures of resolving agents in classical resolution. This technique uses the concept of "families", where the resolving agent is structurally related. The enantiomeric excess is increased from between 20 and 30% to between 90 and 95% when this technique is used. Not many families of resolving agents exist, however common ones include cyclic phosphoric acids, quinine and brucine[44].

This technique leads to precipitation of crystalline diastereomeric salts of high yield and enantiomeric purity. The mechanism behind Dutch resolution is not clear at the moment and the reality is that in many cases the resulting diastereomeric salts are solid solutions which suggests a thermodynamic origin[3].

1.4.5 Dynamic Covalent Bonds

When diboronic acid or polyboronic acid undergo self-condensation, this results in the formation of crystalline porous materials which are termed

covalent organic frameworks (COFs). As in the current research project, this diboronic acid is phenylboronic acid. Recently, research publications have been related to COF-1 (Figure 1.5) which has had drastic expanded interest in the boroxine-containing materials; thus highlighting the versatility of the B_3O_3 ring system[45].
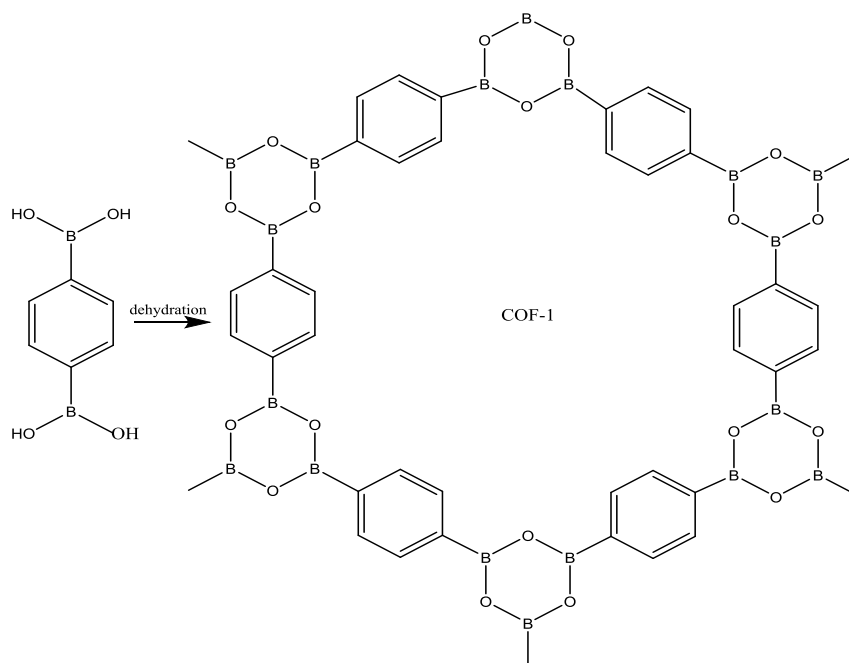
**Figure 1.5: Dehydration of 1,4-benzenediboronic acid
results in the formation of COF-1[46]**

Yaghi, and various co-workers in 2007, showed how COFs were based exclusively on the reversible formation of the boroxine linkages. Optimising the crystallinity of boroxine-based materials requires careful choice of solvent and temperature in order to maximise the error correction associated with the boroxine ring-forming reactions[47]. Recently, Cooper and other co-workers published a paper showing the synthesis and purification of a COF-102 and boronate-based COF-5, using microwave heating[48]. This method was 200 times faster than other reported solvothermal methods[49]. The output of these

new methodologies demonstrated the discovery of new COFs and other microporous polymers.

Boroxines, also known as boronic acid anhydrides, are formed by the dehydration of boronic acids. Boroxine research has gained significant attention in recent years because of its aromatic character and its tendency to form Lewis acid-base adducts with nitrogen-containing ligand.

1.5 Crystallisation

Crystallisation is the process of phase transformation whereby molecules are initially self-assembled in a solution, they then undergo nucleation. This whole process is governed by the laws of thermodynamics and kinetics, as crystallisation is a phase forming route. Consequently, it is important to realise that the formation of the stable form, during crystallisation, is a thermodynamic process, while the formation of the metastable form is a kinetic process. The crystallisation process is affected if stirring is applied, even for slightly soluble substances; to illustrate, Smith and Sweet[50], and Sohnel and Handerson[51,52], found that stirring increases nucleation, the induction time for crystallisation, the growth rate and the number of particles.

The crystallisation process is initiated with the formation of a labile solution, whereby, the solubility equilibrium between solid and solution needs to be re-established, as a degree of solubility mismatch exists. Stability of the crystallisation system depends on the forces of attraction between the solid particles and the thermodynamic conditions are fundamental in the crystal growth process[53]. The formation of the nuclei is defined by the relationship between the critical nuclei size and the degree of supersaturation, other

conditions persuade the nucleation process and relate to the bulk and surface free energies and the kinetics of the process. These nuclei are nano-sized units either from a spontaneous centre (homogeneous nucleation) or from an artificial centre (heterogeneous nucleation)[54]. Nucleation can be induced by agitation, friction or mechanical shock which is dominant at low supersaturation. The growth of crystals can be defined when the size of the particles becomes greater than the critical size, and is therefore visible in a supersaturated or supercooled system. Various theories explain the process of crystal growth, including the following:

The surface energy theory explains that the shape of the crystal is related to the free energy of the faces, and the growth rate of the crystal faces is proportional to their surface energy. Within this model the growth rate and the surface energy are inversely proportional to the lattice density of the plane, so the growth will be faster for the faces having low lattice density[54].

The diffusion theory, proposed by Noyes and Whitney, demonstrates that crystallisation is the reverse process to dissolution, and the growth of the crystal face is a diffusion process. Within this model the difference between the concentration in the bulk solution and the solid surface governs the diffusion and dissolution process[3].

The adsorption layer theory, proposed by Volmer, states that when a unit reaches the crystal face it has to lose one degree of freedom so that it can migrate freely over the crystal face; thus, a dynamic equilibrium between this layer and the bulk of the solution should be attained to adsorb this unit on the layer[50].

The mechanism of crystal growth and the rate of the process may be determined by the size and morphology of the solid, the shape will be cubes or octahedral if the growth takes place on the surface, and it is an elongated shape such as needles, rods or plates if the growth rate is anisotropic.

1.5.1   Methods for Preparation of Multi Component Organic Systems

An important aspect of the successful co-crystal development remains the identification of suitable co-formers. Although the literature review shows many developed synthetic pathways, such as neat or liquid assisted grinding[55,56], slow evaporation of mixed solutions[57], solution-mediated phase transformation (slurrying)[58] and hot-stage microscopy melt interface[59], a trial-and-error approach will be used to screen a large set of possible candidates of co-former identification.

1.5.1.1 Solution Crystallisation

The slow evaporation technique is a basic method whereby a saturated solution must be prepared in a suitable solvent – this solution is left until the crystals are formed. One condition that must be considered is the solubility of both compounds in the same solvent – they must both be comparable and if they are not then the least soluble compound will be recrystallised.

1.5.2 Phase Diagram

1.5.2.1 Phase Diagram in Co-Crystallization

Crystal growth is influenced by various elements, including: crystallographic characteristics, technical parameters of the method used to grow crystals and by kinetics and thermodynamics. The growth of crystals from a solution is

dependent on good knowledge of liquid curves – this is useful when seed crystals are inserted into the solution in order to help the growth of specific forms of crystals; this procedure requires conditions that are close to those of thermal equilibrium[60].

Phase diagrams identify the need or presence of an element or a compound in graphical form by identifying the specific conditions (such as: temperature, pressure and concentration of compounds) at equilibrium in order to reflect the thermodynamic laws and rules between the different phases[50]. The phase diagram is also very useful as it reveals information about the interactions among the components of the solutions.

1.5.2.2 Binary System and Eutectic Points

All of the stable phases which are formed from a two component system can be represented in a binary phase diagram as a function of the concentration and the temperature or pressure. Any changes in the concentration or the temperature are the major factors that control the crystallisation process; therefore, a profile for the overall process can be obtained from the construction of a binary phase diagram as a function of the overall concentration and temperature which are the simplest form of a two component system. To illustrate, Figure 1.6 provides an example of an A and B phase diagram.
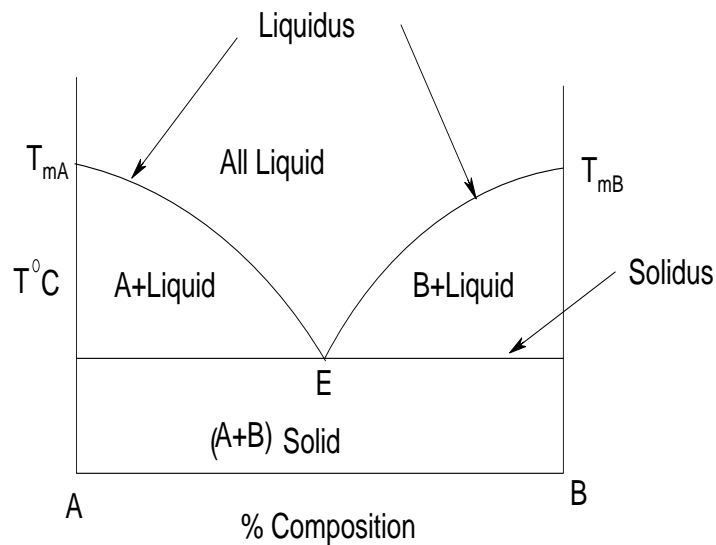
Figure 1.6: A two component binary phase diagram with a simple eutectic[51]

This digram shows that the temperature is the ordinate while the overall composition is the abscissa; furthermore, it it scaled as a molar percentage, but it could also be scaled in a mole fraction. The relation between the temperature and the composition appears as lines or curves, these are called the phase boundries. As can be seen, T_{mA} and T_{mB} are the melting points of component A and component B respectively, the curves T_{mA} E and T_{mB} E are liquidous boundary curves, and the horizontal line separating phase A + liquid and phase B + liquid is the solidus line. Point E is the eutectic point where solid A and solid B, and their liquid, were all in equilibrium; furthermore, the number of phase is recorded as three in accordance with the phase rule whereby the system has zero degrees of freedom and the system is invarient at the eutectic point. By applying the phase rule for a two component system, the degree of freedom is $F = 4 - P$.

1.5.2.3 Ternary System

The construction of ternary phase diagrams is a new approach used to rationalise the preparation of crystals from solutions. The importance of the knowledge of the ternary phase diagram was highlighted in the literature presented by Rodrigues *et al.*[61], and Chiarella *et al.*[62].

The phase equilibria, of a three component system, can be represented on an equilateral triangle in which each component is represented by one of the apices of the triangle, the binary system is represented by each side of the triangle and any point within the triangle will represent the three components of the ternary system. The composition of each component is expressed as being a mole or mass fractions, but it was found that it could lead to some difficulties in the determination of the absolute composition; therefore, it is better to express the composition as being either a molar or mass percentage[63].

1.6   Strategies for Addressing the Project Aims

In order to successfully address the aims of this project a systematic approach will be taken, this will involve first establishing a stable co-crystal using acid-amide interaction and hydrogen bonding through the use of different solvents (acetone, acetonitrile, methanol) of the 1:1, 1:2 and 2:1 molar ratios of the starting materials.

The compounds chosen have complementary donor and acceptor functional groups; to illustrate, isonicotinamide and nicotinamide differ in the position of the nitrogen atom and are co-crystallised with a number of carboxylic acids of

optically pure and racemic compounds in order to determine whether chirality is translated into the secondary structure.

The acid group was chosen as it has been widely studied in the area of crystal engineering and is therefore a good starting point. The complementary hydrogen bonding donor and acceptor sites also makes them good synthons. However carboxylic acid and N interactions are more favoured and form an acid-amide heterosynthon. Therefore we have used the carboxylic acid-amide for the formation of these co-crystals. Nicotinamide has been successfully utilised as a co-former in the preparation of co-crystals with carboxylic acids[16].

1.6.1   α- Hydroxyl Carboxylic Acids in Crystal Engineering

In recent times, amide to carboxylic acid hydrogen bonds have become important in molecular recognition chemistry, where amide hosts have been designed[64] and constructed for binding carboxylic acid[65] and carboxylate ion guests[66]. The hydrogen bonding associated with amide and carboxylic acid functional groups can act as either a proton donor or acceptor. In the literature, many examples of complementary acid-acid and amide-amide association have been acknowledged[67].

Racemic (DL-) and enantiomeric (L- and D-) malic acid species, are very important biological molecules[68,69,70]. They have the same molecular formula, but both the racemic and enantiomeric forms exhibit dissimilarities in terms of their vibrational behaviour which is as a result of differences in their structural features, including: crystal symmetry and geometric distinctions in some functional groups[69].

Malic acids are all capable of forming intramolecular hydrogen bonds that are between an alcohol group and a carboxylic acid group. Among the molecules of malic acid, there are two kinds of hydrogen bond interactions, see Figures 1.7, 1.8 and 1.9.
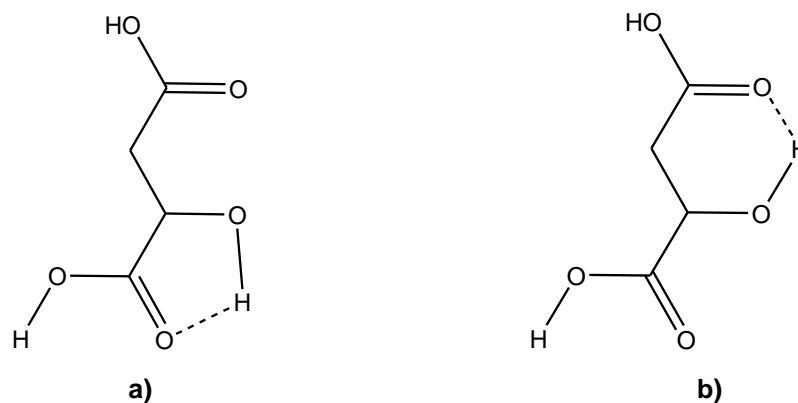
Figure 1.7: Intramolecular hydrogen bonding within malic acid[16]
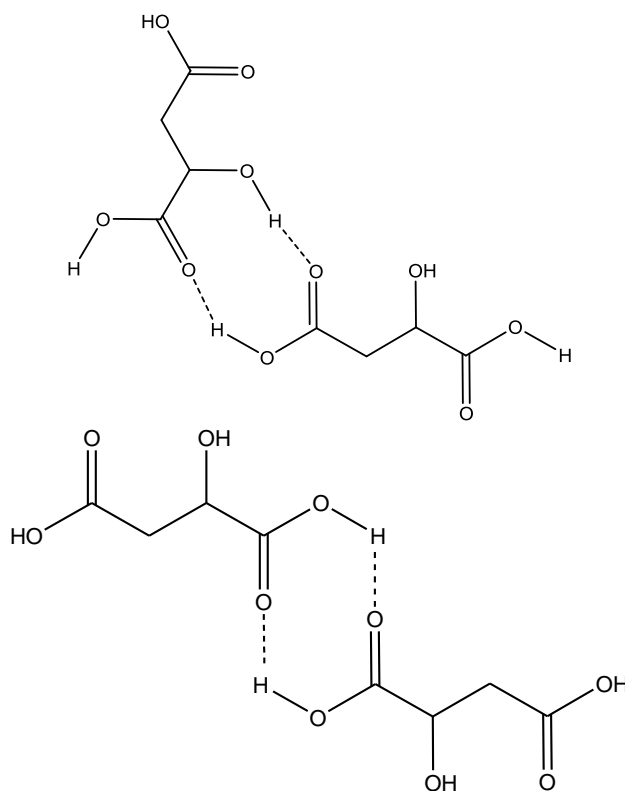
Figure 1.8: Intermolecular hydrogen bonding between malic acid-malic acid[64]
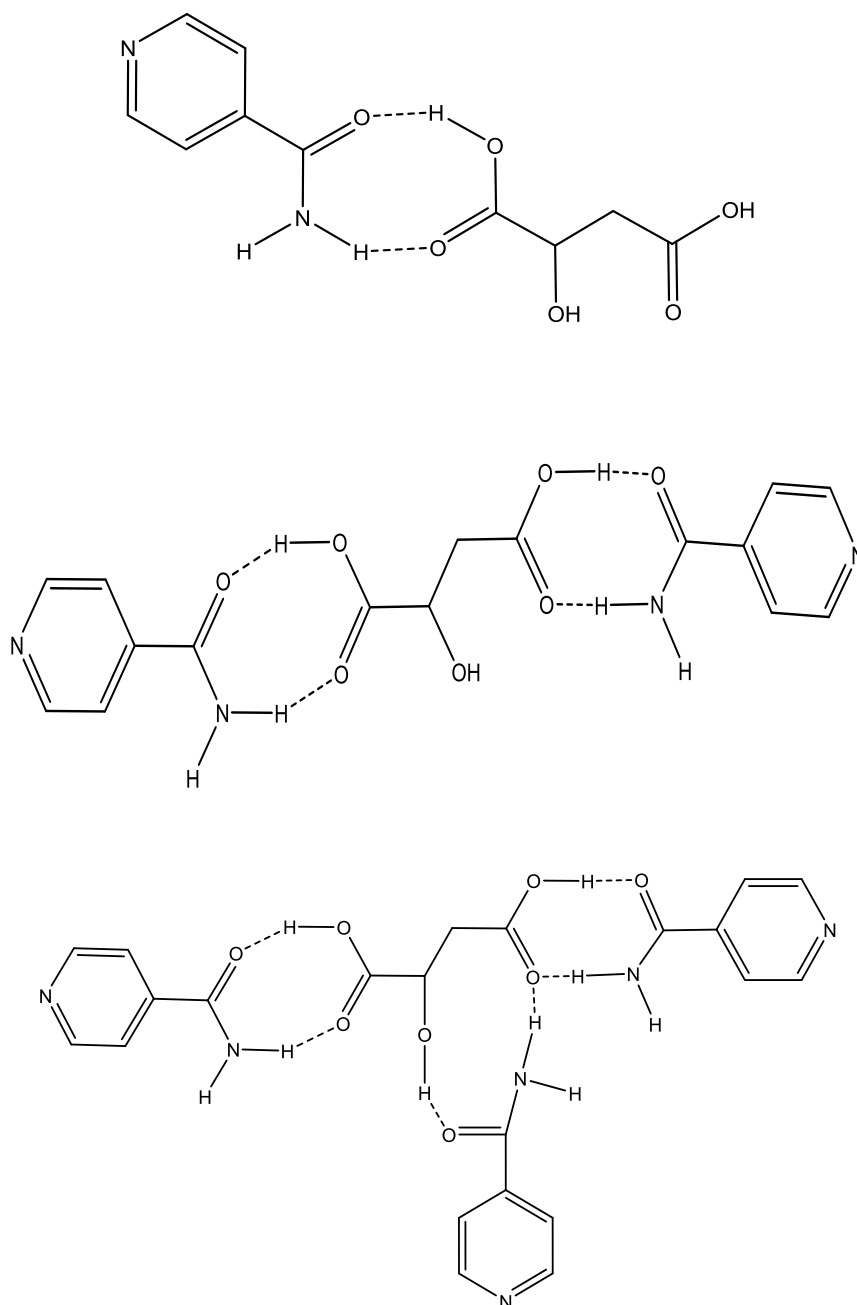
Figure 1.9: Intermolecular hydrogen bonding between malic acid-isonicotinamide[64]

1.6.2 Phenylboronic Acids in Crystal Engineering

Boronic acids and their derivatives are well known in crystal engineering, bioorganic and medicinal chemistry[71,72]. Boronic acids have a tendency to form hydrogen bonded networks, where the boron atom maintains its trigonal

planar geometry which shows a topological resemblance to the centrosymmetric dimer motifs in carboxylic acids and amides[73].

Boronic acids are used in the synthesis of co-crystals and, in addition to the study of centrosymmetric dimer assemblies and condensation products, it should be noted that the interactions made by $-B(OH)_2$ with heterocycles in terms of topology and selectivity are different from the interaction types observed in the assemblies of acids and amides[74].

An important aspect of phenylboronic acid is that it can exist, in principle, in three different conformers (syn-syn; syn-anti and anti-anti, see Figures 1.10a, 1.10b and 1.10c) each of which have separate energy profiles[75]. However in nature these compounds are predominately found in the syn-anti-conformation because it is energetically more favoured. In molecular complexes, the functionality exhibits conformational variety and three conformations are possible for the $-B(OH)_2$ functionality.

syn,anti   syn, syn   anti ,anti

a)   b)   c)
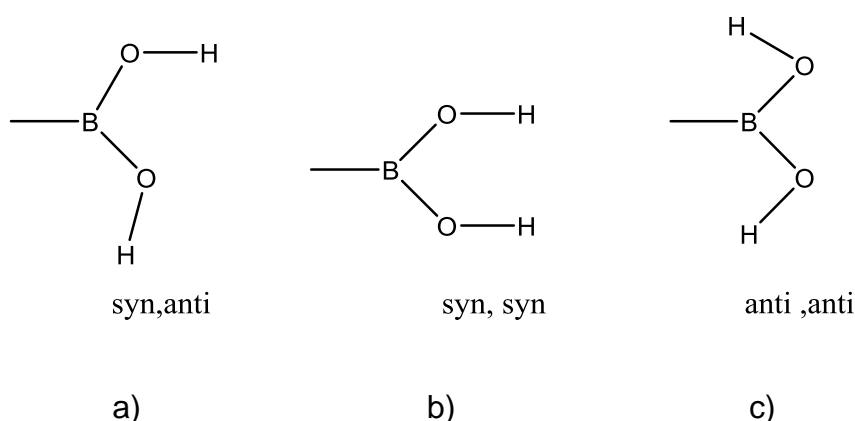
Figure 1.10: Phenylboronic acid with three different conformers: a) syn-anti; b) syn-syn; and, c) anti-anti

Boronic acids also form boroxines, which resemble a six-membered B_3O_3 (boroxine) ring, these are formed when three boronic acid units converge and

undergo cyclodehydration. This property has been efficiently exploited to achieve highly porous covalent organic frameworks[73,74,75].

Various literature has revealed that phenylboronic acids have a tendency to form O-H⋯N hydrogen bonds with several pyridine based linear spacer ligands[45].This tendency of non-covalent interactions with N-donor compounds mutually with the conformational flexibility make this functionality an appealing aspect in crystal engineering. In a co-crystallisation study, by Raju *et al.,* where the system under investigation was 1,2-diazo fragment (alprazolam, 1H-tetrazole, acetazolamide and benzotriazole), and 1,10-phenanthroline and 2,2'-bipyridine, the results obtained revealed that simply the presence of the 1,2-diazo fragment in the co-former does not give assurance of the successful configuration of co-crystals with a syn-syn-conformation of the boronic acid[74].

The complexity in employing phenylboronic acids in the design and synthesis of molecular adducts is obvious from the six types of hydrogen bonding motifs experimentally observed in the adducts of boric/boronic acids with 4,4'-bipyridine. In another study by Desiraju *et al.*, the molecular complexes after synthesis of BPY-BDBA (1,4-benzene-diboronic acid) did not contain cyclic O-H⋯N hydrogen bonds[76]. Instead, the rotational sovereignty enjoyed by the bipyridyl (known as BPY or bpy) unit adopted a completely different pattern. In the complex, although the boronic acid was found in its preferred syn-anti conformation, a linear chain was found connecting the two boronic acid functionalities. These chains are consistent with the heteroatoms of the anti-orientated bipyridyl linkers through O-H⋯N hydrogen bonds. This leads to the formation of a ladder assembly, the ladders belonging to the adjacent

planes are arranged in a staggered manner so as to evade any possible empty space.

1.6.3 Pyridines and Pyridinecarboxamides in Crystal Engineering

The literature indicates that there are many reported complexes of isonicotinamide and nicotinamide. Although it is apparent, from the literature reviewed, that carboxylic acid, and specifically isonicotinamide, form supramolecular synthons which are responsible for molecular complexes.

Miranda *et al.*[77] studied the co-crystal engineering phenomena of stoichiometric molar ratio co-crystal of nicotinamide with lamotrigine (1:1) (a), and lamotrigine nicotinamide co-crystal monohydrate (1:1:1) (b). Single crystal analysis of (b) showed an asymmetric unit which consisted of one molecule of lamotrigine, one molecule of nicotinamide and one water molecule.

The single crystal x-ray structure of nicotinamide (Nic1) was first reported in 1954[78] with a more accurate determination appearing in 1999 (known as CSD refcode: NICOAM01)[79]. The polymorphism of nicotinamide was first discussed in 2001.

Additionally, isonicotinamide is a pyridine derivative with an amido group in ∂Y position, this has pharmaceutical importance since it has anti-tubercular, anti-pyretic and antibacterial properties[80].

The crystal structures of two polymorphs of isonicotinamide were reported in 2003. These two forms, herein designated Iso1 (CSD refcode: EHOWIH02)

and Iso2 (CSD refcodes: EHOWIH, EHOWIH01) which were evidently the only known polymorphs of isonicotinamide[31].

Nicotinamide has two hydrogen bonding groups suitable for the formation of an intermolecular hydrogen bond. The amide group has two hydrogen bond donors and two lone pairs on the carbonyl O atom. A second hydrogen bond acceptor is the lone pair on the N atom of the pyridine ring.

Nicotinamide exist in four polymorphic forms, attained by the recrystallising technique which has four commercially available forms: I, with a melting point of between 126 and 128°C; II, with a melting point of between 112 and 117°C; III, with a melting point of between 107 and 111°C; and, IV, with a melting point of between 101 and 103°C. Form I is the most stable one, with the other three being metastable (the four forms are known as: NICOAM, NICOAM01, NICOAM02 and NICOAM03)[31]. The most stable crystallize in a monoclinic form.[31]

Hydrogen bonded interactions, between the acidic proton of the carboxylic acid with the basic N atom of the pyridine, are very important for the formation of supramolecular structures. This is in accordance with Etter's empirical rule, which states that the best proton donors and acceptors remaining after intramolecular hydrogen bond formation form intermolecular hydrogen bonds[52].

The carboxylic acid proton, being the most acidic proton, is the best hydrogen bonding donor which interacts with the best hydrogen bonding acceptor – this is the basic lone pair of the pyridine N (synthon I). The second

best donor/acceptor pair is the amide syn-proton and the carbonyl oxygen of the amide, which can form a homomeric hydrogen bond ring.

1.6.4 Analytical Strategy

X-ray crystallography was utilised in this project in order to determine the crystal structures and to evaluate the different bonding types used within them. FT-IR analysis showed how the vibration modes will be affected by the formation of supramolecular synthons; this will also indicate the magnitude of deviation of vibrational frequency involved within the modes.

1.6.4.1 Powder X-Ray Diffraction (PXRD)

Each crystalline substance has a unique x-ray diffraction pattern. The number of observed peaks is related to the symmetry of the unit cell (higher symmetry generally means fewer peaks). The d-spacing of the observed peaks are directly related to the repeating distances between the planes of atoms in the structure. Finally, the intensities of the peaks will be noted in terms of how they relate to the different kinds of atoms that are in the repeating planes. The scattering intensities for x-rays are directly related to the number of electrons in the atom; hence, light atoms scatter x-rays weakly, while heavy atoms scatter x-rays more effectively.

These three features of a diffraction pattern: the number of peaks, the positions of the peaks and the intensities of the peaks, define a unique fingerprint x-ray powder pattern for each and every crystalline material. X-ray powder diffraction is a powerful tool that can be used to characterise the products of a solid state synthesis reaction. At the simplest level, diffraction

patterns can be analysed for phase identification; thus, they determine what crystalline substances are present in a given sample.

Each peak in a diffraction pattern arises from a unique set of repeating planes within the structure. These sets of planes are orientated in all directions in three-dimensional space. However, in order to see diffraction from a specific set, the planes must be orientated relative to the incident x-ray beam. Therefore, x-ray powder diffraction relies on a large number of crystallites in random orientations in order to observe the most diffraction peaks. Of course, the proper orientation is only one factor, as diffraction from a particular set of planes may not be observed or the peak intensity may be low due to symmetry (patterns of systematic absences) or other factors that contribute to low intensity.

X-ray diffraction is a useful technique for determining the shape and type of crystal unit cells, as well as the arrangement of atoms within the unit cell. When an x-ray is directed onto an atom, the electrons of the atom will absorb the incoming x-ray and then re-emit it. If the atoms are located on a crystallographic plane, the scattering of x-ray will be mathematically equivalent to the reflection made by the plane. Since the crystallographic planes are parallel to and equally spaced with each other, there will be a path difference between the x-ray diffracted by the two planes (see Figure 1.11)[81].

Thus, it can be noted:

Path difference = AB + BC = $2d_{hkl} \sin\theta$

For scattering-in-phase, the path difference must be equal to an integral number of wavelengths, such as:

$$n\lambda = 2d_{hkl} \sin\theta$$

Where n is an integer and λ is the wavelength of the impinging x-ray – this condition is known as "Bragg's law".
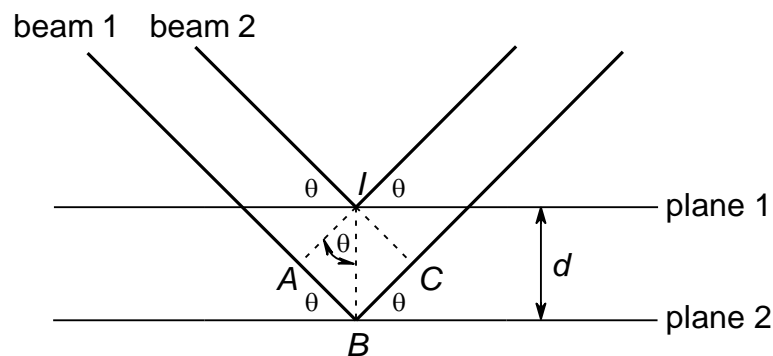
Figure 1.11: X-ray diffracted by two crystallographic planes

1.6.4.2 Symmetry within Crystals

As would be expected the repeating nature of the crystal lattice gives rise to a number of different arrangements, these are described based on the symmetry within the unit cell. This classification describes seven separate crystal systems and the corresponding 32 point groups. A unit cell which possesses only a centre of symmetry, or even no symmetry, is the only system in which there are no shape restrictions. In this case each of the angles α, β and γ must be specified and the crystal system is observed to be triclinic (see Table 1.1)[82].

Table 1.1: The 32 crystal classes and the corresponding crystal systems

Crystal system	Crystal classes	Metric parameters of the unit cell
Triclinic	$1; \bar{1}$	$a \neq b \neq c; \alpha \neq \beta \neq \gamma \neq 90°$
Monoclinic	2; m; 2/m	$a \neq b \neq c; \alpha = \gamma = 90° \beta \neq 90°$ $(\alpha = \beta = 90°, \gamma \neq 90°)$
Orthorhombic	2 2 2; m m 2; m m m	$a \neq b \neq c; \alpha = \beta = \gamma = 90°$
Tetragonal	$4; \bar{4}; 4/m; 4\ 2\ 2; 4\ m\ m;$ $\bar{4}\ 2\ m, 4/m\ m\ m$	$a = b \neq c; \alpha = \beta = \gamma = 90°$
Trigonal	$3; \bar{3}; 3\ 2; 3\ m; 3\ m$	$a = b \neq c; \alpha = \beta = 90°,$ $\gamma = 120°$
Hexagonal	$6; \bar{6}; 6/m; 6\ 2\ 2; 6\ m\ m;$ $\bar{6}\ 2\ m; 6/m\ m\ m$	$a = b \neq c; \alpha = \beta = 90°,$ $\gamma = 120°$
Cubic	$2\ 3; m\ 3; 4\ 3\ 2; \bar{4}\ 3\ m;$ $m\ \bar{3}\ m$	$a = b = c; \alpha = \beta = \gamma = 90°$

Chapter 2

2.0   Experimental

2.1   Instrumental

2.1.1   Powder X-Ray Analysis

Powder x-ray diffraction was recorded with a Bruker D8 diffractometer (wavelength of x-rays: 0.154nm Cu source; voltage: 40kV; filament emission: 30mA). The samples were placed on a sample holder and mounted on the diffractometer, the samples were then scanned from 5 to 50° (2θ) using a 0.01° step width and a one second time count. The receiving slit was 1° and the scatter slit 0.2°. The collected data were analysed using Eva software. It is also worth noting that the data were collected at room temperature.

2.1.2   Infrared (IR) Spectroscopy

The IR spectra of solid samples were recorded as 15mm KBr discs (typically 0.5mg of dry samples in 35mg of dry KBr) and spectra for liquids were obtained as capillary films using NaCl plates. The spectra were recorded with a Nicolet 140 FT-IR spectrophotometer for the range 4000 to 600cm^{-1}. For the solid samples, background spectra were also obtained from the KBr of the same batch that was used in the preparation of the samples. For liquids, the background was recorded as air. All of the discs were prepared immediately before the spectral determination.

2.1.3   NMR Spectra

For ^{1}HNMR Spectra, 20mg of the dry sample was typically placed for dissolution in 0.7cm^3 of the appropriate deuterated solvent. The data were all recorded at 400MHz on a Bruker AC300 spectrometer.

2.2 Reagents

Various general purpose reagent grade (GPR) reagents were purchased from sigma-Aldrich; as such, they could be used without any further purification (see Table 1.2).

Table 2.1: The origin and purity of reagents

Reagents	Source	Purity
Phenylboronic acid	Sigma-Aldrich	≥98% (TLC)
DL-malic acid	Sigma-Aldrich	97%
L-malic acid	Sigma-Aldrich	98%
L-phenyllactic acid	Sigma-Aldrich	≥98%
DL-phenyllactic acid	Sigma-Aldrich	≥98%
4,4'-bipyridine	Sigma-Aldrich	≥98%
4-phenylpyridine	Sigma-Aldrich	≥98%
Nicotinamide	Sigma-Aldrich	≥98%
Isonicotinamide	Sigma-Aldrich	≥98%
Methanol	Fischer Scientific, UK	≥ 99.5%
Acetone	Fischer Scientific, UK	≥ 99.5%
Acetonitrile	Fischer Scientific, UK	≥ 99.5%

2.3 Co-Crystallisation Studies with α-Hydroxy Acids

2.3.1 Crystallisation Studies of DL-Malic Acid with Pyridinecarboxamides

Generally the following method was used, DL-malic acid and isonicotinamide or nicotinamide were dissolved individually in a minimum amount of the solvent (methanol, acetone or acetonitrile), and in accordance with the following stoichiometric starting ratios (1:1, 1:2 and 2:1). The solutions were stirred and warmed (if necessary) until the starting materials were completely dissolved. The solutions were then filtered to avoid the inclusion of undissolved starting materials in the filtrate. The filtered solutions were mixed

and left on the bench for crystallisation at room temperature. The materials obtained from crystallisation were then filtered and dried under suction. This experimental method was repeated using the different solvents and stoichiometric starting ratios (1:1, 1:2 and 2:1). The preparation details for this are presented below in Table 2.2.

Similarly, this experimental method was also repeated using DL-malic acid: nicotinamide, the preparation details for which are presented in Table 2.3.

Table 2.2: Crystallisation studies of DL-malic acid with isonicotinamide

Sample ID	Quantities DL-Malic Acid: Isonicotinamide	Solvent	Yield & Appearance	PXRD 2θ /°
TA-I-17-2a	1 mmol : 1 mmol	Methanol	0.26 g white ppt	10.1, 13.4, 16.1, 16.5, 17.3, 18.2, 18.7, 19.9, 20.3, 21.3, 24.2, 24.8, 26.3, 27.1, 27.7, 28.7, 30.1, 31.0, 32.6, 36.3, 37.1, 38.1
TA-I-17-2b	1 mmol : 2 mmol	Methanol	0.36 g white ppt	16.5, 16.9, 18.7, 18.9, 23.1, 24.7, 25.3, 26.8, 27.1, 29.7, 31.3, 32.4, 33.3
TA-I-17-2c	2 mmol : 1 mmol	Methanol	0.38 g white ppt	8.6, 10.5, 13.8, 16.3, 17.0, 17.7, 18.6, 19.1, 20.3, 21.6, 23.7, 24.5, 25.0, 25.2, 26.6, 27.4, 28.1, 29.1, 30.4, 31.4, 32.2, 33.4, 33.8
TA-I-18-1a	1 mmol : 1 mmol	Acetone	0.63 g white crystals	13.9, 16.5, 17.7, 18.7,19.1, 20.8, 21.2, 21.7, 24.7, 25.3, 25.5, 26.7, 26.9, 27.6, 28.1, 28.3, 29.1, 30.5, 38.3, 39.5
TA-I-18-1b	1 mmol : 2 mmol	Acetone	0.89 g white crystals	7.3, 8.8, 14.6, 16.4,17.6, 18.5, 18.9, 21.4, 22.3, 22.9, 23.8, 24.3, 24.9, 25.2, 25.7, 26.6, 28.0, 28.5, 29.8, 33.2, 35.4, 37.4, 38.3, 39.3
TA-I-18-1c	2 mmol : 1 mmol	Acetone	0.70 g white crystals	10.5,13.8, 16.4, 16.8, 17.6, 19.1, 20.7, 21.1, 21.6, 24.6,25.4, 27.5, 28.1, 29.0, 30.4, 34.1, 36.0, 36.6, 38.2, 39.1, 39.3, 41.9
TA-I-18-3a	1 mmol : 1 mmol	Acetonitrile	0.57 g white crystals	10.4, 13.8, 16.4, 16.9,17.6, 19.1, 20.6, 21.1, 21.6, 22.5, 23.4, 23.9, 24.5, 24.6, 25.4, 27.4, 28.1,28.5, 29.0, 30.4, 31.5, 33.8, 34.1, 36.0, 36.6, 36.6, 38.1, 38.4, 39.2
TA-I-18-3b	1 mmol : 2 mmol	Acetonitrile	0.86 g white crystals	6.8, 13.5, 15.1, 16.9, 18.0, 20.3, 22.0, 22.5, 23.9, 24.2, 24.7, 25.5, 28.1, 28.4, 32.1, 32.7, 34.1,36.2, 37.1, 37.7, 38.3, 38.9
TA-I-18-3c	2 mmol : 1 mmol	Acetonitrile	0.70 g white crystals	10.4, 13.7, 16.4, 16.9, 7.5, 19.1, 20.6, 21.6, 22.5, 23.4, 24.5, 26.0, 27.4, 28.1, 29.0, 30.4, 31.2, 33.8, 34.0, 35.9, 36.6, 38.1, 38.4, 39.3

Table 2.3: Crystallisation studies of DL-malic acid with nicotinamide

Sample ID	Quantities DL-Malic Acid: Nicotinamide	Solvent	Yield & Appearance	PXRD 2θ /°
TA-I-17-3a	1 mmol : 1 mmol	Methanol	0.71 g white ppt	7.7, 15.4, 18.0, 18.5, 21.7, 22.1, 23.2, 27.8
TA-I-17-3b	1 mmol : 2 mmol	Methanol	0.92 g white ppt	7.8, 14.9, 15.5, 17.8, 18.2, 18.5, 19.6, 22.3, 22.7, 23.3, 24.0, 24.6, 25.4, 25.9, , 2
TA-I-17-3c	2 mmol : 1 mmol	Methanol	0.64 g white crystals	7.6, 14.9, 15.3, 17.3, 18.1, 19.3, 20.0, 20.8, 22.2, 23.2, 23.5, 24.5, 25.3, 27.9, 28.8, 31.4, 32.5, 33.4, 37.5
TA-I-18-2a	1 mmol : 1 mmol	Acetone	0.79 g white crystals	7.9, 15.1, 15.6, 18.2, 19.4, 21.0, 21.6, 22.4, 23.3, 24.6, 25.4, 25.8, 26.6, 27.2, 28.0, 28.9, 31.5, 33.2, 33.5, 37.7
TA-I-18-2b	1 mmol : 2 mmol	Acetone	0.86 g white crystals	7.8, 15.0, 15.5, 18.2, 19.4, 20.9, 21.6, 22.3, 23.3, 24.6, 25.5, 26.6, 27.2, 28.0, 28.8, 31.5, 33.4
TA-I-18-2c	2 mmol : 1 mmol	Acetone	0.78 g white crystals	7.7, 14.9, 15.4, 18.0, 19.3, 20.8, 21.5, 22.2, 23.2, 24.4, 25.3, 26.5, 27.0, 7.8, 10.3, 15.0, 15.5, 18.2, 19.1, 19.4, 20.9, 21.6, 22.4, 23.3, 24.6, 25.4, 26.6, 28.0, 28.9, 30.2, 31.5, 32.2, 33.4, 34.3, 34.8, 37.7, 38.5, 40.2, 43.9, 28.7, 33.2
TA-I-18-4a	1 mmol : 1 mmol	Acetonitrile	0.59 g white crystals	7.7, 14.9, 15.4, 16.7, 17.4, 18.1, 19.0, 19.3, 20.9, 21.5, 22.3, 22.8, 23.3, 24.5, 25.3, 25.6, 26.5, 27.9, 28.8, 29.1, 30.1, 31.4, 33.2, 33.4, 34.2, 34.6
TA-I-18-4b	1 mmol : 2 mmol	Acetonitrile	0.72 g white crystals	7.7, 14.9, 15.4, 16.7, 17.4, 18.1, 19.0, 19.3, 20.9, 21.5, 22.3, 22.8, 23.276, 24.484, 25.335, 25.61, 26.5, 27.9, 28.8, 29.1, 30.1, 31.4, 33.2, 33.4, 34.2, 34.6
TA-I-18-4c	2 mmol : 1 mmol	Acetonitrile	0.62 g white crystals	7.8, 15.0, 15.5, 16.8, 17.4, 18.2, 19.0, 19.4, 20.9, 21.6, 22.3, 22.8, 23.3, 24.6, 25.4, 25.7, 26.6, 27.1, 28.0, 28.9, 29.2, 30.2, 31.5, 32.1, 33.2, 33.5, 34.2, 34.7, 36.9, 37.6, 38.5, 39.4, 40.2, 43.9, 47.5

2.3.2 Crystallisation Studies of L-Malic Acid with Pyridinecarboxamides

Generally the following method was used, L-malic acid and isonicotinamide or nicotinamide were dissolved in the minimum amount of solvent (methanol, acetone, acetonitrile or ethyl acetate) with three stoichiometric starting ratios (1:1, 1:2 and 2:1). The same procedure was followed as above (see the start of Section 2.3). The preparation details for the L-malic acid are given in Table 2.4.

Similarly, this experimental method was repeated using DL-malic acid: nicotinamide. The preparation details for which are given in Table 2.5.

Table 2.4: Crystallisation studies of L-malic acid with isonicotinamide

Sample ID	Quantities L-Malic Acid: Isonicotinamide	Solvent	Yield & Appearance	PXRD 2θ /°
TA-I-22-2a	1 mmol : 1 mmol	Methanol	0.68 g white crystals	Oil no value
TA-I-22-2b	1 mmol : 2 mmol	Methanol	0.85 g white crystals	15.1, 16.8, 17.9, 21.9, 22.4, 23.8, 24.2, 24.6, 25.5, 28.0, 28.4, 32.8, 34.0, 37.6, 38.8
TA-I-22-2c	2 mmol : 1 mmol	Methanol	0. 67 g white crystals	16.9, 21.2, 23.9, 25.5, 31.5, 35.0, 36.1, 37.2, 38.3, 39.4, 12.0
TA-I-22-3a	1 mmol : 1 mmol	Acetone	0.72 g white crystals	6.7, 15.2, 16.8, 17.9, 20.1, 21.9, 22.4, 23.8, 24. 24.6, 25.5, 28.0, 28.4, 32.1, 34.0, 37.6, 38.9, 39.2
TA-I-22-3b	1 mmol : 2 mmol	Acetone	0.86 g white crystals	6.7, 13.4, 15.1, 16.8, 17.9, 20.1, 21.9, 22.4, 23.8, 24.2, 24.6, 25.5, 28.0, 28.4, 32.1, 32.8, 33.9, 37.5, 38.8, 39.2
TA-I-22-3c	2 mmol : 1 mmol	Acetone	0.90 g oil	
TA-I-22-4a	1 mmol : 1 mmol	Acetonitrile	0.72 g beige crystals	6.6, 9.2, 10.6, 12.4, 13.1, 13.6, 15.2, 16.4, 17.2, 17.4, 18.3, 18.6, 19.1, 19.6, 20.3, 1.2, 21.9, 23.2, 24.3, 24.9, 26.3, 27.5, 29.6
TA-I-22-4b	1 mmol : 2 mmol	Acetonitrile	0.74 g beige crystals	11.7, 16.7, 21.0, 22.0, 23.6, 25.2, 26.7, 27.5, 29.4, 30.3, 31.2, 34.0, 34.7, 35.6, 36.2, 37.1, 38.0, 39.0
TA-I-22-4c	2 mmol : 1 mmol	Acetonitrile	0.68 g beige crystals	15.1, 16.7, 17.8, 20.9, 21.8, 22.4, 23.8, 24.3, 24.5, 25.3, 25.5, 26.9, 28.0, 28.3, 34.0, 34.9, 35.8, 37.0, 37.5, 38.9, 39.2, 40.8
TA-I-23-1a	1 mmol : 1 mmol	Ethyl acetate	0.63 g white crystals	11.7, 16.8, 17.2, 18.9, 21.0, 22.1, 23.7, 25.3, 26.7, 27.7, 28.0, 30.5, 31.4, 34.0, 34.9, 35.9, 36.3, 37.1, 38.1, 39.3, 46.3
TA-I-23-1b	1 mmol : 2 mmol	Ethyl acetate	0.86 g white crystals	15.3, 16.9, 18.1, 20.3, 21.2, 22.0, 22.7, 23.1, 24.0, 24.7, 25.6, 28.2, 28.5, 34.1, 37.6, 39.0
TA-I-23-1c	2 mmol : 1 mmol	Ethyl acetate	0.74 g white crystals	11.8, 16.8, 17.3, 18.9, 21.0, 22.2, 23.7, 25.3, 26.8, 27.7, 28.0, 29.6, 30.5, 31.4, 34.9, 35.9, 36.4, 37.1, 38.1, 39.3, 46.4

Table 2.5: Crystallisation studies of L-malic acid with nicotinamide

Sample ID	Quantities L-Malic Acid: Nicotinamide	Solvent	Yield & Appearance	PXRD 2θ /°
TA-I-23-3a	1 mmol : 1 mmol	Methanol	0.72 g white crystals	7.5, 17.6, 18.3, 19.3, 20.0, 20.9, 21.3, 22.4, 22.8, 23.9, 24.7, 25.7, 26.8, 27.1, 28.0, 29.0, 29.6, 30.2, 31.0, 31.6, 33.5, 34.1, 35.1, 36.1, 36.8 , 37.3, 37.7, 38.3, 39.0, 39.4
TA-I-23-3b	1 mmol : 2 mmol	Methanol	0.96 g white crystals	6.7, 12.5, 14.7, 18.6, 19.6, 21.4, 24.5, 25.0, 25.4, 25.5, 26.1, 26.4, 29.2, 32.7, 34.1, 37.4, 38.0, 39.7
TA-I-23-3c	2 mmol : 1 mmol	Methanol	0.86 g white crystals	19.3, 20.9, 21.3, 22.7, 23.8, 25.7, 28.0, 28.9
TA-I-23-2a	1 mmol : 1 mmol	Acetone	0.75 g white crystals	14.4, 19.0, 21.1, 25.2, 26.0, 27.7, 28.9
TA-I-23-2b	1 mmol : 2 mmol	Acetone	0.98 g white crystals	8.6, 14.6, 18.5, 19.7, 21.4, 24.4, 24.0, 24.9, 25.4, 26.2, 27.9, 29.1, 31.6, 32.6
TA-I-23-2c	2 mmol : 1 mmol	Acetone	0.69 g white crystals	19.4, 21.0, 21.4, 22.9, 24.0, 25.8, 28.2, 29.1, 35.2
TA-I-24-1a	1 mmol : 1 mmol	Acetonitrile	0.62 g white crystals	17.3, 17.9, 18.9, 20.1, 20.6, 21.0, 22.2, 22.5, 23.5, 25.4, 26.4, 27.7, 28.6, 29.2, 31.2, 33.2, 34.8, 36.0, 37.0, 40.2
TA-I-24-1b	1 mmol : 2 mmol	Acetonitrile	0.57 g white crystals	12.2, 14.3, 17.3, 18.9, 19.4, 20.1, 20.6, 21.0, 22.1, 22.5, 23.5, 24.6, 25.2, 25.9, 26.4, 27.7, 28.7, 28.8, 29.3, 30.1, 31.2, 33.2, 33.8, 34.8, 35.9, 37.1, 37.9, 38.6, 40.2
TA-I-24-1c	2 mmol : 1 mmol	Acetonitrile	0.57 g white crystals	18.9, 20.5, 21.0, 22.2, 22.5, 23.5, 25.3, 26.4, 27.6, 28.5, 29.2, 31.2, 33.1, 34.7, 36.9

2.3.3 Crystallisation Studies of DL-3-Phenyllactic Acid with Pyridinecarboxamides

DL-3-phenyllactic acid and the corresponding molar ratio of isonicotinamide or nicotinamide were dissolved individually in the minimum amount of solvent (methanol, acetone and acetonitrile). The samples were heated when acetone and acetonitrile were used; but, the samples dissolved in methanol at room temperature. The preparation details for this are given in Table 2.6

Likewise, this experimental method was repeated using DL-3-phenyllactic: nicotinamide, the preparation details for which are given in Table 2.7.

Table 2.6: Crystallisation studies of DL-3-phenyllactic acid with isonicotinamide

Sample ID	Quantities **DL-3-Phenyllactic Acid: Isonicotinamide**	Solvent	Yield & Appearance	PXRD 2θ /°
TA-I-31-2a	1 mmol : 1 mmol	Methanol	0.56 g white crystals	8.1, 10.2, 16.0, 17.8, 18.9, 23.9, 24.6, 25.5, 26.3, 28.8, 30.6, 31.4, 32.0, 33.6, 38.2
TA-I-31-2b	1 mmol : 2 mmol	Methanol	0.45 g white crystals	8.1, 16.0, 17.8, 18.9, 23.2, 23.6, 23.8, 24.6, 25.6, 26.6, 28.8, 31.5, 36.6, 38.8
TA-I-31-2c	2 mmol : 1 mmol	Methanol	0.61 g white crystals	8.1, 12.2, 15.1, 15.9, 17.0, 17.8, 19.4, 20.7, 21.6, 22.8, 23.9, 24.6, 25.6, 28.8, 32.6, 34.7, 39.4
TA-I-31-1a	1 mmol : 1 mmol	Acetone	0.53 g white crystals	8.1, 15.9, 17.8, 18.8, 23.7, 23.9, 24.6, 25.5, 28.7, 30.4, 31.5, 37.9, 39.1
TA-I-31-1b	1 mmol : 2 mmol	Acetone	0.27 g white solid	8.0, 10.2, 17.8, 23.0, 23.7, 24.4, 25.3, 28.5, 31.4
TA-I-31-1c	2 mmol : 1 mmol	Acetone	0.32 g white solid	8.0, 15.7, 17.7, 18.7, 19.3, 20.4, 23.5, 23.7, 24.5, 25.4, 26.1, 28.7, 30.6, 31.3, 34.4
TA-I-31-3a	1 mmol : 1 mmol	Acetonitrile	0.62 g white crystals	17.5, 22.8, 23.3, 25.2, 28.3
TA-I-31-3b	1 mmol : 2 mmol	Acetonitrile	0.57 g white crystals	11.2, 17.4, 22.0, 22.8, 23.3, 24.2, 25.1, 28.3, 34.6, 36.5
TA-I-31-3c	2 mmol : 1 mmol	Acetonitrile	0.4 g white crystals	17.5, 22.9, 23.3, 25.1, 28.4

Table 2.7: Crystallisation studies of DL-3-phenyllactic acid with nicotinamide

Sample ID	Quantities DL-3-Phenyllactic Acid: Nicotinamide	Solvent	Yield & Appearance	PXRD 2θ /°
TA-I-32-3a	1 mmol : 1 mmol	Methanol	0.42 g white crystals	8.3, 10.2, 12.5, 16.8, 17.8, 18.5, 20.1, 22.0, 22.8, 23.4, 25.1, 25.3, 28.3, 30.4, 31.5 , 33.9, 37.2, 37.8
TA-I-32-3b	1 mmol : 2 mmol	Methanol	0.16 g white crystals	9.7, 12.0, 16.3, 17.3, 18.1, 19.6, 21.6, 22.3, 22.9, 24.8, 27.8, 36.7
TA-I-32-3c	2 mmol : 1 mmol	Methanol	0. 62 g white crystals	11.6, 15.0, 19.2, 19.7, 20.0, 22.3, 22.4, 24.9, 25.9, 27.5, 28.6, 30.4, 33.8, 34.7, 37.1, 38.9
TA-I-32-2a	1 mmol : 1 mmol	Acetone	0.52 g white solid	8.1, 9.7, 14.4, 16.3, 16.8, 18.1, 18.7, 19.7, 21.0, 21.6, 22.3, 22.9, 23.4, 23.8, 24.8, 28.0, 28.8, 31.0, 33.1, 33.3
TA-I-32-2b	1 mmol : 2 mmol	Acetone	0.69 g white crystals	8.0, 9.0, 9.8, 12.1, 13.3, 14.7, 16.4, 17.4, 18.1, 18.5, 18.9, 19.7, 21.6, 22.4, 23.0, 24.9, 26.7, 27.9, 30.0, 31.1, 33.6, 36.7, 37.4
TA-I-32-2c	2 mmol : 1 mmol	Acetone	0.73 g white crystals	5.9, 8.3, 9.9, 12.9, 16.4, 17.0, 17.8, 18.5, 18.7, 19.8, 20.9, 21.1, 23.2, 24.0, 24.9, 26.5, 28.2, 37.6
TA-I-32-4°	1 mmol : 1 mmol	Acetonitrile	0.60 g white solid	6.0, 9.9, 16.5, 17.1, 17.8, 18.6, 19.8, 21.1, 22.6, 23.5, 25.1, 26.9, 28.3
TA-I-32-4b	1 mmol : 2 mmol	Acetonitrile	0.79 g white crystals	8.5, 10.3, 12.6, 16.9, 17.8,18.6, 20.1, 22.1, 22.8, 23.4, 25.3, 28.3, 34.0, 37.2, 37.8
TA-I-32-4c	2 mmol : 1 mmol	Acetonitrile	0.88 g white solid	6.3, 10.2, 9.2 10.2, 11.9, 13.3, 13.7, 16.8, 17.4, 18.2, 19.0, 20.1, 21.4, 21.6, 23.7, 24.6, 26.9, 27.1, 28.6, 33.3

2.3.4 Crystallisation Studies of L-3-Phenyllactic Acid with Pyridinecarboxamides

L-3-phenyllactic acid and the corresponding molar ratio of the isonicotinamide were dissolved individually in the minimum amount of solvent (methanol, acetone, acetonitrile or ethyl acetate) at room temperature. This experimental method was repeated using the different solvents and stoichiometric starting ratios (1:1, 1:2 and 2:1). The preparation details for which are given in Table 2.8.

Similarly, this experimental method was repeated using L-3-phenyllactic: nicotinamide, the preparation details for which are given in Table 2.9.

Table 2.8: Crystallisation studies of L-3-phenyllactic acid with isonicotinamide

Sample ID	Quantities L-3-Phenyllactic Acid: Isonicotinamide	Solvent	Yield & Appearance	PXRD 2θ /°
TA-I-52-2a	1 mmol : 1 mmol	Methanol	0.72 g white crystals	7.2, 8.6, 9.7, 11.3, 15.3, 17.4, 18.1, 19.9, 22.3, 22.6, 23.6, 24.8, 25.6, 28.4, 30.2, 30.4, 35.6, 37.1, 37.2
TA-I-52-2b	1 mmol : 2 mmol	Methanol	0.57 g white crystals	7.1, 9.5, 11.3, 14.1, 14.7, 15.2, 17.3, 18.1, 19.6, 21.8, 22.6, 23.0, 23.9, 24.8, 28.2, 30.1, 35.5, 37.0
TA-I-52-2c	2 mmol : 1 mmol	Methanol	0. 70 g white crystals	7.4, 8.1, 8.7, 9.7, 11.5, 14.5, 15.0, 15.5, 16.4, 17.5, 18.0, 18.2, 18.4, 19.9, 20.4 , 20.8, 21.4, 22.8, 23.6, 24.2, 25.0, 26.0, 28.4, 30.4, 33.2, 35.7, 37.2, 39.3
TA-I-52-1a	1 mmol : 1 mmol	Acetone	0.75 g white crystals	7.6, 10.1, 11.8, 15.2, 15.7, 17.7, 18.5, 20.2, 23.0, 24.0, 25.3, 28.7, 30.6, 36.0
TA-I-52-1b	1 mmol : 2 mmol	Acetone	0.98 g white crystals	7.8, 10.2, 15.3, 17.9, 18.2, 18.7, 20.3, 23.0, 23.2, 24.2, 25.4, 28.8, 30.2, 30.8, 37.7
TA-I-52-1c	2 mmol : 1 mmol	Acetone	0.69 g oil	
TA-I-52-3°	1 mmol : 1 mmol	Acetonitrile	0.62 g oil	
TA-I-52-3b	1 mmol : 2 mmol	Acetonitrile	0.57 g oil	
TA-I-52-3c	2 mmol : 1 mmol	Acetonitrile	0.57 g oil	

Table 2.9: Crystallisation studies of L-3-phenyllactic acid with nicotinamide

Sample ID	Quantities L-3-Phenyllactic Acid: Nicotinamide	Solvent	Yield & Appearance	PXRD
TA-I-53-2a	1 mmol : 1 mmol	Acetone	oil	
TA-I-53-2b	1 mmol : 2 mmol	Acetone	oil	
TA-I-53-2c	2 mmol : 1 mmol	Acetone	oil	
TA-I-53-3a	1 mmol : 1 mmol	Methanol	white crystals	18.0, 20.2, 25.5, 27.2
TA-I-53-3b	1 mmol : 2 mmol	Methanol	white crystals	5.2, 14.9, 17.6, 19.9, 22.3, 25.2, 25.8, 27.3, 37.0, 38.7
TA-I-53-3c	2 mmol : 1 mmol	Methanol	oil	
TA-I-53-4°	1 mmol : 1 mmol	Acetonitrile	0.62 g white crystals	14.8, 15.4, 22.2, 22.8, 27.7, 37.0, 39.1
TA-I-53-4b	1 mmol : 2 mmol	Acetonitrile	0.57 g white crystals	25.8, 25.0, 34.4, 30.3
TA-I-52-4c	2 mmol : 1 mmol	Acetonitrile	0.57 g oil	

2.4 Co-crystallisation Studies with Phenylboronic Acids

2.4.1 Crystallisation Studies of Phenylboronic Acid with Pyridinecarboxamides

Phenylboronic acid and the corresponding molar ratio of isonicotinamide or nicotinamide were dissolved individually in the minimum amount of solvent (methanol, acetone, acetonitrile or ethyl acetate) at room temperature. Again, the solutions were stirred and warmed (if necessary) until the starting materials were completely dissolved. This experimental method was repeated using the different solvents and stoichiometric starting ratios (1:1, 1:2 and 2:1). The preparation details for this are shown in Table 2.10.

This experimental method was repeated using phenylboronic acid: nicotinamide, Table 2.11 shows the preparation detail for this.

Table 2.10: Crystallisation studies of phenylboronic acid with isonicotinamide

Sample ID	Quantities Phenylboronic Acid: Isonicotinamide	Solvent	Yield & Appearance	PXRD 2θ /°
TA-I-19-1a	1 mmol : 1 mmol	Acetone	0.63 g white crystals	9.4, 15.5, 17.1, 17.8, 18.6, 19.5, 20.8, 21.5, 23.0, 23.5, 28.1, 28.6, 29.2, 31.4, 34.6, 35.8, 37.9
TA-I-19-1b	1 mmol : 2 mmol	Acetone	0.9 g beige needles	9.4, 15.7, 17.1, 17.8, 18.7, 19.6, 20.7, 21.4, 23.1, 23.4, 23.6, 26.1, 26.5, 28.2, 28.5, 29.0, 29.2, 31.8, 36.0, 37.9, 48.7
TA-I-19-1c	2 mmol : 1 mmol	Acetone	0.62g brown solid	7.4, 14.4, 15.6, 17.9, 18.9, 20.7, 22.8, 23.4, 28.4, 29.1, 31.7, 35.9, 48.4
TA-I-19-2a	1 mmol : 1 mmol	Acetonitrile	0.61g brown crystals	15.9, 17.2, 17.8, 18.2, 21.4, 21.6, 23.1, 23.4, 23.6, 24.1, 28.3, 28.9, 29.4, 31.9, 35.0, 36.0, 38.1, 39.9, 41.3, 45.4, 47.5
TA-I-19-2b	1 mmol : 2 mmol	Acetonitrile	0.92 g orange-yellow crystals	9.5, 15.9, 17.3, 17.8, 18.8, 19.4, 19.8, 20.9, 21.7, 23.5, 23.7, 26.0, 28.2, 29.1, 29.4, 30.0, 31.0, 31.4, 31.9, 34.8, 36.1, 38.1
TA-I-19-2c	2 mmol : 1 mmol	Acetonitrile	0.58 g orange-yellow crystals	9.4, 9.7, 10.8, 11.5, 12.1, 12.5, 17.0, 18.9, 20.8, 22.1, 23.6, 24.1, 24.8, 25.1, 28.4, 29.3, 29.8
TA-I-19-3a	1 mmol : 1 mmol	Methanol	0.67 g brown needle	9.2, 15.4, 16.8, 17.5, 18.4, 19.4, 20.6, 21.1, 22.2, 23.0, 23.3, 25.8, 27.4, 27.7, 27.9, 28.5, 28.7, 29.1, 34.3, 35.4, 37.5, 37.9
TA-I-19-3b	1 mmol : 2 mmol	Methanol	0.97 g brown crystals	9.2, 9.5, 10.4, 10.8, 11.3, 11.9, 12.9, 13.9, 14.4, 15.3, 16.4, 16.8, 17.7, 18.6, 19.3, 19.9, 20.1, 20.7, 21.5, 22.2, 23.1, 23.4, 23.7, 24.5, 24.9, 25.4, 26.2, 27.7, 28.1, 28.8, 29.2, 29.7, 36.0, 40.5
TA-I-19-3c	2 mmol : 1 mmol	Methanol	0.92 g brown-orange crystals	7.9, 9.4, 11.5, 14.5, 15.7, 17.1, 17.5, 17.8, 18.7, 19.7, 21.4, 21.6, 22.2, 22.6, 23.1, 23.4, 23.5, 24.9, 25.4, 25.7, 26.1, 27.7, 28.2, 28.7, 29.1, 31.7, 35.1, 35.6, 36.1, 36.7, 38.1, 39.7, 41.1, 42.1, 45.0, 45.7, 47.3, 48.5

Table 2.11: Crystallisation studies of phenylboronic acid with nicotinamide

Sample ID	Quantities Phenylboronic Acid: Nicotinamide	Solvent	Yield & Appearance	PXRD 2θ /°
TA-I-20-2a	1 mmol : 1 mmol	Acetone	0.55 g beige solid	7.8, 9.2, 12.2, 14.5, 15.4, 15.9, 17.7, 18.7, 19.9, 20.8, 22.0, 23.2, 25.6, 26.3, 26.7, 27.9, 30.0
TA-I-20-2b	1 mmol : 2 mmol	Acetone	0.72 g beige solid	7.7, 9.2, 14.5, 16.0, 18.7, 20.0, 20.9, 21.9, 23.3, 25.1, 25.6, 26.9, 27.9, 30.1, 36.3
TA-I-20-2c	2 mmol : 1 mmol	Acetone	0.9 g beige solid	5.1, 6.5, 7.1, 8.1, 8.5, 8.9, 9.5, 9.9, 10.4, 11.5, 12.4, 13.0, 13.7, 14.5, 15.8, 16.3, 16.5, 17.1, 18.1, 19.0, 19.5, 19.8, 20.2, 21.1, 21.8, 23.2, 23.6, 24.3, 24.8, 26.1, 26.6, 27.1, 28.1, 28.3, 29.5
TA-I-20-3a	1 mmol : 1 mmol	Methanol	0.57g white solid	7.4, 9.2, 10.9, 14.2, 16.0, 18.0, 18.7, 19.2, 20.7, 20.9, 22.1, 22.7, 23.3, 25.2, 26.6, 27.4, 28.0, 29.6, 30.1, 32.5, 33.7, 38.2, 41.6
TA-I-20-3b	1 mmol : 2 mmol	Methanol	0.83 g creamy white solid	9.5, 11.3, 14.9, 16.3, 19.1, 19.5, 21.2, 22.3, 23.6, 24.7, 25.5, 25.9, 27.4, 28.3, 29.9, 30.4, 32.9, 34.0, 38.5
TA-I-20-3c	2 mmol : 1 mmol	Methanol	0.9 g creamy white solid	6.5, 9.1, 10.4, 12.1, 12.3, 13.0, 13.5, 15.1, 16.2, 17.1, 17.3, 18.2, 18.5, 19.5, 20.1, 21.1, 21.7, 23.1, 24.2, 24.7, 26.1, 27.4, 28.9
TA-I-20-4a	1 mmol : 1 mmol	Acetonitrile	0.57 beige oily	No value
TA-I-20-4b	1 mmol : 2 mmol	Acetonitrile	0.86 g beige solid	8.2, 8.4, 11.9, 14.8, 16.2, 18.5, 20.5, 23.4, 24.4, 25.4, 26.1, 26.7, 27.0, 27.3
TA-I-20-4c	2 mmol : 1 mmol	Acetonitrile	0.74 g beige solid	7.8, 9.6, 11.1, 12.2, 13.4, 14.5, 15.6, 16.3, 17.8, 19.3, 19.4, 20.0, 21.9, 23.0, 24.0, 25.1, 25.6, 26.3, 27.0, 27.9, 29.8, 32.3, 36.6, 38.4, 40.5

2.4.2 Crystallisation Studies of Phenylboronic Acid with 4,4'-Bipyridine and 4-Phenylpyridine

Phenylboronic acid and the corresponding molar ratio of the 4,4-dipyridyl or 4-phenylpyridine were dissolved individually in the minimum amount of solvent (methanol, acetone or acetonitrile) at room temperature. This experimental method was repeated again using the different solvents and stoichiometric starting ratios (1:1, 1:2 and 2:1). Once the solutions were mixed they turned a bright yellow, they were then left to crystallise. The preparation details for which are shown in Table 2.12.

Likewise, this experimental method was repeated using phenylboronic acid: 4-phenylpyridine, Table 2.13 shows the preparation details for this.

Table 2.12: Crystallisation studies of phenylboronic acid with 4,4'-bipyridine

Sample ID	Quantities Phenylboronic Acid: 4,4'-Bipyridine	Solvent	Yield & Appearance	PXRD
TA-I-54-1a	1 mmol : 1 mmol	Acetone	0.55 g yellow solid	12.0, 13.2, 19.7, 20.2, 24.2, 25.5, 26.5, 27.3, 29.4, 33.5, 37.1
TA-I-54-1b	1 mmol : 2 mmol	Acetone	0.72 g yellow solid	11.3, 12.0, 13.2, 18.1, 19.6, 20.1, 21.3, 24.2, 25.4, 26.2, 26.4, 27.2, 28.7, 29.3, 31.1, 33.4, 36.0, 37.1, 38.3, 38.5
TA-I-54-1c	2 mmol : 1 mmol	Acetone	0.80 g yellow solid	9.3, 10.0, 15.5, 16.1, 16.9, 18.5, 20.0, 21.2, 22.8, 23.6, 25.5, 26.5, 29.3
TA-I-54-2a	1 mmol : 1 mmol	Methanol	0.76 g yellow solid	5.7, 7.4, 10.3, 10.8, 11.3, 12.1, 12.4, 13.0, 14.3, 14.6, 15.1, 16.1, 16.5, 17.5, 18.2, 18.7, 19.2, 19.7, 20.2, 21.5, 22.2, 22.9, 23.6, 24.1, 24.6, 25.5, 26.5, 27.3, 27.8, 28.3, 29.3, 29.7, 30.3, 30.8, 31.0, 31.7, 32.6, 33.5, 34.6, 35.9, 36.4, 37.1, 38.3, 38.5
TA-I-54-2b	1 mmol : 2 mmol	Methanol	0.98 g yellow solid	5.7, 8.2, 9.4, 10.1, 11.3, 12.0, 12.6, 13.3, 14.0, 14.7, 15.6, 16.6, 17.1, 17.4, 18.2, 18.8, 19.0, 19.8, 20.1, 21.5, 22.3, 22.7, 23.5, 24.0, 24.2, 25.6, 26.3, 26.6, 27.2, 29.4, 30.9, 31.2, 32.6, 33.6, 34.2, 37.2, 38.2, 38.6
TA-I-54-2c	2 mmol : 1 mmol	Methanol	0.69 g yellow solid	5.7, 8.2, 9.4, 10.1, 11.3, 12.0, 12.6, 13.3, 14.0, 14.7, 15.6, 16.6, 17.1, 17.4, 18.2, 18.8, 19.0, 19.8, 20.1, 21.5, 22.3, 22.7, 23.5, 24.0, 24.2, 25.6, 26.3, 26.6, 27.2, 29.4, 30.9, 31.2, 32.6, 33.6, 34.2, 37.2, 38.2, 38.6
TA-I-55-1a	1 mmol : 1 mmol	Acetonitrile	0.71g yellow solid	11.3, 12.1, 13.3, 18.2, 19.7, 20.2, 21.6, 23.3, 25.6, 26.5, 27.3, 29.4, 31.2, 32.8, 37.2, 38.4
TA-I-55-1b	1 mmol : 2 mmol	Acetonitrile	0.92 g yellow solid	11.4, 12.2, 13.4, 14.7, 18.3, 19.8, 20.3, 21.7, 23.3, 24.4, 25.7, 26.5, 27.3, 29.4, 31.3, 32.9, 33.6, 37.2, 38.4, 38.8
TA-I-55-1c	2 mmol : 1 mmol	Acetonitrile	0.64 g yellow solid	5.6, 9.1, 10.4, 11.11, 11.64, 12.3, 12.9, 14.0, 14.6, 15.4, 16.4, 17.1, 17.3, 18.7, 19.2, 20.2, 20.6, 21.3, 21.7, 23.04, 23.5, 24.4, 25.2, 26.3, 26.6, 26.8, 27.5, 28.6, 29.1, 29.8, 30.8, 31.9, 32.4, 33.2, 39.3

Table 2.13: Crystallisation studies of phenylboronic acid with 4-phenylpyridine

Sample ID	Quantities Phenylboronic Acid: 4-Phenylpyridine	Solvent	Yield & Appearance	PXRD
TA-I-56-2a	1 mmol : 1 mmol	Acetone	0.62 g yellow solid	5.8, 6.9, 7.8, 8.0, 9.1, 10.1, 12.0, 12.8, 13.3, 14.0, 14.6, 15.3, 15.9, 16.9, 17.5, 18.0, 18.2, 18.5, 19.4, 19.6, 20.9, 21.2, 22.1, 22.3, 22.7, 23.2, 23.9, 24.6, 24.9, 25.4, 25.6, 26.2, 27.3, 27.8, 28.6, 29.5, 33.0, 33.7, 34.8, 35.1, 35.8
TA-I-56-2b	1 mmol : 2 mmol	Acetone	0.43 g yellow solid	9.8, 10.6, 12.7, 16.7, 17.8, 18.7, 18.9, 19.7, 20.0, 20.7, 21.5, 22.0, 22.3, 23.0, 23.5, 23.8, 25.1, 25.8, 26.2, 26.3, 27.8, 29.3, 29.9, 30.6, 32.4, 33.1, 35.8
TA-I-56-2c	2 mmol : 1 mmol	Acetone	0.70 g yellow solid	7.8, 8.0, 8.8, 9.5, 9.9, 11.5, 11.8, 13.1, 14.3, 15.6, 16.4, 16.9, 17.5, 17.8, 18.1, 18.6, 19.0, 19.5, 20.6, 20.7, 21.2, 21.9, 22.6, 23.2, 23.8, 24.6, 24.9, 25.4, 26.2, 27.2, 27.7, 28.6, 29.7, 30.0, 31.2, 31.6, 32.8, 33.6, 35.1, 35.9, 37.2, 38.7
TA-I-56-1a	1 mmol : 1 mmol	Methanol	0.69 g yellow solid	8.0, 8.9, 10.1, 11.9, 13.4, 15.8, 16.5, 17.0, 17.5, 17.8, 18.2, 18.5, 18.7, 19.1, 19.8, 20.1, 20.7, 21.1, 21.2, 22.0, 23.3, 23.8, 24.5, 24.7, 27.8, 28.7, 29.5, 29.9, 30.1, 30.7, 31.6, 33.6, 34.7, 35.1, 35.7, 35.9
TA-I-56-1b	1 mmol : 2 mmol	Methanol	0.76 g yellow solid	7.9, 8.1, 8.9, 9.7, 12.0, 13.4, 14.8, 15.5, 17.0, 17.6, 18.1, 18.4, 18.8, 19.2, 19.7, 20.0, 20.7, 21.4, 22.1, 22.7, 23.2, 23.7, 24.1, 27.3, 27.7, 28.7, 29.5, 34.1, 34.9, 39.2
TA-I-56-1c	2 mmol : 1 mmol	Methanol	0.93 g yellow solid	8.0, 8.2, 10.1, 11.1, 11.9, 11.5, 13.3, 14.2, 15.4, 15.9, 16.6, 16.9, 17.5, 18.1, 18.5, 19.6, 19.9, 20.1, 20.6, 21.1, 22.0, 22.5, 22.8, 23.3, 23.9, 24.8, 26.4, 27.7, 28.5, 30.3, 31.1, 32.1, 33.5, 36.0, 37.9, 39.3
TA-I-56-3a	1 mmol : 1 mmol	Acetonitrile	0.70 g yellow solid	8.0, 9.1, 9.7, 10.1, 11.9, 12.9, 13.4, 15.5, 17.0, 17.5, 17.8, 18.2, 18.7, 19.0, 19.3, 19.8, 20.7, 21.2, 21.4, 22.1, 22.9, 23.3, 23.8, 25.1, 26.4, 27.8, 28.2, 28.6, 29.4, 29.8, 39.1

Sample ID	Quantities Phenylboronic Acid: 4-Phenylpyridine	Solvent	Yield & Appearance	PXRD
TA-I-56-3b	1 mmol : 2 mmol	Acetonitrile	0.71 g yellow solid	8.2, 9.2, 9.7, 9.9, 12.1, 15.0, 17.1, 17.8, 18.4, 19.3, 19.5, 19.9, 20.9, 21.5, 22.1, 22.6, 23.4, 23.9, 25.1, 26.4, 26.7, 28.0, 28.7, 28.4, 29.6, 30.9, 35.1, 36.1
TA-I-56-3c	2 mmol : 1 mmol	Acetonitrile	0.61 g yellow solid	8.1, 9.1, 9.7, 10.1, 12.1, 13.0, 13.5, 14.3, 15.8, 16.6, 17.1, 17.8, 18.2, 18.6, 19.2, 19.7, 19.9, 20.1, 20.8, 21.2, 22.1, 22.7, 23.3, 23.9, 24.7, 25.8, 26.6, 27.7, 28.8, 29.6, 30.0, 30.8, 33.4, 36.1

2.6   Single Crystal X-Ray Studies

Single crystal x-ray diffraction studies were undertaken with a Bruker X8 diffractometer. Single crystals were selected from either mother liquors or they were separated from solids, they were then coated with perfluoroalkane oil and mounted into the diffractometer's nitrogen cryostream. From the resulting diffraction data, structure solution and refinement were carried out with the Bruker APEX2 v2011.4-1 software. Data collection and the initial structure solution and refinement were carried out by Professor Ian Scowen at the University of Bradford.

Table 2.14: Crystal data and structure refinement for TA-1-17-3b (DL-malic acid: nicotinamide)

Identification code	tai_17_3b_t
Empirical formula	C20 H24 N4 O12
Formula weight	512.43
Temperature	173(2) K
Wavelength	0.71073 Å
Crystal system	Orthorhombic
Space group	Pca2(1)
Unit cell dimensions	a = 18.629(3) Å $\quad$ α= 90°.
	b = 5.2842(8) Å $\quad$ β= 90°.
	c = 22.841(4) Å $\quad$ ɣ = 90°.
Volume	2248.5(6) Å^3
Z	4
Density (calculated)	1.514 Mg/m^3
Absorption coefficient	0.127 mm^{-1}
F(000)	1072
Crystal size	0.754 x 0.348 x 0.226 mm^3
Theta range for data collection	2.19 to 24.66°.
Index ranges	-18<=h<=21, -5<=k<=5, -25<=l<=23
Reflections collected	16447
Independent reflections	3047 [R(int) = 0.0537]
Completeness to theta = 24.66°	86.4 %
Absorption correction	Multi-scan (Bruker SAINT)
Refinement method	Full-matrix least-squares on F^2
Data / restraints / parameters	3047 / 1 / 335
Goodness-of-fit on F^2	1.080
Final R indices [I>2sigma(I)]	R1 = 0.0477, wR2 = 0.1130
R indices (all data)	R1 = 0.0631, wR2 = 0.1197
Absolute structure parameter	-1.2(17)
Largest diff. peak and hole	0.263 and -0.284 e.Å^{-3}

Table 2.15: Crystal data and structure refinement for TA-1-23-3b (L-malic acid: nicotinamide)

Identification code	tai_23_3b_2_0m
Empirical formula	C16 H18 N4 O7
Formula weight	378.34
Temperature	173(2) K
Wavelength	0.71073 Å
Crystal system	Triclinic
Space group	P1
Unit cell dimensions	a = 4.7631(2) Å α= 96.829(3)°.
	b = 8.8253(4) Å β= 95.279(3)°.
	c = 10.6620(5) Å ɣ = 105.603(3)°.
Volume	424.99(3) Å^3
Z	1
Density (calculated)	1.478 Mg/m^3
Absorption coefficient	0.118 mm^{-1}
F(000)	198
Crystal size	0.234 x 0.320 x 0.489 mm^3
Theta range for data collection	2.87 to 32.00°.
Index ranges	-6<=h<=6, -12<=k<=13, -15<=l<=15
Reflections collected	7290
Independent reflections	4822 [R(int) = 0.0135]
Completeness to theta = 32.00°	93.0 %
Absorption correction	Multi-scan (Bruker SAINT)
Refinement method	Full-matrix least-squares on F^2
Data / restraints / parameters	4822 / 3 / 312
Goodness-of-fit on F^2	1.021
Final R indices [I>2sigma(I)]	R1 = 0.0370, wR2 = 0.0845
R indices (all data)	R1 = 0.0516, wR2 = 0.0919
Absolute structure parameter	0.8(8)
Largest diff. peak and hole	0.295 and -0.191 e.Å^{-3}

Table 2.16: Crystal data and structure refinement for TA-1-31-3c (DL-3-phenyllactic acid: isonicotinamide)

Identification code	tai_31_3c_0m
Empirical formula	C15 H16 N2 O4
Formula weight	288.30
Temperature	173(2) K
Wavelength	0.71073 Å
Crystal system	Triclinic
Space group	P-1
Unit cell dimensions	a = 5.3395(5) Å $\quad$ α= 78.849(9)°.
	b = 11.3914(15) Å $\quad$ β= 82.062(8)°.
	c = 11.6131(13) Å $\quad$ ɣ = 81.076(9)°.
Volume	680.36(13) Å^3
Z	2
Density (calculated)	1.407 Mg/m^3
Absorption coefficient	0.103 mm^{-1}
F(000)	304
Crystal size	0.126 x 0.318 x 0.460 mm^3
Theta range for data collection	2.79 to 27.50°.
Index ranges	-6<=h<=6, -14<=k<=14, -15<=l<=15
Reflections collected	17283
Independent reflections	3114 [R(int) = 0.0822]
Completeness to theta = 27.50°	99.9 %
Absorption correction	Multi-scan (Bruker SAINT)
Refinement method	Full-matrix least-squares on F^2
Data / restraints / parameters	3114 / 0 / 206
Goodness-of-fit on F^2	0.790
Final R indices [I>2sigma(I)]	R1 = 0.0531, wR2 = 0.1298
R indices (all data)	R1 = 0.1038, wR2 = 0.1567
Largest diff. peak and hole	0.316 and -0.296 e.Å^{-3}

Table 2.17: Crystal data and structure refinement for TA-1-52-1a (L-3-phenyllactic acid: isonicotinamide)

Identification code	tai_52_1a_0m
Empirical formula	C15 H16 N2 O4
Formula weight	288.30
Temperature	173(2) K
Wavelength	1.54178 Å
Crystal system	Triclinic
Space group	P1
Unit cell dimensions	a = 5.3040(2) Å $\quad$ α= 80.398(3)°.
	b = 11.4994(4) Å $\quad$ β= 81.767(3)°.
	c = 11.7480(5) Å $\quad$ ɣ= 82.135(3)°.
Volume	694.52(5) Å^3
Z	2
Density (calculated)	1.379 Mg/m^3
Absorption coefficient	0.841 mm^{-1}
F(000)	304
Crystal size	0.3 x 0.3 x 0.4 mm^3
Theta range for data collection	3.85 to 66.62°.
Index ranges	-6<=h<=6, -13<=k<=13, -13<=l<=13
Reflections collected	14779
Independent reflections	3555 [R(int) = 0.0722]
Completeness to theta = 66.62°	97.2 %
Absorption correction	Multi-scan (Bruker SAINT)
Refinement method	Full-matrix least-squares on F^2
Data / restraints / parameters	3555 / 3 / 411
Goodness-of-fit on F^2	1.071
Final R indices [I>2sigma(I)]	R1 = 0.0528, wR2 = 0.1276
R indices (all data)	R1 = 0.0689, wR2 = 0.1415
Absolute structure parameter	-0.1(3)
Largest diff. peak and hole	0.208 and -0.308 e.Å^{-3}

Table 2.18: Crystal data and structure refinement for TA-1-20-3a (phenylboronic acid: isonicotinamide)

Identification code	tai_20_3a_0m
Empirical formula	C12 H13 B N2 O3
Formula weight	244.05
Temperature	173(2) K
Wavelength	0.71073 Å
Crystal system	Triclinic
Space group	P-1
Unit cell dimensions	a = 5.4403(3) Å α= 95.815(4)°.
	b = 9.4941(5) Å β= 96.296(4)°.
	c = 12.4001(6) Å γ = 102.275(4)°.
Volume	616.91(6) Å^3
Z	2
Density (calculated)	1.314 Mg/m^3
Absorption coefficient	0.094 mm^{-1}
F(000)	256
Crystal size	0.50 x 0.41 x 0.12 mm^3
Theta range for data collection	2.59 to 32.19°.
Index ranges	-8<=h<=7, -14<=k<=14, -17<=l<=18
Reflections collected	24707
Independent reflections	4168 [R(int) = 0.0698]
Completeness to theta = 32.19°	95.7 %
Absorption correction	Multi-scan (Bruker SAINT)
Max. and min. transmission	0.9887 and 0.9543
Refinement method	Full-matrix least-squares on F^2
Data / restraints / parameters	4168 / 0 / 179
Goodness-of-fit on F^2	1.003
Final R indices [I>2sigma(I)]	R1 = 0.0532, wR2 = 0.0947
R indices (all data)	R1 = 0.1275, wR2 = 0.1182
Largest diff. peak and hole	0.267 and -0.227 e.Å^{-3}

Table 2.19: Crystal data and structure refinement for RBi_1_0m (phenylboronic acid: isonicotinamide)

Identification code	rbi_1_0m
Empirical formula	C12 H13 B N2 O3
Formula weight	244.05
Temperature	173(2) K
Wavelength	0.71073 Å
Crystal system	Monoclinic
Space group	P2(1)/n
Unit cell dimensions	a = 12.0598(8) Å $\quad$ α= 90°.
	b = 5.1459(2) Å $\quad$ β= 101.963(2)°.
	c = 19.2537(11) Å $\quad$ γ = 90°.
Volume	1168.91(11) Å^3
Z	4
Density (calculated)	1.387 Mg/m^3
Absorption coefficient	0.099 mm^{-1}
F(000)	512
Crystal size	0.120 x 0.177 x 0.470 mm^3
Theta range for data collection	3.34 to 23.70°.
Index ranges	-13<=h<=9, -4<=k<=5, -17<=l<=16
Reflections collected	4848
Independent reflections	1142 [R(int) = 0.0248]
Completeness to theta = 23.70°	64.9 %
Absorption correction	Multi-scan (Bruker SAINT)
Refinement method	Full-matrix least-squares on F^2
Data / restraints / parameters	1142 / 0 / 215
Goodness-of-fit on F^2	0.932
Final R indices [I>2sigma(I)]	R1 = 0.0344, wR2 = 0.0743
R indices (all data)	R1 = 0.0463, wR2 = 0.0833
Largest diff. peak and hole	0.113 and -0.170 e.Å^{-3}

Table 2.20: Crystal data and structure refinement for TA-1-61-3a (3-nitrophenylboronic acid: isonicotinamide)

Identification code	tai_61_3a_0m_a
Empirical formula	C12 H12 B N3 O5
Formula weight	289.06
Temperature	173(2) K
Wavelength	0.71073 Å
Crystal system	Triclinic
Space group	P-1
Unit cell dimensions	a = 5.0091(5) Å $\quad$ α= 65.845(6)°.
	b = 11.6769(11) Å $\quad$ β= 79.684(7)°.
	c = 12.6083(13) Å $\quad$ γ = 80.152(6)°.
Volume	658.08(11) Å^3
Z	2
Density (calculated)	1.459 Mg/m^3
Absorption coefficient	0.113 mm^{-1}
F(000)	300
Crystal size	0.11 x 0.14 x 0.35 mm^3
Theta range for data collection	2.05 to 25.00°.
Index ranges	-5<=h<=5, -13<=k<=13, -14<=l<=14
Reflections collected	11617
Independent reflections	2289 [R(int) = 0.0711]
Completeness to theta = 25.00°	99.3 %
Refinement method	Full-matrix least-squares on F^2
Data / restraints / parameters	2289 / 0 / 192
Goodness-of-fit on F^2	0.909
Final R indices [I>2sigma(I)]	R1 = 0.0550, wR2 = 0.1217
R indices (all data)	R1 = 0.0950, wR2 = 0.1387
Largest diff. peak and hole	0.210 and -0.241 e.Å^{-3}

Table 2.21 Crystal data and structure refinement for TA-1-56-2c ([PhBO]₃[4-Phpy]₄[4-Phpy])

Identification code	tai_56_2c_0m
Empirical formula	C63.50 H52.50 B6 N2.50 O6
Formula weight	1011.44
Temperature	173(2) K
Wavelength	0.71073 Å
Crystal system	Monoclinic
Space group	C2/c
Unit cell dimensions	a = 47.2140(10) Å α= 90°.
	b = 13.4209(3) Å β= 108.5010(10)°.
	c = 18.7318(3) Å ɣ = 90°.
Volume	11256.0(4) Å^3
Z	8
Density (calculated)	1.194 Mg/m^3
Absorption coefficient	0.074 mm^{-1}
F(000)	4232
Crystal size	0.322 x 0.528 x 0.681 mm^3
Theta range for data collection	2.54 to 29.76°.
Index ranges	-54<=h<=59, -15<=k<=17, -25<=l<=25
Reflections collected	66823
Independent reflections	12798 [R(int) = 0.0627]
Completeness to theta = 29.76°	79.6 %
Absorption correction	None
Refinement method	Full-matrix least-squares on F^2
Data / restraints / parameters	12798 / 0 / 705
Goodness-of-fit on F^2	0.983
Final R indices [I>2sigma(I)]	R1 = 0.0525, wR2 = 0.1016
R indices (all data)	R1 = 0.1448, wR2 = 0.1316
Largest diff. peak and hole	0.194 and -0.227 e.Å^{-3}

Table 2.22: Crystal data and structure refinement for TA-1-54-1c ([PhB(OH)$_2$][4,4'-bipy])

Identification code	twin4
Empirical formula	C20H20BN2O6
Temperature	173
Space group	C2
Volume	2183.67 (16) Å^3
a, b, c (Å)	9.2670 (4), 17.6376 (7), 14.1413 (6)
α, β, γ (°)	90, 109.134 (2), 90
Z	4
Radiation type	Mo Kα
μ (mm−1)	0.09
Data collection	
No. of measured, independent and observed [I > 2σ(I)] reflections	1382, 1382, 1335
Rint	0.0000
θmax (°)	22.0
(sin θ/λ)max (Å−1)	0.526
Refinement	
R[F2 > 2σ(F2)], wR(F2), S	0.078, 0.225, 1.14
No. of reflections	1382
No. of parameters	302
No. of restraints	1
H-atom treatment and constrained refinement	H atoms treated by a mixture of independent
	w = 1/[σ2(Fo2) + (0.1004P)2 + 19.9417P]
	Where P = (Fo2 + 2Fc2)/3
(Δ/σ)max	0.267
Δρmax, Δρmin (e Å−3)	0.44, −0.30
Absolute structure	Flack H D (1983), Acta Cryst. A39, 876-881
Absolute structure parameter	−5 (7)

Table 2.23: Crystal data for TA-1-54-2a ([(PhBO)3(4,4'-bipy)][PhB(OH)2])

Identification code	t_a
Chemical formula	$C_{16}H_{15}BN_2O_2$
Mr	278.11
space group	P21/c
Temperature (K)	173
a, b, c (Å)	22.417 (9), 14.497 (5), 10.223 (4)
α, β, γ (°)	90, 99.157 (11), 90
V (Å3)	3280 (2)
Z	8
Radiation type	Mo Kα
μ (mm−1)	0.07
Crystal size (mm)	0.25 × 0.24 × 0.05
Data collection	
No. of measured, independent and observed [I> 2σ(I)] reflections	40735, 3325, 1996
Rint	0.215
θmax (°)	20.6
(sin θ/λ)max (Å−1)	0.495
Refinement	
R[F2> 2σ(F2)], wR(F2), S	0.080, 0.201, 1.09
No. of reflections	3325
No. of parameters	414
H-atom treatment and constrained refinement	H atoms treated by a mixture of independent
(Δ/σ)max	0.357
Δρmax, Δρmin (e Å−3)	0.29, −0.25

Chapter 3

3.0   An Investigation into the Preparation of Crystalline Multicomponent Systems from Chiral Formers: Malic Acid

3.1   Introduction and Aims of the Study

In this study, an attempt has been made to evaluate the influence of a chiral centre that is adjacent to molecular synthons, in order to identify the potential translation of information into the solid form. The co-crystallisation of pyridinecarboxamides has been compared in terms of both the racemic mixture of malic acid and the enantiomerically pure form of the acid (L-malic acid).
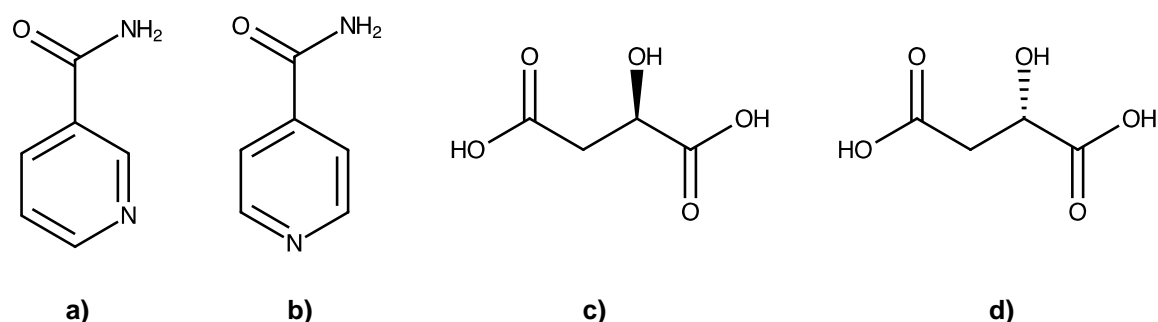
Figure 3.1: The co-crystallisation of: a) nicotinamide; b) isonicotinamide; c) L-malic acid (R-form); and, d) D-malic acid (S-form)

With regards to Figure 3.1 above, nicotinamide and isonicotinamide were used in the co-crystallisation process with the acid co-formers. The two molecules are structurally similar but differ in position of the N atom in the pyridine rings. The formers have been selected to promote acid-amide interactions as primary motifs for the assembly of multicomponent products. This study is designed to provide some insight into the role of the chiral centres that are adjacent to the primary hydrogen bonding motif.

Malic acid was crystallised independently with both nicotinamide and isonicotinamide. Crystallisation studies were performed in a range of different solvents (methanol, acetone and acetonitrile) with different molar ratios of the starting material (1:1, 1:2 and 2:1). The products were isolated as white crystalline powders after slow evaporation of the solvent occurred at room temperature (Table 2.2 and 2.3 Chapter 2).

This section will now focus on explaining the phenomena of transformation of chiral information based on the preparation of solid state multicomponent systems from mixtures of chiral and achiral formers. In addition, an understanding of the competition between the homodimers of carboxamides and acid-amide dimers in rings should also be gained. The alternative hetero interaction between the pyridine N to acid provides a single point attachment between the formers which may be structurally analogous to the interaction with 4,4'-bipyridine (isonicotinamide) or 3,3'-bipyridine (nicotinamide). Only two structures of α-hydroxy acids with isonicotinamide are known: D-tartaric acid (JAWUZ)[83] and DL-mandelic acid (LUNPAL)[84], with nicotinamide with citric acid (CUYXUG)[85]; and racemic and enantiopure mandelic acid (JILZOUΦ1 and JILZOU, respectively)[83].

The key stages in this study are:

Co-crystallisation from different starting stoichiometric ratios and a range of solvents with different polarities.

Characterisation using powder x-ray diffraction data to confirm the formation of new material.

Characterisation of new materials using NMR (to identify stoichiometries) and IR techniques (co-crystal formation).

3.2   Phase Chemistry

3.2.1   Crystallisation Studies of DL-Malic Acid with Pyridinecarboxamides

3.2.1.1 Isonicotinamide

Solutions of DL-malic acid and isonicotinamide were prepared in ratios of 1:1, 1:2 and 2:1 in methanol, acetonitrile and acetone. After slow evaporation of the solvent, at room temperature, white crystalline solids were isolated. The resulting products were analysed with powder x-ray diffraction and solid state infrared spectroscopy. In addition, stoichiometric ratios of the crystalline products were established using a solution nuclear magnetic resonance spectroscopy (^{1}HNMR).

Comparison of the PXRD patterns of the starting materials (DL-malic acid and isonicotinamide), against the multicomponent system, allows for evaluation and the drawing of initial conclusions as to whether the complexation reactions were successful. The PXRD were compared to the isolated polymorphs (EHOWIH, EHOWIH01, EHOWIH02) of isonicotinamide from the database[86].

The sample TA-I-17-2a showed a presence of new peaks at 13.9, 19.9, 21.8, 22.8 and 24.2° (see Figure 3.2). Similarly, the non-stoichiometric product of TA-I-17-2b showed unique peaks at 17.6, 19.7, 22.9, 24.5, 27.8 and 47.5°. In addition, TA-I-17-2c showed distinctive peaks at 16.7 and 17.3°, indicating

that a new phase was present. Detailed analysis of the PXRD is provided to support this chapter, this can be found in Appendix A.

Both stoichiometric and non-stoichiometric products showed no significant peak appearances that were in the region of 39 to 40°. The data obtained by analysis can be used to depict the conclusion that the starting materials have formed a new phase (TA-I-17-2a, TA-I-17-2b, TA-I-17-2c). The non-stoichiometric products (2:1) showed the presence of peaks that corresponded with the starting materials, specifically DL-malic acid in the following regions of 19.0, 26.6 and 33.3°.

The multicomponent formation of DL-malic acid/isonicotinamide was also investigated using acetone (TA-I-18-1a, 1b and 1c) and acetonitrile (TA-I-18-3a, 3b and 3c) as the solvent. The use of x-ray powder diffraction is likely to be very useful in demonstrating the important aspects with regards to the nature of the interactions and the effect of the solvent within the formation of a multicomponent system. The XRD powder patterns for the materials formed, provides confirmation that TA-I-18-1a showed peaks at 21.4, 21.9 and 25.5° which was similar to the results identified for TA-I-17-2a and TA-I-18-3a.

Analysis of non-stoichiometric products, through the use of acetone and acetonitrile, also agree well with the results of the multicomponents by methanol; as such, TA-I-18-3b showed a peak at 28.41 and TA-I-18-3c showed a peak at 28.88, along a 2θ scale. When reviewing the PXRD patterns, it is interesting to notice that the molar ratio 1:1 and 2:1 products

show somewhat similar traces of peaks on the new phase. However, the ratio 1:2 products (specifically at 2θ: 15.1, 25.5 and 24.7) showed a mixture of multicomponent systems and starting materials, specifically isonicotinamide and its polymorphic form (EAOWIH01) which do not appear in the other ratios.

To summarise, the samples in methanol (2:1, 1:1 and 1:2) all produced a new phase. The 2:1 and 1:1 had the same new phase, and the 1:2 ratio also produced a new phase; additionally, the 2:1 ratio also had some excess DL-malic acid. In acetonitrile, all of the ratios produced the same new phase; however, the 1:1 ratio showed two new phases with some traces of isonicotinamide and the 1:2 ratio produced a new phase with the excess of isonicotinamide polymorphic form (EAOWIH02). In acetone the same new phase was present for all three ratios. Hence, the solvents and the ratios of starting material used seem to have had an effect on the phase that is produced (Figure 3.2 and 3.3).
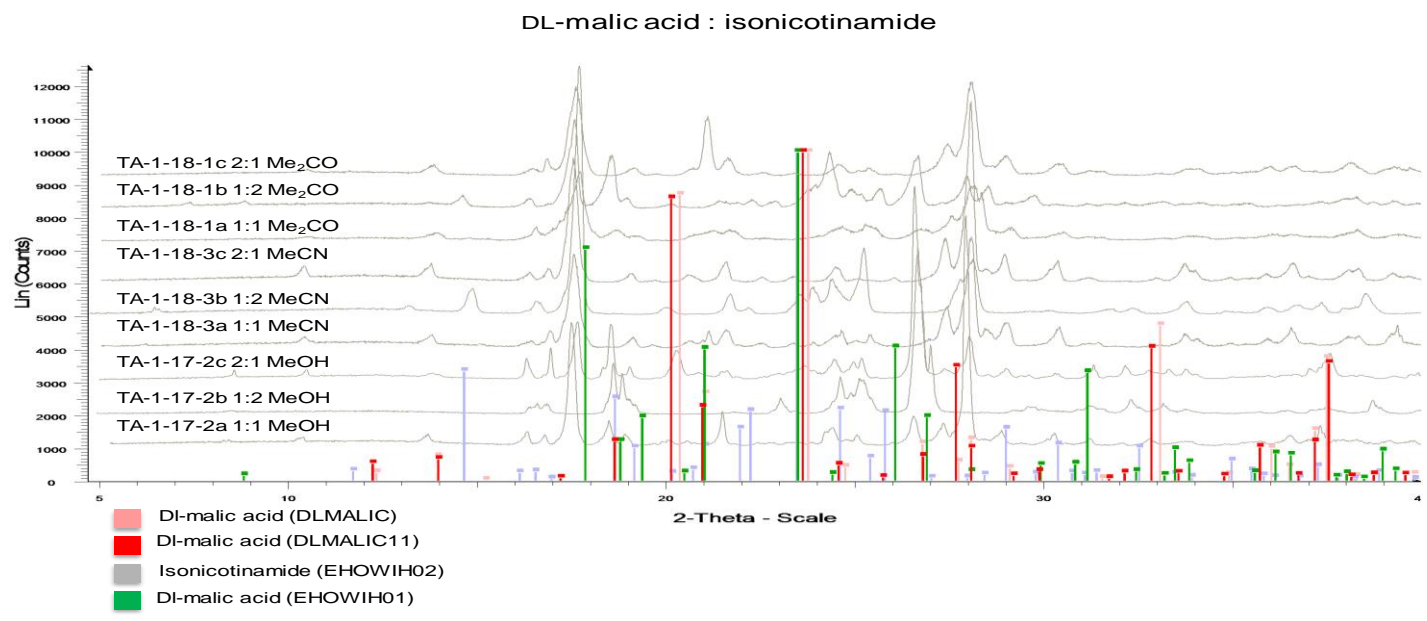
Figure 3.2: X-ray powder diffraction patterns of isonicotinamide and DL-malic acid, and products of crystallisation with a range of solvents
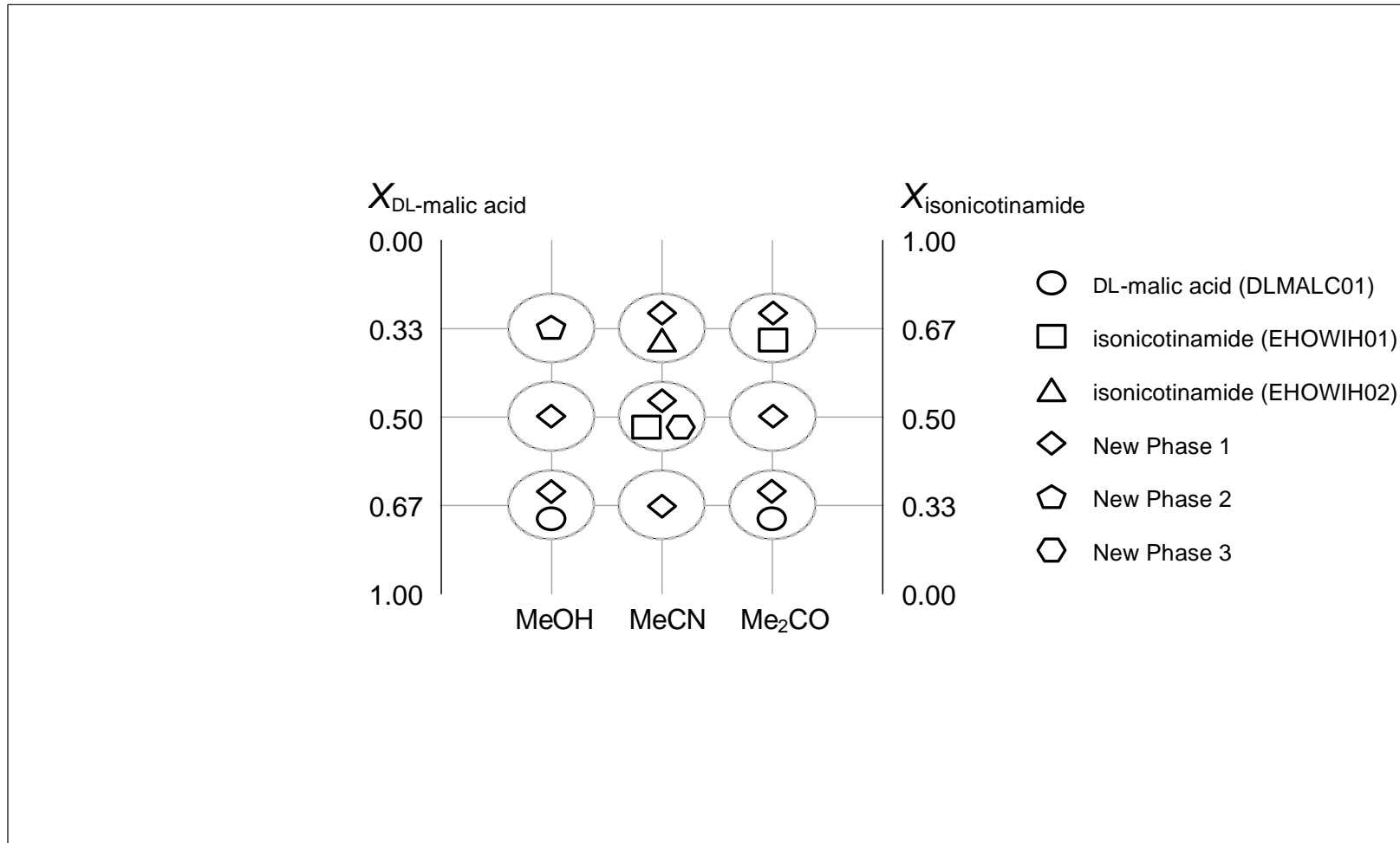
Figure 3.3: Representation of crystalline phases identified from the co-crystalisations of DL-malic acid: isonicotinamide

In order of establish whether DL-malic acid is present in the product (by implication that the product contains a co-crystal phase), the ^{1}HNMR experiment was undertaken. From the integral values of different peak intensities for protons in different environments on DL-malic acid and isonicotinamide, it is evident that this new material contains the starting components. Thus, indicating that both the DL-malic acid and isonicotinamide are present in the co-crystal (see Table 3.1).

The different systems were dissolved $(CD_3)_2OD$ as a solvent. A peak at 2.08ppm represents the residual proton in the deuterated-acetone, and the peak at 4.0ppm represents the water in the system. The structures used in the assignments of the ^{1}HNMR spectra are detailed below in Figure 3.4.
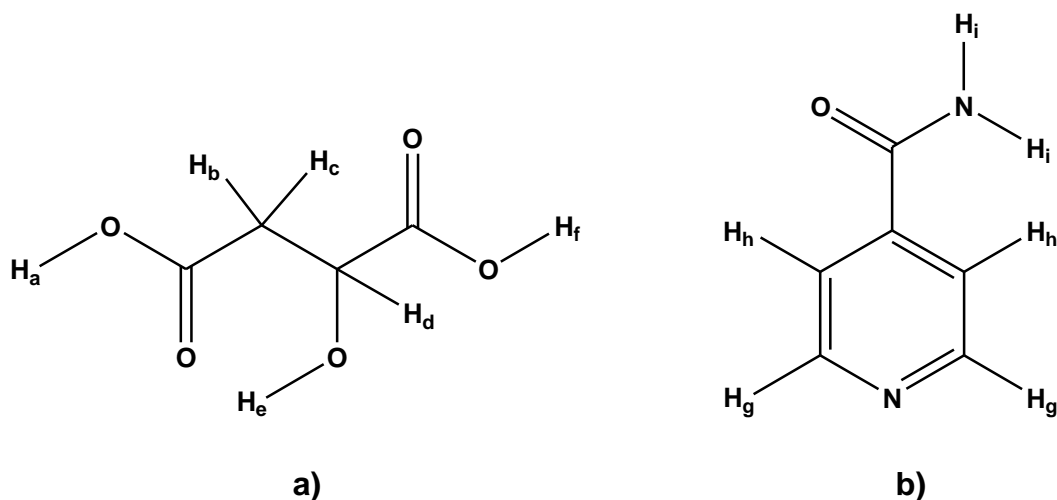
Figure 3.4: Structures used in the assignment of the ^{1}HNMR spectra of sample: a) malic acid; and, b) isonicotinamide

Table 3.1: ^{1}HNMR spectral data of sample and its starting materials for: DL-malic acid and isonicotinamide (Appendix AA 3.1)

Sample TA-I-17-2b			DL-Malic Acid			Isonicotinamide		
Shift (ppm)	Multiplicity, Integration	Assignment	Shift (ppm)	Multiplicity, Integration	Assignment	Shift (ppm)	Multiplicity, Integration	Assignment
2.08	S	Acetone-d_6	2.10	bs, 1H	H_e	--	--	--
2.60	dd, 0.5H	H_b	2.53	dd, 1H	H_b, H_c	--	--	--
2.81	dd, 0.5H	H_c	2.78	dd, 1H		--	--	--
4.30	S	water	--	--	--	--	--	--
4.51	dd, 0.5H	H_d	4.42	dd, 1H	H_d	--	--	--
--	--	--	--	--	--	6.05	s, 2H	NH_2
7.77	d, 2H	H_h	--	--	--	7.96	d, 2H	H_h
8.70	d, 2H	H_g	--	--	--	9.06	d, 2H	H_g
			11.00	bs, 2H	H_a, H_f			

The ^{1}HNMR spectrum of isonicotinamide exhibited two doublets for the aromatic protons in the range of 7.96 to 9.06ppm. The structure of isonicotinamide was confirmed in the ^{1}HNMR spectrum of sample TA-I-17-2b, where a doublet was observed in the deshielded region of 8.70ppm for two H_g protons corresponding to CH protons in the neighbourhood of the heteroatom – nitrogen in this case. The other set of two aromatic protons (H_h) resonated in the region 7.77ppm, again as a doublet.

The structure of malic acid was also confirmed in the ^{1}HNMR spectrum of sample TA-I-17-2b, whereby a doublet of doublets in the region of 2.60 and 2.81ppm for each of two diastereotopic protons H_b and H_c, were observed. The methine proton of the chiral centre appeared as a doublet of doublets in the region of 4.50ppm, it also appeared to be deshielded due to the fact that this proton is in the neighbourhood of a highly electronegative oxygen atom. All the signals of the protons of malic acid appeared to be deshielded with a slight change in their chemical shift values – this was evidenced by the comparison of chemical shift values of neat malic acid and that of sample TA-I-17-2b, as can be seen in Table 3.1. It is worth noting that this might be the result of complexation.

The ^{1}HNMR spectrum obtained for sample TA-I-17-2b shows similarities to the isonicotinamide between 7.77 and 9.10ppm, as well as similarities to the DL-malic acid between 2.60 and 4.51ppm, thus indicating that a multicomponent system is formed successfully from malic acid and isonicotinamide.

The ^{1}HNMR spectrum of the multicomponent system sample shows common peaks/shifts in both of the starting materials; thus, suggesting that some complexation between the two has occurred. Similar behaviours were observed for multicomponent systems TA-I-18-1a and TA-I-18-3a, they utilised the same starting materials but different solvents (acetone and acetonitrile) in the multicomponent preparation.

These conclusions are supported by the data obtained using FT-IR spectroscopy, an overlay of the sample TA-I-17-2a and non-stoichiometric TA-I-17-2b. In addition, the TA-I-17-2c product, along with both starting materials of DL-malic acid and isonicotinamide are shown in Table 3.2; the formation of a new complex when compared with the starting materials can be clearly observed.

Table 3.2: FT-IR assignment of TA-I-17-2 (a) (b) and (c) for DL-malic acid and isonicotinamide, and products of crystallisation (1:1) (1:2) and (2:1) in MeOH

Assignment is made using the literature[87,69]

Iso-nicotinamide (cm^{-1})	DL-Malic Acid (cm^{-1})	TA-I-17-2a (cm^{-1})	TA-I-17-2b (cm^{-1})	TA-I-17-2c (cm^{-1})	Assignment
	3445 s	3490		3490 s	_(OH) of CHOH
3370, 3186		3384, 3205	3389, 3295,3228	3384s, 3204	ú NH$_2$ ú NH$_2$
3076, 3064, 3053, 3041		3095		3091 w	ú CH , ú CH
	3030 s, br	292,628, 952,773	298,929, 282,839	2898 w	_(OH) of COOH hydrogen bond mode _s(CH$_2$_
	2911 sh				ú CH$_2$
	2624 m, br				Combinations H$_2$ bond mode, dimer
		2465	2407	2557 w	
			1958		
	1739 vvs, 1716 vs	1716, 1684	1685	1725 s	(C= O) of dimeric COOH out-of-phase
		1609	1611		
1667					ú CO
1624, 1596					δNH$_2$, ú ring +δCCH , ú ring

1552		1548	1554	1548	ύ ring
1496					δCCH +ύ ring
1410		1414	1411	1415	δCCH +ύ ring
	1442 s-m				_(C–O) Cu(OH) of COOH, (acid II)
	1410 s-m				υ(CH$_2$_scis)
1395					ύ CN + δCC , δCCH+δCCO
	1385 w				υ(CH) of CHOH
	1359 m.-w				δ(CH$_2$) SCIS, δ(CH$_2$)$_{wag}$
	1290 s, d		1292		υ(OH) C_(C–O) of COOH(acid III)
	1277 sh				υ(CH$_2$)twist,(OH), (C–O)
	1267 sh	1262		1268	δ(CH) of CHOD
1265					ū ring
1228		1221	1229	1221	δCCH (74)+ύ ring (14)
	1219 m				δ(CH$_2$)
	1185 s	1182	1169		δ(CH$_2$) twist, δ(CH$_2$)scis
1148					ring+CCH+CN+CC
1122					CCH+ ring
	1103 s	1107	1098	1104	(CH$_2$)$_{SCIS}$, ū(C-O),δ(OH)
1085			1060		δ CCH +ύ ring
1063					NH$_2$ rock +ύCN
	1033 w	1027	1026	1029	ύ(C–C), (CH)
969					CH
	968 m		962	965	(C–C), υ(C-O)tors (acid IV)
955		959			ū CH
	951m				δ(OD)+ υ(C-O)of COOD(acidIII)
	885m,	891	884	890	δ(C-O), (C-CH$_2$), (C-H)
875					ᵞCH
853		855		859	ᵞCH+ᵞ CC +ᵞCO
	825vvw				δ(C-O), (C-CH$_2$), (C-H)
	790 vw				δ(CH$_2$)
778					γring +γco
755					δ ring + ύcc + ύring
	750 vw				O-C=O def.coupled with OH
	724 vvw				Def
708					ring + CO
	667 m				υ(C–H), υ(C–CH$_2$),
669			695		ring+ring
629					δ CCO + ύ ring
542					NH$_2$ twist + ring + CC

S=strong, v=very, m=medium, w=week, sh=shoulder, as=anti,symmetric, sym,symmetric, i.p=in-plane

In order to achieve an experimental assignment of the molecular vibrations of racemic and enantiomeric forms of malic acids and isonicotinamide, and to explain the observed differences, the three different ratios have been examined and compared against the literature reviewed[88,80].
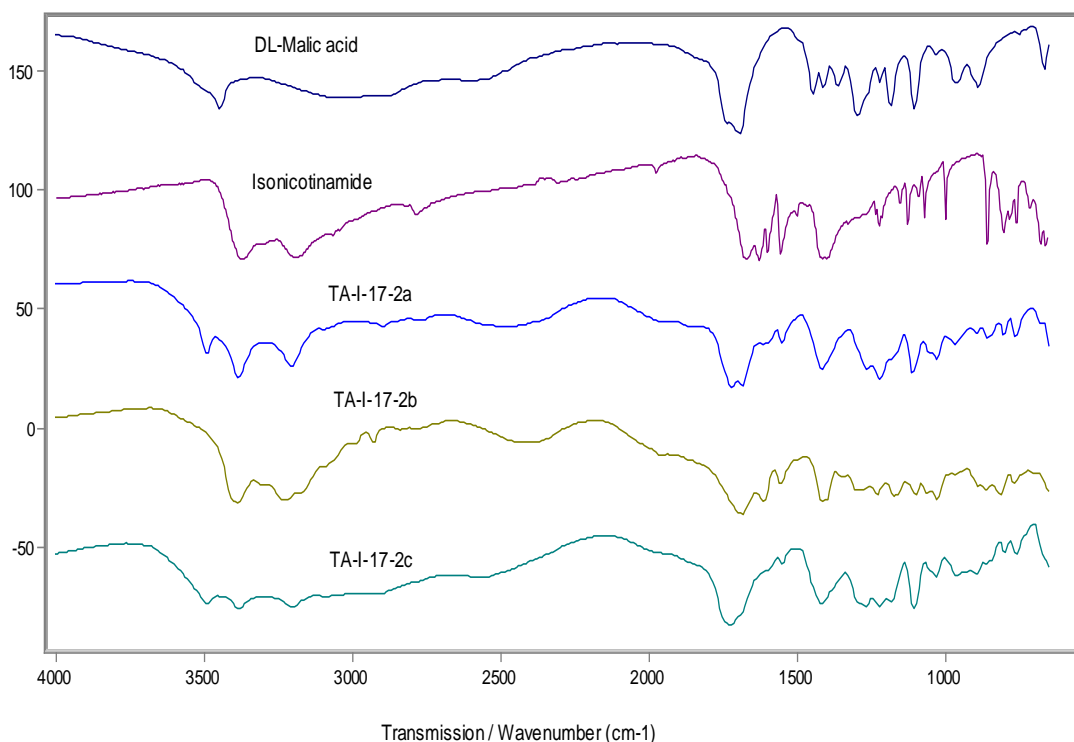
Figure 3.5: IR spectra of DL-malic acid, isonicotinamide and multicomponent in methanol solvent, in different ratios

Inspection of the solid state FT-IR data for the products obtained from crystallisation were compared to those obtained from the starting materials. The FT-IR clearly shows that the infrared trace of the 1:1 and 2:1 ratios are fairly similar; however, the trace for the 1:2 ratio clearly shows some differences (see Figure 3.5).

Baranska *et al.* studied, in detail, the vibrational spectra of both the racemic and enantiomeric forms of malic acid. With regards to measuring the

vibrational spectra of the racemic (DL), and the enantiomeric forms of malic acid in the range of 4000 to 450 cm^{-1}, this allowed for a comparative study of the current results to be made with the literature[89].

Baranska *et al.* reported significant distinctions in the spectra of the racemic and enantiomeric forms; but, it should be noted that no differences were observed between the spectra of L- and D-malic acid[89]. In the 3500 to 3000cm^{-1} region, a sharp band was observed at 3445cm^{-1}. According to Van Loock *et al.*[90], this suggests that the OH of the CHOH group in DL-malic acid might not be involved in hydrogen bonding. In comparison to the multicomponent complexes, a peak at 3445cm^{-1}, in the starting material, was shifted to 3490cm^{-1} for both of the multicomponent ratios of 1:1 and 2:1 (TA-I-17-2a and TA-I-17-2c). Whereas, for ratio 1:2 (TA-I-17-2b), it was absent (see Figure 3.6a).

The spectrum of isonicotinamide is dominated by two stretching modes at 3370 and 3186cm^{-1}, and they have been assigned to the hydrogen bonded NH$_2$ group. In contrast, the multicomponent compounds showed characteristic peaks at 3384 and 3205cm^{-1} in TA-I-17-2a (1:1), with peaks at 3389cm^{-1}, 3228cm^{-1} for TA-I-17-2b (1:2), and peaks at 3384 and 3204cm^{-1} for TA-I-17-2c, this could be assigned to NH$_2$.
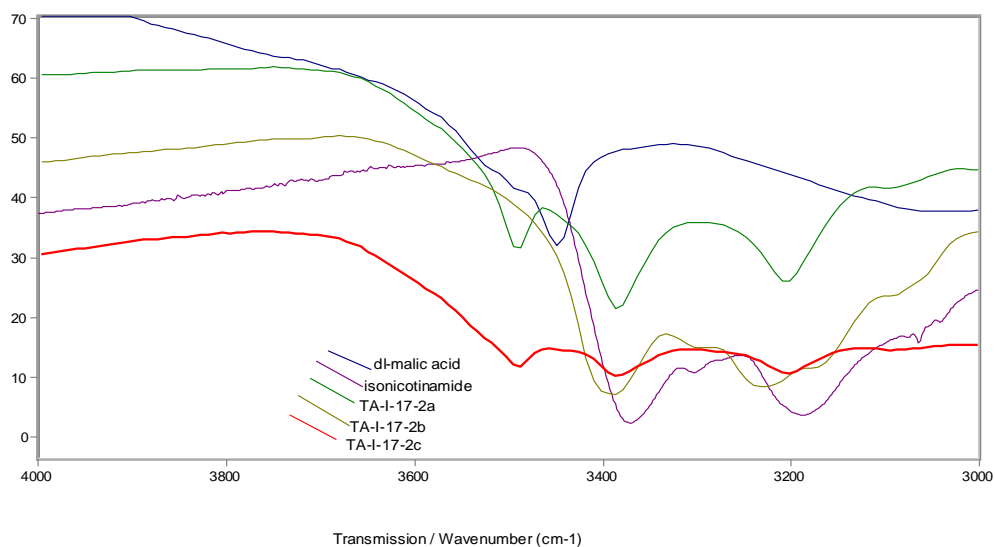
Figure: 3.6a: IR spectra of DL-malic acid, Isonicotinamide, and TA-I-17-2a, 2b and 2c in methanol for the region of 3500 to 3000cm^{-1}
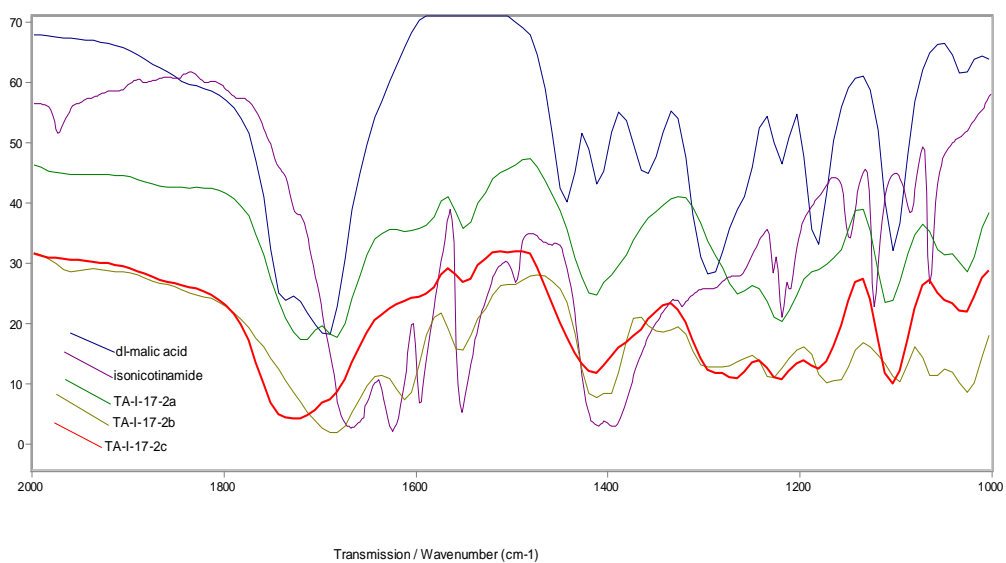
Figure 3.6b: IR spectra of DL-malic acid, isonicotinamide, and TA-I-17-2a, 2b and 2c in methanol for the region of 2000 to 1000 cm^{-1}

In the 3000 to 2000cm^{-1} region no significant peaks were observed. Whereas, for the vibrational spectra of the multicomponent system for the region of 2000 to 1000cm^{-1} (see Figure 3.6b), several important observations can be made. According to Baranska *et al.,* the IR spectrum of the racemate DL-malic acid has a multiplet structure with two prominent bands of C=O at

82

1739 and 1716cm^{-1}. In contrast, the multicomponent complex of TA-I-17-2a (1:1) had peaks at 1716cm^{-1}, and TA-I-17-2b (2:1) had a peak at 1725cm^{-1} – this can be assigned to the C=O group. For isonicotinamide, due to the H-bonding effect, the NH$_2$ bending mode is expected to be higher; in contrast, the C=O stretching mode is lower in frequency value than the corresponding values of the free molecule. Thus, no signs of these peaks were observed in the multicomponent systems.

3.2.1.2 Nicotinamide

The equimolar solution of DL-malic acid and nicotinamide were dissolved in methanol, acetone and acetonitrile for the different stoichiometric ratios, they were then left to re-crystallise at room temperature. Once crystallised, white crystalline solids were obtained which could then be analysed. The PXRD analysis of the starting materials for each of the samples of: TA-I-17-3a, TA-I-17 3b and TA-I-17-3c, were compared in order to demonstrate whether complexation had been successful.

The PXRD patterns clearly showed that the multicomponent system of TA-I-17-3a showed new peaks at 7.7, 17.9, 19.3, 21.40 and 21.7°, these peaks are not as a result of the starting material or the polymorphs of the starting material. Similarly, the non-stoichiometric product of TA-I-17-3b also showed peaks at 7.7, 17.8, 18.1, 18.4, 31.1 and 39.1°, along the 2θ scale; finally, TA-I-17-3c showed peaks at 7.8,14.9, 20.8, 27.9 and 33.7° (Figure 3.7).

The PXRD pattern of the 1:1 nicotinamide: DL-malic acid mole ratio mixture was somewhat the same as that obtained for the 1:2 mixture, although an

increase in intensity of the 15.3°, 2θ peak, was observed. In the pattern of the stoichiometric multicomponent system, TA-I-17-3a had scattering peaks which ranged between 30 and 37° (2θ) and were therefore effectively of negligible intensity.

The same analysis was performed for each of the different solvents (acetone and acetonitrile). Multicomponents TA-I-18-2a, 2b and 2c (all used acetone as the solvent) and TA-I-18-4a, 4b, 4c (used acetonitrile as the solvent) all showed new characteristic peaks for both the stoichiometric and non-stoichiometric products at 7.7 to 7.81°, along the 2θ scale – this is in agreement with the results of TA-I-17-3a, 3b, 3c (which used methanol as the solvent). An interesting observation is that the peak appearance decreases when the polarity of the solvent increases (thus, peak appearance for methanol < acetone < acetonitrile). The PXRD data clearly shows that the starting materials have been converted into the same new phase with all of the solvents. However, when methanol was used in the 1:2 and 1:1 ratio, the starting material nicotinamide was present, and in the 2:1 ratio DL-malic acid was present (see Figure 3.7 and 3.8).

DL-malic acid : nicotinamide

TA-1-18-2c 2:1 Me$_2$CO
TA-1-18-2b 1:2 Me$_2$CO
TA-1-18-2a 1:1 Me$_2$CO
TA-1-18-4c 2:1 MeCN
TA-1-18-4b 1:2 MeCN
TA-1-18-4a 1:1 MeCN
TA-1-17-3c 2:1 MeOH
TA-1-17-3b 1:2 MeOH
TA-1-17-3a 1:1 MeOH

DL-malic acid (DLMALC11

Nicotinamide (NICOAM01)

Single Crystal (tai_17_3b_t)
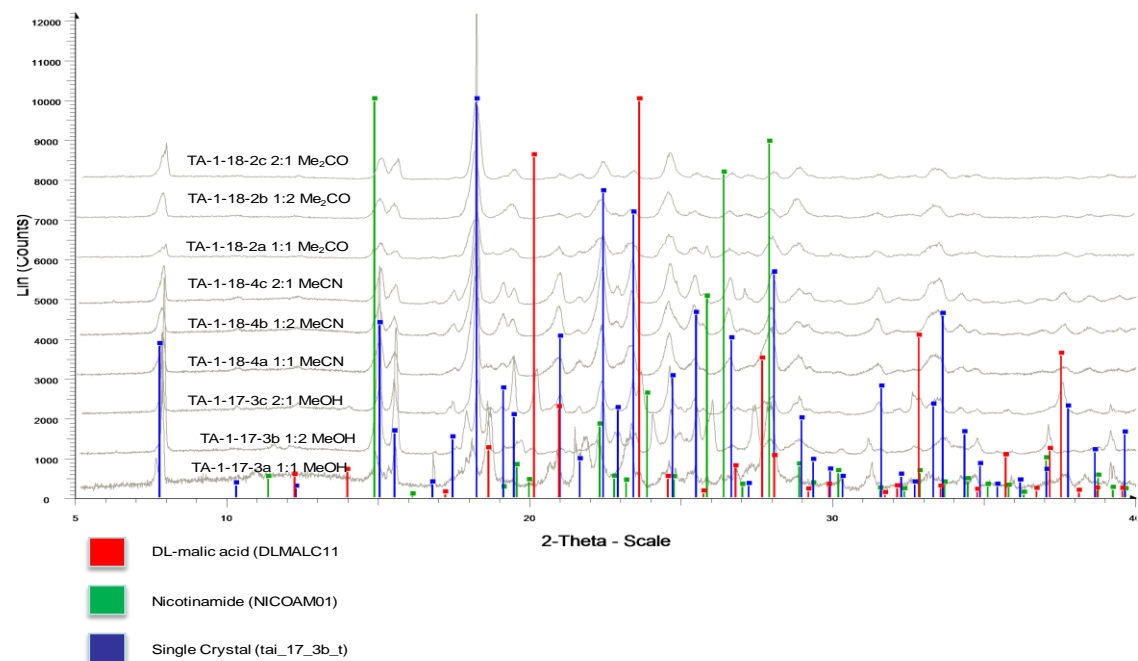
Figure 3.7: X-ray powder diffraction patterns of nicotinamide and DL-malic acid and products of crystallisation

Graphical representation of crystalline phases identified from co-crystallis
DL-malic acid : nicotinamide
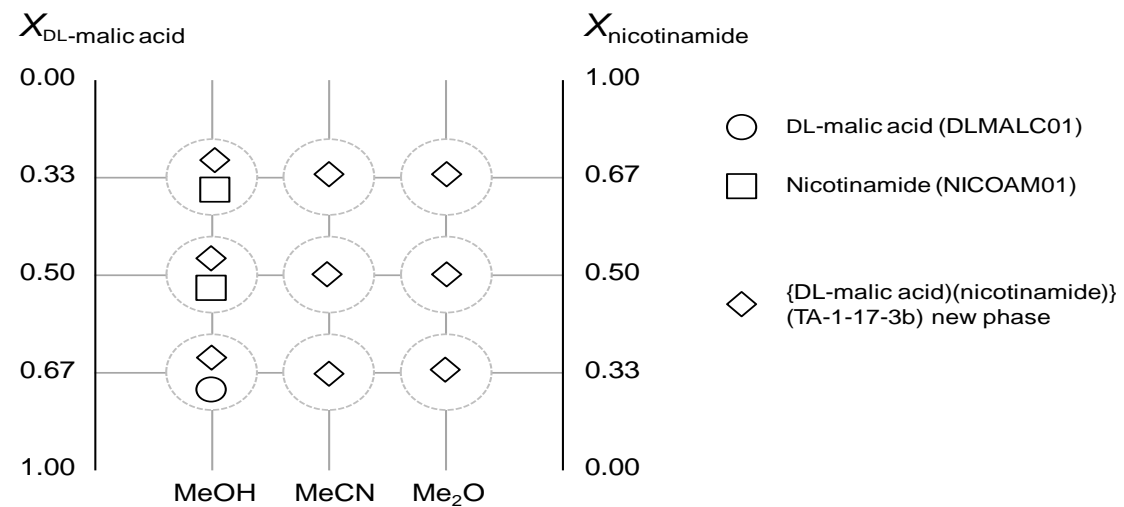
Figure 3.8: Representation of crystalline phases identified from co-crystallisations of DL-malic acid: nicotinamide

Table 3.3: FT-IR assignment of TA-I-17-3(a) (b) and (c) for DL-malic acid and nicotinamide and products of crystallisation (1:1) (1:2) and (2:1) in MeOH

Nic-otinamide (cm⁻¹)	DL-Malic Acid (cm⁻¹)	TA-I-17-3a (cm⁻¹)	TA-I-17-3b (cm⁻¹)	TA-I-17-3c (cm⁻¹)	Assignment
	3445 s	3474,3405	3475	3474	_(OH) of CHOH
3366, 3167		3214,	3367	3344, 3218	ú NH$_2$, ú NH$_2$
2782, 2316		2765, 2491	2779		ú CH (99), ú CH
	3030 s, br	3076	3170		_(OH) of COOH hydrogen bond mode _s(CH$_2$)
	2911 sh	2931		2976, 2932	ú CH$_2$
		2851		2853	
	2624 m, br				Combinations H$_2$ bond mode,dimer
	1739 vvs, 1716 vvs, 1690 vvs	1717		1719	(C= O) of dimeric COOH out-of-phase
		1690			
1680		1670		1672	ú CO
1483, 1618		1614,1575,1424	1600,1616	1615, 1578	CN $_{amide}$ Stretch
1341					CH ip bend
1410				1428	δCCH +ú ring
	1442 s-m		1480		_(C–O) Cυ(OH) of COOH, (acid II)
	1410 s-m	1401		1400	υ(CH$_2$_scis
1395					ú CN + δCC , δCCH+δCCO
	1385 w		1398		υ(CH) of CHOH
	1359 m.-w	1368, 1302	1344	1367, 1303	δ(CH$_2$) $_{SCIS}$, δ(CH$_2$)$_{wag}$
	1290 s, d		1299		υ(OH) C_(C–O) of COOH(acid III)
	1277 sh				υ(CH$_2$)twist,(OH), (C–O)
	1267 sh				δ(CH) of CHOD
1230		1239	1241	1247	CC stretch
1200		1201		1201	CH ip bend
	1219 m	1222	1224	1221	δ(CH$_2$)
	1185 s	1192	1198	1191	δ(CH$_2$) twist, δ(CH$_2$)scis
1154		1150			CC stretch
1122		1110	1110	1112	CH ip bend
	1103 s				(CH$_2$)$_{SCIS}$, ū(C-O),δ(OH)
1027			1029		NH$_2$ rock
1063		1044		1043	NH$_2$ rock +úCN
	1033 w			1005	ú(C–C), (CH)
972		994			CH op bend
936			939		CH op bend
	968 m			970	(C–C), υ(C-O)tors (acid IV)
	951m	942			δ(OD)+υ(C-O)of COOD(acidIII)

		907	902	901	
	885m,	886			δ(C-O), (C-CH$_2$), (C-H)
827			830	833	CH op bend
853					Vvw
	825vvw	834			δ(C-O), (C-CH2), (C-H)
	790 vw	795	790	794	δ(CH$_2$)
777					γring + ring def
	750 vw	750		751	O-C=O def.coupled with OH
	724 vvw			713	Def
702			705	703	Ring op. Bend γ ring
	667 m	643			υ(C–H), υ(C–CH$_2$),

The FT-IR spectra of nicotinamide and *DL*-malic acid, as well as their multicomponent products, showed evidence of a number of differences in both the fingerprint region and the high frequency region. To identify the formation of successful complexes, classification of NH$_2$, C-O and C-N amide stretching and ∂ NH$_2$ vibrations are important as they present useful information on the intermolecular H-bonding interactions within the multicomponent system as well as for any nicotinamide molecules.

The FT-IR spectra also showed that absorption bands (of around 1650cm^{-1}) were observed in the carbonyl, CN amide stretch for the multicomponent system; thus, TA-I-18-4a consisted of a broadened and overlapping envelope that contains the out-of-plane deformation modes that can imitate the starting materials[80]. However, careful examination of the outline of the band system of the stoichiometric and non-stoichiometric (TA-I-18-4b, TA-I-18-4c) multicomponent systems in this region (700 to 1400cm $^{-1}$) identified that any contributions of the scarcely shifted bands are generally due to the initial starting material. As such, a lack of shift in the vibrational frequencies indicates that the patterns of molecular motion of the supramolecular synthon

are not significantly different and are therefore relative to those of the initial reactants. This point indicates that both homosupramolecular synthons (i.e., nicotinamide and malic acid) are not strongly changed upon formation of the heterosupramolecular synthon of the multicomponent system.

3.2.2 Crystallisation Studies of L-Malic Acid with Pyridinecarboxamides

L-malic acid was crystallised together with isonicotinamide. The crystallisation was performed using different solvents (methanol, acetone and acetonitrile) as well as the different starting molar ratios of 1:1, 1:2 and 2:1. The solid products were formed once the solutions containing the individual components were mixed; these products were isolated as white crystalline solids.

The overlaid PXRD pattern of the starting materials were compared against the sample TA-I-22-2a, 2b and 2c in order to draw initial conclusions as to whether complexation had been successful. The PXRD patterns obtained for L-malic acid and isonicotinamide, and their multicomponents are shown in Table (Figure 3.9). Interestingly, TA-I-22-2a and 2b showed new characteristic peaks at 15.1, 16.8, 23.8, 27.9, 28.4, 32.8, 33.9 and 37.6°, none of these peaks resembled the L-malic acid, isonicotinamide or its polymorphic forms; thus, verifying the preposition that a new phase was present.

In addition, an excess of L-malic acid in TA-I-22-2c also showed new characteristic peaks at 11.9, 16.9, 23.9, 35.0 and 37.1°; thus, indicating that they have no correspondence in the diffraction pattern, as its starting material

and its polymorphic forms represent a new phase once the methanol was used as a solvent.

Further investigation was then conducted using acetone and acetonitrile, as two other solvents. Although both starting materials exhibited a strong scattering peak at around 19.4 and 24.4°, along the 2θ scale; the L-malic acid also showed evidence of characteristic scattering peaks at 15.3 and 20.9° (2θ scale), and isonicotinamide showed a characteristic scattering peak of 25.9° along the 2θ scale. The 1:1 molar ratio of the starting materials which used acetone as a solvent gave rise to multicomponent system TA-I-22-3a; this was nearly same as when methanol was used as the solvent. The PXRD pattern of TA-I-22-3a and 3b revealed different scattering peak at 15.2, 16.8, 28.4 and 32.1°; thus, illustrating that they produced the same phase.

The XRD powder pattern for each of the isolated products that were prepared using acetonitrile as the solvent also shows evidence of a new phase by the appearance of a few new peaks that were not present in the multicomponent system – they were formed by the use of methanol and acetone. The 1:1 molar ratio product, TA-I-22-4a showed very prominent characteristic peaks at 6.6, 9.2, 10.5, 12.4, 13.1, 13.6, 15.4, 17.2, 18.6 and 21.2°, this strongly suggests that a new phase was formed which is very different from its starting materials and the polymorphic forms associated with it (Figure 3.9). On the other hand, the non-stoichiometric product for the 1:2 molar ratio, TA-I-22-4b, shows unique peaks at 11.7, 16.7, 22.9, 29.4, 30.4 and 31.4°. The

90

2:1 molar ratio also presents peaks on the 2θ scale of: 15.1, 16.7, 17.8, 23.8, 24.5, 28.3 and 37.5°. This suggests that all three ratios in acetonitrile produced a new phase.

L-malic acid : isonicotinamide

Figure 3.9: X-ray powder diffraction patterns of isonicotinamide and L-malic acid and products of crystallisation with a range of solvents

Graphical representation of crystalline phases identified from co-crystallisations of L-malic acid : isonicotinamide

Figure 3.10: Representation of crystalline phases identified from co-crystallisations of L-malic acid: isonicotinamide formatting

Further investigation using FT-IR analysis was carried on the samples above in order to confirm the presence of all of the important functional groups and to ensure that the differences in the sample occurred as a result of the starting material, in order to truly indicate whether complexation/hydrogen bond formation had occurred (see Table 3.4, below).

Table 3.4: FT-IR assignment of TA-I-22-2(a) (b) and (c) for L-malic acid and isonicotinamide and products of crystallisation for (1:1) (1:2) and (2:1) in MeOH

Iso nicotinamide FT-IR (cm^{-1})	L-Malic Acid FT-IR (cm^{-1})	TA-I-22-2a FT-IR (cm^{-1})	TA-I-22-2b FT-IR (cm^{-1})	TA-I-22-2c FT-IR (cm^{-1})	Assignment
	3537 vs, br	3501			υ(OH) of CHOH
3370, 3186			3168		ύ NH2 (100), ύ NH2 (100)
3076, 3064, 3053, 3041		3099			ύ CH (99), ύ CH (100)
	3393 sh	3347, 3214	3380		_(OH) of COOH hydrogen bond mode _s(CH2_
		2926	2978, 1917		
		2849	2784		
	2670 sh	2579			ύ (OD) of CHOD
			1958		
	1721 vs	1704			(C= O) of dimeric COOH out-of-phase
1667		1666	1635	1617	ύ CO
1624, 1596					δNH2 , ύ ring +δCCH , ύ ring
1552		1553	1552, 1504	1505	ύ ring
1496		1428			δCCH +ύ ring
1410		1416		1414	δCCH +ύ ring
	1413 s-m				u(CH)$_2$_scis
1395		1351,1332	1392, 1321	1354, 1333	ύ CN + δCC , δCCH+δCCO
	1288 m				(OD)+(C-O)of COOD
1265		1250	1242		ū ring
1228		1232		1231	δCCH (74)+ύ ring (14)

94

	1224 m	1218			δ(CH$_2$)
	1186 m				δ(CH2) twist, δ(CH2)scis
1148		1154	1156		ring+CCH+CN+CC
1122			1122		CCH+ ring
	1107 s		1094	1104	(CH2)$_{SCIS}$, ū(C-O),δ(OH)
1085					δ CCH +ú ring
1063		1063	1060		NH$_2$ rock +úCN
	1036 w				ú(C–C), (CH)
		1019	1026	1019, 1027	
994		980		981	Ring
969		964	951	944	CH
955		939			ū CH
		907		905	
	899 vw				δ(C-O), (C-CH$_2$), (C-H)
		884		884	
875					ᵧCH
853					ᵧCH+ᵧ CC +ᵧCO
		861	860	861, 824	
	757 vw			795	δ(CH$_2$)
778				776	γring +γco
755			759		δ ring (30)+ úcc(17)+ úring
708					ring + CO
	660 m				υ(C–H), υ(C–CH2),
669			682		ring+ring
629					δ CCO + ú ring
542				563	NH2 twist + ring + CC

The infrared absorption spectra of isonicotinamide, L-malic acid, and their 1:1, 1:2 and 2:1 molar ratios, for the multicomponent products of TA-I-22-2a, 2b and 2c, were found to exhibit a number of differences in both the fingerprint region as well as the high frequency region (see Table 3.4). In order to appraise the trends, in the spectra of multicomponents more effectively, the origins of the major absorbance peaks of starting materials needed to be compared with the stoichiometric and non-stoichiometric products. The results shown above clearly show differences in the vibrational

modes observed in TA-I-22-2a, 2b, 2c, these could be as a result of structural differences and the binding fashion. The vibrations spectra of starting materials and products in the region of 3500 to $1300cm^{-1}$ is interesting, these regions are characteristic of -OH vibrations, --CH and --C vibrations, as well as symmetric and asymmetric stretching vibrations of carboxylic groups forming dimeric rings as the CH deformation bands and coupled vibrations of the COOH group. The region below 1300 to $900cm^{-1}$ is less characteristic because a number of overlapping bands, such as the -CO and -CC bands and the CH and OH for the deformation vibrations.

The IR spectrum in the region of 3500 to $3000cm^{-1}$ for L-malic acid shows vibration modes of OH of the CHOH bond, but only TA-I-22-2a shows this kind of bonding at $3501cm^{-1}$. Similarly, N stretching wavenumbers were contributed from isonicotinamide in this region; for example, amino hydrogens are involved in H-bonding interactions[91]. In solid isonicotinamides, due to the H-bonding effect, the N bending mode is expected to be higher; whereas, the multicomponents of TAI-22-2b and TA-I-22-2c showed stretching modes which were lower in value than the corresponding values of the starting materials.

L-malic acid showed a well developed band that appeared at $2670cm^{-1}$, this may have been as a result of the shift in the broad band with the maximum at $3537cm^{-1}$, which was assigned to υ(OH) of CHOH. Similarly, the multicomponent system of TA-I-22-2a showed bands at 2926, 2849 and $2579cm^{-1}$ and TA-I-22-2b showed just two bands which were observed at 2978 and $2784cm^{-1}$. These bands may be ascribed only to the υ(OH)

vibration of the CHOH moiety. In the region of 2000 to 1000cm^{-1}, L-malic

acid contributes only one -CO band at 1721cm^{-1}, whereas the IR spectrum of

the TA-I-22-2a was at 1706 cm^{-1}, and TA-I-22-2b and TA-I-22-2c had two

prominent bands of 1553 to 1540cm^{-1} (see Table 3.3).

Similar investigation was carried out for the multicomponent system prepared

using acetone as a solvent in order to determine whether the solvent

participate in the bonding pattern or whether it was just a suitable medium for

the preparation of multicomponents.

Table 3.5: FT-IR assignment of TA-I-23-3 (a) (b) and (c) for L-malic acid and isonicotinamide, and products of crystallisation for (1:1) (1:2) and (2:1) in Me$_2$CO

Iso-nicotinamide	L-Malic Acid	TA-I-23-3a	TA-I-23-3b	TA-I-23-3c	Assignment
FT-IR (cm^{-1})	FT-IR (cm^{-1})	FT-IR (cm^{-1})	FT-IR (cm^{-1})	FT-IR (cm^{-1})	
	3537 vs, br	3493	3492		_(OH) of CHOH
3370, 3186		3167	3167	3158	ú NH$_2$ (100), ú NH$_2$ (100)
3076, 3064, 3053, 3041				3098	ú CH (99), ú CH (100)
	3393 sh	3381	3381	3323	_(OH) of COOH hydrogen bond mode _s(CH$_2$)
		2783	2783		
		2483	2483		
	2670 sh				ú (OD) of CHOD
		1956	1956	1958	
	1721 vs			1725	(C= O) of dimeric COOH out-of-phase
1667		1695	1694		ú CO
1624, 1596		1635	1685	1614, 1600	δNH2 , ú ring +δCCH , ú ring
1552		1548	1547	1503	ú ring
1496					δCCH +ú ring

1410					δCCH +ύ ring
	1413 s-m			1413	υ(CH)₂_scis
1395		1394			ύ CN + δCC , δCCH+δCCO
		1322	1323	1333	
	1288 m				(OD)+(C-O)of COOD
1265		1243	1242	1238	ū ring
1228					δCCH ύ ring
	1224 m				δ(CH₂)
	1186 m	1163	1163	1187	δ(CH₂) twist, δ(CH₂)scis
1148					ring+CCH+CN+CC
1122		1124	1124		CCH+ ring
	1107 s			1100	(CH2)scis, ū(C-O),δ(OH)
1085		1091	1091		δ CCH +ύ ring
1063		1058	1058		NH2 rock +ύCN
	1036 w	1034		1028	ύ(C–C), (CH)
994		995			Ring
969					CH
955			945	945	ū CH
	899 vw				δ(C-O), (C-CH₂), (C-H)
875				885	ᵞCH
853		859	859	821	ᵞCH+ᵞ CC +ᵞCO
	757 vw				δ(CH₂)
778					γring +γco
755		753	753	756	δ ring (30)+ ύcc(17)+ ύring
708				706	ring + CO
	660 m	676	686		υ(C–H), υ(C–CH2),
669					ring+ring
629					δ CCO + ύ ring
542					NH₂ twist + ring + CC

98

To identify the formation of successful complexes, classification of NH_2, C-O and C-N amide stretching and ∂NH_2 vibrations were deemed to be very important as they can reveal useful information about the intermolecular H-bonding interactions in a multicomponent system, as well as for the L-malic acid and isonicotinamide molecules.

Similarly, in the case of L-malic acid, the υ(C=O) doublet band indicates the presence of two kinds of dimeric carboxyl rings which are responsible for shape and intensity in the IR spectrum. According to Wolfs and Desseyn's formation of υ(C-O) ∂(OH), band combined vibration of the COOH group is an important aspect[70,89].

The FT-IR spectra (See Table 3.5) also showed that absorption bands (of around 1650cm^{-1}) were observed in the carbonyl, CN amide for the multicomponent system of TA-I-23-3a, which consisted of a broadened and overlapped envelope that contained the out-of-plane deformation mode which were imitative from the starting materials[89]. The lack of movement within the vibrational frequencies in TA-I-23-3a, 3b and 3c indicates that the patterns of molecular motion of the supramolecular synthon are not significantly different or relative to those of the initial reactants.

In order of establish whether L-malic acid is present in the product (by implication the product contains a co-crystal phase), the ^{1}HNMR experiment was undertaken. From the integral values of different peak intensities for protons in the different environments on L-malic acid and isonicotinamide that were obtained from the NMR spectra, it is clearly evident that this new

material contains the starting components in the 1:1, 1:2 and 2:1 stoichiometric ratio. Thus, indicating that both the DL-malic acid and isonicotinamide are present in the co-crystal.

The structures used in the assignments of the ^{1}HNMR spectra are detailed below in Figures 3.11a and 3.11b.

a)   b)
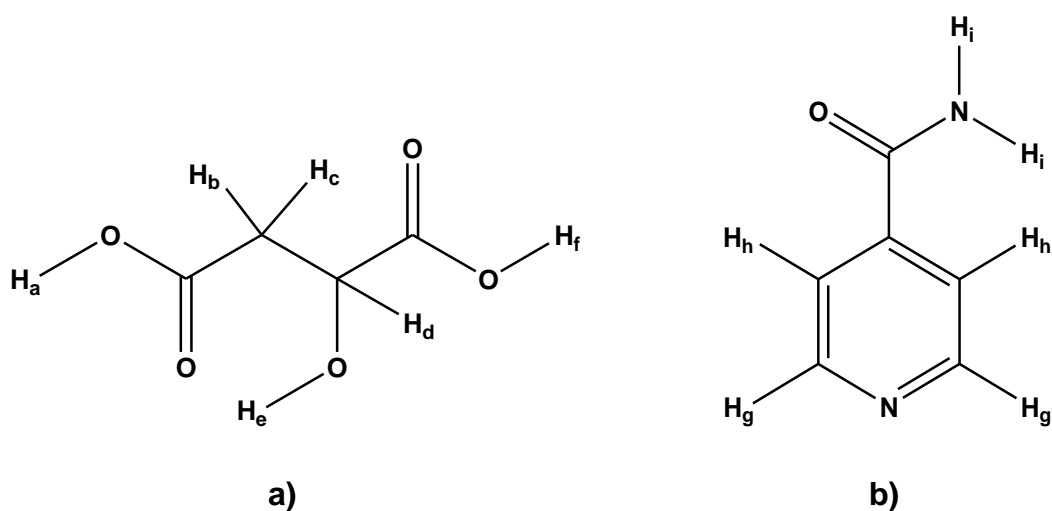
Figure 3.11: Structures used in the assignments of the ^{1}HNMR spectra: a) L-malic acid; and, b) isonicotinamide

Table 3.6: ^{1}HNMR spectral data of sample and its starting materials i.e. L-malic acid and isonicotinamide

Sample TA-I-22-4b			L-malic acid			Isonicotinamide		
Shift (ppm)	Multiplicity, Integration	Assignment	Shift (ppm)	Multiplicity, Integration	Assignment	Shift (ppm)	Multiplicity, Integration	Assignment
2.08	S	Acetone-d_6	2.10	bs, 1H	H_e	--	--	--
2.60	dd, 0.5H	H_b	2.53	dd, 1H	H_b, H_c	--	--	--
2.81	dd, 0.5H	H_c	2.78	dd, 1H		--	--	--
4.30	S	water	--	--	--	--	--	--
4.51	dd, 0.5H	H_d	4.42	dd, 1H	H_d	--	--	--
--	--	--	--	--	--	6.05	s, 2H	NH_2
7.77	d, 2H	H_h	--	--	--	7.96	d, 2H	H_h
8.70	d, 2H	H_g	--	--	--	9.06	d, 2H	H_g
			11.00	bs, 2H	H_a, H_f			

The ^{1}HNMR spectrum of isonicotinamide, exhibited two doublets which are a mirror image of each other for aromatic protons in the range of 7.96 to 9.06ppm. The structure of isonicotinamide was confirmed in the ^{1}HNMR spectrum of sample TA-I-22-4b, where a doublet was observed in the deshielded region of 8.70ppm for two H_g protons corresponding to CH protons in the neighbourhood of the heteroatom, nitrogen in this case. The other set of two aromatic protons (H_h) resonated in the region of 7.77ppm as a doublet (see Table 3.6).

The structure of malic acid was also confirmed in the ^{1}H NMR spectrum of sample TA-I-22-4b, which showed a doublet of doublets in the region 2.60 and 2.81ppm for each of the two diastereotopic protons H_b and H_c. The methine proton of the chiral centre appeared as a doublet of doublets in the region of 4.50ppm, it also appeared deshielded due to the fact that the proton was in the neighbourhood of a highly electronegative oxygen atom. All the signals of the protons of malic acid appeared deshielded with a slight change in the chemical shift values, as is evident by the comparison of the chemical shift values of the neat malic acid and that of sample TA-I-17-2b, as shown in (Table 3.1). This may well be the result of complexation.

The ^{1}HNMR spectrum obtained for sample TA-I-22-4b shows similarities to the isonicotinamide between 7.77 and 9.10ppm, with similarities to the L-malic acid, ranging between 2.60 and 4.51ppm; thus, indicating that a multicomponent system can be formed successfully from malic acid and isonicotinamide.

One important observation to share is that the integration values of malic acid are half those of the integration values of isonicotinamide. The protons H_b, H_c and H_d of malic acid have integration values of 0.52, 0.52 and 0.54 for each of these protons, respectively. This clearly indicates that one molecule of malic acid might be coordinated with two molecules of isonicotinamide as shown below in terms of the expected structure of sample TA-I-22-4b in Figure 3.12.

The ^{1}HNMR spectrum obtained for sample TA-I-22-4a also shows similarities to the isonicotinamide, between 7.78 and 9.12ppm, with similarities to the L-malic acid of between 2.61 and 4.52ppm; thus indicating that a multicomponent system can be formed successfully from malic acid and isonicotinamide.

The ^{1}HNMR spectrum obtained for sample TA-I-22-3c shows similarities to the isonicotinamide between 7.78 and 8.67ppm, as well as similarities to the L-malic acid of between 2.61 and 4.51ppm; thus indicating that a multicomponent system can be formed successfully from malic acid and isonicotinamide.

Most importantly, the integration value of signals of malic acid and isonicotinamide clearly indicate that one molecule of malic acid might be best coordinated with two molecules of isonicotinamide, as shown below by the expected structure of the sample (see Figure 3.12).
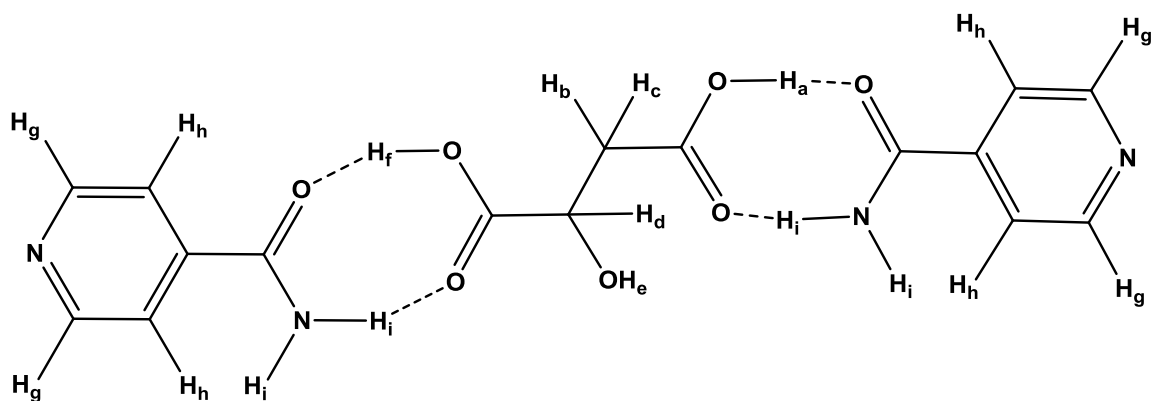
Figure 3.12: Expected structure of SAMPLE of one molecule of malic acid with two molecules of isonicotinamide

3.2.2.1 Nicotinamide

L-Malic acid was crystallised together with nicotinamide in various solvents. The crystallisation was performed using the same method used to crystallise the L-malic acid with isonicotinamide. Thus, PXRD, NMR and FT-IR were used to characterise whether a new phase had formed.

The spectral PXRD data, shown below (see Figure 3.13) clearly shows that samples, TA-I 23-3a, 3b and, 3c, do not represent any of the starting materials of L-malic acid or nicotinamide, or its polymorphic forms. Sample TA-I-23-3a illustrated a presence of new peaks at 14.4, 18.9 and 25.9°, along the 2θ scale. This sample also had fewer amorphous regions than the starting materials; thus indicating a more defined and stable structure.

Similarly, the non-stoichiometric molar ratio product sample of TA-I-23-3b showed characteristic peaks at 8.6, 14.6, 18.5, 19.5, 21.5, 24.1, 29.1, 32.6, 37.3 and 38.1°. In addition, TA-I-23-3c also showed some new peaks at 21.49, 22.97, 24.01, 28.2 and 35.28°, along the 2θ scale. Nonetheless, these

results show that some form of new phase had been formed in both the stoichiometric and non-stoichiometric samples. The different stoichiometries in methanol all produced a new phase, but in the 1:1 and 2:1 ratios an additional new phase was also present (see Figure 3.13 and 3.14).

Further investigation was conducted using the same starting materials with different solvents for the preparation of the co-crystal in order to study the effect of the solvent in the co-crystallisation and bonding pattern. The PXRD pattern shows a new phase for each of the products; to illustrate, the 1:1 (TA-I-24-1a, 1b and 1c) ratio shows some new unique peaks, but these new peaks were not present in either the starting material or its polymorphic form. The different stoichiometries in acetonitrile all produced the same new phases. (see Figure 3.13 and 3.14).

The 1:1 ratio (TA-I-23-2a) in acetone shows unique peaks at 7.5, 17.6, 18.3, 21.3, 26.7, 28.0, 28.9, 31.0, 37.0, 37.3, 38.3 and 39.3°. Similarly, the ratio 2:1 (TA-I-23-2c) shows smaller peaks that do not correspond with the starting materials at 21.3, 28.0 and 28.9° along the 2θ scale. The different stoichiometric products formed using acetone all produced a new phase, but in 1:1 and 1:2 ratios an additional new phase was also exist. Thus, it is concluded that complexation occurred within the system bonded network (see Figure 3.13 and 3.14).

However, it can also be concluded that new phases were formed through the use of all three solvents (acetone, acetonitrile and methanol). This conclusion was further supported by the FT-IR data obtained, which clearly shows

similarities and dissimilarities between both the starting materials and the multicomponent products.

L-malic acid : nicotinamide
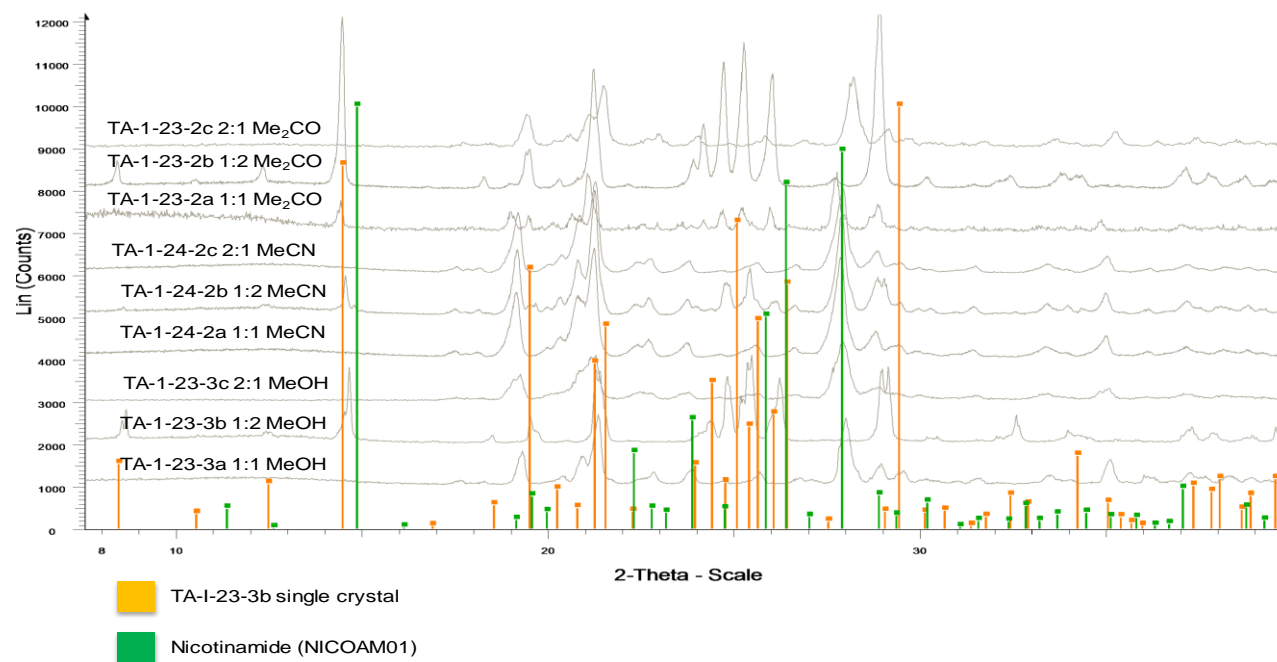
Figure 3.13: X-ray powder diffraction patterns of nicotinamide and L-malic acid, and products of crystallisation with a range of solvents

Graphical representation of crystalline phases identified from L-malic acid : nicotinamide
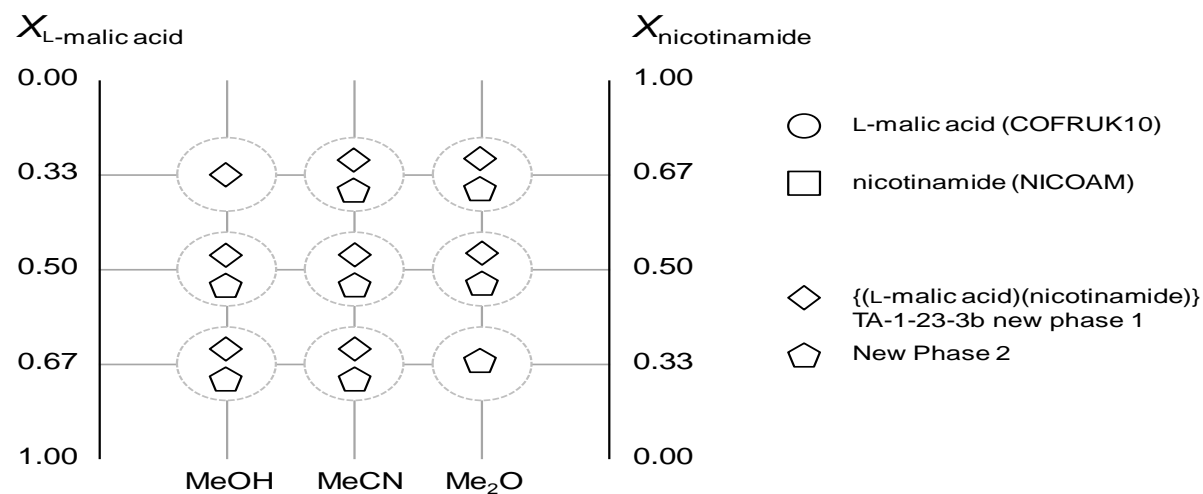
Figure 3.14: Representation of crystalline phases identified from co-crystallisations of L-malic acid

The FT-IR spectra of enantiomeric (L) forms of malic acid, nicotinamide and their multicomponent systems were accepted as having significant differences in the spectra between them.

3.3   X-Ray Structure Analysis

3.3.1   Single Crystal Analysis of DL-Malic Acid and Nicotinamide TA-1-17-3b

The single crystal structure of nicotinamide and DL-malic acid was obtained from a colourless block in the orthorhombic space group of Pca2$_1$. The asymmetric unit of the crystal confirms the presence of a stoichiometric complex (1:1) co-crystal, where two molecules of malic acid form hydrogen bonding with two molecules of nicotinamide. The asymmetric unit essentially describes a hydrogen bonded dimer; this is a formed pseudosymmetric centred dimer that is formed by intermolecular hydrogen bonding between carboxylate oxygen and the secondary alcohol of malic acid. This is augmented by the hydrogen bonding to the isonicotinamide; the nicotinamide essentially bridges the two malic acids of the dimer which forms a carboxylate COH to pyridine nitrogen and amide nitrogen to the alcohol OH of the second malic acid (see Figure 3.15).

The dimer assembly forms a type of planar unit within the crystal packing, the remaining carboxylate acids of the malic acid molecules lie above and below the plane linking the two further nicotinamide units through the acid COH group to the amide carboxyl groups. This further propagates the structure parallel to the a-axis. These linked dimers are shown on the b-axis in Figure 3.16; however, when viewed down the c-axis, the dimers are a complex

network of interconnected dimer units stabilised by aromatic π-π interactions between nicotinamide. This is in addition to the hydrogen bonded systems.
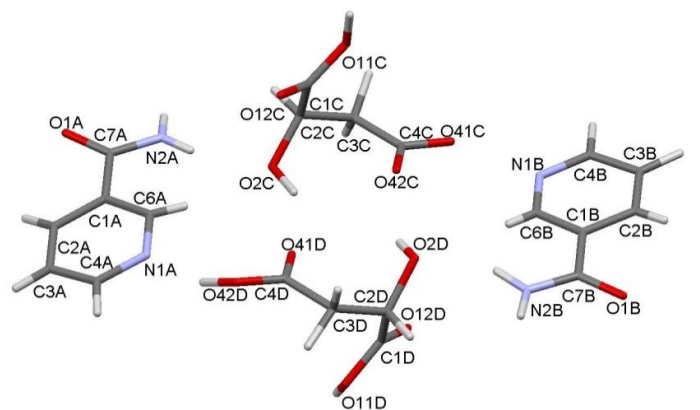
a)
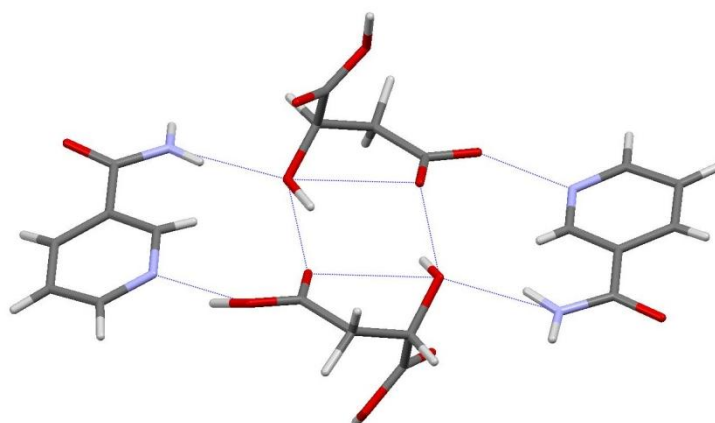
b)

Figure 3.15: The asymmetric unit of the DL-malic acid: nicotinamide co-crystal showing: a) the numbering scheme adopted; and, b) the hydrogen bonding of the pseudo-centrosymmetric dimer
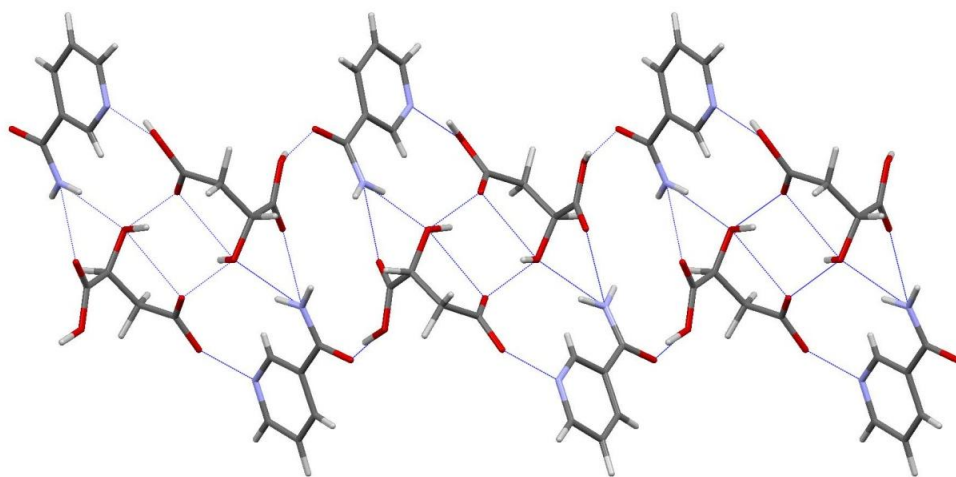
a)
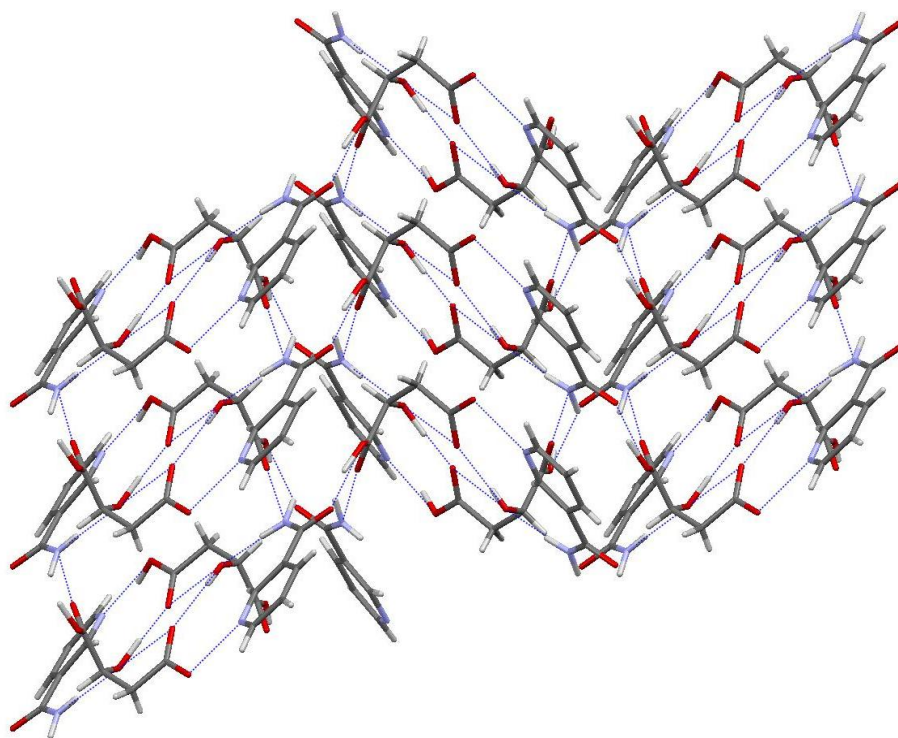
b)

Figure 3.16: The crystal packing of DL-malic acid: nicotinamide co-crystal showing: a) linked dimer units viewed down the b-axis of the unit cell; and, b) the crystal packing network viewed down the c-axis of the unit cell

3.3.2 Single Crystal Analysis of L-Malic Acid and Nicotinamide (TA-1-23-3b)

The 1:2 co-crystal is crystallised in the P1 space group with two molecules of nicotinamide and a single molecule of the S-enantiomer of malic acid in the asymmetric unit. In this case, the generation of a non-centrosymmetric crystal lattice is consistent with the inclusion of the single malic acid enantiomer in the solid state structure.

Again, the crystal packing in this system is the linkage of π-π stacked assemblies of nicotinamide through H-bonds to each acid unit of malic acid. In this case, however, no significant H-bonding is observed in the malic acid "bridges"; thus, the structural units repeat solely through translation of the unit cell (see Figure 3.17).
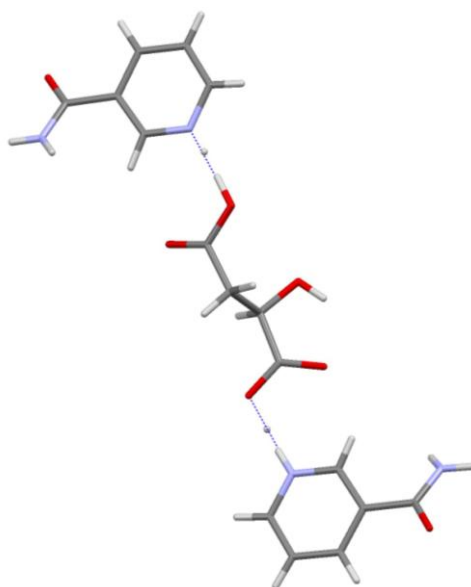
a)
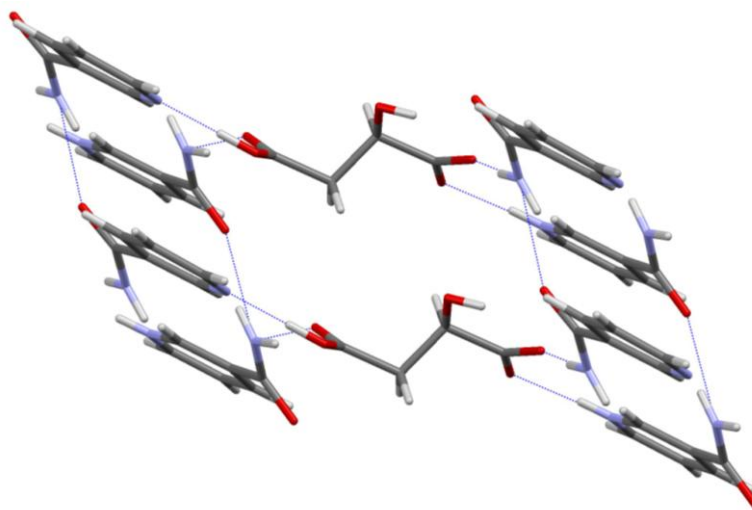
b)

Figure 3.17: The asymmetric unit of the L-malic acid: nicotinamide co-crystal showing: a) the asymmetric unit; and, b) the crystal packing

3.3   Discussion

The initial results for these systems show that while the resulting co-crystal systems showed interesting and predictable hydrogen bonding patterns, the transmission of chiral information into chiral solid state was surprising and the resulting crystal structures can be described as being relatively unusual.

It is apparent that recognition between enantiomeric molecular forms plays a significant role in the assembly of these systems. This mechanism can be considered independently from the H-bonding networks that support the heteromolecular interactions (e.g. acid-amide recognition). Discrimination and control of such interactions could therefore play a role in transmitting chiral molecular information into solid state multicomponent assemblies.

In both cases, the use of nicotinamide and isonicotinamide with DL-malic acid, usually carboxylic acid, to amide hydrogen bonding exists and is further stabilised by additional hydrogen bonding from the amide-amide and carboxylic-carboxylic acid. The analysis and data interpretation has shown that the newly formed multicomponents differed from their starting materials, specifically with regards to the single crystal analysis which revealed that supramolecular synthon motifs were formed.

The study revealed that similar supramolecular synthons were observed by other complexes of carboxylic acid with isonicotinamide and nicotinamide. Although single crystal structure analysis was not performed – this could have provided confirmation of explicit supramolecular synthons within the system; nonetheless, the PXRD provided a good overview of the amorphous and crystalline phases. Use of the different solvents (acetone, acetonitrile and methanol) indicated slight changes in the PXRD patterns – this can be explained further by the preposition given by Seaton *et al.*[18] with regards to considering the solvent, the solute interactions and the weaker discrete acid-amide interactions which suggest that it could be a good source for solvent selectivity. Consequently, a more detailed study related to solubility would help to identify explicit solvents and their solute interactions could be identified to explain this difference further. These results also explain that solvents can play an important role in the selective growth of a desired molecular complex. Similarly, FT-IR data analysis of nicotinamide and isonicotinamide co-crystals has helped to support the literature by revealing

that it is the primary hydrogen bonded interaction that combines nicotinamide

with the carboxylic acid molecule.

Chapter 4

4.0   An Investigation into Multicomponent Crystalline Systems from Chiral Co-Formers and Achiral Analogues: DL- 3-Phenyllactic Acid and L-phenyllactic acid.

4.1   Introduction and Aims of the Study

This chapter will provide a review of the investigation of DL-phenyllactic acid, L-phenyllactic acid, as potentials to form co-crystals with amides. The amide species includes nicotinamide and Isonicotinamide. By using these acids and compounds, crystallisation was carried out with different stoichiometric ratios; the co-crystals were then analysed using powder x-ray diffraction and solid state infrared spectroscopy. In addition, in order to confirm the stoichiometric ratios of the products produced, ^{1}HNMR was used. Infrared spectroscopy was used to investigate the intermolecular bonds.

The main concept to consider, when selecting compounds for co-crystallisation, is whether they hold functional characteristics that will allow them to act as hydrogen bond donors and acceptors; in addition, it is also important that the general rules for hydrogen bonding, in terms of the design of hydrogen bonded solids are considered. Furthermore, the compounds that are polymorphic display structural flexibility which will ultimately increase the chances of co-crystallisation. Therefore, in order to achieve the overall aim of this project, it is imperative that the following aspects are considered and understood: the basis of crystal engineering, the intermolecular interactions involved in crystal packing, as well as how crystals are formed and an

understanding of the factors which affect crystals. Moreover, an understanding of the solvent and crystal relationship will also be useful.

Therefore to investigate the preparation of solid state co-crystal systems from mixtures of chiral and achiral forms, in order to analyse how the transformations take place.

4.2   Phase Chemistry

4.2.1   Crystallisation Studies of DL-3-Phenyllactic Acid with Pyridinecarboxamides

4.2.1.1 Isonicotinamide

DL-3-phenyllactic acid was crystallised together with isonicotinamide. The crystallisations were performed using different solvents and different starting molar ratios. The solid products were left to re-crystallise in the form of white crystalline solids and oils.

The spectral PXRD data (see Figure 4.1) clearly shows that the samples TA-I-31-1a, 1b and 1c were very different from the starting materials of isonicotinamide and phenyllactic acid.

Despite the fact that both starting materials exhibited a strong scattering peak at around 19.6 and 25.8°, phenyllactic acid exhibited a characteristic scattering peak at 10.9, 15.0 and 25.6°; similarly, isonicotinamide exhibited a characteristic scattering peak at 18.8, 20.9, 23.4 and 31.3° Interestingly the 1:1, 1:2, 2:1 molar ratio of the products for TA-I-31-1a, 1b and 1c, all showed characteristic peaks in the same region at 17.5, 22.9, 23.3, 25.2 and 28.4°;

thus indicating that a new phase had formed, however peak appeared for TA-I-31-1b showed peak at 18.2, 31.1 which corresponds to isonicotinamide. Similarly TA-I-31-1c also showed few peaks that correspond to DL-phenyllactic acid. The PXRD results of the samples prepared using methanol as the solvent also followed somewhat similar result patterns. A similar new phase was produced using acetonitrile as solvent however, 1:2 molar ratio product showed existence of isonicotinamide (see Figure 4.1 and 4.2).

DL-3-phenyllactic acid : isonicotinamide
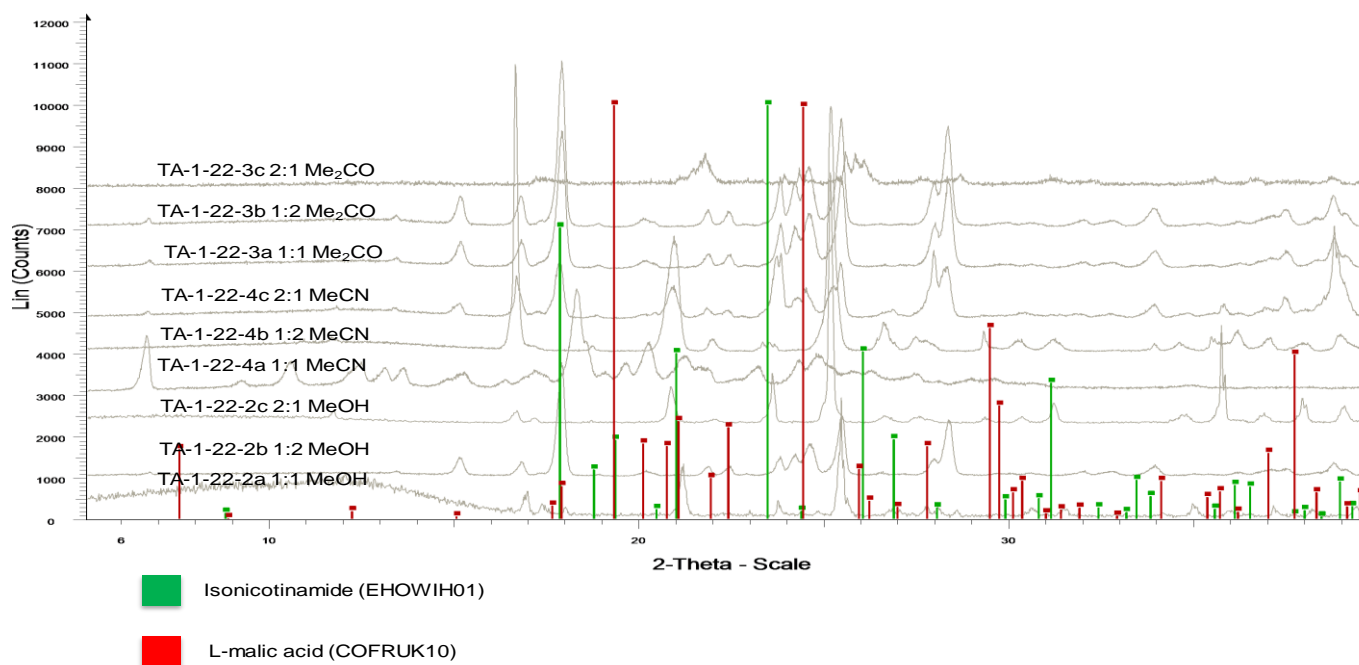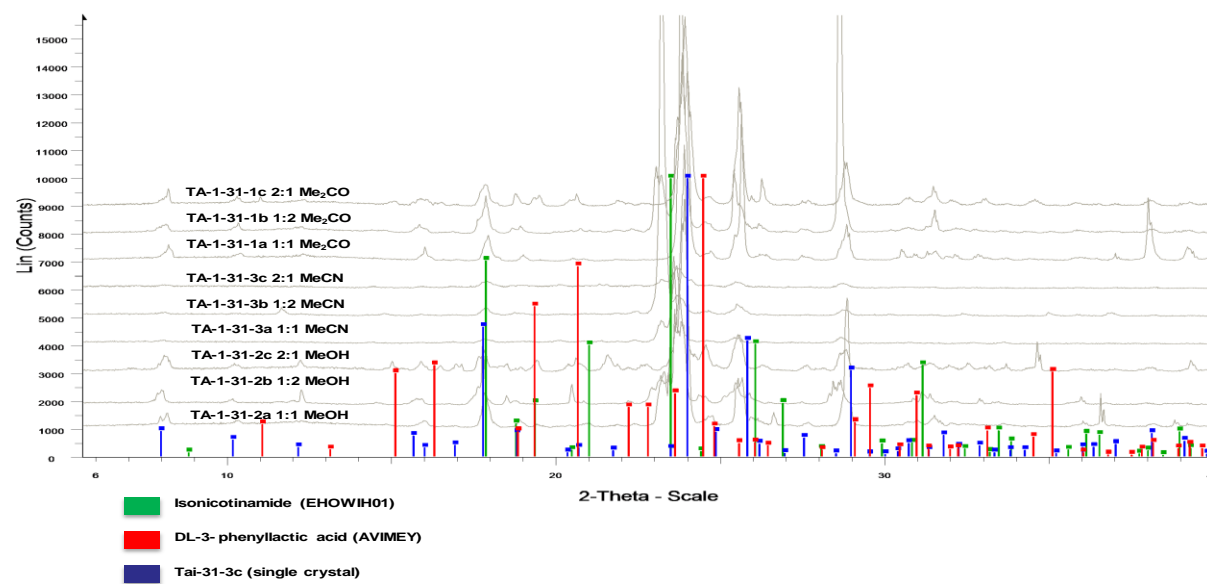

Figure 4.1: X-ray powder diffraction patterns of isonicotinamide and DL-phenyllactic acid, and products of crystallisation with a range of solvent

Graphical representation of crystalline phases identified from co-crystallisations of DL-3-phenyllactic acid : isonicotinamide
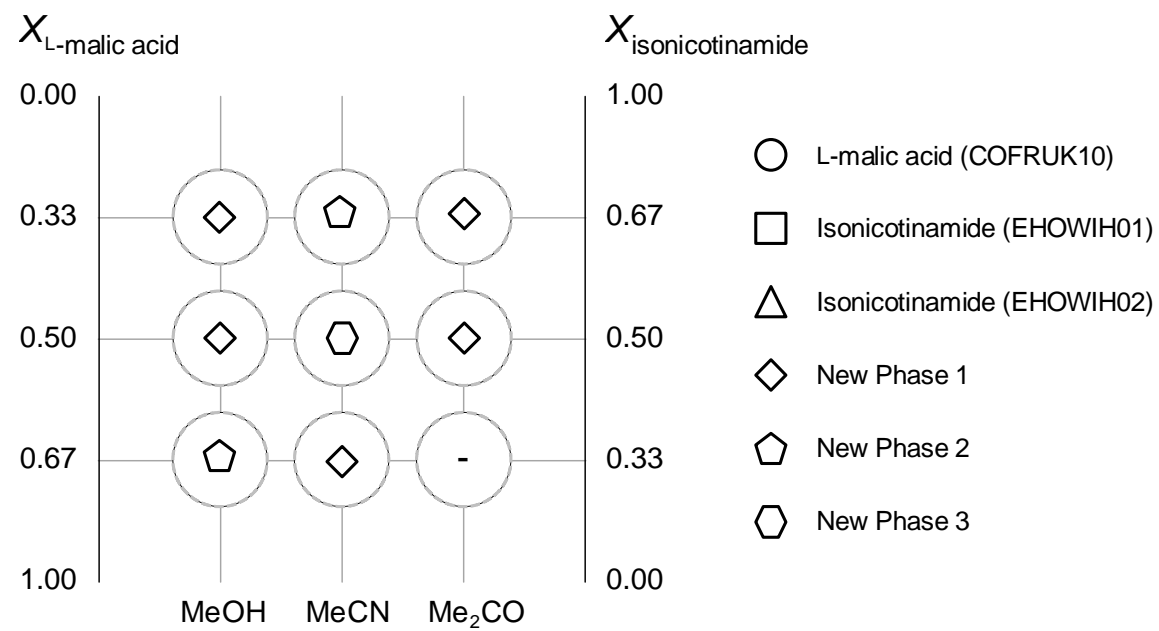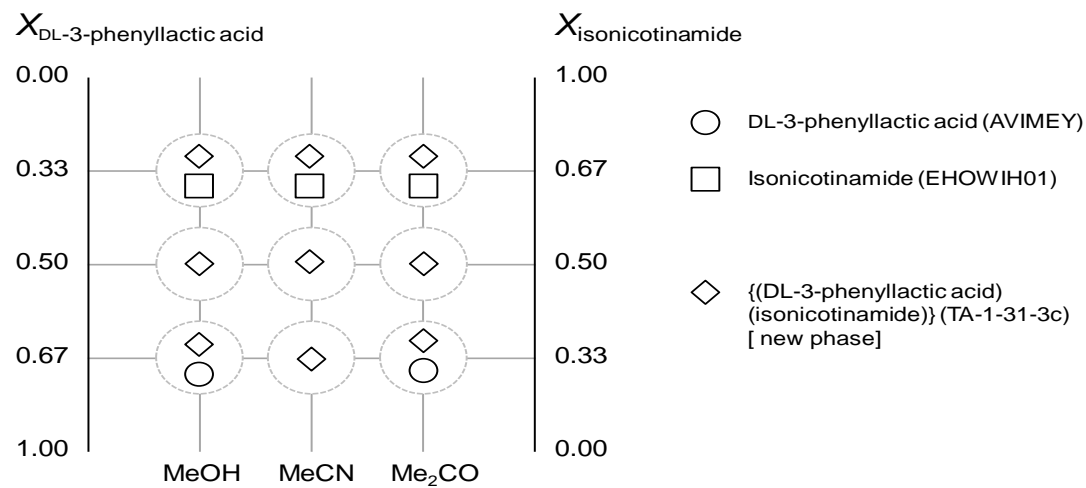

Figure 4.2: Representation of crystalline phases identified from co-crystallisations of DL-3-phenyllactic acid: isonicotinamide

Further investigation using FT-IR analysis was performed on all of the samples above in order to confirm the presence of important functional groups, and to ensure that the differences in the samples (from the starting materials) were assessed to indicate whether complexation/hydrogen bond formation had occurred.
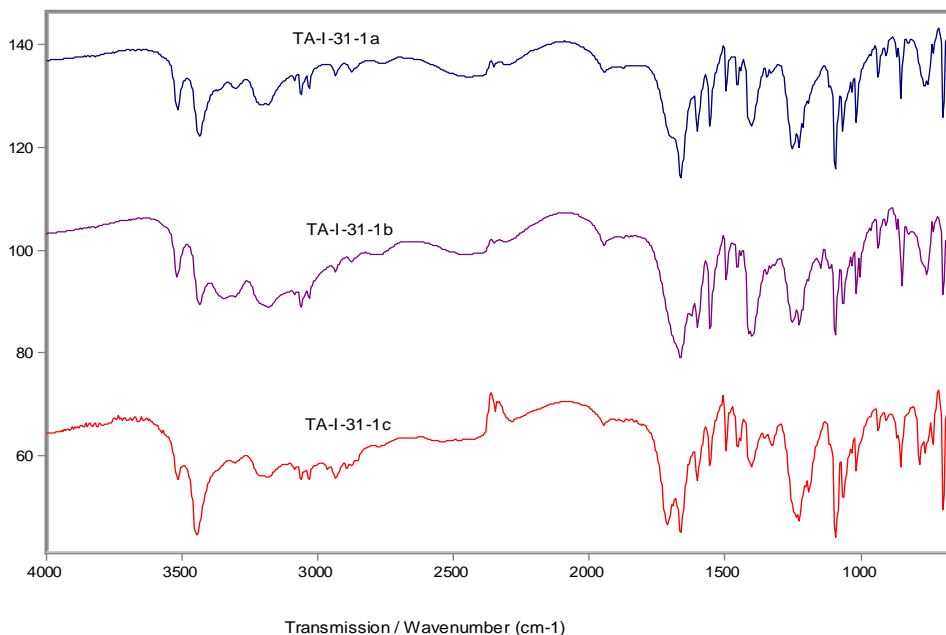
Figure 4.3: Comparative FT-IR spectra for TA-I-31-1a, 1b and 1c in ratios 1:1, 1:2 and 2:1 in Me$_2$CO

The comparative FT-IR spectra for multicomponent systems of TA-I-31-1a, 1b and 1c (Figure 4.3), explained several characteristic bands which were distinguishable between TA-I-32-3a, 3b and 3c; these results can be used to assess the relative strengths of the hydrogen bonding interactions in the solid state. Phenyllactic acid generally showed two different types of O-H..O interactions; these products also identified alcohol OH group as the donor and carboxylic acid O=C group as the acceptor. The O---O and H---O distances arising from these types of interactions are shorter, but they

substantiated the finding that stronger O-H..O hydrogen bonds were observed from the IR data. The multicomponent TA-I-31-1a provided a sharp band at 3517cm^{-1}; interestingly, TA-I-31-1b and 1c also showed peaks at this position, but they were less intense then 1a which is a characteristic of OH stretching (Figure 4.3). A similarly sharp OH stretching band also appeared at 3442cm^{-1} for the IR spectrum of TA-I-31-2a. This absorption band corresponds to the stretching frequency of the alcohol O-H bond, which would be expected to shift to lower wavenumbers as the strength of an O-H..O hydrogen bond increases.
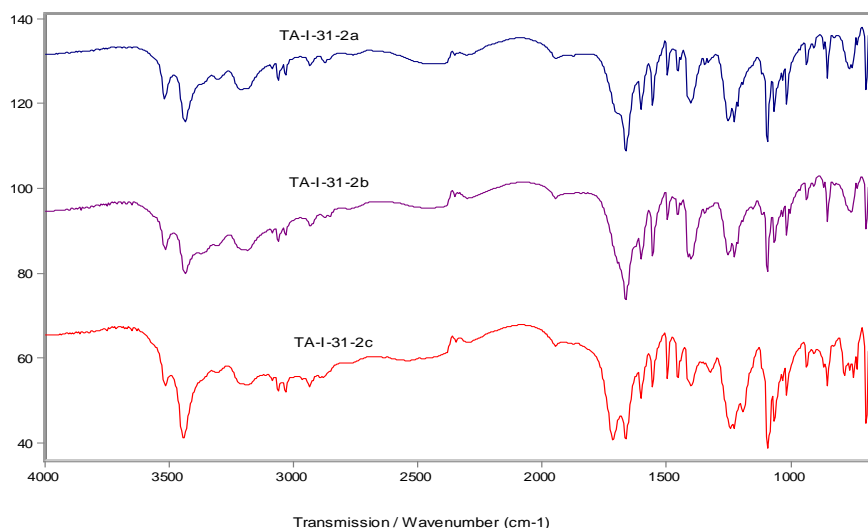
Figure 4.4: Comparative FT-IR spectra TA-I-31-2a, 1b and 1c in ratios 1:1, 1:2 and 2:1 in MeOH

4.2.1.2 Nicotinamide

DL-3-phenyllactic acid was also crystallised together with nicotinamide. The crystallisation was again performed using different solvents and different starting molar ratios. However, it should be noted that some products were oils and were not characterised with PXRD.

The PXRD patterns obtained for DL-phenyllactic acid, nicotinamide and its multicomponents are shown in Figure 4.5. By looking at the result patterns, it is quite obvious that TA-I-32-2a and 2b were different from their starting materials. This was evidenced by the appearance of new characteristic peaks at 8.2, 9.8, 14.4, 16.3, 19.7, 21.1 and 22.9°, none of these peaks resembled the DL-phenyllactic acid or nicotinamide, or its polymorphic form. This substantiates the preposition that multicomponent formation had occurred.

The system with excesses of DL-phenyllactic acid in TA-I-32-2c also showed new characteristic peaks at 5.9, 8.3, 9.9, 12.9, 16.4, 17.8, 19.8, 20.9 and 21.1°. Thus, the 1:1 and 1:2 ratio in acetone produced the same new phase, but the 2:1 ratio in the same solvent different new phase was present with exist of DL-phenyllactic acid (Figure 4.6). Further investigation was performed using acetonitrile as the solvent. Samples of TA-I-32-4a and 4c showed somewhat similar peaks which indicated a new phase formation; in addition, TA-I-32-4a (1:1), in particular, showed that an additional new phase was also present.

The PXRD analysis was performed on the samples prepared by DL-phenyllactic acid and nicotinamide which used methanol for preparation. The multicomponent systems of TA-I-32-3a and 3b showed new peaks at 8.3, 10.2, 12.5, 16.8, 22.0, 25.1 and 31.5°. TA-I-32-3c also showed peaks at 19.3, 24.9, 28.6 and 30.4°. Therefore, the different stoichiometries in methanol all produced a new phase with excess of nicotinamide in 2:1 ratio.

DL-3-phenyllactic acid :nicotinamide

TA-1-32-2c 2:1 Me$_2$CO
TA-1-32-2b 1:2 Me$_2$CO
TA-1-32-2a 1:1 Me$_2$CO
TA-1-32-4c 2:1 MeCN
TA-1-32-4b 1:2 MeCN
TA-1-32-4a 1:1 MeCN
TA-1-32-3c 2:1 MeOH
TA-1-32-3b 1:2 MeOH
TA-1-32-3a 1:1 MeOH

Lin (Counts)

2-Theta - Scale

Nicotinamide (NICOAM01)

DL-3- phenyllactic acid (AVIMEY)

Figure 4.5: X-ray powder diffraction patterns of nicotinamide and DL-phenyllactic acid, and products of crystallisation with a range of solvents

Graphical representation of crystalline phases identified from co-crystallisations DL-3-phenyllactic acid : nicotinamide
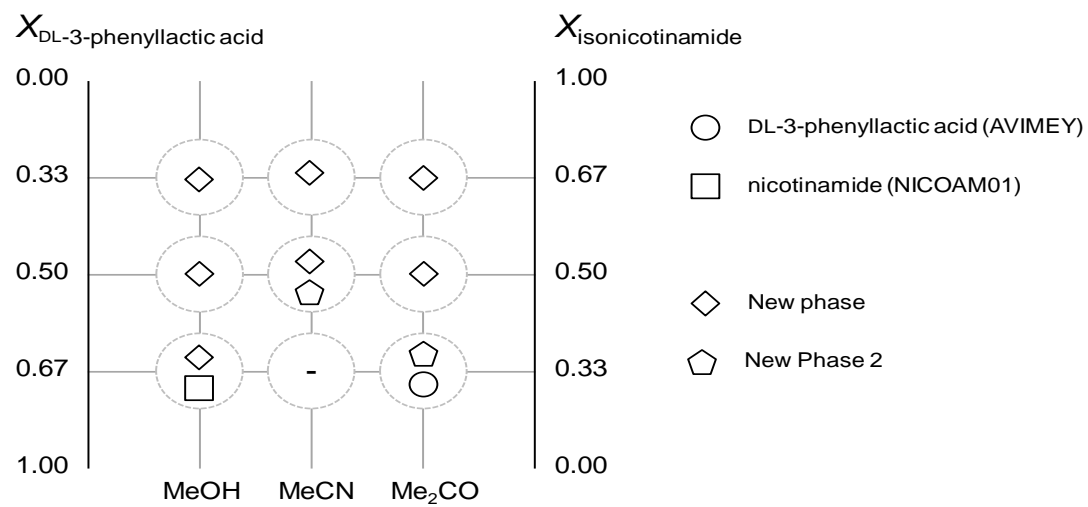
Figure 4.6: Representation of crystalline phases identified from co-crystallisations of DL-3-phenyllactic acid: nicotinamide

An extended FT-IR study of the multicomponent systems helped to indicate the presence of functional groups which were expected in the samples of successful co-crystallisation of the two starting materials. In this regard, Figure 4.7 shows an overlaid IR pattern of TA-I-32-2a, 2b and 2c. The visual inspection of the FT-IR pattern illustrates that the region of 650 to 1800cm^{-1} was very similar for all three multicomponent systems.
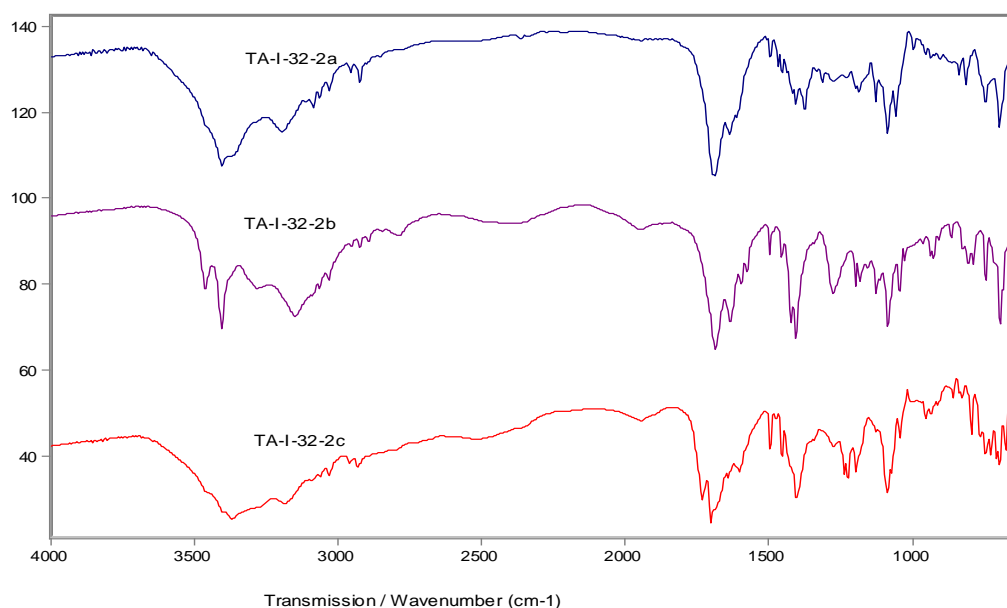
Figure 4.7: Comparative FT-IR spectra TA-I-32-2a, 2b and 2c in ratios 1:1, 1:2 and 2:1 in Me$_2$CO

4.2.2 Crystallisation Studies of L-3-Phenyllactic Acid with Pyridinecarboxamides

4.2.2.1 Isonicotinamide

L-phenyllactic acid was crystallised together with isonicotinamide. This crystallisation was performed using different solvents and different starting molar ratios. The solid products were left to re-crystallise and form white crystalline solids.

127

The spectral PXRD data illustrates that the samples of TA-I-52-1a and 1b (see Figure 4.8), differed from the starting materials of isonicotinamide and L-phenyllactic acid. TA-I-52-1c presented as oil and PXRD was therefore not possible on this sample. The PXRD patterns for TA-52-1a and 1b gave similar diffraction patterns which provided evidence of the same phase. The presence of new peaks at 7.6, 10.1, 15.2, 17.7, 25.3, 28.7, 30.6 and 35.9°, along the 2θ scale supports this proposal. The data obtained via analysis can be used to portray the initial conclusion that the starting materials efficiently reached complexation as they formed multicomponent systems for TA-I-52-1a and TA-I-52-1b.

The multicomponent formation of L-phenyllactic acid and isonicotinamide was also investigated using methanol (TA-I-52-2a, 2b and 2c) as the solvent. X-ray powder diffraction was then used to identify the important aspects with regards to the nature of the interactions and the effect of solvents in multicomponent system formation.

The PXRD patterns for the materials formed corroborates that TA-I-52-2a showed peaks at 7.2, 8.6, 9.7,11.3, 15.3, 17.4, 18.1, 19.9, 22.3, 23.6 and 24.8°; this showed the same phase as which was obtained with acetone. All three compounds showed very different diffraction pattern , indicating that new phases were produced with the different ratios; however the isonicotinamide was remaining in 1:1 ratio and the L-phenyllactic in 2:1 ratio (Figure 4.8 and 4.9).

In summary, three new phases were produced from the different ratios of the starting materials and solvents. Furthermore, the type of phase produced was not dependent on the solvent used or the ratio of the starting material.

Further investigation was performed on the samples of TA-I-52-1a, 1b and 1c for the starting materials of L-phenyllactic acid and isonicotinamide, using FT-IR spectral data for characterisation of the systems. The results indicated that some complexation/co-ordination between the two occurred as the spectrum of the multicomponent system showed common peaks in both of the starting materials and products.

The FT-IR spectra and literature confirm that O---O and H---O distances arising from these types of interactions are less when compared to stronger O-H---O hydrogen bonds[92]; in addition, a sharp band at $3492cm^{-1}$ was characteristic of OH stretching. This absorption band maintained correspondence with the stretching frequency of the alcohol O-H bond, it would therefore be expected that this would shift to lower wavenumbers as the strength of the O-H---O hydrogen bond increases[80]. Although the peak maxima of TA-I-52-1a signified bands which were more difficult to quantify, a qualitative comparison of the spectra shows that the O-H stretching bands in the spectrum shifted slightly to lower wavenumbers; thus corroborating that shorter O---O and H---O distances in the structure of TA-I-52-1a can be compared to the phenyllactic acid and isonicotinamide hydrogen bond. The spectra also indicated strong IR absorption bands for the carbonyl group at 1726 and $1710cm^{-1}$, respectively.

L-3-phenyllactic acid : isonicotinamide
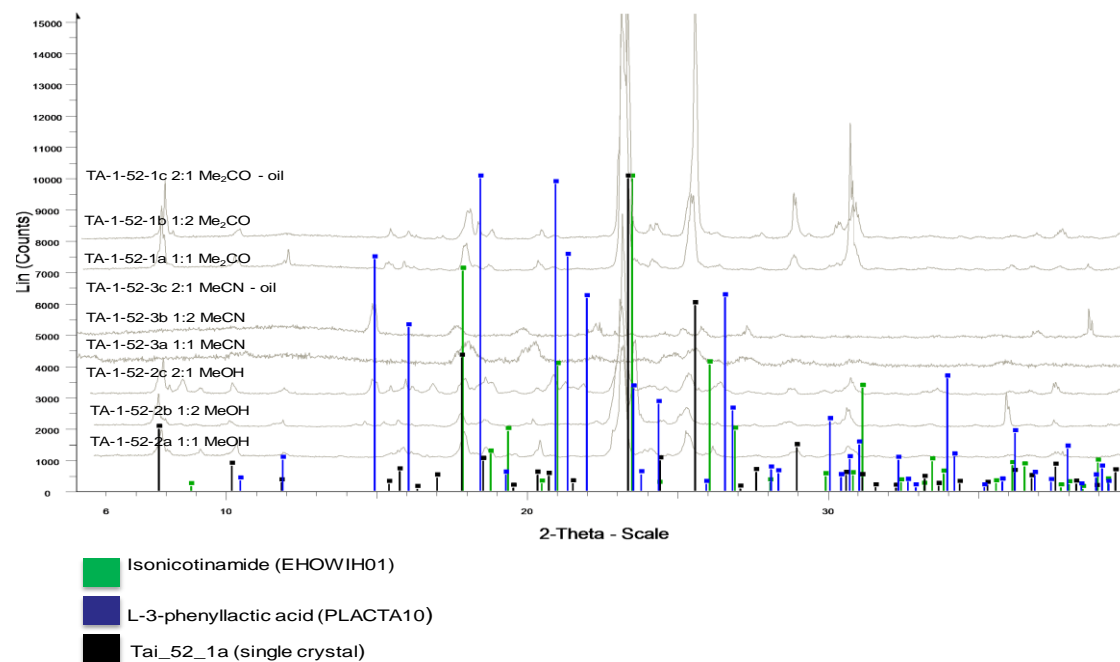
Figure 4.8: X-ray powder diffraction patterns of isonicotinamide and L-phenyllactic acid, and products of crystallisation with a range of solvents

Graphical representation of crystalline phases identified from co-crystallisations of L-3-phenyllactic acid : isonicotinamide
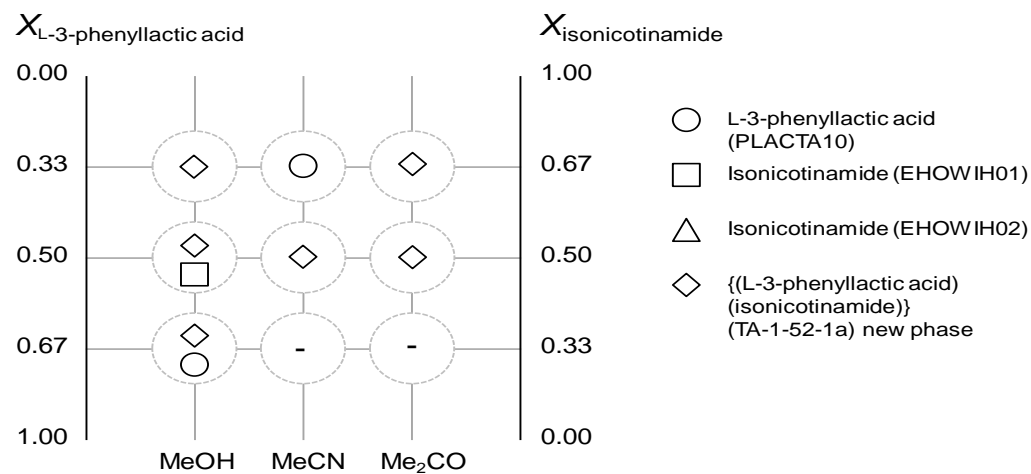
Figure 4.9: Representation of crystalline phases identified from co-crystallisations of L-phenyllactic acid: isonicotinamide

4.2.2.2 Nicotinamide

L-phenyllactic acid was crystallised together with nicotinamide. This crystallisation was performed using different solvents and different starting molar ratios. The solid products were left to re-crystallise and form white crystalline solids. The stoichiometric ratios for nicotinamide and L-phenyllactic acid were isolated as white crystalline solids.

The PXRD patterns obtained for L-phenyllactic acid and nicotinamide in the 1:1 ratio for TA-I-53-3a are shown in Figure 4.10. L-Phenyllactic acid exhibited a characteristic scattering peak at 14.9 and 20.6°, and nicotinamide exhibited a characteristic scattering peak at 15.1 and 19.2°. The 1:1 stoichiometric multicomponent product of TA-I-53-3a and 3b exhibited different scattering peaks from their starting material, but the same peaks were observed at 18.1, 20.1 and 25.6° and thus exhibited the same phase. Additionally, TA-I-53-3b had additional peaks which correspond with the starting material of nicotinamide. TA-I-53-3c was oil and therefore was not characterised using the PXRD.

Similar analysis was carried out using the solid products of TA-I-53-4a and 4b with the 1:1 and 1:2 ratios in acetonitrile. Peaks appeared at positions that were compared with TA-I-53-3a and 3b. Although the products of TA-I-53-4a and 4b showed new peaks at 14.8 and 15.4°, which indicate a new phase, in TA-I-53-4a, the peaks recorded at 22.84 corresponded with 22.15 and 27.7° which corresponded directed with the starting material of nicotinamide. In general it was observed that the L-3-phenyllactic acid/nicotinamide system

showed no new phase for the 1:2 product, with any three solvents (MeOH, MeCN, and Me_2CO). The 1:1 multicomponent system product showed new phase 1 with MeOH, new phase 2 and some traces of nicotinamide with MeCN and no multicomponent formation when Me_2CO was used. Similarly, the 1:2 product showed a new phase 1 and some traces of nicotinamide with MeOH and new phase 2 with acetonitrile; however, no new phase with Me_2CO.

L-3-phenyllactic acid :nicotinamide

Figure 4.10: X-ray powder diffraction patterns of nicotinamide and L-phenyllactic acid, and products of crystallisation with a range of solvents

Graphical representation of crystalline phases identified from co-crystallisations of L-3-phenyllactic acid : nicotinamide

Figure 4.11: Representation of crystalline phases identified from co-crystallisations of L-phenyllactic acid: nicotinamide

4.3 X-Ray Structure Analysis

4.3.1 Single Crystal Analysis of DL-3-Phenyllactic Acid and Isonicotinamide (TA-1-31-3c) in MeCN

The crystal structure of DL-3-phenyllactic acid and isonicotinamide displayed the geometry of the crystal as triclinic. It shows the dimeric nature of the isonicotinamide molecules which are linked with DL-3-phenyllactic acid, along with a network of hydrogen bonds among the assemblage of appropriate functional groups.

The co-crystal TA-I-31-3c was crystallised in the triclinic P1 space group with a= 5.3395 (5) Å, b = 11.3914 (15) Å, c = 11.6131 (13) Å, and α = 78.849 (9)°, β= 82.062 (8)°, γ = 81.076 (9)° which shows a single molecule of DL-3-phenyllactic acid and isonicotinamide in each of the asymmetric units. The phenyllactic acid molecule adopts a V-shape conformation in that the two molecules are twisted (see Figure 4.12).
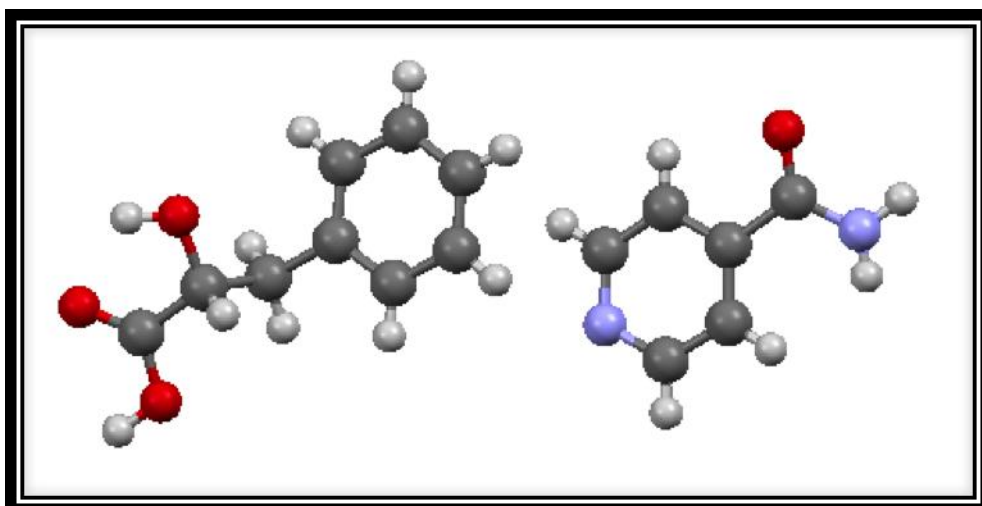
Figure 4.12: The asymmetric unit of the DL-3-phenyllactic acid: isonicotinamide co-crystal

Crystal structure analysis was also performed to rationalise the hydrogen bonding preferences of acceptors and donors in the presence of other competing functional groups. Isonicotinamide has one type of donor (amine NH_2) as it has two acidic protons, but there is only one type of acceptor, namely, the carbonyl O atom which is capable of forming hydrogen bonds in the co-crystal. Phenyllactic acid has two types of donors, namely: the carboxylic hydroxyl group ($OH_{carboxylic}$) and the alcoholic hydroxyl group ($OH_{hydroxyl}$), which, in total, bear two acidic protons. In addition, there are three types of acceptors, namely, the carbonyl O atom and the O atom of ($OH_{carboxylic}$), as well as the O atom of the alcoholic hydroxyl group ($OH_{alcohlic}$), all of which are capable of forming hydrogen bonds in the multicomponent complex.

The DL-phenyllactic acid molecule possesses two strong hydrogen bonding functional groups: a carboxylic acid and a hydroxyl group. The hydrogen bonded unit in the co-crystal possesses two molecules of isonicotinamide and one molecule of phenyllactic acid as shown in Figure 4.13. In this structure, the robust synthon holds the heteroaryl ring and phenyl ring within the same plane.
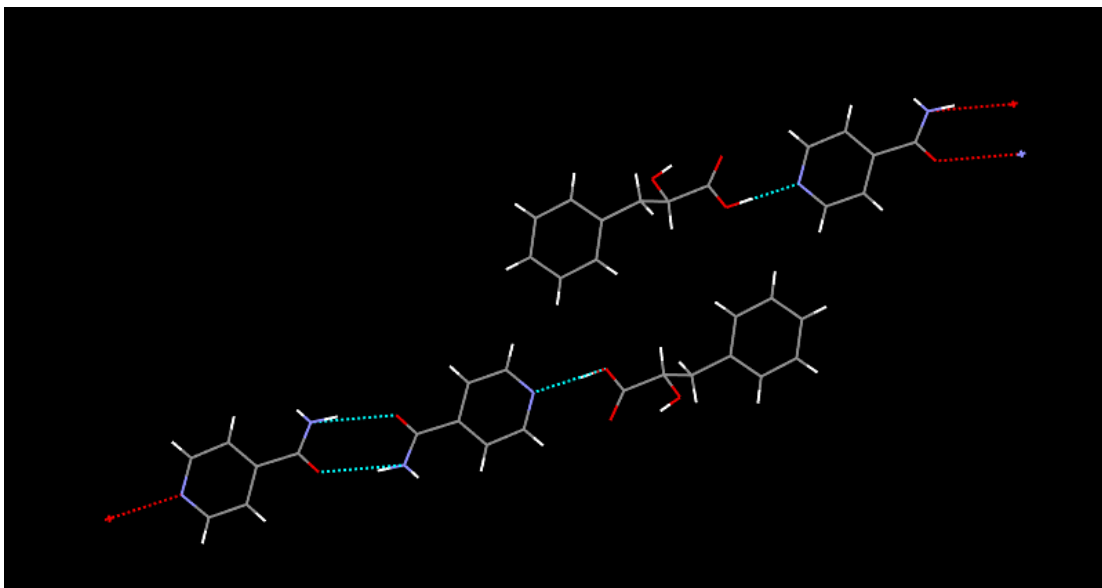
Figure 4.13: The hydrogen bonded unit in the co-crystal of two molecules of isonicotinamide and one molecule of DL-3- phenyllactic acid

In Figure 4.13, it can be seen that the amine group of isonicotinamide uses its hydrogens to form N-H- - - $O_{carbonyl\ of\ isonicotinamide}$ hydrogen bonds; furthermore, the oxygen atom of carbonyl functionality is the hydrogen bond accepter which forms C=O---N-H hydrogen bonds with the adjacent isonicotinamide molecule which eventually leads to the formation of a dimer.
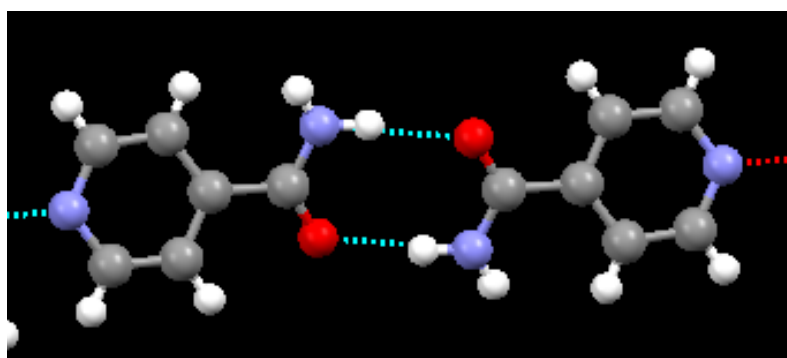
Figure 4.14: The structure crystal showing the primary intermolecular interaction between the acid and the N-heterocyclic nitrogen atom as well as the amide-amide dimer

In Figure 4.14, it can be seen that the primary intermolecular interaction is the O-H---N hydrogen bond between the acid and the N-heterocyclic nitrogen atom as well as the amide-amide dimer. The presence of the COOH functional group, within the compound, promotes the intermolecular O−H⋯O hydrogen bonds, this further links the molecules through intermolecular C−H⋯O and C−H⋯π interactions.
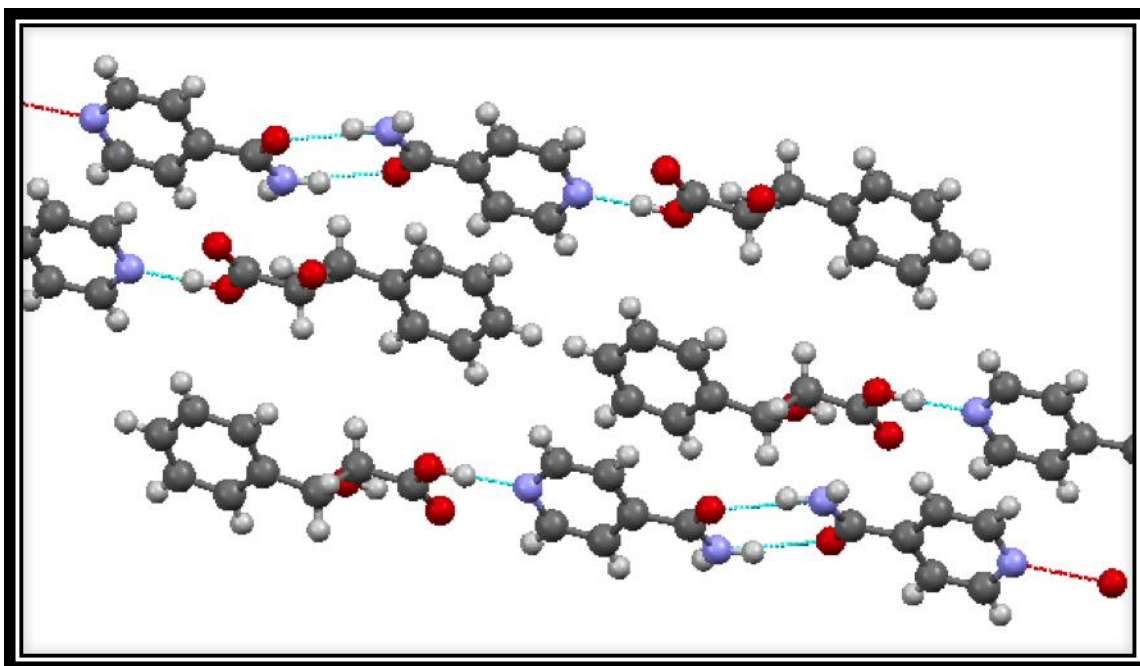
Figure 4.15: Formation of amide-amide dimmer in TA-I-31-3c

The alcoholic OH of DL-phenyllactic acid protrudes almost perpendicularly from either side of the chain, hence this hydroxyl functionality is not involved in the hydrogen bonding.

Each of the hydrogen bonded units of DL-3- phenyllactic acid consists of DL-phenyllactic acid, one distinct molecule of isonicotinamide which is bound through hydrogen bonds. The DL-phenyllactic acid molecule is bound to the isonicotinamide molecule through the O–H---N$_{\text{(pyridyl ring)}}$.

Each hydrogen bonded unit of isonicotinamide consists of two distinct molecules of isonicotinamide and one DL-phenyllactic acid molecule, which is bound through the hydrogen bond. The isonicotinamide molecule is bound to the other molecule of isonicotinamide through $C=O_{(Isonicotinamide)}$---N–$H_{(isonicotinamide ')}$ and N–H---- $C=O$. The isonicotinamide molecule is bound to one molecule of DL-3-phenyllactic acid through the $N_{(pyridine\ ring\ )}$---O–$H_{carboxyl}$ hydrogen bonds. The nicotinamide molecule also shows interactions to another molecule of DL-phenyllactic acid through a pair of $N_{(pyridine\ ring)}$ with the ring carbons
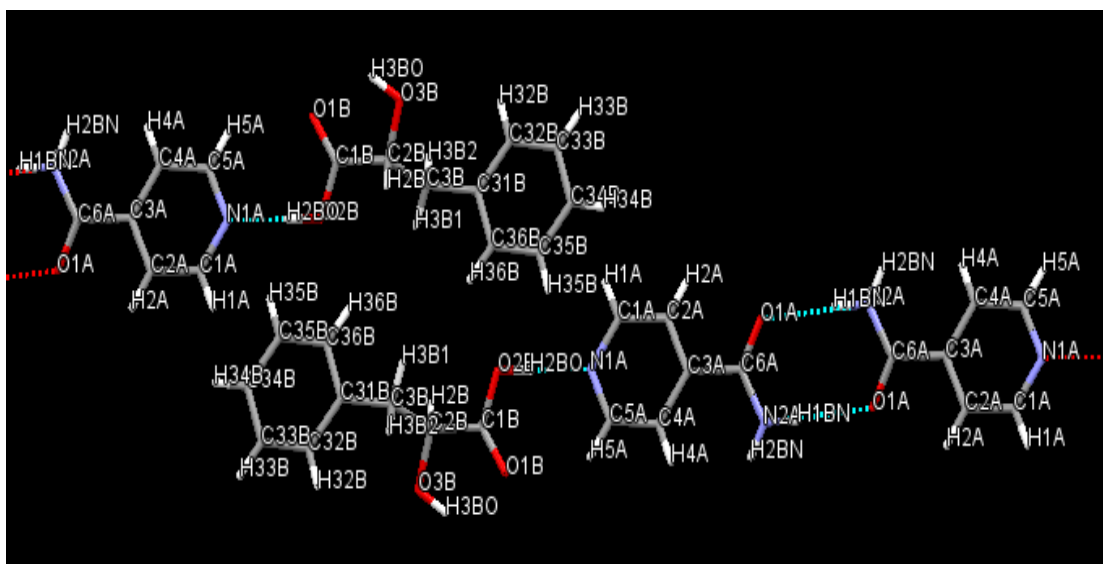
Figure 4.16: Labelling scheme adopted to show extended hydrogen network with co-crystal

Isonicotinamide was found to co-crystallise with the DL-3-phenyllactic acid supramolecular assemblies which involve hydrogen bonds between the nicotinamide pyridyl nitrogen and carboxylic hydrogen of DL-3-phenyllactic acid which also assembled the nicotinamide nitrogens and carboxamides group of adjacent isonicotinamide molecules. An extended network of H-

bonds among the assemblage of appropriate functional groups supports this crystal structure. These findings are noteworthy, because they indicate the co-crystal properties. Furthermore, the crystal structure, displayed in Figure 4.15, also indicates that OH was not primarily involved in the intramolecular O-H- - -O(carbonyl) hydrogen bond interactions.

These crystal structures also agree with the IR spectral analysis. This vibrational analysis showed that the N-H stretching vibration displayed a shift in wavenumbers, around 3310cm^{-1}, which is indicative of complexation. Similarly, the OH stretching band also appeared with a shift below 3442cm^{-1}, in the IR spectrum. This absorption band corresponds to the stretching frequency of the alcohol O-H bond, which can be expected to shift to lower wavenumbers as the strength of an O-H- - -O hydrogen bond increases[93].

Aryl and heteroaryl rings, and the chain of phenyllactic acid, are packed in an antiparallel manner over the other similar pairs from adjacent 2D sheets to interdigitate the structure via π---π interactions.

This supramolecular heterosynthon is a two-point recognition event as there are two ranges corresponding to O−H⋯N (heteroaryl) and N−H⋯O=C interactions. In this case, the supramolecular synthons are entirely different. The DL-phenyllactic acid-pyridine OH$_{acid}$ ⋯N $_{pyridine}$ supramolecular heterosynthon is formed and the primary amide is hydrogen bonded to the other carboxamides group. The lone pair interaction of the carbonyl of carboxamide is shown with the NH$_2$ group of other carboxamide groups which exhibit a hydrogen bond.
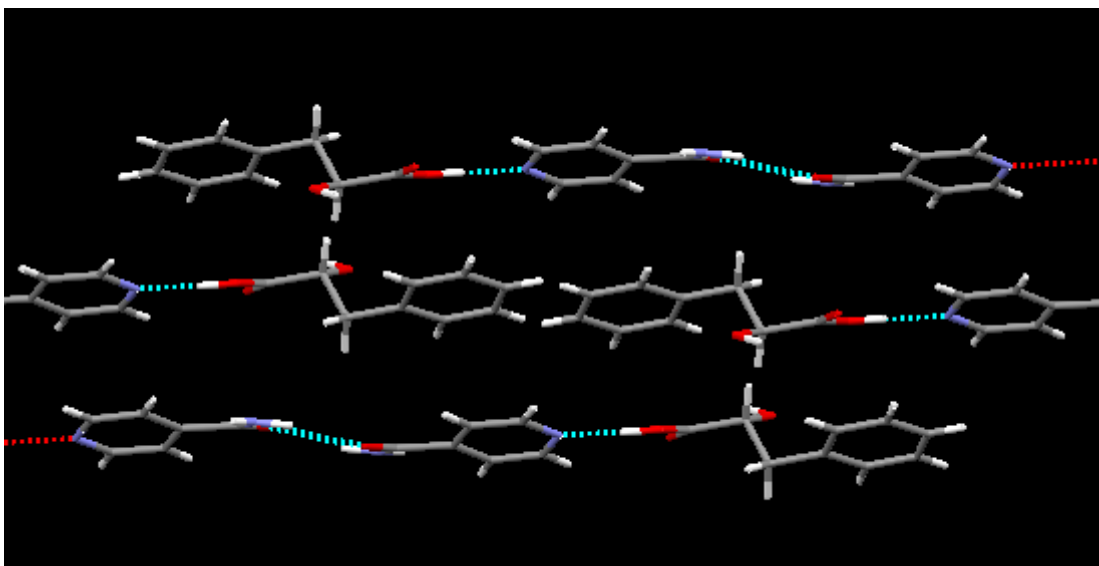
Figure 4.17: 2D sheets indicating π---π interaction within TA-I-31-3c

4.3.2   Single Crystal Analysis of L-3-Phenyllactic Acid and Isonicotinamide (TA-1-52-1a)

The crystal structure of the multicomponent complex of L-phenyllactic acid and isonicotinamide displayed the geometry of the crystal as triclinic. It shows the dimeric nature of the isonicotinamide molecules which are linked with L-3-phenyllactic acid along with a network of hydrogen bonds that are among the assemblage of appropriate functional groups (Figure 4.18).
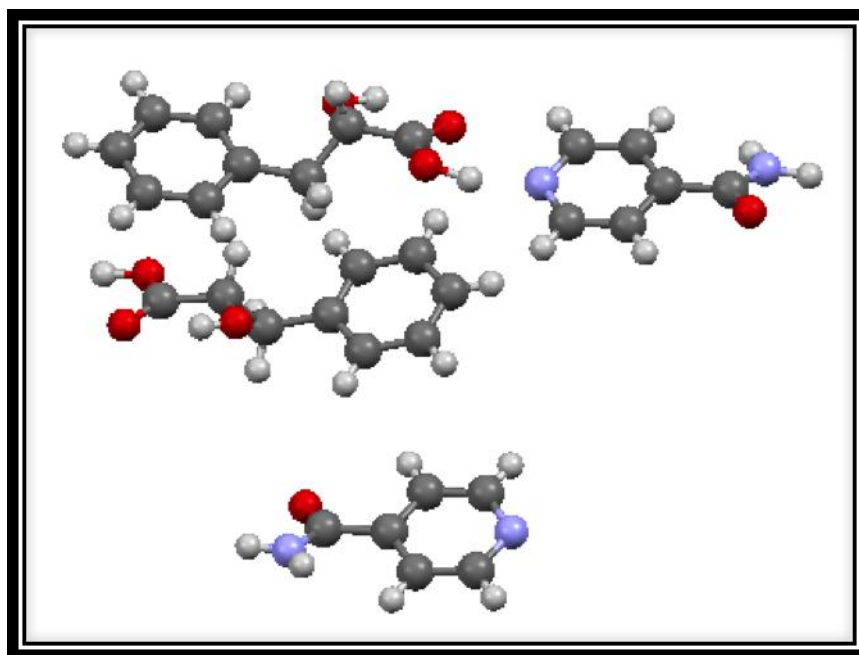
Figure 4.18: Asymmetric unit of L-3- phenyllactic acid:isonicotinamide

The co-crystal TA-I-52-1a_0m crystallises in the triclinic P1 space group with a = 5.3040 (2) Å, b = 11.4994 (4) Å, c = 11.7480 (5) Å, and α = 80.398 (3)°, β = 81.767 (3)°, γ = 82.135 (3)° which shows two molecules of each of L-3-phenyllactic acid and isonicotinamide within the asymmetric unit. The L-3-phenyllactic acid molecule adopts a zigzag conformation. The crystal structure analysis was also performed to rationalise the hydrogen bonding preferences of acceptors and donors in the presence of other competing functional groups.

As previously discussed, isonicotinamide has one type of donor (amine NH_2) that in total bears two acidic protons; in addition, there is one type of acceptor, namely, the carbonyl O atom that is capable of forming hydrogen bonds in the co-crystal. Phenyllactic acid has two types of donors, namely, the carboxylic hydroxyl group ($OH_{carboxylic}$) and the alcoholic hydroxyl group

(OH_hydroxyl) which in total bear two acidic protons with three types of acceptors, namely, the carbonyl O atom and the O atom of (OH_carboxylic) as well as the O atom of the alcoholic hydroxyl group (OH _alcohlic) – these are capable of forming hydrogen bonds in the co-crystal (see Figure 4.20).
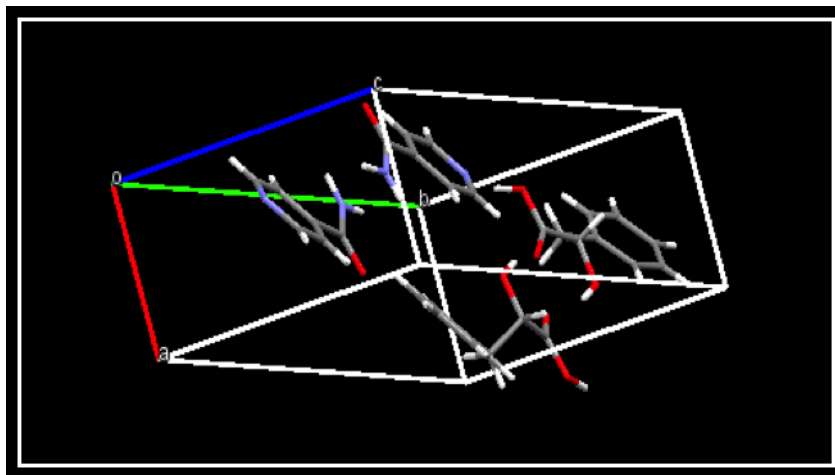
Figure 4.19: Basic unit showing hydrogen bonds in the co-crystal

The L-3-phenyllactic acid molecule possesses two strong hydrogen bonding functional groups: a carboxylic acid and a hydroxyl group. The hydrogen bonded unit in the co-crystal possess two molecules of isonicotinamide and two molecules of phenyllactic acid, as shown in the packing diagram within the structure. This robust synthon holds the heteroaryl ring and phenyl ring in the same plane (see Figure 4.20).
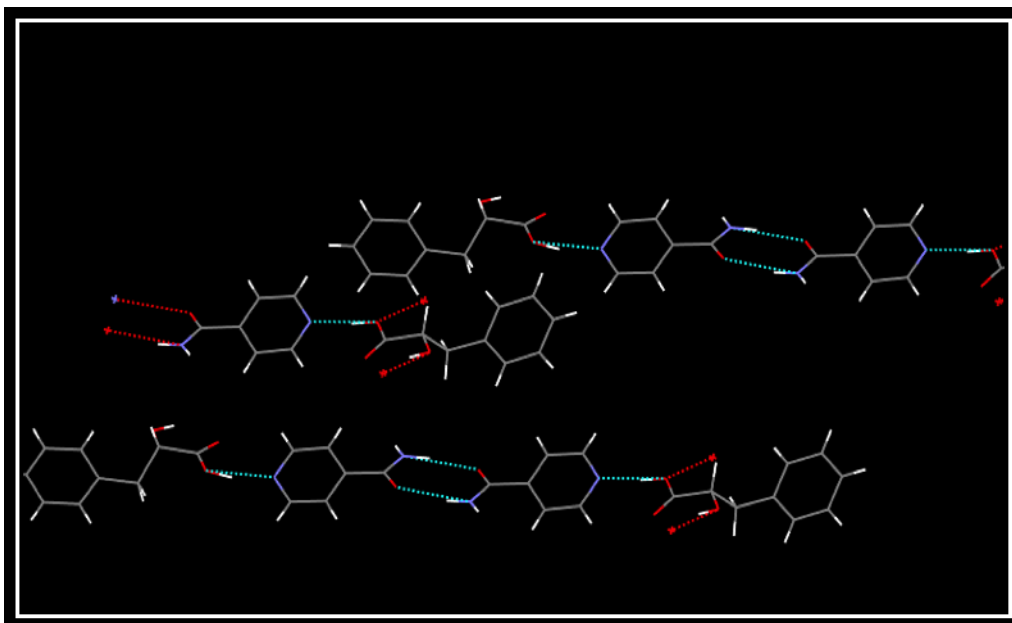
Figure 4.20: Formation of dimer in L-3- phenyllactic`acid: isonicotinamide co-crystal

In Figure 4.20 (the packing diagram), the amino group of isonicotinamide uses its hydrogens to form N-H- - - $O_{carbonyl\ of\ isonicotinamide}$ hydrogen bonds with the oxygen atom of carbonyl functionality, here the hydrogen bond accepter forms C=O- - - N-H hydrogen bonds with the adjacent isonicotinamide molecule – this eventually leads to the formation of a dimer.

This diagram reveals that the primary intermolecular interaction is the O-H---N hydrogen bond between the acid and the N-heterocyclic nitrogen atom as well as the amide-amide dimer and the OH- - -OH interaction. Further linking of the molecules through intermolecular C−H···O and C−H···π interactions occurs, but alcoholic OH of L-*3*-phenyllactic acid protrudes almost perpendicularly from either side of the chain hence this hydroxyl functionality is not involved in the hydrogen bonding.

Each hydrogen bonded unit of L-3-phenyllactic acid consists of two molecules of L-phenyllactic acid and one distinct molecule of isonicotinamide which are bound through hydrogen bonds. The L-phenyllactic acid molecule is bound to the molecule of isonicotinamide through O–H---N$_{(pyridyl\ ring)}$ as well as bound to another molecule of L-phenyllactic acid.

Each hydrogen bonded unit of isonicotinamide consists of two distinct molecules of isonicotinamide and one L-phenyllactic acid molecule, bound through hydrogen bonds. The isonicotinamide molecule is bound to the other molecule of isonicotinamide through C=O$_{(Isonicotinamide)}$---N–H$_{(isonicotinamide')}$ and N–H---C=O. The isonicotinamide molecule is bound to one molecule of L-3-phenyllactic acid through N$_{(pyridine\ ring)}$---O–H$_{carboxyl}$ hydrogen bonds. The isonicotinamide molecule also demonstrates interactions with another molecule of L-phenyllactic acid through a pair of N$_{(pyridine\ ring)}$, with the ring carbons.

The crystal structure also displays that OH of L-3- phenyllactic acid was not primarily involved in intramolecular O-H---O(carbonyl) hydrogen bond interactions. Instead O-H was involved in intermolecular hydrogen bonding with another molecule of L-phenyllactic acid via the O-H----O-H hydrogen bond – such interactions were not observed in cases of co-crystals that were formed by DL-3-phenyllactic acid.
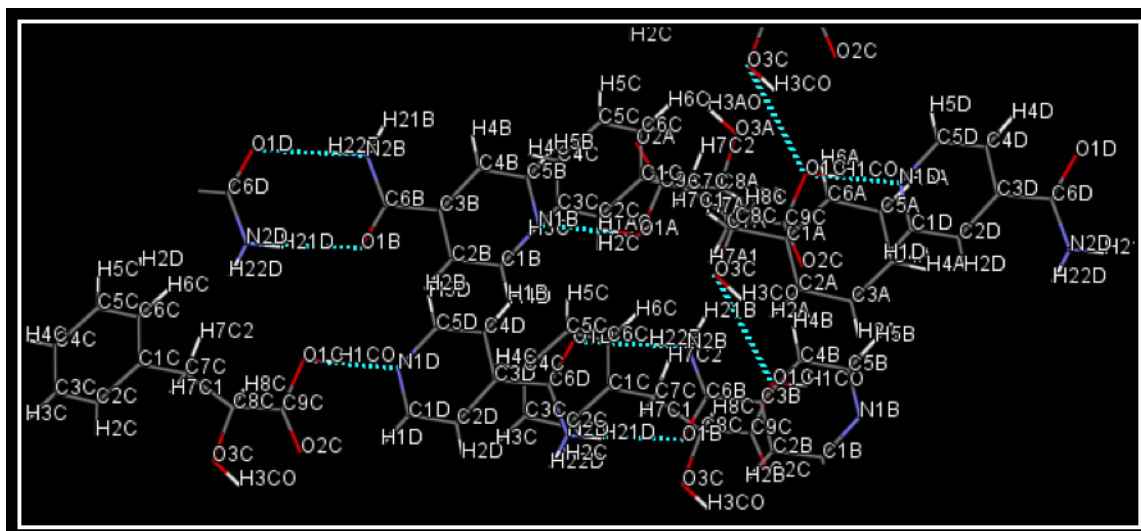
Figure 4.21: Labelling scheme adopted to show extended hydrogen bonded network

The crystal structure is also in agreement with the IR spectral analysis. The vibrational analysis showed that the N-H stretching vibration displaying a shift in wavenumbers, around 3310cm^{-1}, which is indicative of complexation. Similarly, the OH stretching band also appeared with a shift that was below 3442 cm^{-1}, within the IR spectrum. This absorption band corresponds with the stretching frequency of the alcohol O-H bond, which would be expected to shift to lower wavenumbers as the strength of an O-H- - -O hydrogen bond increases.

Aryl and heteroaryl rings, and chains of phenyllactic acid, are packed antiparallel with the other similar pairs from adjacent 2D sheets to interdigitate the structure via π---π interactions.

This supramolecular heterosynthon is a three-point recognition event as there are three ranges which correspond to O−H···N(heteroaryl) and N−H···O=C interactions, and O-H- - -O-H interactions. In this case, the

147

supramolecular synthons are entirely different. The L-*3*-phenyllactic acid-pyridine $OH_{acid} \cdots N_{pyridine}$ supramolecular heterosynthon is formed and the primary amide is hydrogen bonded to the other carboxamide group. The lone pair interaction of the carbonyl of carboxamide is shown with the NH_2 group of the other carboxamide group which exhibits a hydrogen bond.

4.4   Discussion

A comparative study of the multicomponent systems, using both homochirality and racemic of the 3PLA with amide (isonicotinamide and nicotinamide), using the different molar ratios for each of the starting materials and different solvent (acetone, acetonitrile and methanol), was provided in this part of the research. This study has revealed crystal structures of co-crystals of DL-phenyllactic acid and isonicotinamide; as such, both of the compounds crystallised in the triclinic space group, thus showing the dimeric nature of nicotinamide molecules that were linked with phenyllactic acid along with a network of hydrogen bonds that were among the assemblage of appropriate functional groups.

The DL-phenyllactic acid molecule possesses two strong hydrogen bonding functional groups: a carboxylic acid and a hydroxyl group. In addition, the hydrogen bonded unit, in the co-crystal, possessed the two molecules of isonicotinamide and nicotinamide, and one molecule of phenyllactic acid, as shown in the packing diagram (see Figure 4.21). In the structure, the robust synthon held the heteroaryl ring and the phenyl ring in the same plane. Each hydrogen bonded unit of DL-3-phenyllactic acid consists of DL-phenyllactic acid and one distinct molecule of isonicotinamide bound through

hydrogen bonds. The DL-3-phenyllactic acid molecule was bound to the molecule of isonicotinamide through O–H---N$_{(pyridyl\ ring)}$. Furthermore, homochiral crystals were grown using an aprotic, and a less polar solvent system. The research considered the use of an ideal racemic system to investigate homochiral versus heterochiral nucleation, as a means for resolving enantiomers.

Chapter 5

5. 0 An Investigation into Multicomponent Crystalline Systems from Phenylboronic Acids and Pyridinecarboxamides

5.1 Introduction and the Aims of the Study

Hydrogen bonding, π-π stacking, and N-H---π and C-H---π interactions play a considerable role in governing the specific functional structures of important biomolecules[13,94,15]. These non-covalent interactions are also the basis of crystal engineering, supramolecular chemistry, self-assembly, molecular recognition and DNA intercalation[17,18,95]. Although the foundation of hydrogen bonding and stacking, or π-hydrogen bonding interactions, are different from these, hydrogen bonding arises from electrostatic interaction, while dispersion forces dominate the π---π stacking and π-hydrogen bonding interactions[18].

The aspiration of this current part of the research is to investigate the potential for modification of the hydrogen bonding environment that has originated from the interaction of boronic acids and amides. These modifications of the hydrogen bonding regime, from benzoic acids where the carboxylic acid provides an O, OH donor-acceptor system and the phenylboronic acid unit which provides an OH, OH donor-donor system, aim to:

Prepare and characterise co-crystal systems of boronic acid.

Investigate and confirm that a boroxine ring forming reaction is a dynamic covalent process.

Investigate the thermodynamic equilibriums that exist between boronic acid monomers and boroxinestrimers.

Identify how the use of different solvents (acetone, acetonitrile and methanol) effect the formation of a multicomponent system.

Study the effect of changing the molar ratio of isonicotinamide and nicotinamide to phenylboronic acid for the final products.

Where possible, characterise the system by single crystal analyses.

Perform a comparative study of selected multicomponent systems by both the single crystal and by its PXRD pattern.

Characterise the systems with FT-IR, PXRD and single crystal analyses.

5.2 Phase Chemistry

5.2.1 Crystallisation Studies of Phenylboronic Acid and Pyridinecarboxamides

5.2.1.1 Isonicotinamide

The phenylboronic acid and isonicotinamide multicomponent systems were prepared through the use of slow evaporation of the saturated equimolar (ratio 1:1) and non-equimolar (ratios 1:2 and 2:1) solutions within the different solvents of methanol, acetone and acetonitrile. The products (white crystalline solid) were then analysed using PXRD, FT-IR and single crystal analysis.

The PXRD patterns obtained for isonicotinamide, phenylboronic acid, as stoichiometric (TA-I-19-1a) and non-stoichiometric products (TA-I-19-1b and TA-I-19-1c), are shown in Figure 5.1. While both solids exhibited a strong scattering peak at around 20.8 and 25.8° (on the 2θ scale), phenylboronic acid exhibited a characteristic scattering peak at 15.27° and isonicotinamide exhibited a characteristic scattering peak at 23.44°. The 1:1 stoichiometric product of TA-I-19-1a evidenced peaks at 15.4, 17.1, 20.8, 21.5, 23.5, 28.6, 34.6, 35.8 and 37.91°; similarly, the non-stoichiometric product of TA-I-19-2b also exhibited strong scattering peaks at 15.69, 17.7, 21.3, 23.6, 26.5, 28.4, 29.1 and 48.6°, similarly TA-I-19-1c which showed new peaks at 7.4, 14.4, 15.6, 18.9, 22.8, 23.4, 28.4, 29.1 and 35.9°. All different stoichiometries in acetone produced the same new phase with excess of the starting material, thus indicating that complexation had occurred (Figure 5.1 and 5.2)

The comparative XPRD patterns obtained for phenylboronic acid, isonicotinamide, its polymorphic forms and the multicomponent products prepared using acetonitrile are shown in Figure 5.1. The 1:1 stoichiometric product of TA-I-19-2a exhibited altered scattering peak at 15.9, 21.5, 23.7, 29.4, 31.9, 39.9 and 47.5° along the 2θ scale with excess of isonicotinamide. Similarly, the non-stoichiometric molar ratio products of TA-I-19-2b also showed new characteristic peak appearances at 9.6, 19.4, 19.9 and 29.16° which is different from the new phase was present in 1:1 ratio. In addition, TA-I-19-2c also showed the appearance of new peaks similar to the new phase was produced in 1:1 ratio, which is indicative of the formation of a multicomponent system; however, the peaks at 12.1, 18.9, 20.9, 22.1, 24.2,

29.4 and 29.9⁰, along the same 2θ scale, showed similarities with the starting material isonicotinamide. Thus representing that some of the excess of the starting material remained in the mixture in its solid form (see Figure 5.1 and 5.2).

The comparative study of the PXRD pattern shows that the starting material and the multicomponent systems using methanol as solvent revealed the appearance of new peaks. TA-I-19-3a (the 1:1 molar ratio product of the starting material) showed not much difference from the starting materials. The pattern of 1:1 more corresponding with isonicotinamide. On the other hand, TA-1-19-3b presented new significant peaks at 9.3, 10.9, 11.4, 11.9, 14.5, 16.5, 17.8, 19.3, 19.9, 20.2, 28.88 and 29.22⁰, along the 2θ scale.

Correspondingly, TA-I-19-3c showed new peaks at 7.9, 9.4, 11.5, 14.6, 15.8, 17.0, 17.6, 19.7, 21.4, 21.7, 22.7, 23.1, 24.9 and 35.1, along the 2θ scale. In addition isonicotinamide also existed in this ratio. Thus indicating that hydrogen bonded multicomponent system formation occurred within all of the samples.

phenylboronic acid :isonicotinamide
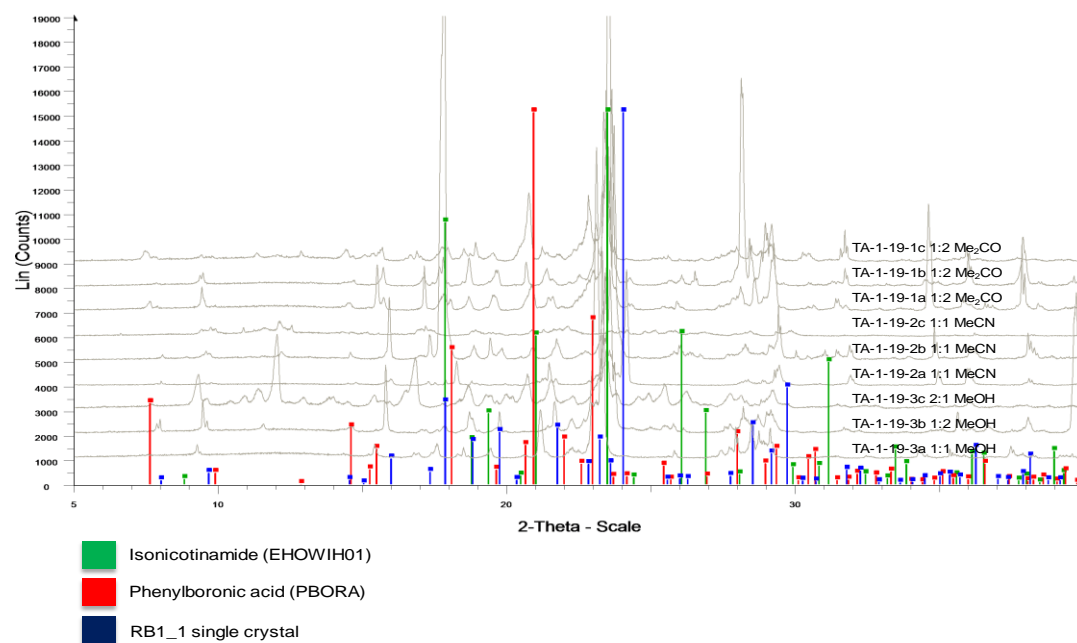
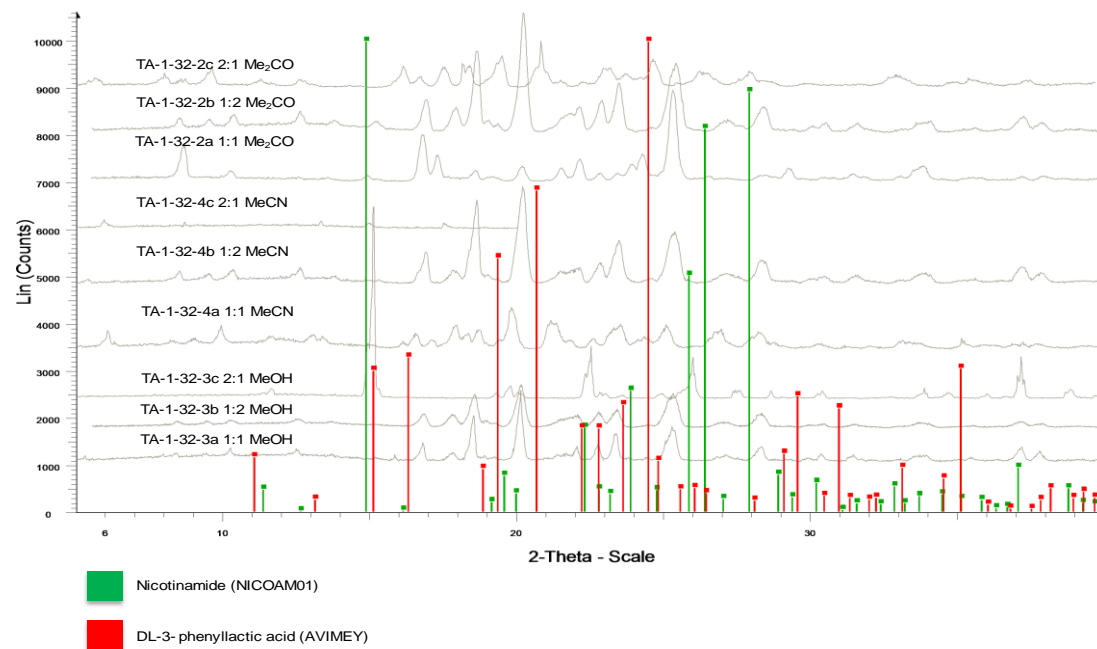Figure 5.1: X-ray powder diffraction patterns of isonicotinamide and phenylboronic acid, and products of crystallisation with a range of solvents

Graphical representation of crystalline phases identified from co-crystallisations of phenylboronic acid : isonicotinamide
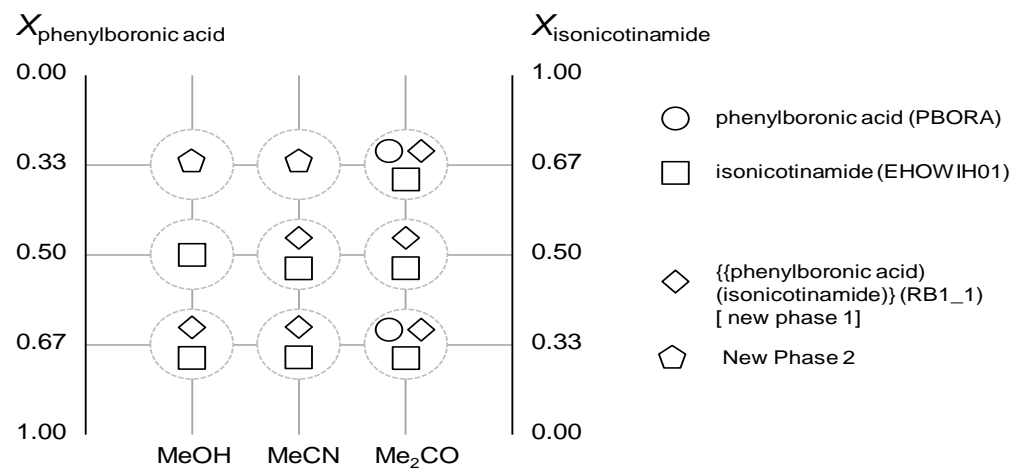
Figure 5.2: Representation of crystalline phases identified from co-crystallisations of phenylboronic acid and isonicotinamide

In a research study conducted by Seaton *et al.,* the use of isonicotinamide and benzoic acid [1:1] co-crystallisation revealed that solvent selectivity could be streamlined in a supramolecular manner by reflecting the interactions and the varying solvent volumes which also effect it (Figure 5.3)[18,96].
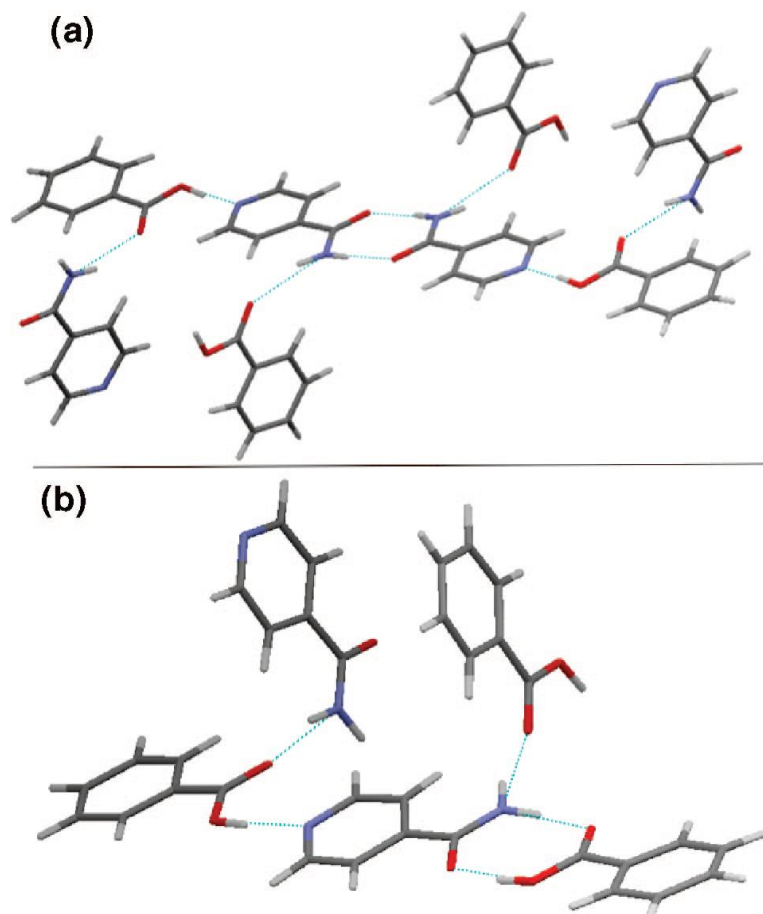
Figure 5.3: Comparison of the main intermolecular interactions between: a) 1:1; and, b) 2:1 benzoic acid: isonicotinamide molecular complees[18]

The literature also indicated that the isonicotinamide, benzoic acid co-crystal showed a C=O---HO hydrogen bond which was in competition with the discrete amide-acid interaction. Generally, sensitivity to a particular solvent would vary the packing volume of the $-NH_2$ vs $-CO_2$ H moieties which would

also have an effect on the functional groups on the solvents for both the acid-amide and the amide-amide associations[18].

The crystal structure can be further stabilised by various C-H---O and π---π stacking interactions. Due to the presence of phenylboronic acid and its ability to form tetrameric motifs which consist of acid-acid homosynthons, such motifs are generally composed of hydrogen bonded complexes, with obvious (B)O-H---N, (B)O-H---O, C-H---O, C-H---N, C-H---π, C-H---B and very strong π---π stacking interactions[97].

Further investigation was also carried out using the FT-IR technique, see Figure 5.4.
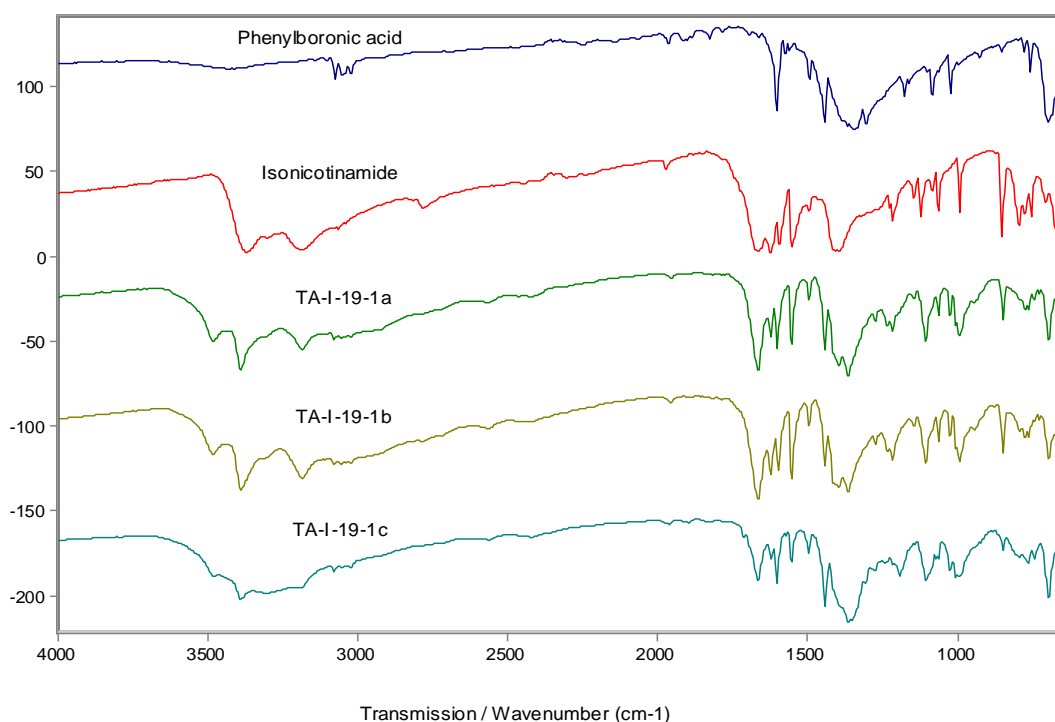
Figure 5.4: Comparative FT-IR spectra for TA-I-19-1a, 1b and 1c in ratios 1:1, 1:2 and 2:1 in Me$_2$CO

Table 5.1: FT-IR assignments for samples TA-I-19-1a, TA-I-19-1b and TA-I-19-1c in Me$_2$CO

Iso-nicotinamide FT-IR (cm^{-1})	Phenylboronic Acid FT-IR (cm^{-1})	TA-I-19-1a FT-IR (cm^{-1})	TA-I-19-1b FT-IR (cm^{-1})	TA-I-19-1c FT-IR (cm^{-1})	Assignment
		3482	3482	3480	
3370, 3186		3309 3186	3388 3186	3388	ύ NH2 (100), ύ NH2 (100)
	3273, 3081, 3024	3079 2568	3079	3097 3023	OH and VOD
3076, 3064, 3053, 3041			3055 3042 3023		ύ CH (99), ύ CH (100)
1624, 1596, 1667					δNH2 , ύ ring +δCCH , ύ ring ,ύ CO
		2568	2567		
	2419		2465		
	1964	1958	1959		
	1894		1891		
				1713	
		1666	1666	1667	C=O
		1621	1626	1621	
	1604		1601	1603	C=C stretch
	1572	1554	1553	1554	C=C stretch
1552					ύ ring
	1499	1497	1497	1498	C=C stretch
1496					δCCH +ύ ring
		1444	1441	1441	
1410					δCCH +ύ ring
1395		1397			ύ CN + δCC ,
	1350	1366	1366	1357	
	1275, 1191	1275	1275	1275	C-O stretch
1265					ū ring
1228		1234 1219	1233 1219		δCCH (74)+ύ ring (14)
	1161				C-O stretch
1148		1146	1146		ring+CCH+CN+CC
1122		1119	1119		CCH+ ring

	1095		1107	1106	C-O stretch
	1072		1076	1073	C-O stretch
1085					δ CCH +ύ ring
1063		1063		1064	NH2 rock +ύCN
	1029	1027	1027	1028	B-C stretch
	1007		1008	1008	
994			993		Ring
	972				B-O sym. Stretch
969					CH
955					ū CH
	923				Csp2- H bending
875					γCH
853		851			γCH+γ CC +γCO
	803				B-O sym. Stretch
	697, 857		846	846	BO2 out- of –Plane
778					γring +γco
	764	761	766	760	Boroxole ring
755					δ ring (30)+ ύcc(17)+ ύring
708				724	ring + CO
	697, 857				BO2 out- of –Plane
669					ring+ring
629					δ CCO + ύ ring
542					NH2 twist + ring + CC

Many strong and clear stretching modes appeared in the FT-IR spectra for the phenylboronic acid, isonicotinamide and their respective multicomponent systems of TA-I-19-1a, 1b and 1c (Table 5.1). These stretching modes reflect the arrangement of phenylboronic acid and isonicotinamide after the formation of co-crystals. The C=O stretching mode appeared at 1666cm^{-1} for TA-I-19-1a, 1667cm^{-1} for TA-I-19-1b and 1666cm^{-1} for TA-I-19-1c, while the C-N stretching mode appeared at 1397cm^{-1} for TA-I-19-1a. Similarly, the

symmetric and asymmetric CH_2 stretching modes were assigned at 3065 to 2568cm^{-1} for TA-I-19-1a, and 2901 to 2922cm^{-1} for TA-I-19-1b. On the basis of these results, it can be assumed that the TA-I-19-1a and TA-I-19-1b multicomponent systems had relatively well-ordered constructions when compared to TA-I-19-1c (see Figure 5.4).
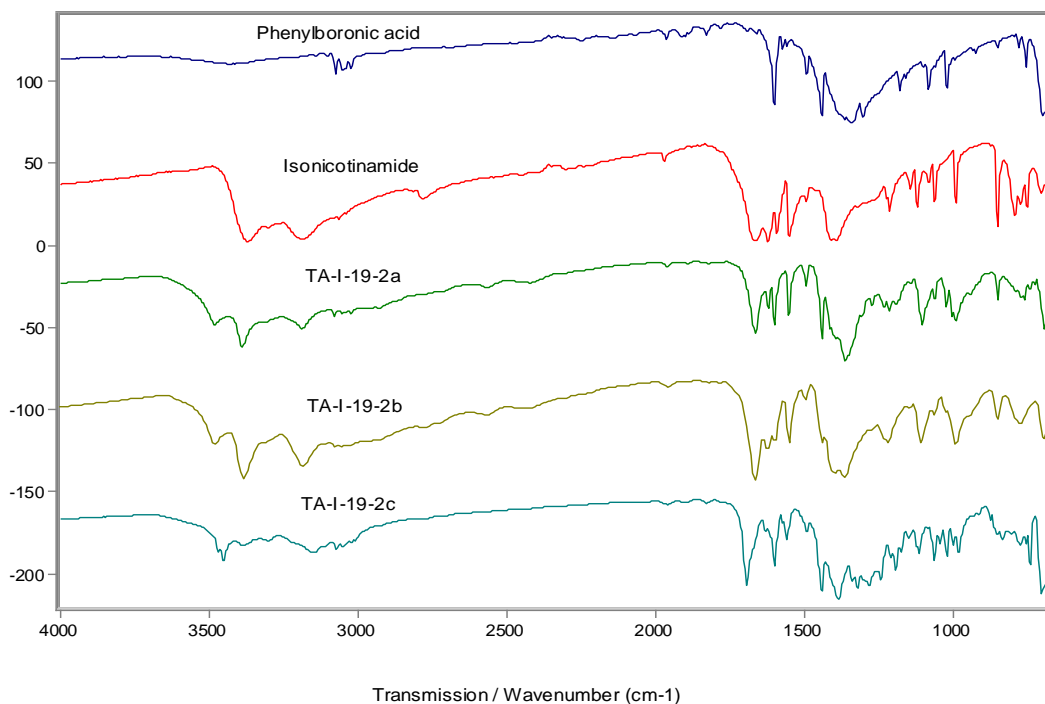
Figure 5.5: Comparative FT-IR spectra for TA-I-19-2a, 2b and 2c in ratios 1:1, 1:2 and 2:1 in MeCN

The comparative plots of the FT-IR spectra for TA-I-19-2a, 2b and 2c all had the characteristics expected of hydrogen bonded complexes, including the presence of both N-H stretching (~3481cm^{-1} shown by both TA-I-19-2a and TA-I-19-2b, and at ~3451cm^{-1} bending [~1495cm^{-1}] modes), see Figure 5.5. Consequently, the proposed multicomponent systems of TA-I-19-2a, 2b and 2c agree well with the results obtained from the PXRD pattern which is indicative that hydrogen bonded multicomponent system formation occurred.

The results obtained are similar to the results of TA-I-19-1a, 1b and 1c which were attained by using acetone as the solvent.
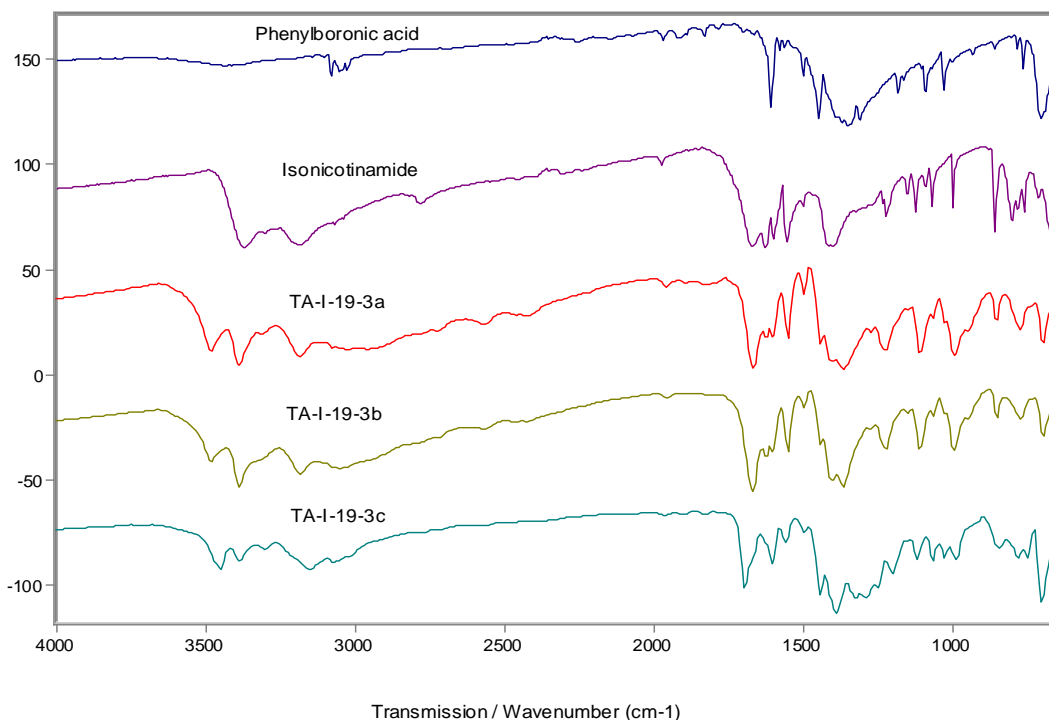
Figure 5.6: Comparative FT-IR spectra for TA-I-19-3a, 3b and 3c, in ratios 1:1, 1:2 and 2:1 MeOH

The TA-I-19-3a sample showed correspondence with phenylboronic acid, with peaks at 991cm^{-1} (ring deformation), 1604cm^{-1} (C=C stretch) and 3083 ($^{\upsilon}$OH), as well as consistencies with isonicotinamide which were fairly obvious at 755cm^{-1} (C-H wag), 1218cm^{-1} (C-N stretch), 1297cm^{-1} (ring deformation) and 3185cm^{-1} ($^{\upsilon}$NH$_2$) (O-C-H stretch). However, the multicomponent systems of TA-I-19-3a, 3b and 3c showed slightly different patterns at 2959, 2568, 1823 and 1624cm^{-1} which is representative that multicomponent formation occurred within these systems[98,99]. These results were similar to those obtained by the different solvents in TA-I-19-1a and TA-

162

I-19-2a, this is indicative that the solvent was not directly involved in the hydrogen bonding pattern.

5.2.1.2 Nicotinamide

The PXRD pattern shows the comparative study of the starting materials with the polymorphic forms. The resulting patterns showed that TA-I-20-2a had new peaks at 7.81, 9.22, 15.99, 17.77 and 26.77⁰, along the 2θ scale which indicates a new phase . The non- stoichiometric product of TA-I-20-2b showed peaks similar to the peaks present in the sample made from a 1:1 ratio. These peaks were showed at 7.79, 9.23, 14.51, 26.99 and 36.31⁰,along the 2θ scale. The different ratios 1:1 and 1:2 both show same new phase with excess of nicotinamide. However, TA-I-20-2c showed a few new peaks at 5.28 to 8.92, 10.39, 12.44, 13.01,14.50, 1585, 24.83, 26.66, 27.06, 28.08, 28.30 and 29.56⁰, along the 2θ scale which is different from the phase that was presented in 1:1 and 1:2. This is indicative that multicomponent formation occurred within these systems (Figure 5.7 and 5.8).

Further analysis was performed using the same system of phenylboronic acid and nicotinamide with methanol as the solvent. The product obtained was analysed with both PXRD and single crystal analyses. The PXRD pattern showed that the multicomponent system of TA-I-20-3a showed new peaks at 7.41, 9.28, 10.95, 4.22, 16.08, 18.05, 19.23, 20.70, 20.93, 26.63, 38.24 and 41.61⁰, along the 2θ scale. The non-stoichiometric product of TA-I-20-3b showed peaks that corresponded with nicotinamide, but new peaks were also identified at 9.50, 11.29, 14.90, 16.37 and 28.43⁰, along the 2θ scale. Finally, TA-I-20-3c showed new peaks at 6.54, 9.12, 10.46, 12.34, 13.02, 13.52,

17.08, 21.79 and 26.18⁰, along the 2θ scale, but a few peaks were identified at 15.17, 17.35, 18.24, 20.16, 21.17 and 28.92⁰ which corresponds with the starting materials or the polymorphic forms (Figure 5.7 and 5.8). The same system of phenylboronic acid and nicotinamide with acetonitrile as the solvent was used. The non-stoichiometric product 1:2 and 2:1 ratios all produced different phase with excess of nicotinamide at 2:1 ratio (Figure 5.7 and 5.8).
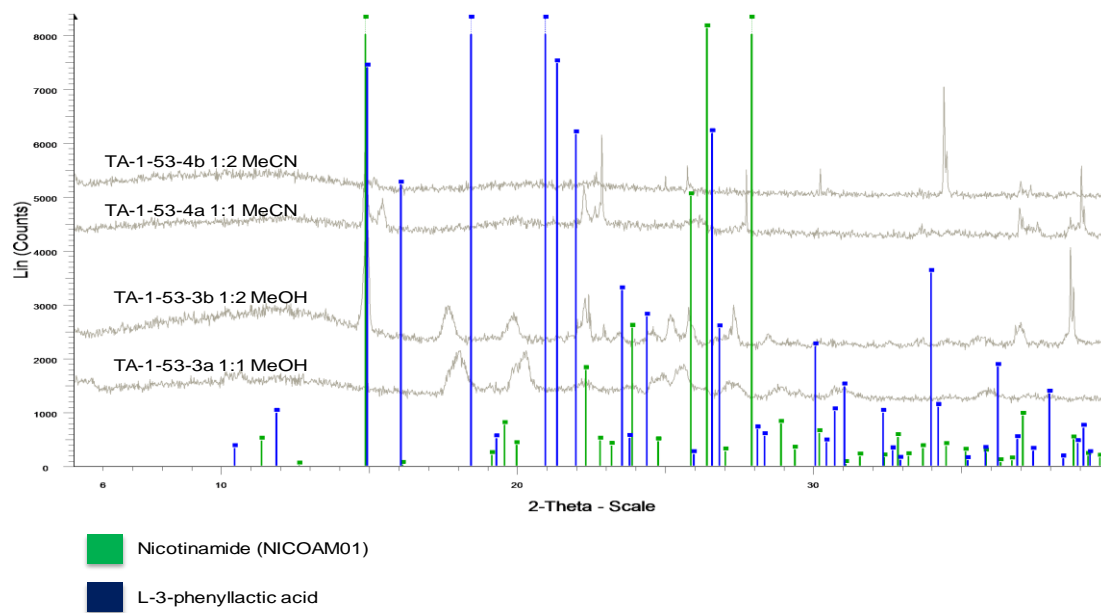
phenylboronic acid :nicotinamide
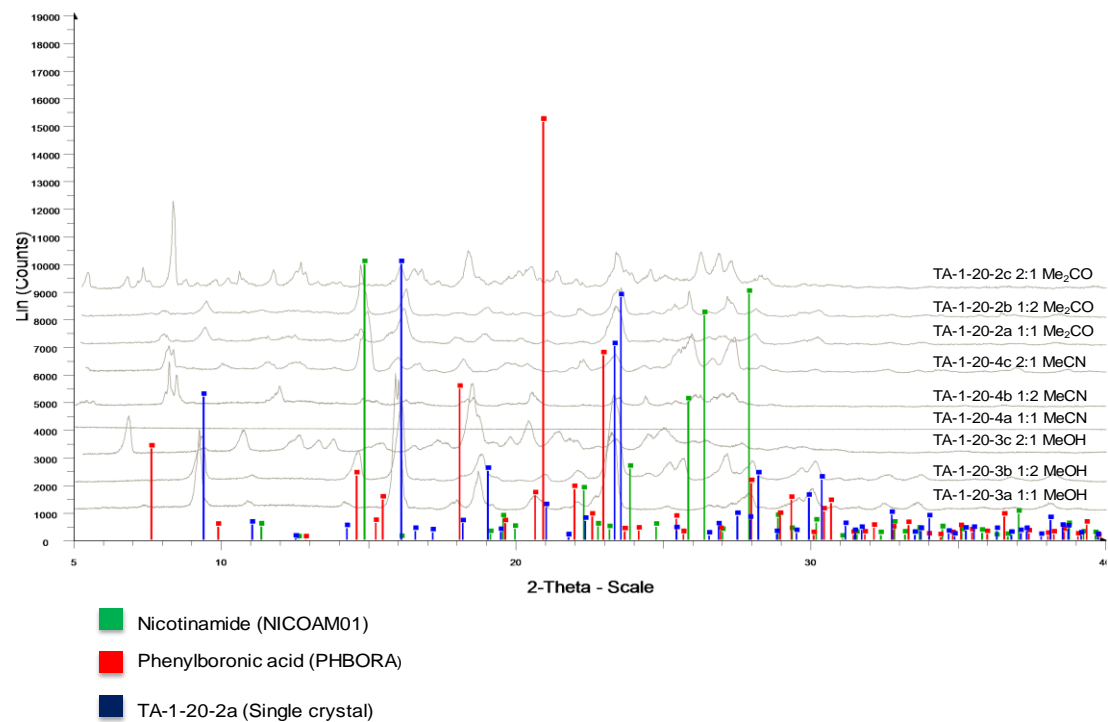
Figure 5.7: X-ray powder diffraction patterns of nicotinamide and phenylboronic acid, and products of crystallisation with a range of solvents

Graphical representation of crystalline phases identified from co-crystallisations of phenylboronic acid : nicotinamide
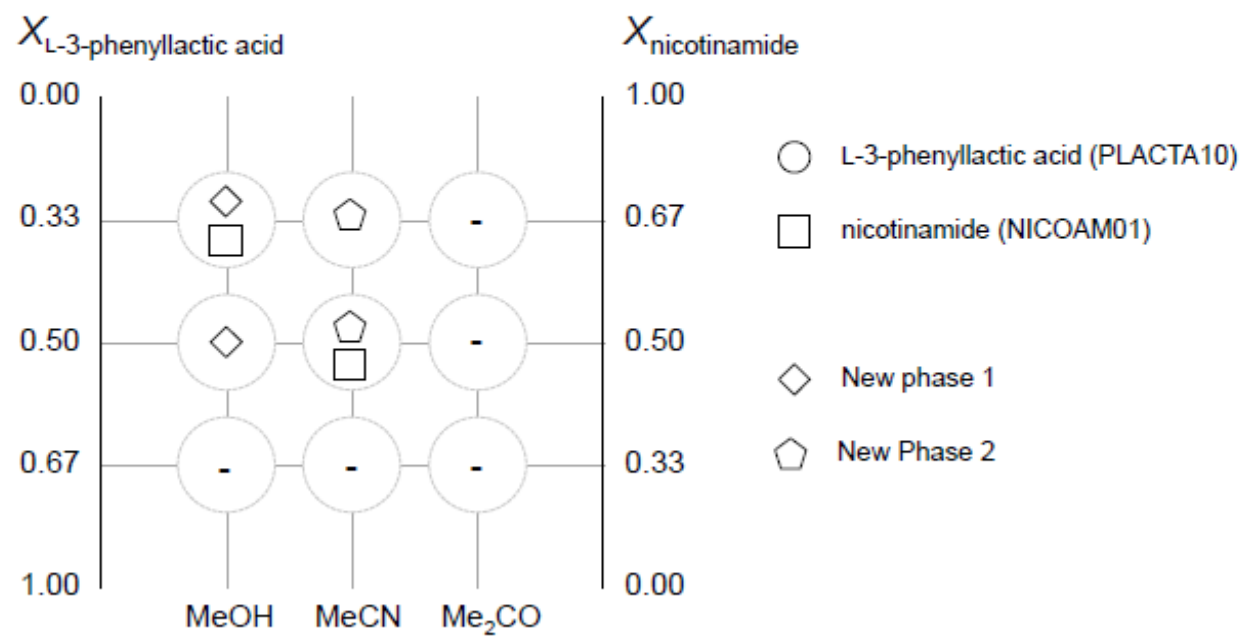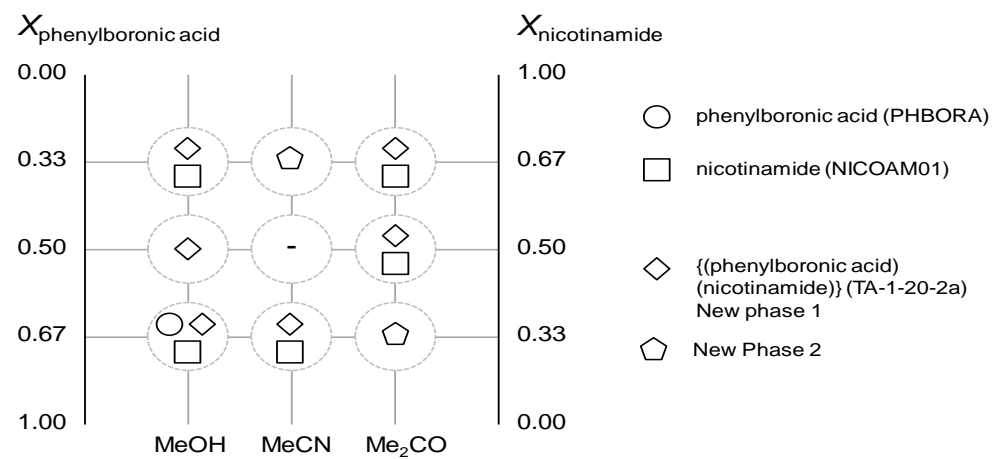

Figure 5.8: Representation of crystalline phases identified from co-crystallisations of phenylboronic acid and nicotinamide

Similar results were also observed for the PXRD pattern of these same systems when they used acetonitrile was used as the solvent.

Further investigation was then carried out using the FT-IR analysis for the ranges of 600 to 4000cm^{-1} (Figure 5.9).
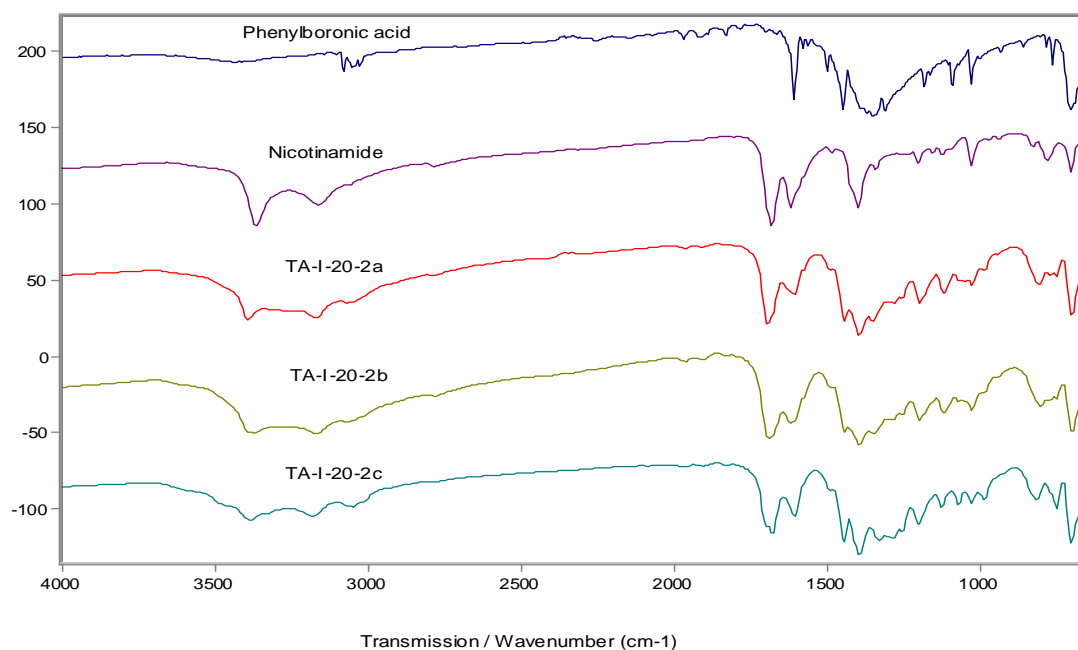
Figure 5.9: Comparative FT-IR spectra for TA-I-20-2a, 2b and 2c, in ratios 1:1, 1:2 and 2:1 in Me$_2$CO

The results indicate that nicotinamide (NH$_2$) presented symmetric and asymmetric stretching wavenumbers at 3366 and 3161cm^{-1}, for TA-I-20-2a at 3392, 3257 and 3314cm^{-1}, for TA-I-20-2b at 3371 and 3172cm^{-1}, and for TA-I-20-2c at 3383cm^{-1}. There was clearly an increase in hydrogen bonding through the NH$_2$ hydrogens which affected the NH$_2$ bending mode on the formation of the multicomponent systems[63]. Analogous wavenumber shifts were also obtained in aniline and phenylenediamine complexes[96,100]. The C-O stretching wavenumber was observed at 1693cm^{-1} in nicotinamide and at 1693, 1689 and 1678 cm^{-1}, respectively for TA-I-20-2a, 2b and 2c (Figure

167

5.8). Similar stretching and bending mode were also observed for TA-I-20-3a, 3b and 3c, as well as for TA-I-20-4a, 4b and 4c for the different solvents.

5.3   X-Ray Structure Analysis

5.3.2   Single Crystal Analysis of Polymorphic Forms of Phenylboronic Acid and Nicotinamide (TA-1-20-3a and RBi_1)
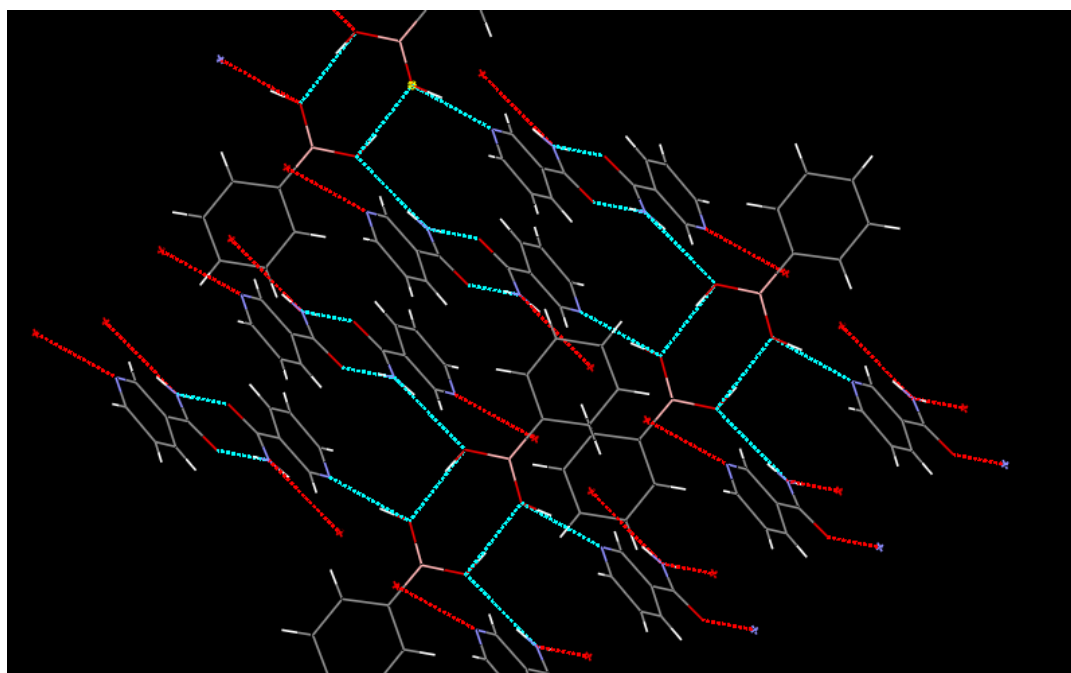
Figure 5.10: Triclinic crystal packing of the co-crystal of phenylboronic acid: nicotinamide

The crystal structure of the co-crystal of phenylboronic acid and nicotinamide displays the geometry of the crystal as triclinic. It shows that the dimeric nature of phenylboronic acid is linked with the nicotinamide molecules along with an extended network of H-bonds that are among the assemblage of appropriate functional groups.

The boronic acid group has a trigonal geometry and is fairly coplanar with the benzene ring. The CBO2 plane is quite coplanar with the benzene ring, with

a respective twist around the C–B bond for the two molecules of PhB (OH)$_2$. Each dimeric phenylboronic acid ensemble is also linked with hydrogen bonds to four other nicotinamide molecules in order to give an infinite array of layers.

Each hydrogen bonded unit of phenylboronic acid consists of phenylboronic acid, two distinct molecules of nicotinamide and other phenylboronic acid molecules which are bound through hydrogen bonds. The phenylboronic acid molecule is bound to the two distinct molecules of nicotinamide through O–H---N–H$_{(Nicotinamide)}$. The phenylboronic acid molecule is bound to the other molecule of phenylboronic acid through a pair of O–H---O hydrogen bonds.

Furthermore, each hydrogen bonded unit of nicotinamide consists of two distinct molecules of nicotinamide and one phenylboronic acid molecule, bound through hydrogen bonds. The nicotinamide molecule is bound to the other molecule of nicotinamide through C=O$_{(Nicotinamide)}$---N–H$_{(Nicotinamide')}$ and N–H$_{(Nicotinamide)}$--- C=O$_{(Nicotinamide')}$. The nicotinamide molecule is bound to one molecule of phenylboronic acid through N$_{(pyridine\ ring\ of\ nicotinamide)}$---O–H hydrogen bonds. The nicotinamide molecule also demonstrated interactions with another molecule of phenylboronic acid through a pair of N$_{(pyridine\ ring\ of\ nicotinamide)}$ with the ring carbons.

169
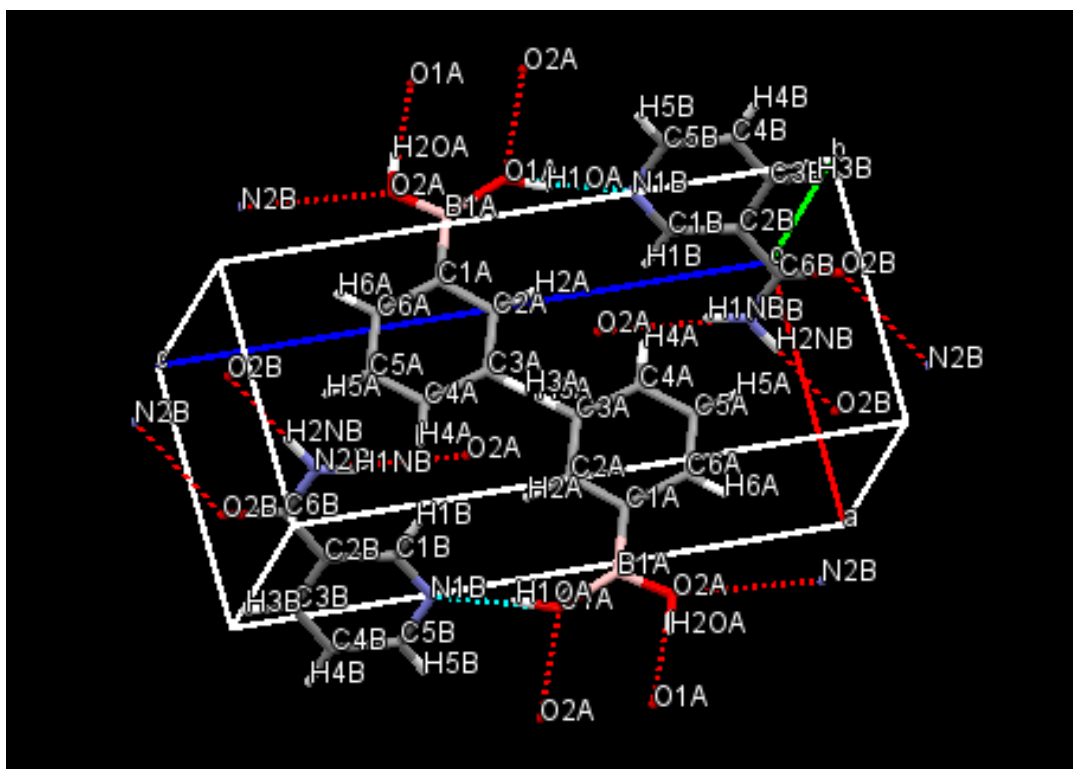
Figure 5.11: Extended hydrogen bonding network within co-crystal

Due to the behaviour of phenylboronic acid and its property which allows it to form hydrogen bonded dimers, phenylboronic acid and nicotinamide were found to co-crystallize with nicotinamide to form supramolecular assemblies. These assemblies involved hydrogen bonds that were between the B(OH)2 groups and the nicotinamide nitrogens and the carboxamide group. Furthermore, an extended network of H-bonds, found among the assemblage of the appropriate functional groups, supports the crystal structure. Consequently, these findings indicate noteworthy co-crystal properties.
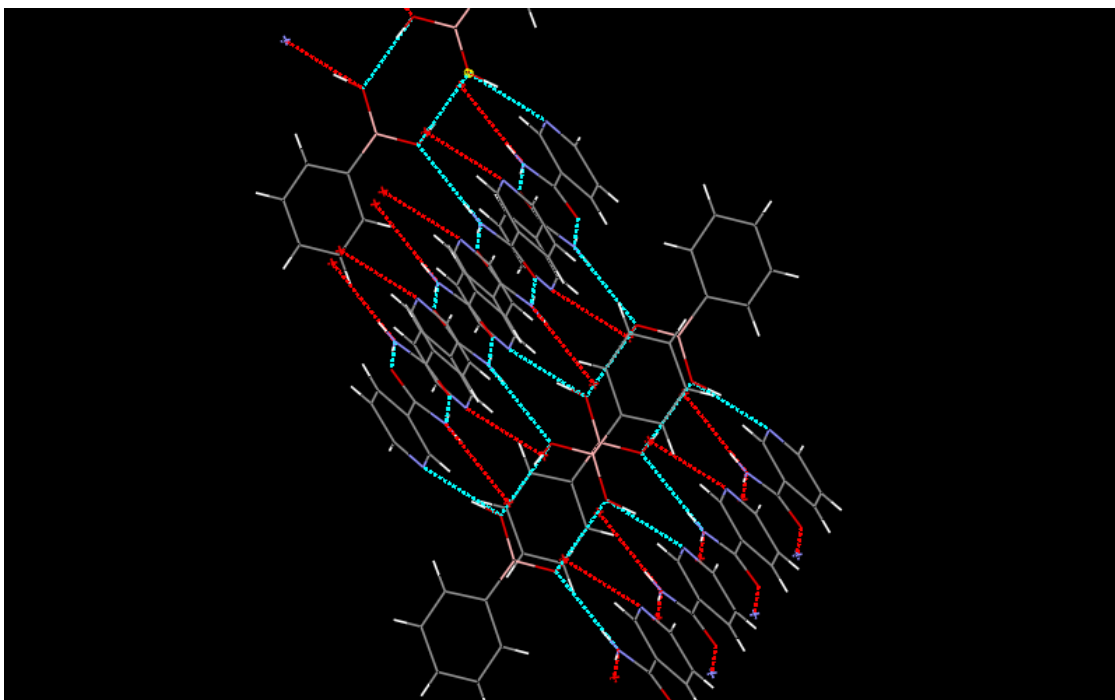
Figure 5.12: Formation of supramolecular hetrosynthon in TA-I-20-3a

The nicotinamide molecules look like a novel ribbon-shaped conformation. The catenated dimer, sometimes referred to as an amide tape or ribbon, is a chain of translational related dimers linked along a 5.1 Å short axis by N−H---O bonds. This supramolecular heterosynthon is a two-point recognition event as there are two ranges which correspond to the O−H---O and N−H---O interactions.

In this case, the supramolecular synthons are entirely different. The phenylboronic acid-pyridine OH_{acid} ---$N_{pyridine}$ supramolecular heterosynthon is formed and the primary amide is hydrogen which is bonded to the carboxamide group. The lone pair interaction of the carbonyl of carboxamide is shown with the NH_2 group of the other carboxamide group which is exhibiting a hydrogen bond.
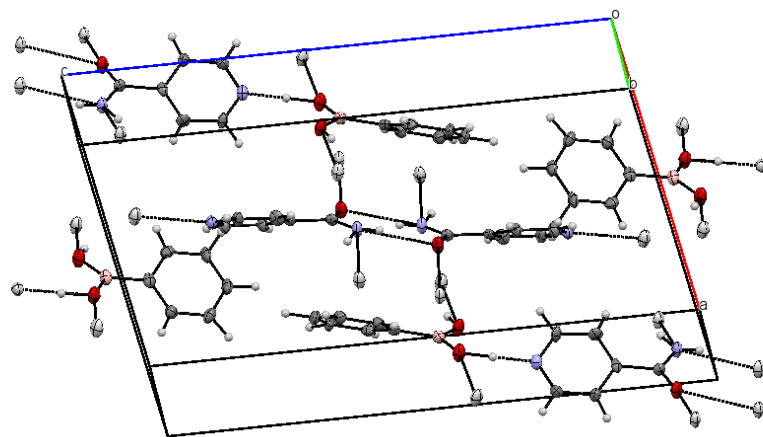
a)
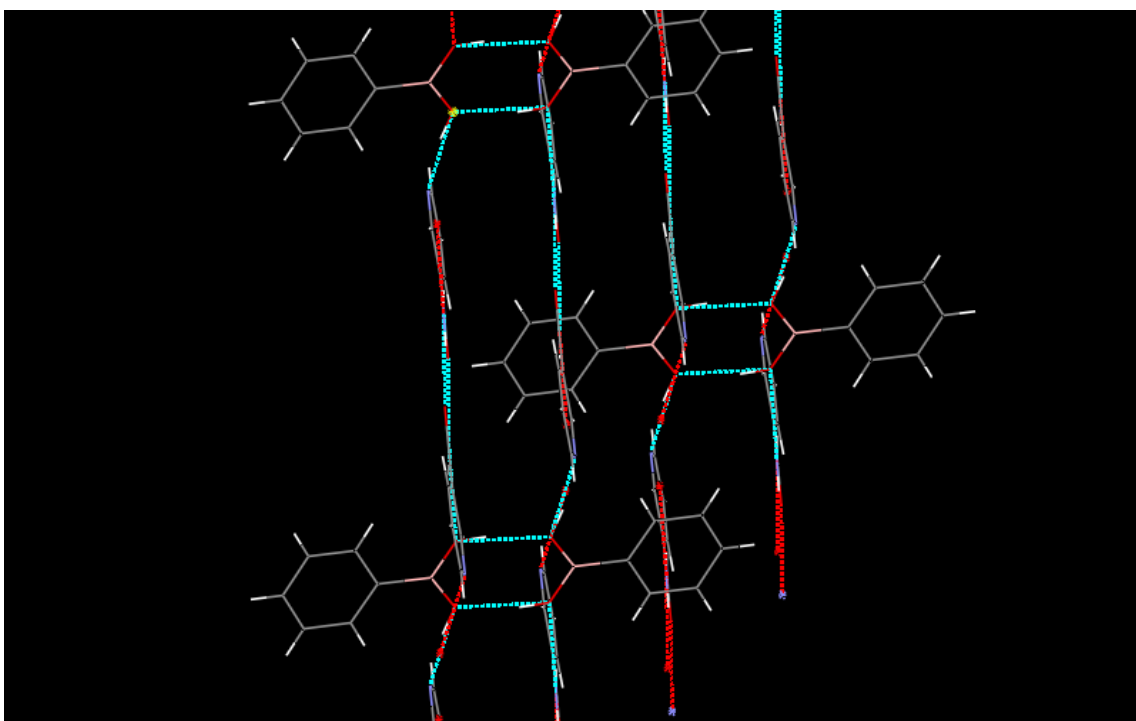
b)
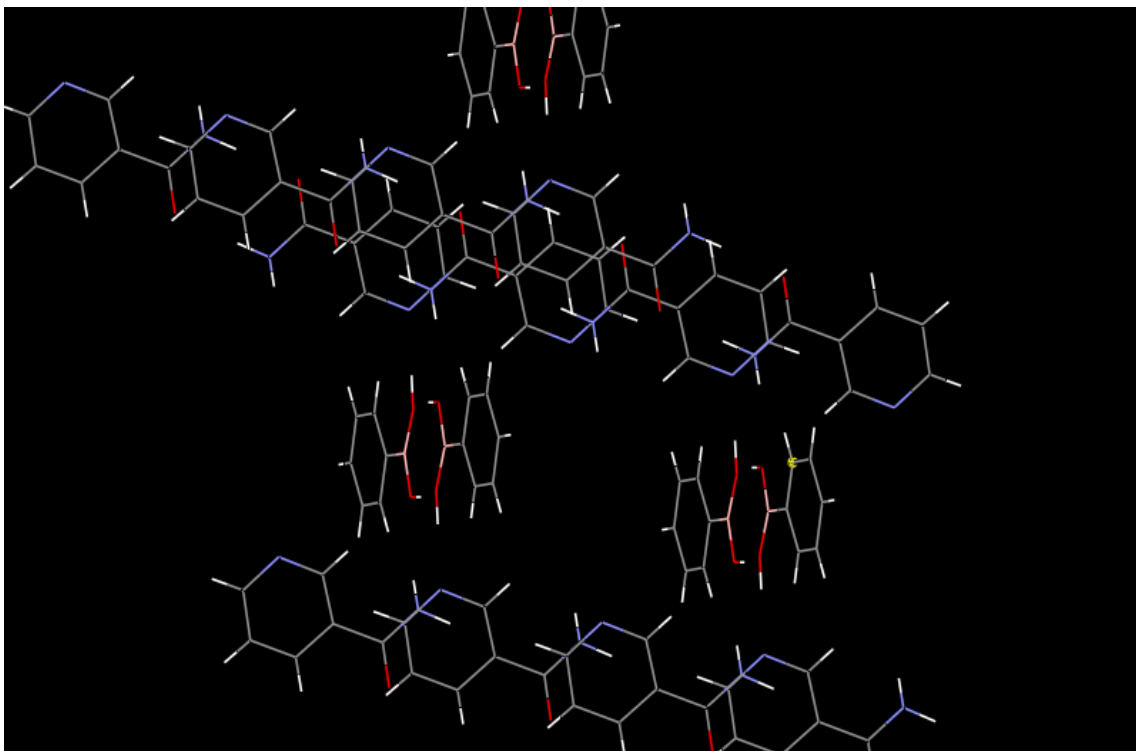
c)

Figure 5.13: The crystal packing of the phenylboronic acid: nicotinamide co-crystal showing: a) and b) Formation of ladder like structure by hetrosynthon, and c) The hydrogen bonding network

5.4 Discussion

The study of the multicomponent system of phenylboronic acid and nicotinamide was investigated by stoichiometric and non-stoichiometric mixtures, through the use of the PXRD, IR and single crystal analyses. The infrared absorption spectroscopy explains about the nature of interactions in the multicomponent system, specifically for identifying strong O-H stretching interactions which were involved in the specified formation of hydrogen bonding networks. All of the systems, whether stoichiometric or non-stoichiometric, produced multicomponent formations.

Single crystal analysis proved to be significantly helpful to the study as it detailed the hydrogen bonding network in the multicomponent system. The structure displayed the equivalent supramolecular synthons as expected for the boronic acid with isonicotinamide. The study also revealed that solvents only act as a medium of multicomponent formation as they did not take direct involvement in the bonding process. Consequently, consideration of the competition of the solvent- solute interactions and the weaker, more discrete, acid-amide interactions suggests that solvent selectivity is of value; however, further studies into explicit solvent-solute interactions are needed in order to explain this difference further. These results therefore highlight how the choice of solvent can play an important role in the selective growth of a desired molecular complex[18].

Chapter 6

6.0 An Investigation into Multicomponent Crystalline Systems from Phenylboronic Acids and Pyridine Co-Formers

Exploiting the dynamic covalent chemistry of the boroxine ring construction (see Figure 6.1), in the development of multicomponent systems, is based on the proliferation of hydrogen bonded networks as a means for assembly. This current research study focused on the binary systems of phenylboronic acid, with regards to 4,4'-bipyridine and 4-phenylpyridine. This research study also focused on determining the effect of different solvents and different molar ratios of starting materials on the multicomponent system.
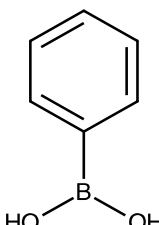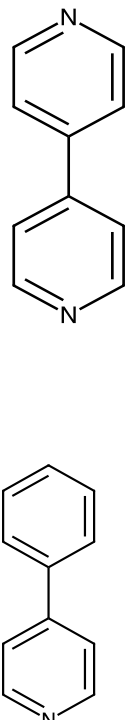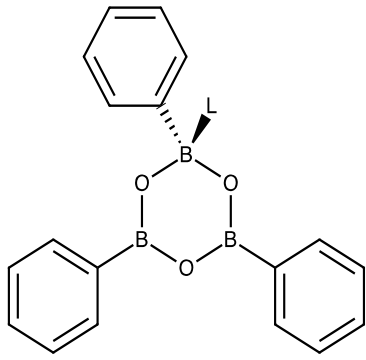
Acidic Donor	Basic Acceptor	Proposed Structure of Boroxine
Phenylboronic Aacid	4,4'-Bipyridine/ 4 Phenylpyridine	Boroxine (L is representation of legand)

Figure 6.1: The binary systems of phenylboronic acid, with regards to 4,4'-bipyridine and 4-phenylpyridine

6.1   Introduction and Aims of the Study

The main aim of this study was to investigate the potential for modification of the hydrogen bonding environment, within the hydrogen bonded multicomponent system of boroxines. This study also aimed to determine how the use of different solvents (acetone, acetonitrile and methanol) and the use of different molar ratios (1:1, 1:2 and 2:1), of the starting materials, could be used to drive the systems between the boronic acid co-crystal and the boroxine adduct; as such, it aimed to:

Prepare and characterise co-crystal systems of boronic acid.

Investigate and confirm that the boroxine ring forming reaction is a dynamic covalent process.

Investigate the thermodynamic equilibrium that exist between boronic acid monomer and boroxinestrimers.

Characterise the obtained multicomponent system in terms of the FT-IR, the PXRD and ^{1}HNMR.

6.2   Phase Chemistry

6.2.1   Crystallisation Studies of Phenylboronic Acids with Pyridines

6.2.1.1 4,4'-Bipyridine

Phenylboronic acid and 4,4'-bipyridine were dissolved in acetone in ratios of 1:1, 1:2 and 2:1. An analysis of the starting materials, against the samples of

TA-I-54-1a, TA-I-54-1b and TA-I-54-1c allowed for comparison and the drawing of initial conclusions as to whether a new phase was isolated.

The powder x-ray diffraction (PXRD) obtained for the multicomponent system were formed in 1:1, 1:2 and 2:1 ratios of phenylboronic acid and 4,4'-bipyridine, they also used acetone as the solvent for their formation.

The PXRD patterns obtained for phenylboronic acid, 4,4'-bipyridine and the 1:1 co-crystal product of TA-I-54-1a indicated that phenylboronic acid exhibited a characteristic scattering peak at 15.3 and 20.9°, and 4,4'-bipyridine exhibited a characteristic scattering peak at 22.4 and 25.0° .The 1:1 stoichiometric co-crystal products exhibited different scattering peaks at 20.2 and 25.5°, which is indicative that they did not correspond to the diffraction patterns of the starting materials; thus indicative that a new phase was formed.

The current research result patterns of phenylboronic acid with 4,4'-bipyridine can be compared to the research by Rodriguez-Cuamatzi *et al.*; the findings suggest that similar behaviours occurred when boric acid and 4,4'-bipyridine formed a co-crystal synthesis [(ba)(bpy)(H_2O)] using the stoichiometric, 1:1 ratio (Figure 6.2)[97]. Similarly, the current study also used acetone as the solvent which was not dried prior to use; interestingly, the moisture from the solvent also showed its effect on the bonding pattern.
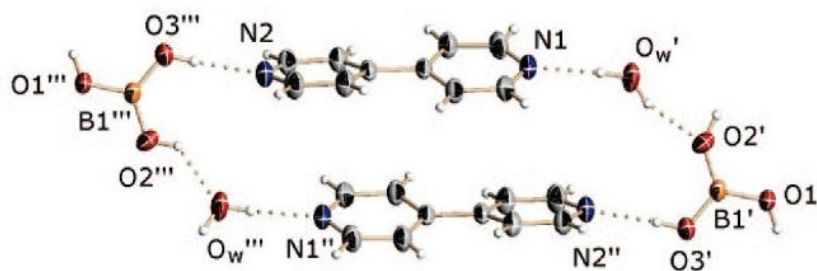
Figure 6.2: Hydrogen bonding motifs found in the crystal structures of [(ba)(bpy)(H$_2$O)]

The XRPD pattern of the non-stoichiometric multicomponent system was barely distinguishable from its starting material of phenylboronic acid and 4,4'-bipyridine, or from TA-I-54-1a. The pattern of 1:2 molar ratio of phenylboronic acid demonstrated similar peak appearances at 26.4°, with respect to phenylboronic acid; although, one peak had a scattering angle of 20.1° along the 2θ scale. This appeared to double in relative intensity. The XRPD pattern of the multicomponent system of the 2:1 phenylboronic acid molar ratio produced a major scattering peak that shifted slightly to 27.2° on the 2θ scale. Thus, strong new peaks were observed at the scattering angles of 26.4°, along the 2θ scale (Figure 6.3).

The XRPD pattern of a phenylboronic acid-rich multicomponent signifies more of a progression in the physical phases than the 4,4'-bipyridine did in terms of its rich molar ratio fraction. To illustrate, TA-I-54-1b showed more regular peak appearances then the TA-I-54-1c sample (which identified very few peaks). These insignificant peak appearances, in the region of 30 to 46°, were identified along the 2θ scale.

phenylboronic acid :4,4'-bipyridine
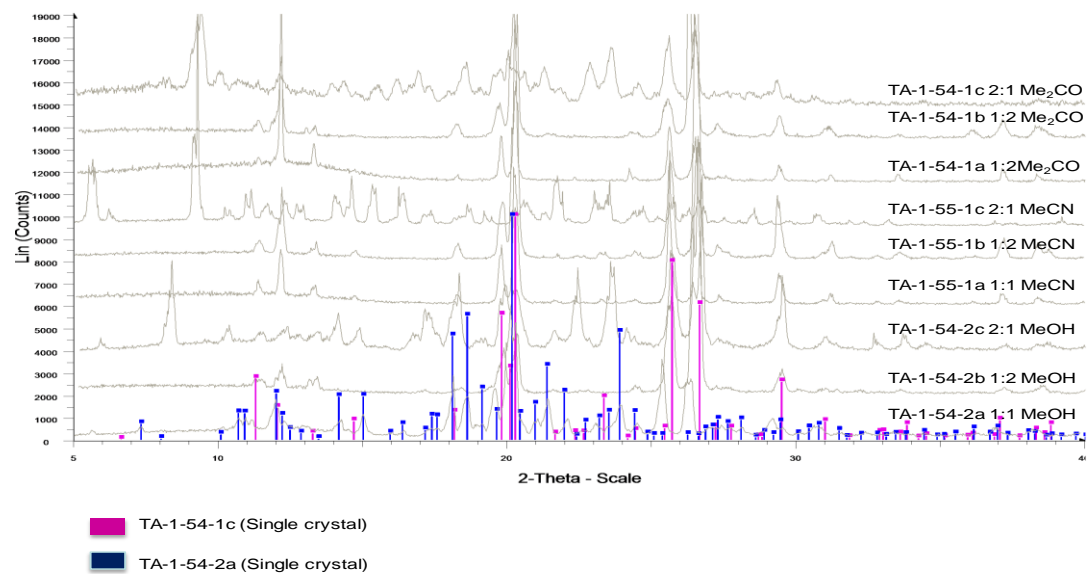
Figure 6.3: X-ray powder diffraction patterns of 4,4' bipyridine and phenylboronic acid, and products of crystallisation with a range of solvents

Graphical representation of crystalline phases identified from co-crystallisations of phenylboronic acid : 4,4' -bipyridine
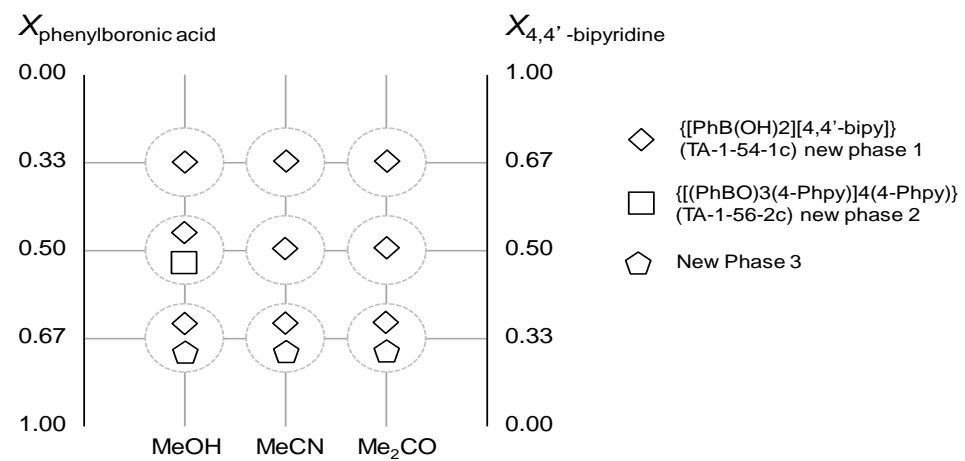
Figure 6.4: Representation of crystalline phases identified from co-crystallisations of 4,4' bipyridine and phenylboronic acid

The study conducted by Rodriguez-Cuamatzi *et al.* demonstrated similar interactions for multicomponent complexes. During their study, they concluded that the supramolecular structures that were outlined by [(1,4-bdba)(bpy)$_2$] (**1**) and [(3-apba)(bpy)$_2$] **(2)**, for boronic acid and 4,4'-bipyridine concluded that the molecules interacted with each other through a hydrogen bonding motif [where each dihydroxyboryl group is connected to two bpy molecules through O-H---N hydrogen bonds. This was similar to that found for the 1:2 adduct between phenylboronic acid and bpy ([(pba)(bpy)$_2$] (see Figure 6.5). This conclusion will be helpful for the prediction of structures of supra-molecular synthons[101].
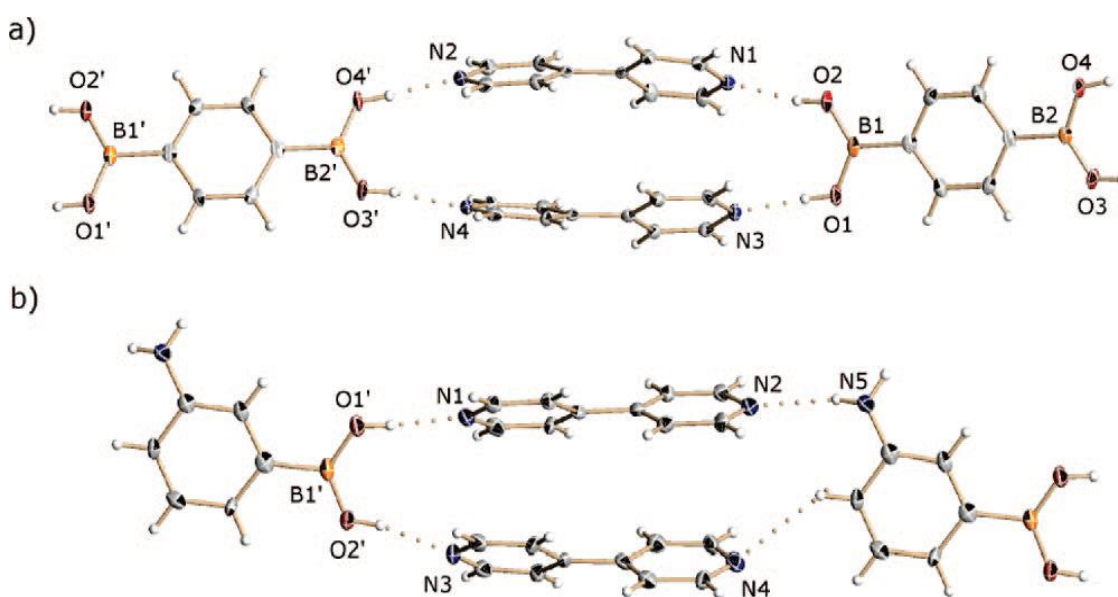
Figure 6.5: Hydrogen bonding motifs found in the crystal structures of: (a) [(1,4-bdba)(bpy)2] (1); and, (b) [(3-apba)(bpy)(2)

The samples of TA-I-54-1b were also analysed using single crystal analysis (provided by Professor Scowen, University of Bradford); the results of which clearly illustrate that the primary hydrogen bonding motif, comprised of

hydrogen bonded networks with significant (B)O-H---N, (B)O-H---O, C-H---O, C-H---N, C-H---π, π---π and C-H---B interactions.
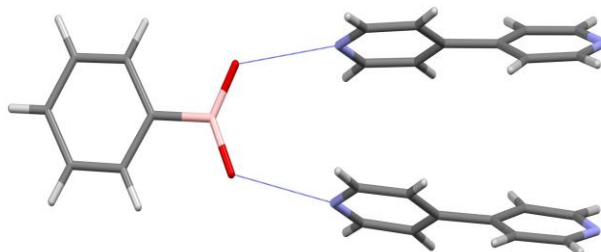
Figure 6.6: Primary hydrogen bond motif of TA-I-54-1b

The secondary hydrogen bonding motif for sample TA-I-54-1b (as provided by Professor Scowen) also demonstrates the outcome in the hydrogen bonding network by the intervention of the water molecule (see Figure 6.6). The motif clearly showed linkage of the parallel strands of N-H---π hydrogen bonding. The imperative facet of this motif is the emergence of the centroid (signified by the pink sphere in Figure 6.7). It is worth noting that the centroid is in the vicinity of the electron density which is positioned in the centre of this aromatic system. The strong N-H bonds are generally formed in areas where centroid π electron density lies within the neighbouring phenylboronic acid.
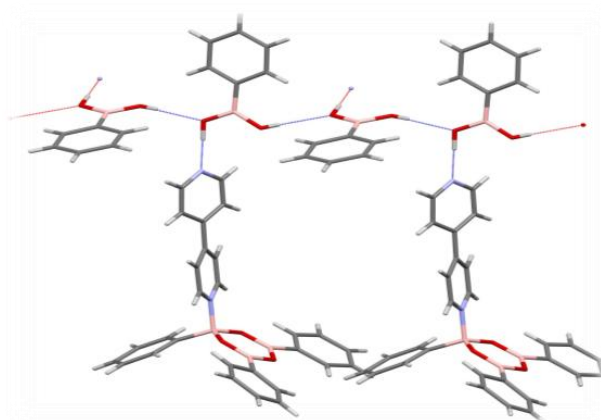
Figure 6.7: The secondary hydrogen bonding motif for sample TA-I-54-1b

The secondary hydrogen bonding motifs, as depicted by Rodriguez-Cuamatzi *et al.* explained four types of secondary interactions that occurred between the C-H acid hydrogen atoms of the pyridyl moieties and the neighbouring boronic acid molecules[149] as the following interactions: (i) C-H---O, (ii) C-H---N, (iii)C-H---π and (iv) C-H---B. All of the C-H---O, C-H---N and C-H---π interactions were within the previously established limits[102,103]. However, in this case the boron atoms were involved in pπ---pπ-interactions with the oxygen atoms, this provides them with electron density. Interestingly, a search of the CSD database[104] revealed 27 entries for boronic acids, eight of which showed intermolecular C-H---B interactions in their crystal. Therefore, it can be suggested that C-H---B interactions play a non-negligible role in the structures of supramoleculars.

As in most of the known crystal structures of boronic acids[97], the hydroxyl groups that are attached to the boron atoms have syn-configuration. In the hydrogen bonded macrocycles, the pyridine rings of opposite bpy molecules have slightly displaced parallel-sandwich geometries[105] which are almost coplanar to each other, thus they form centroids. According to Rodriguez-Cuamatzi *et al.*, within each bpy molecule, the pyridine rings are twisted around the central C-C bonds, by angles ranging from 28.6 to 37.5° [97]. Thus, based on these progress result patterns, and by observing the behaviour of boronic acid and 4,4'-bipyridine, the predicted macromolecule structures will resemble the structures presented in Figure 6.8.
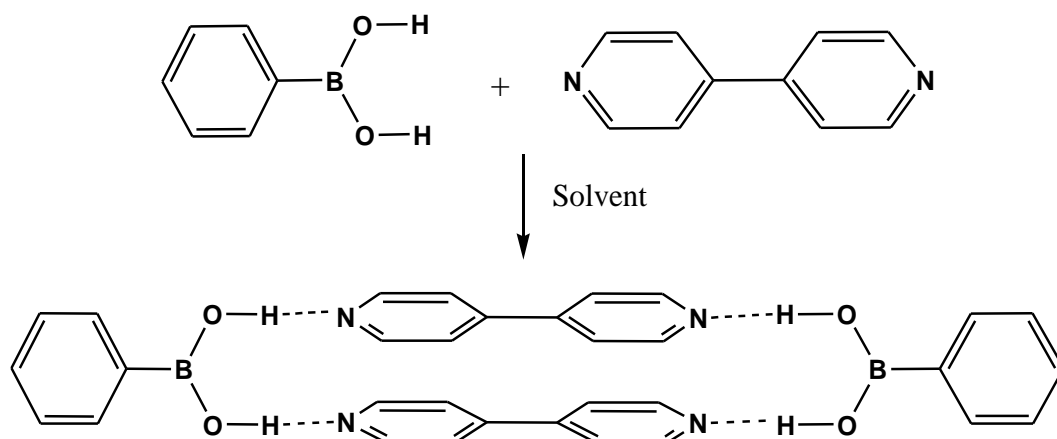
Figure 6.8: Predicted macromolecule structures of boronic acid with 4,4'-bipyridine

An interesting aspect of this analysis "the formation of boroxines ring", is that not much is observed in the 1:1 ratio multicomponent adduct – this is supported by the work presented by Kua *et al.*[106]. They noted that the trimerisation of phenylboronic acids to form arylboroxine rings (step 1), is enthalpically unfavourable. In contrast, the formation of stable 1:1 adducts (step 2), was highly favourable, thermodynamically; in fact, it was sufficiently favourable to drive the two-step reaction forward toward formation of the products. The main reason for this reaction is substitution of the π-electron-withdrawing groups, in the para position of the phenyl ring, which was disfavoured in step 1; whereas, the π-electron-donors behaved in total opposition to this. Conversely, the substituents that were overall electron-withdrawing tended to favour step 2, whereas electron donors disfavoured it (Figure 6.9)[106].

Figure 6.9: Two-step reaction sequence of boroxine construction followed by adduct formation

Further investigation was performed on the data collected from TA-I-54-1a, TA-I-54-1b and TA-I-54-1c, and its starting materials in order to verify the initial conclusions (see Table 6.1). FT-IR analysis was also performed to determine whether or not the anticipated hydrogen bonded multicomponent structure had been formed (Figure 6.10).

Transmission / Wavenumber (cm-1)

Figure 6.10: Comparative FT-IR spectra of TA-I-54-1a, 1b and 1c, in ratios 1:1, 1:2 and 2:1 in Me$_2$CO

186

Table 6.1: FT-IR assignments for samples TA-I-54-1a, TA-I-54-1b and TA-I-54-1c in Me$_2$CO

Phenyl boronic acid cm^{-1}	4,4'-bipyridine cm^{-1}	TAI-54-1a cm^{-1}	TAI-54-1B cm^{-1}	TAI-54-1c cm^{-1}	Assignment $\bar{\upsilon}$ (cm^{-1})
	3429	3860, 3721 3637	3446	3436	O-H, stretch
3273 3081 3024	3025 2927 2895			3020,3050	OH and VOD
2419	2362	2342,2361	2360,2342	2340	
1964	1942			1956	
1894	1868				
		1722,1710			
	1654	1692,1665 1620		1626	C=N stretch
1604	1592	1594	1594	1601	C=C stretch
1572		1572,1567			C=C stretch
	1540 1532	1548,1530	1532	1543	C=C stretch
1499	1488	1480		1493	C=C stretch
1439	1406	1440,	1447	1442,1417	B-O asym. stretch
	1409	1401	1400	1390	
1350		1377,1341	1374,1341	1340,1326	
1275, 1191	1218		1211	1280,1212 1199	C-O stretch
1161	1123			1176,1122	C-O stretch
1095			1066	1085	C-O stretch
1072	1075	1023	1042		C-O stretch
1029	1038		1023	1069	B-C stretch
1007		1001	1001	1019 1001	
972	988	990	990	980	B-O sym. stretch
923	850		845	826	C$_{sp2}$- H bending
803	803	801	801	811	B-O sym. stretch
764	733	781,781		769	Boroxole ring
697, 857		715, 668	688,651	746, 707,672	BO2 out- of -Plane

The FT-IR spectra of the starting materials and corresponding multicomponent systems of TA-I-54-1a, TA-I-54-1b and TA-I-54-1c showed many strong and clear stretching modes (Figure 6.9). These stretching modes reflected the arrangement of phenylboronic acid with 4,4'-bipyridine utilising hydrogen bonded network assemblies. As shown in Table 6.1, some stretching modes were confirmed, such as an O-H stretching mode (in the region of $3637cm^{-1}$ in TA-I-54-1a, and approx $\sim 3446cm^{-1}$ in both TA-I-54-1b and TA-I-54-1c) which supported the proposition that formation of multicomponent systems was successful. In contrast, the C=N stretching mode appeared at $\sim 1620cm^{-1}$ (for TA-I-54-1a and TA-I-54-1c) and the C=C stretching mode, for all three multicomponents, occurred in the region of $\sim 1600cm^{-1}$. In particular, the symmetric and asymmetric B-O stretching modes of phenylboronic acid, and three multicomponent adducts, were assigned at $\sim 1430cm^{-1}$ and $\sim 850cm^{-1}$, respectively.

The B-O-H deformation (δBOH) can be easily recognised in the spectrum of phenylboronic acid; however, in multicomponent systems, its frequency is lowered slightly. A strong band at $1007cm^{-1}$ in the spectrum of phenylboronic acid, which shifts to $990cm^{-1}$ upon multicomponent formation, is identified with this vibration. The bands located at 1197 and $929cm^{-1}$, and at 1183 and $914cm^{-1}$, have been assigned to δ BOH in the phenylboronic acid and multicomponent system.

On the basis of these results, it is possible to assume that the multicomponent systems of TA-I-54-1a, TA-I-54-1b and TA-I-54-1c have relatively well-ordered constructions.
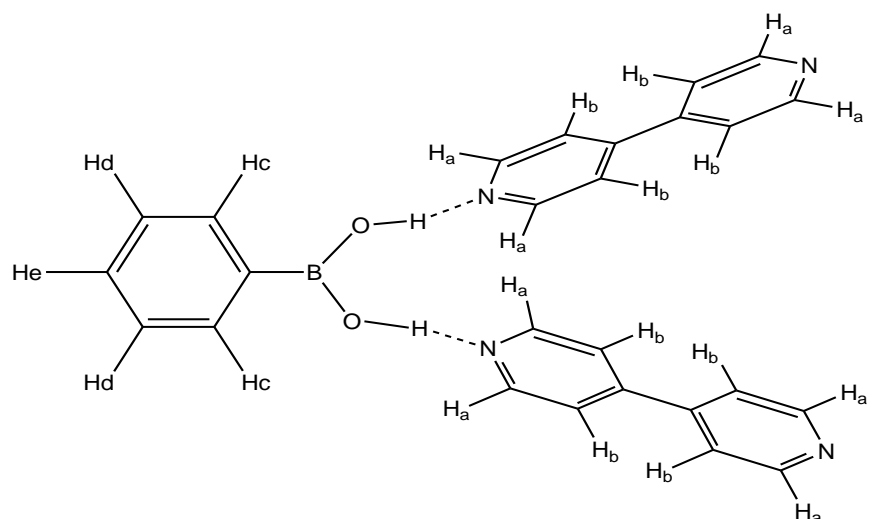
Figure 6.11: Predicted macromolecule structures showing N-H bonding pattern between phenylboronic acid and 4,4'dipyridyl

The crystal structure of the co-crystal of phenylboronic acid and 4,4'-dipyridyl was shown as belonging to space group C2. It showed phenylboronic acid linked with 4,4'-dipyridyl molecules through hydrogen bonds which provided an infinite array of layers which contained discrete termolecular coordinating structures. The boronic acid group has a trigonal geometry and is fairly coplanar with the benzene ring, and the CBO2 plane is quite coplanar with the benzene ring.
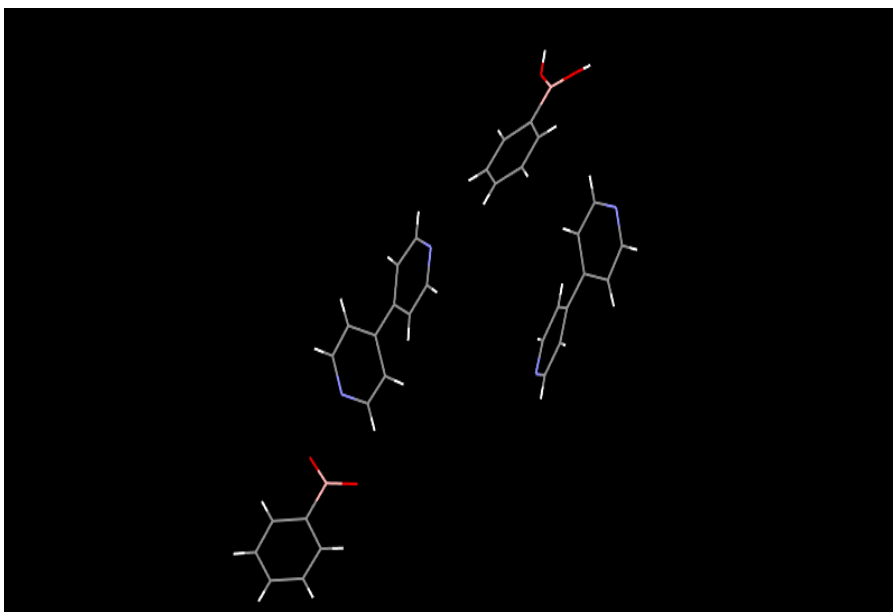
Figure 6.12: Crystal structure showing basic unit of phenylboronic acid and 4,4'-dipyridyl molecule

Each hydrogen bonded unit of phenylboronic acid consists of phenylboronic acid and two distinct molecules of 4,4'-dipyridyl which are bound through hydrogen bonds. The phenylboronic acid molecule is bound to the two distinct molecules of 4,4'-dipyridyl through O–H---N.

In packing each hydrogen bonded unit of 4,4'-dipyridyl, one molecule of 4,4'-dipyridyl and half a molecule of phenylboronic acid were bound through N---O–H hydrogen bonds. The 4,4'-dipyridyl molecule was bound to one molecule of phenylboronic acid; the 4,4'-dipyridyl molecule also showed weak interactions with another molecule of phenylboronic acid through a pair of N with the ring carbons.

The crystal structure also supported the IR spectral data, as discussed previously. A strong band of B-O-H deformation at 1002 and 929cm^{-1}, that was easily recognised in the IR spectrum indicated the complexation of

phenylboronic acid, while also ruling out the possibility of triphenylboroxine formation.

As no peaks were observed in the IR spectrum, in the region of 1080 to 1090cm^{-1}, which corresponds to the B-C stretching vibrations of phenylboronic acid, again this ruled out the possibility of phenylboronic anhydride formation.

The crystal structure therefore clearly indicates the conformation of BOH in boronic acid, being syn-syn. Each 4,4'-dipyridyl ring is stacked parallel to the other 4,4'-dipyridyl ring, this could be as a result of the π-π interactions of the two aromatic rings.
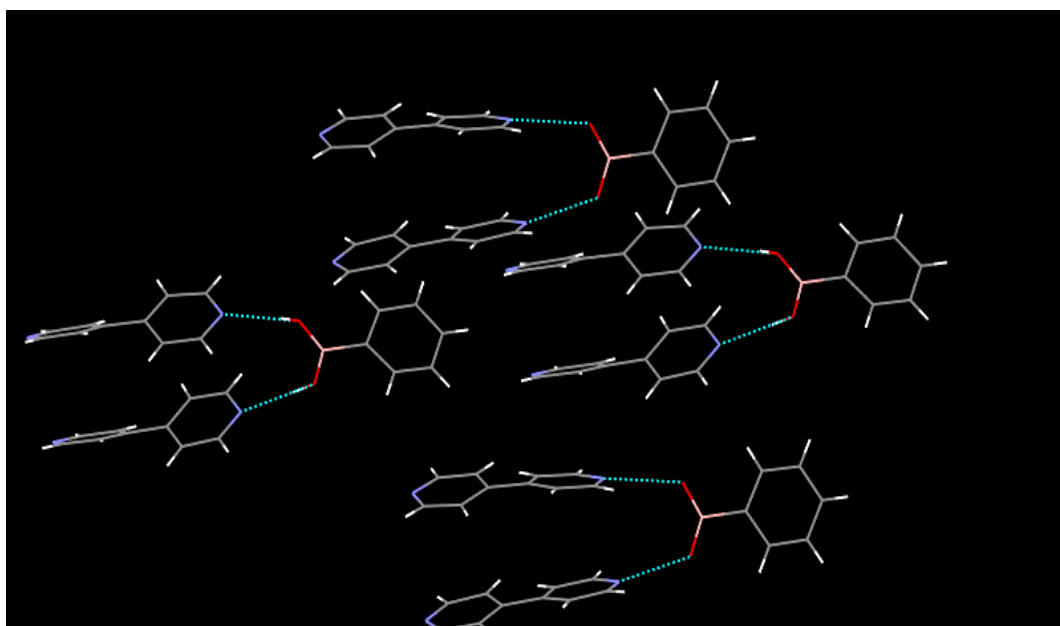
Figure 6.13: Crystal structure indicating the π-π interactions of the two aromatic rings

As shown in the packing diagram, the hydrogen bonded dimers of phenylboronic acid did not appeared in the crystal structure due to the fact that the concentration of phenylboronic acid is half of the concentration of

4,4'-dipyridyl. An extended network of H-bonds, among the assemblage of appropriate functional groups, supports the crystal structure. These findings are noteworthy as they are indicative of co-crystal properties. In this case, phenylboronic acid-pyridine OH---N supramolecular heterosynthon is formed.
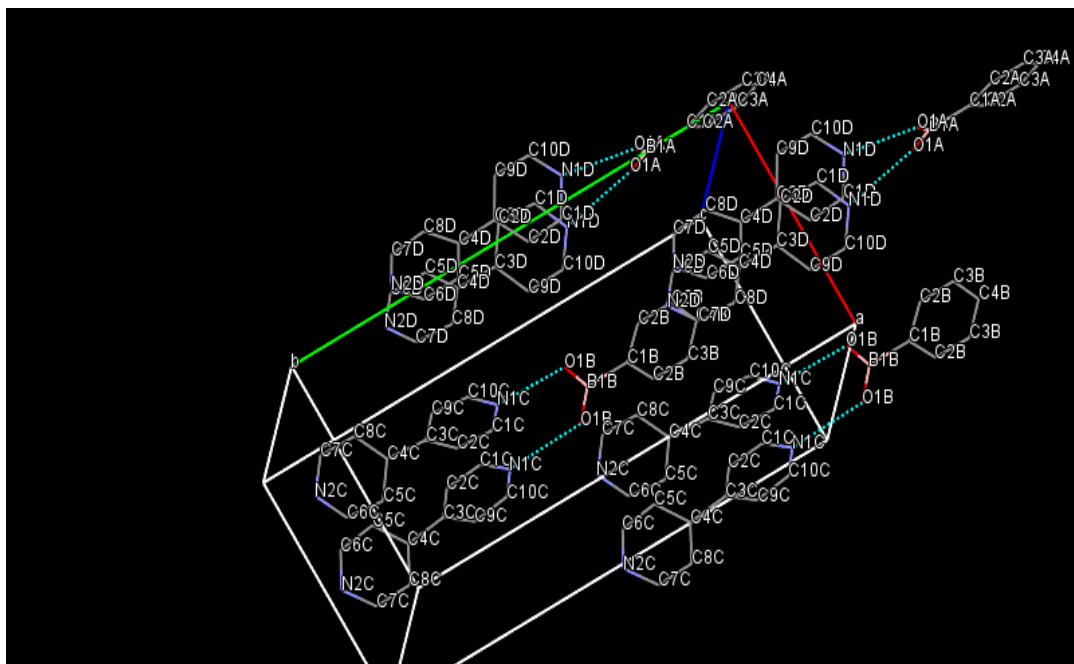
Figure 6.14: Supramolecular heterosynthon is formed within Twin4 TA-I-54-1b

The co-crystal is a multiple component crystal in which all components are solid under ambient conditions, when used in their pure form; thus, in order to study the phenomena in more detail, different solvents were used (acetonitrile and methanol) during the multicomponent system formation (Figure 6.3 and 6.4). The solid products (TA-I-54-2a and TA-I-55-1a) were analysed using powder x-ray diffraction (PXRD) and infrared (IR) analysis. Peaks appeared at positions within the multicomponent system for TA-I-54-1a (when acetone was used as the solvent – see Figure 6.3.), the results were similar to the multicomponent system of TA-55-1a (where acetonitrile

was used as the solvent) at angles 12.11, 13.25, 19.71, 20.23, 25.59, 26.53, 29.41 and 37.14⁰, along the 2θ scale; however, new peaks also appeared at 31.18 and 32.80⁰, along the 2θ scale.

When comparing the multicomponent systems of TA-54-1a and TA-55-1a with the system of TA-I-54-2a (using methanol as the solvent), somewhat different PXRD patterns were shown (see Figure 6.3) and totally new peaks appeared in the region of 5.74, 7.43, 10.26, 14.33, 27.84, 30.81, 34.61, 35.90, 36.40 and 37.05⁰, along the 2θ scale. These peaks were not linked to either the starting materials (phenylboronic acid, 4,4'-bipyridine) or the other multicomponent systems which had been formed using acetone and acetonitrile as solvents. Thus, indicating that sample TA-I-54-2a had formed a multicomponent complex while also being indicative that hydrogen bonding is stronger. In addition, it is well known that methanol is a very polar solvent which also enhances the hydrogen bonding network.

Wakabayashi *et al.* discuss solvent behaviour for these boroylpyridines as being dependent on their dipole moment; thus, greater polar solvents provide better stabilisation, due to greater solvation which favours the cyclic trimers[107].

Table 6.2: FT-IR assignments for samples TA-I-54-2a, TA-I-54-2b and TA-I-54-2c in MeOH

Phenyl-boronic acid cm^{-1}	4,4'-bipyridine cm^{-1}	TAI-54-2a cm^{-1}	TAI-54-2B cm^{-1}	TAI-54-2c cm^{-1}	Assignment $\bar{\upsilon}$ (cm^{-1}) [36]
	3429	3436	3430	3436	O-H, stretch

3273, 3081 3024	3025 2927 2895	2919	3044 2921	3043, 2921 2852	C_{sp2}-H stretch
2419	2362	2361,2342	2360,2342	2361,2342	
1964	1942	1954	1932		
1894	1868				
	1654	1629	1619	1630	C=N stretch
1604	1592	1601		1602	C=C stretch
1572		1540	1531		C=C stretch
	1540 1532		1532	1540	C=C stretch
1499	1488		1483		C=C stretch
1439		1442	1447	1442,	B-O asym. stretch
	1409	1413	1400	1414	
1350		1396,1341	1376,1313	1394,1325	
1275, 1191	1218	1283,1211 1193	1211	1283,1211 1196	C-O stretch
1161	1123		1116	1149	C-O stretch
1095			1098	1085	C-O stretch
1072	1075	1069	1065,1041		C-O stretch
1029	1038	1023	1023	1069	B-C stretch
1007		1003		1030	
972	988	989	990		B-O sym. stretch
923	850		845	864,832	C_{sp2}- H bending
803	803	802	801	814	B-O sym. stretch
764	733		781,733	703	Boroxole ring
697, 857		705 669	668	672	BO2 out- of -Plane

All major peaks of the IR spectra were assigned according to the literature[98,99] for stoichiometric molar mass ratio products (TA-I-54-2a, TA-I-54-2b and TA-I-54-2c) which indicates that all expected major functional groups were present upon successful co-crystallisation of the two reactants. The hydrogen bonded O-H groups were indicated at 3436, 3430, 3436cm^{-1} respectively, confirming that the hydrogen bonded network formed a supramolecular structure, since neither starting material indicates the presence of boroxol ring formation (see Table 6.2). This IR spectrum of multicomponent complexes suggests the bidentate bridging nature of 4,4'-bipyridine as well as the polymeric nature of the complex. Although, the infrared spectrum of 4,4'-bipyridine exhibits fewer absorption bands compared with the spectrum of the ligand, on co-ordination they change from non-planarity to planarity.

6.2.1.2 4-Phenylpyridine

The spectral PXRD data shown in Figure 6.15 noticeably illustrates that the samples of TA-I-56-1a, TA-I-56-1b and TA-I-56-1c are neither of the starting materials 4-phenylpyridine nor phenylboronic acid. The appearance of new peaks in the 1:1 stoichiometric ratio produced (TA-I-56-1a) 8.02, 11, 23 and 27⁰, along the 2θ scale, also supports this. The product obtained has also demonstrated that more peaks appeared in the multicomponent system which demonstrates less amorphous regions than the starting materials and therefore allocate it as a more discrete and well structured structure.

The PXRD results undoubtedly showed that non-stoichiometric molar ratio multicomponents TA-I-56-1b(1:2 molar ratio) showed the indication of

multicomponent formation with existence of 4-phenylpyridine. However, TA-I-56-1c (2:1molar ratio) showed peak positions and peak intensities that differed from the reference patterns (TA-I-56-1a) and starting material but concluding that multicomponent formation had taken place within system(see Figure 6.15 and 6.16). These results support the concepts drawn by the research conducted by Peddireddi *et al.*, about the optimisation of π-π interactions in these supramolecular synthons[74]. In this multicomponent formation, the trigonal planar boron can act as a Lewis acid, the addition of a Lewis base 4-phenylpyridine may lead to the formation of 1:1 adducts. In the adduct, a new B-N bond is formed and boron adopts a tetrahedral environment. The base donates electron density to the tetrahedral boron, which in the Lewis structure carries a formal negative charge (nitrogen has the formal positive charge).

phenylboronic acid :4-phenylpyridine

Legend:
- Phenylboronic acid (PHBORA)
- Tai_56_2c_0m (single crystal)
- 4-phenylpyriden (exptl pattern)
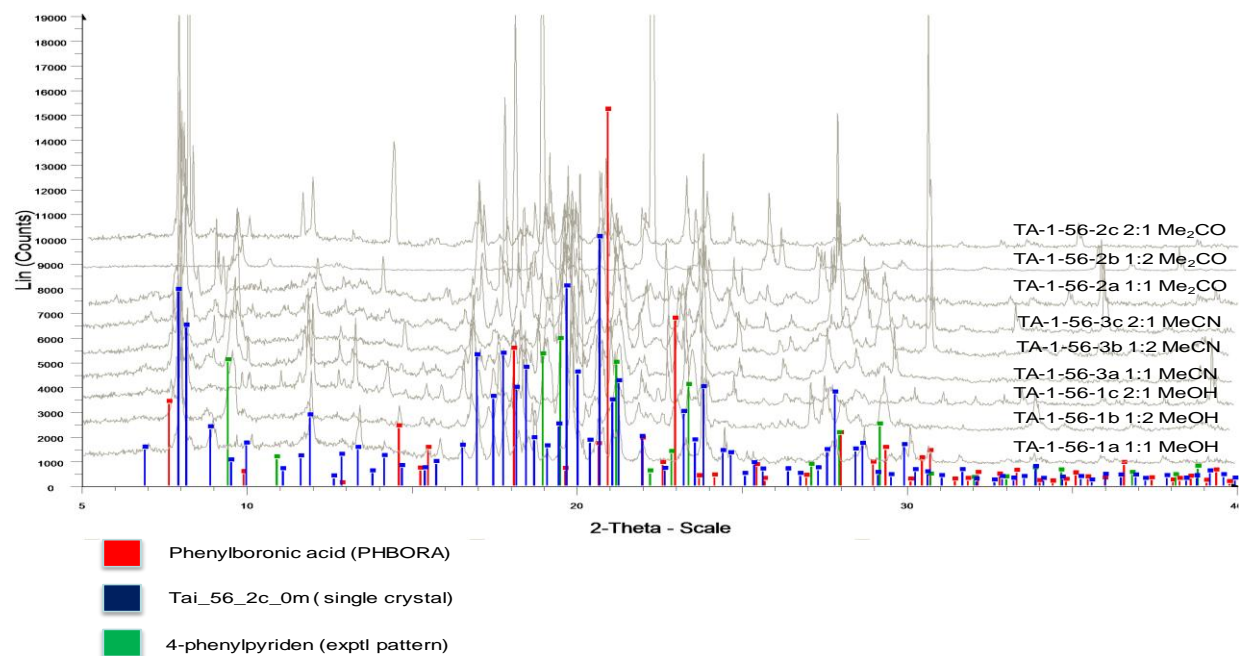
Figure 6.15: X-ray powder diffraction patterns of 4-phenylpyridine and phenylboronic acid, and products of crystallisation with a range of solvents

Graphical representation of crystalline phases identified from co-crystallisations of phenylboronic acid : 4-phenylpyridine
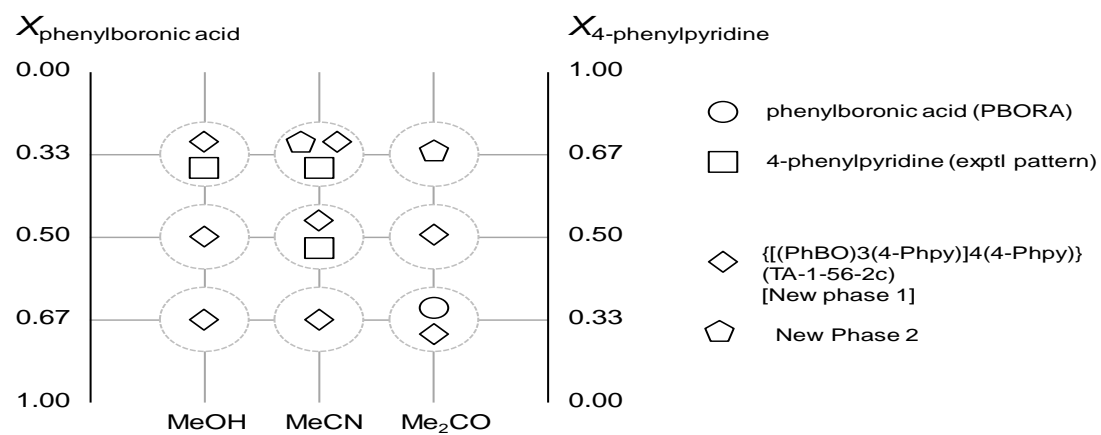
Figure 6.16: Representation of crystalline phases identified from co-crystallisations of 4-phenylpyridine and phenylboronic acid

Peddireddi *et al.* concluded that π-stacking can be engineered into co-crystalline condensed ladders using boronic acids[74,108]. In their studies they used the system of 4-methoxyphenylboronic acid with 4,4'-bpe producing the 1D infinite ladder (4-methoxyphenylboronic acid, 4,4'-bpe). The structure contained both syn and anti conformations of the hydroxyl groups, with O-H---O hydrogen bonds being nearest to the neighbour boronic acids. The rungs were sustained with O-H---N type hydrogen bonds (see Figure 6.17).
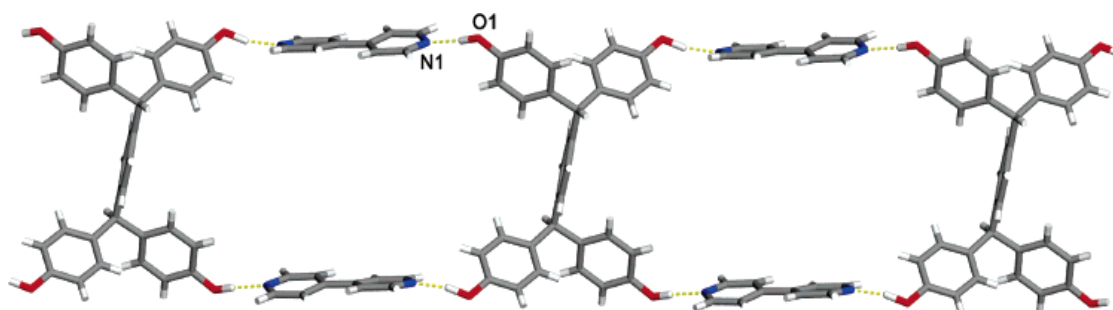
Figure 6.17: The self-assembly of (1,4-di[bis(4-hydroxyphenyl)methyl]benzene).(4,4-bpy) into a 1D ladder[108]

Inspired by the work of Peddireddi *et al.*[74], and observing the interaction of one N atom in the supramolecular synthons, the predicted structure of this multicomponent complex, using 1:1 ratio of the starting material can be presented below in Figures 6.18a and 6.18b.
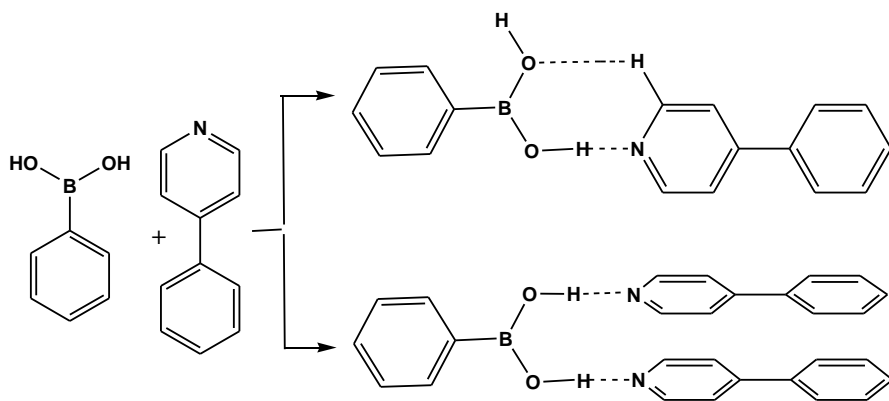
Figure 6.18a: Predicted molecular structures of phenyl boronic acid with 4-phenylpyriden 1:1 ratio
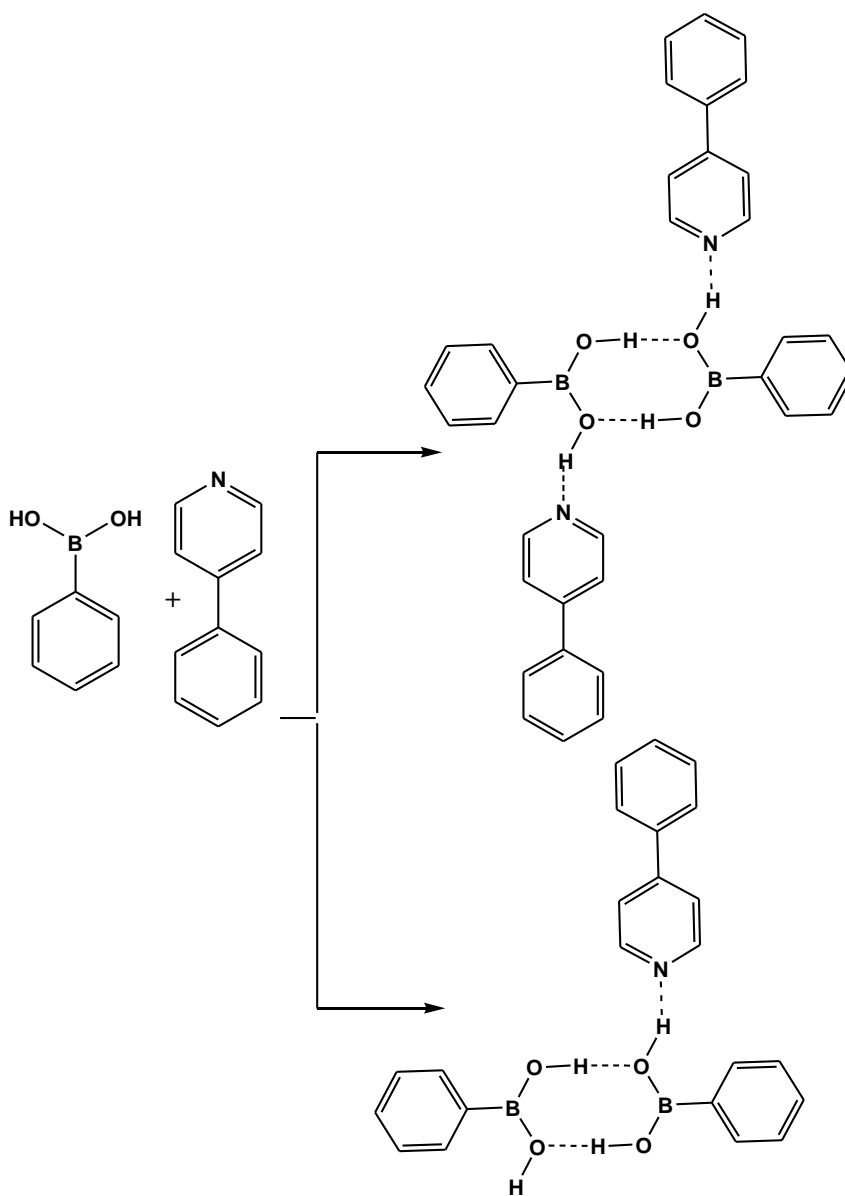
Figure 6.18b: Predicted molecular structures of phenyl boronic acid with 4-phenylpyriden 1:1 ratio

As discussed earlier, self-assembly of 4,4'-bpy with phenylboronic acid produced a finite three component assembly. The assemblies contained only syn hydroxyl conformations and were held together via two O-H---N bonds. The finite structures were subsequently linked into molecular tapes through weak C-H---N forces; however, the hydrogen bonded network of 4-phenylpyridine with phenylboronic acid is able to produce 1D infinite ladders (phenylboronic acid, 4-phenylpyridine) of H_2O. As the solvents used to form the multicomponent systems were not dried prior to use, the moisture within the solvents also participated in the hydrogen bonded assemblies. The structure, composed of only syn hydroxyl groups, was propagated through O-H---O hydrogen bonds. Thus, water molecules may also have participated in forming the rung of the ladder (see Figure 6.19). The fortuitous incorporation of the water molecule addresses a further need concerning the ability/requirement to reliably construct ladders using a boronic acid-based synthon.
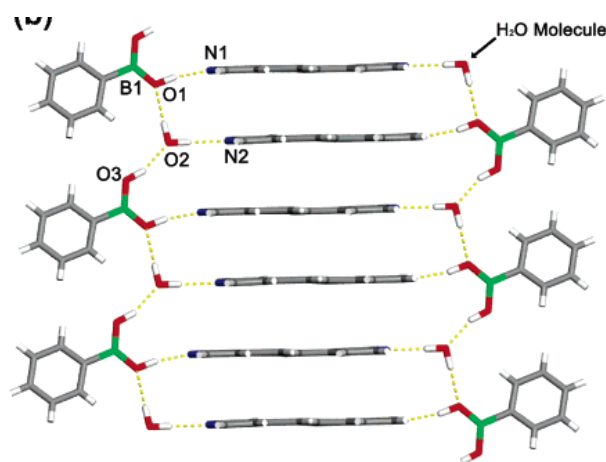
Figure 6.19: Ladder structures based on (phenylboronic acid).(4,4'-bpe).H2O[74]

These initial conclusions have been confirmed by the FT-IR data attained; to illustrate, the overlaid spectra (shown in Appendix D) clearly shows the differences in peak appearance between TA-I-56-1a, TA-I-56-1b and TA-I-56-1c (see Table 6.3) for their starting materials.

Table 6.3: FT-IR assignments for samples TA-I-56-1a, TA-I-56-1b and TA-I-56-1c in Me$_2$CO

Phenyl boronic acid cm^{-1}	4-phenyl pyridine cm^{-1}	TAI-56-1a cm^{-1}	TAI-56-1B cm^{-1}	TAI-56-1c cm^{-1}	Assignment $\bar{\upsilon}$ (cm^{-1})
	3436	3847, 3662	3446	3638	O-H, stretch
3273 3081 3024	3058	3074	3075 3056 3032	3074	C$_{sp2}$-H stretch
2419					
1964	1958			1962	
1894					
		1710		1722	
	1667	1665	1629	1665,1630	C=N stretch
1604		1603,	1600	1601	C=C stretch
1572	1587	1573			C=C stretch
	1543	1551,1513	1558, 1543	1551,1536 1530,1513	C=C stretch
1499	1482	1486	1482	1485,	C=C stretch
1439	1446	1446,1426	1444	1441,1426	
	1409	1402	1408	1402	B-O asym. stretch
1350	1340,1333	1330,1281	1330,1281	1303,1281	
1275, 1191	1232 1189	1256 1216	1256 1216	1256 1216	C-O stretch
1161	1162	1200,1175	1199,1124	1200,1124	C-O stretch
1095	1103	1124			C-O stretch
1072	1072	1084	1084	1085	C-O stretch B-C stretch
1029	1041	1069,1029	1070,1042	1069	
1007	1002	1001	1001	1001	
972	986	982	982	982	B-O sym. stretch
923	917	851	829	817,780	C$_{sp2}$- H bending

803	830	846,816		810	B-O sym. stretch
764	761	780,746	761,764	768	Boroxole ring
697, 857	740	729,702, 691	729,702 688	746,729, 702,691	BO2 out- of -Plane

Although the literature review clearly suggests the well-known multicomponent complexes of phenylboronic acid for 1:1 adducts, it also indicated that the solvents do not generally participate directly in the hydrogen bonding assemblies which lead to multicomponent system formation[97,109,45,110]. To substantiate this proposal, this contemporary research study will now be further expanded in order to categorise the potentially stable multicomponent adducts of the above system in order to study the effect of hydrogen bonding in these complexes through the use of different solvents and different molar mass ratios. Interesting aspects of a computational study conducted by Kua *et al.* anticipated that the "formation of 1:2 adducts of arylboroxine*pyridine are less favourable enthalpically as compared to 1:1 adducts"[111]. In order to assess this piece of evidence further, the multicomponents adduct were also primed with molar mass ratios of 1:2 for: TA-I-56-2b where acetone was used as the solvent, TA-I-56-3b where acetonitrile was used as the solvent, and, for: 2:1 for TA-I-56-2c and TA-I-56-3c – these samples were then analysed using the PXRD and IR techniques (Figure 6.15).

Wakabayashi *et al.* studied the chemistry of borylpyridines by explaining how changes by structural modification conjecture in the self-assembling attribute occurred[107]. Their aim was to study the planned synthesis of more sophisticated systems using 3-[4'-(diethylboryl)phenyl]pyridine (3) and 3-[3'-

(diethylboryl)phenyl]pyridine (4), having a spacer, p and m-phenylene unit, respectively, which then became three-dimensional supramolecules[107]. They concluded that three provided an equilibrium mixture of oligomers along with cyclic trimer, as a foremost constituent by means of intermolecular boron-nitrogen co-ordination bonds. The current research pattern of pyridine shows somewhat similar behaviours to the work of Wakabayashi *et al.* The results suggested that scuttling of component molecules involved the breaking of the intermolecular B-N coordination[112,113] which can be satisfactorily explained by the reduced Lewis acidity of the boron atom in three and four, because the boron atoms in three and four were bonded to the π-electron-donating benzene ring but not directly to the pyridine one.

Although the samples of TA-I-56-1a, 1b and 1c were prepared using methanol as the solvent, they showed successful multicomponent formation. To study the effect of the solvent on the multicomponent system when using the same starting materials but different solvents, acetone (TA-I-56-2a, 2b and 2c) and acetonitrile (TA-I-3a, 3b and 3c) were employed. Although all of the samples were synthesised in the same way, they differed slightly in their physical appearance.

For this reason, the IR spectra for TA-I-56-1a, TA-I-56-2a and TA-I-56-3a will now be compared in order to establish whether they are indeed the same. Irrespective of their slight differences in their physical appearance, the results obtained clearly indicate (see Table 6.3 and 6.4) that identical peaks in the IR spectrum were identified; thus, indicating that despite the visual appearance,

the compounds appeared to be identical when FT-IR analysis was performed.

Table 6.4: FT-IR assignments for sample TA-I-56-2a, TA-I-56-2b and TA-I-56-2c in Me$_2$CO

Phenyl boronic acid cm^{-1}	4-phenyl pyridine cm^{-1}	TAI-56-2a cm^{-1}	TAI-56-2B cm^{-1}	TAI-56-2c cm^{-1}	Assignment $\bar{\upsilon}$ (cm^{-1})
	3436		3436	3436	O-H, stretch
3273, 3081 3024	3058	3074 3053 3032	2360 2342	3074 3053 3032	C$_{sp2}$-H stretch
2419		2360,2342		2360,2342	
1964	1958	1962		1962	
1894		1899		1899	
	1667		1616	1630	C=N stretch
1604		1603	1601	1601	C=C stretch
1572	1587	1573		1573	C=C stretch
	1543	1551	1550	1551	C=C stretch
1499	1482	1486		1486	C=C stretch
1439	1446	1426	1444	1444	B-O asym. stretch
	1409	1403	1407	1400	
1350	1340,1333	1330,1256	1345,1328	1330,1280	
1275, 1191	1232 1189	1216	1215	1256 1216	C-O stretch
1161	1162	1200,1175		1200,1175	C-O stretch
1095	1103	1124	1123	1124	C-O stretch
1072	1072	1084		1084	C-O stretch B-C stretch
1029	1041	1069	1020	1069	
1007	1002		1003		
972	986				B-O sym. stretch
923	917				C$_{sp2}$- H bending
803	830	846,816	826	846,816	B-O sym. stretch
764	761	780	782,759	709,	Boroxole ring
697, 857	740	675	710,667	675	BO2 out- of -Plane
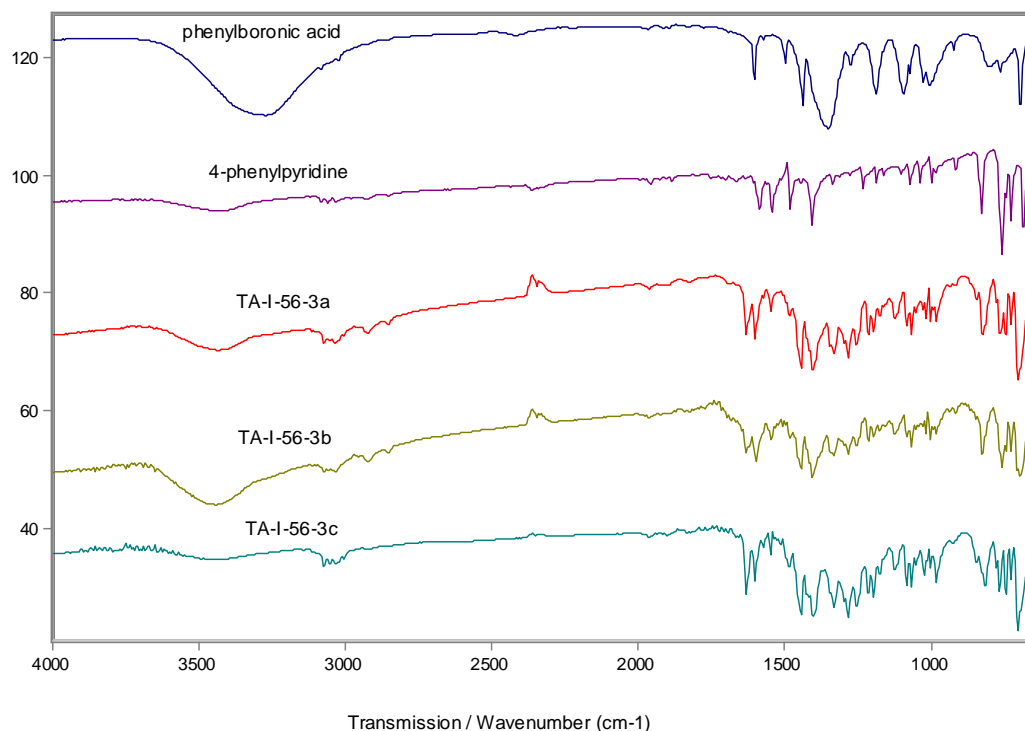
Figure 6.20: Comparative FT-IR spectra for TA-I-56-3a, 3b and 3c, in ratios 1:1, 1:2 and 2:1 in MeCN

6.3   X-Ray Structure Analysis

6.3.1   Single Crystal Analysis of {[(PhBO)$_3$(4-Phpy)]$_4$(4-Phpy)} (TA-1-56-2c)

The crystal structure of the co-crystal of phenylboronic acid and 4-phenylpyridine (t_a), for TA_I_56_2c with a ratio of 1:1 in acetone, displayed the space group as P2$_1$/c, showing the existence of two molecules of 2,4,6-triphenyl-1,3,5,2,4,6-trioxatriborinane   (cyclotrimeric   anhydride   of phenylboronic acid) and three molecules of 4-phenylpyridine. The crystal structure unambiguously exhibited two tetracoordinated adducts of 2,4,6-triphenyl-1,3,5,2,4,6-trioxatriborinane with 4-phenylpyridine molecules.
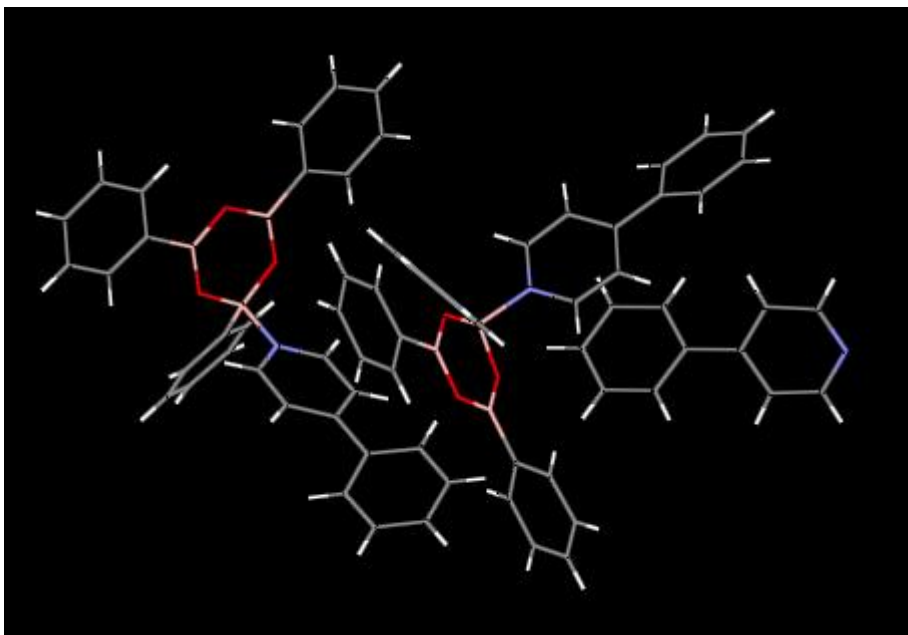
Figure 6.21: Crystal packing of two molecules of cyclotrimeric anhydride of phenylboronic acid and three molecules of 4-phenylpyridine

The crystal structure of the sample revealed that in each, 2,4,6-triphenyl-1,3,5,2,4,6-trioxatriborinane was formed by self-condensation of three triphenylboronic acid molecules, one boron atom adopted a tetrahedral configuration with the 4-phenylpyridine nitrogen atom coordinated; the other two boron centres adopted a trigonal planar configuration with the other 4-phenylpyridine left unbound.

The boroxine ring was in coordination with 4-phenylpyridine in the tetracoordinated adduct, a strong $N^{\delta+}$–$B^{\delta-}$ dipole that points away from the plane of the phenyl ring which may be induced by this B_3O_3 ring interaction which has almost a planar geometry. The two CBO_2 planes were fairly coplanar with two of the benzene rings, but one of the benzenes was out of plane due to the formation of the tetracoordinated adduct. No dimers of phenylboronic acid were seen.

In packing each of the hydrogen bonded units, the tetracoordinated 2,4,6-triphenyl-1,3,5,2,4,6-trioxatriborinane and 4-phenylpyridine were bound through hydrogen bonds. The 4-phenylpyridine interacted through phenyl rings, this is indicative of π-π interactions; in addition, the 4-phenylpyridine molecule was also shown as interacting with another molecule of cyclotrimeric phenyl boroxine through a pair of N with the ring carbons.
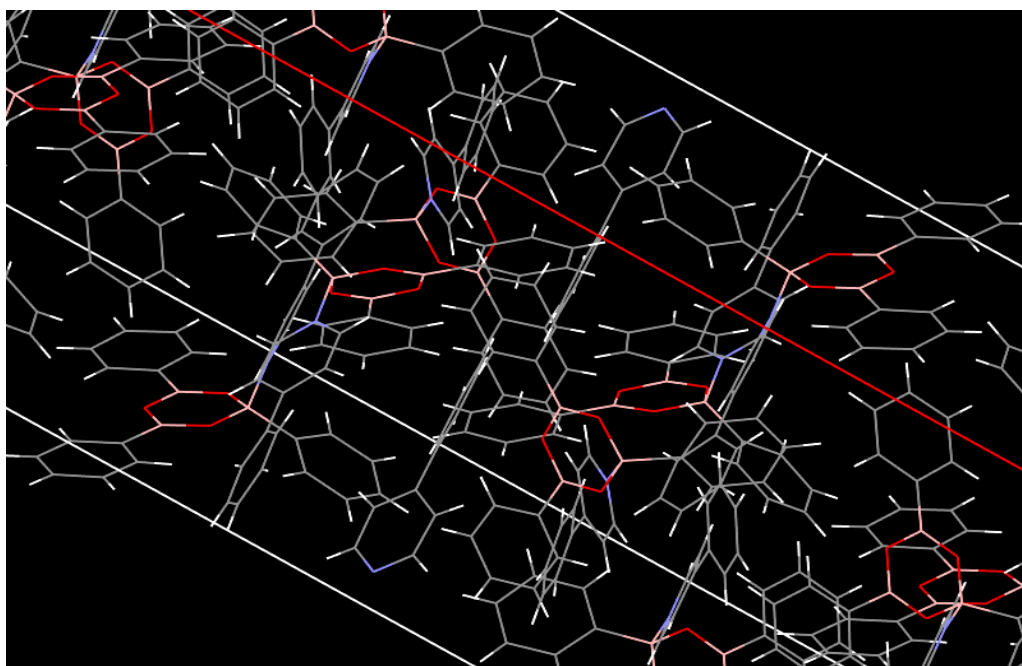
Figure 6.22: The supramolecular of phenylboronic acid: 4-phenylpyriden showing cascade of ladders across horizontal and vertical axes

Due to the formation of 2,4,6-triphenyl-1,3,5,2,4,6-trioxatriborinane and its property to form hydrogen bonded supramolecular assemblies, an extended network of H-bonds among the assemblage of appropriate functional groups was identified as supporting the crystal structure. These findings indicate noteworthy co-crystal properties. In this case, the 2,4,6-triphenyl-1,3,5,2,4,6-trioxatriborinane-4-phenylpyridine supramolecular heterosynthon was formed along with an extended network of H-bonds among the assemblage of

appropriate functional groups. The supramolecular structure appeared like a cascade of ladders across horizontal and vertical axes (see Figure 6.22).

The crystal structure is also in agreement with the IR spectral analysis, as discussed previously. Absence of a band of B-O-H deformation at 1002 and 929cm^{-1}, in the IR spectrum indicates a triphenylboroxine formation which rules out the possibility of phenylboronic acid. Furthermore, the vibrational analysis also showed the B-C stretching vibration, a doublet was displayed at 1104 and 1087cm^{-1} which corresponds with the presence of 2,4,6-triphenyl-1,3,5,2,4,6-trioxatriborinane and rules out the possibility of phenylboronic acid.
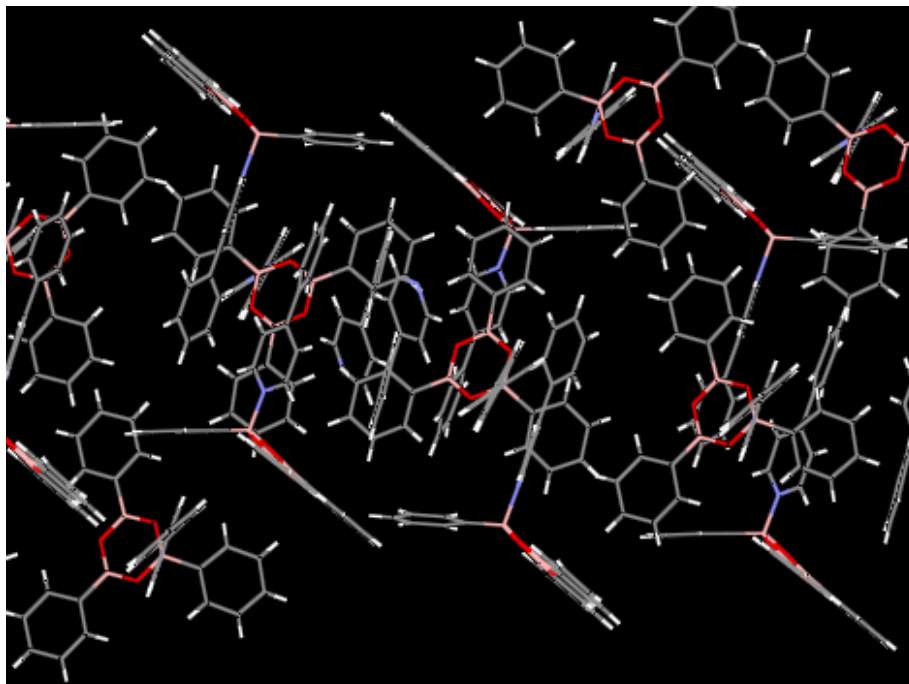
Figure 6.23: the formation of 2,4,6-triphenyl-1,3,5,2,4,6-trioxatriborinane tetracoordinate adduct within co-crystal TA-I-56-2c-

Some characteristic modes in the boroxine ring in terms of the stretching of the boron and oxygen atoms were observed. The symmetric stretching

frequency of the boron atoms of the main ring were observed at 1280.3 and 1468cm^{-1} and the symmetric stretching frequency of the oxygen atoms of the main ring was observed at 824.5cm^{-1}. These results indicate the formation of 2,4,6-triphenyl-1,3,5,2,4,6-trioxatriborinane tetracoordinate adduct. The crystal data and experimental information for sample TA-I-56-2c-0m is given in Table 2.21 and Table 2.13

The x-ray structure analysis of the boroxines gives evidence for the existence of a π-ring system in 2,4,6-triphenyl-1,3,5,2,4,6-trioxatriborinanes. The structural data and geometric parameters (B-O bond lengths and O-B-O bond angles) of the boroxine derivatives are shown in Table 2.21 In addition, there were increases in the bond angles toward 120°, since the phenyl ring on the boron pulls the lone pair of oxygen electrons toward boron; thus, increasing the molecular aromaticity.
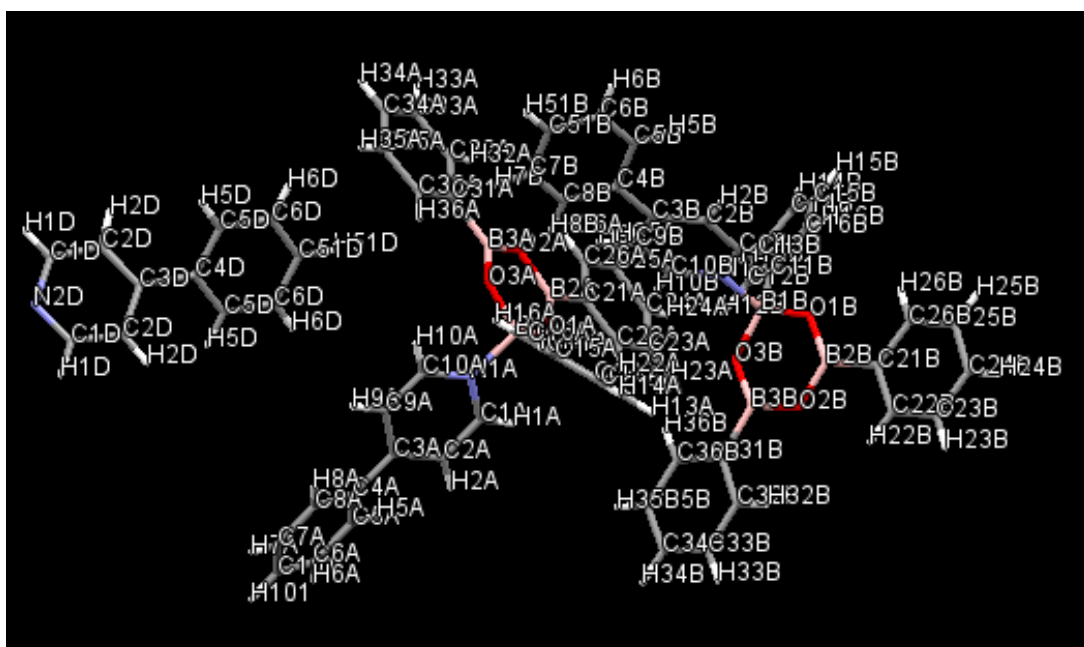
Figure 6.24: Crystal packing showing the symmetric stretching

From the table of geometric parameters (Table 2.21), it was also observed that the B–O bond of sample TA-I-56-2c increased to around 1.43–1.48 Å, which is as much as 0.10 Å longer than the corresponding bonds in 2,4,6-triphenyl-1,3,5,2,4,6-trioxatriborinanes. As previously discussed, this supports the formation of tetracoordinated boroxine adducts. Longer bond length of the tetracoordinate adduct shows lesser bond strength than 2,4,6-triphenyl-1,3,5,2,4,6-trioxatriborinanes whereby the bond strength originates from the conjugation between the lone pairs on the oxygen's and boron's empty orbital; as a result, B–O linkage holds a partial double bond character.
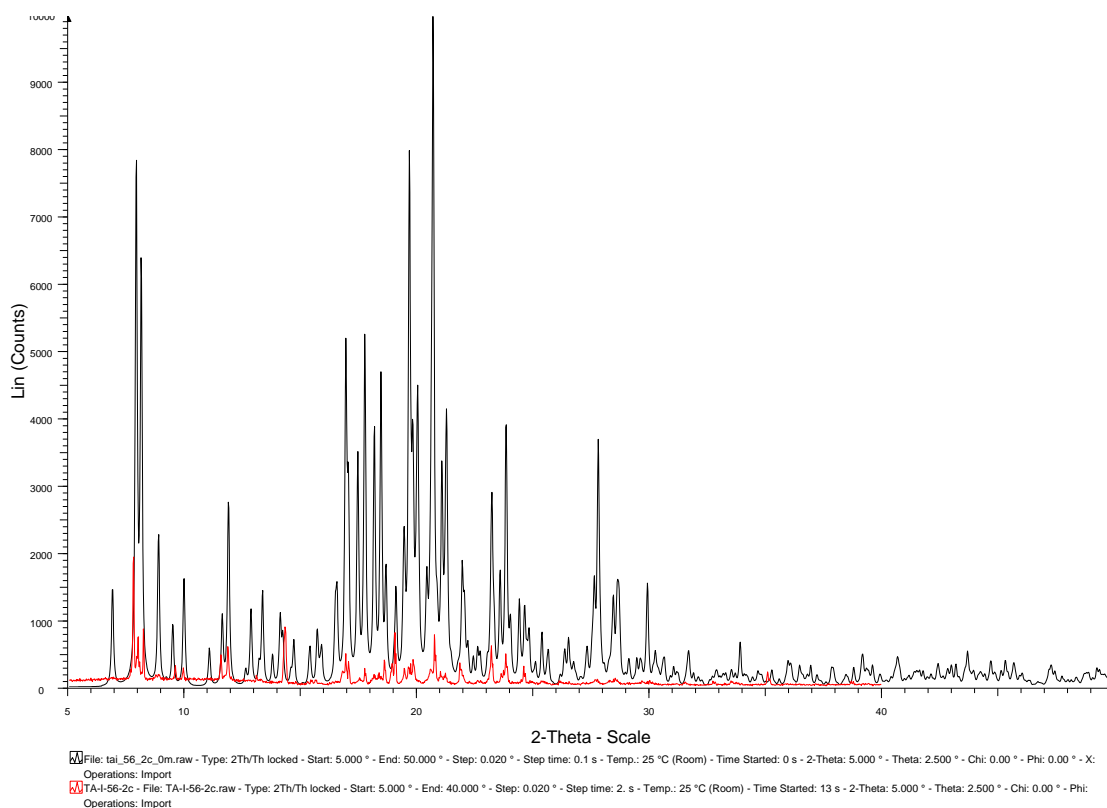
Figure 6.25: Overlay pattern of PXRD of T-I-56-2c and its single crystal

6.3.2   Single Crystal Analysis of {[PhB(OH)$_2$][4,4'-bipy]} (TA-1-54-2a)

The co-crystal structure of phenylboronic acid and 4-4'dipyridyl (t_a) for TA-I-54-2a, in ratio 1:1 in methanol as the solvent, displayed the space group as P2$_1$/c which showed the formation of triphenylboroxine. The structure-directing potential of boronic acid has led to the development of a self-organisation in the form of tetracoordinated adduct of 2,4,6-triphenyl-1,3,5,2,4,6-trioxatriborinane. It is clear within the crystal structure that boron (of boroxines) coordinates with 4,4'bipyridyl (basic molecule) to complete its octet; furthermore, it also exists as a stable tetracoordinated adduct.
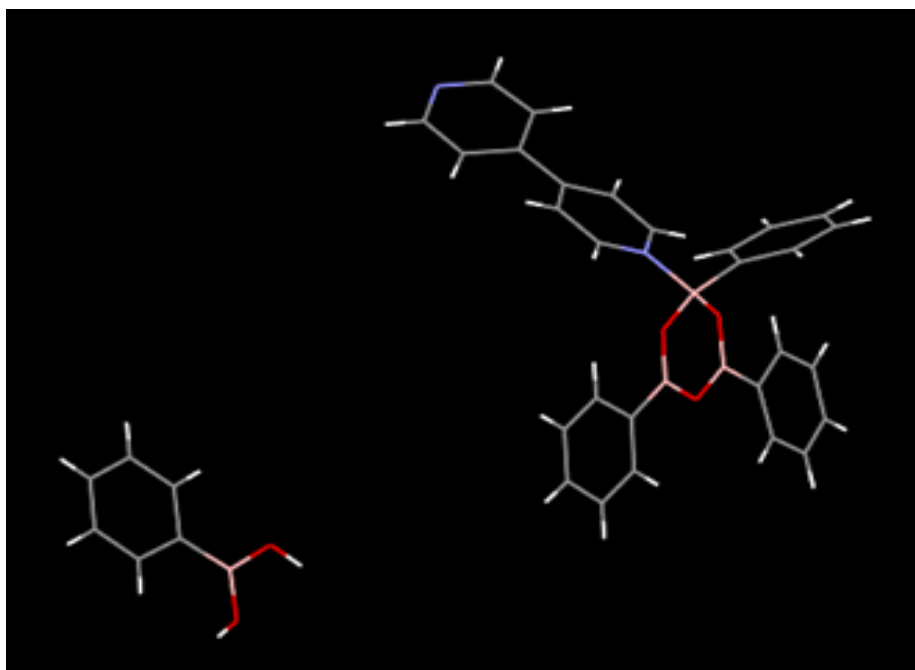
Figure 6.26:   Self-organisation of boronic acid to form tetra-coordinated adduct of 2,4,6-triphenyl-1,3,5,2,4,6-trioxatriborinane

In the tetracoordinated adduct, where a boroxine ring is coordinating with 4-4'dipyridyl, a strong N$^{\delta+}$–B$^{\delta-}$ dipole, that points away from the plane of the phenyl ring, may be induced by this interaction. The B–O bond of

212

tetracoordinated 2,4,6-triphenyl-1,3,5,2,4,6-trioxatriborinane is increased to about 1.44-1.48 Å, which is as much as 0.10 Å longer than the corresponding bonds in tricoordinated boroxines. As previously discussed, this indicates the considerable strength of the B–O bonds in trigonal boronic acid derivatives. This bond strength originates from the conjugation between the lone pairs on the oxygen's and boron's empty orbital; as a result, the B–O linkage holds a partial double bond character. The B_3O_3 ring has almost planar geometry as the two CBO_2 planes are fairly coplanar with two of the benzene rings. No dimers were seen as B---O---H bonds have syn-anti configuration. Each non-dimeric phenylboronic acid is also linked with the hydrogen bonds 4-4'dipyridyl molecules which are incorporated into an array of layers.

In packing one hydrogen bonded unit, it consists of a tetracoordinated adduct of 2,4,6-triphenyl-1,3,5,2,4,6-trioxatriborinane and 4-4'dipyridyl and other phenylboronic acid molecules which are bound through hydrogen bonds. The non-dimeric phenylboronic acid molecule is bound to the molecule of 4-4'dipyridyl through O–H---N. The phenylboronic acid molecule is bound to the triphenylboroxine ring oxygen through a pair of O–H$_{(phenylboronic\ acid)}$ ---O$_{(boroxine)}$ hydrogen bonds. Thus, the 4-4'dipyridyl molecule also showed interactions to another molecule of phenylboronic acid, through a pair of N, with the ring carbons (Figure 6.27)
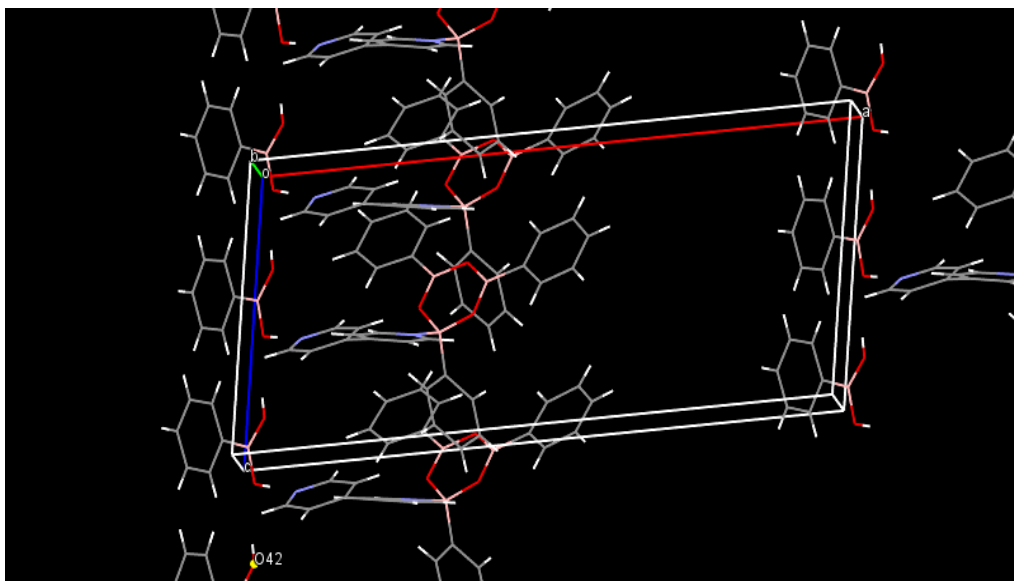
Figure 6.27: Interaction of phenylboronic acid molecule to the triphenylboroxine ring.

Due to the formation of the tetracoordinated adduct of 2,4,6-triphenyl-1,3,5,2,4,6-trioxatriborinane and its property which allows it to form hydrogen bonded supramolecular assemblies, involving hydrogen bonds between BO_2, $B(OH)_2$ groups and the 4-4'dipyridyl nitrogens. An extended network of H-bonds among the assemblage of appropriate functional groups supports the crystal structure. These findings indicate noteworthy co-crystal properties. This supramolecular heterosynthon is a two-point recognition event as there are two ranges corresponding to O−H---O and O-H---N interactions. In this case, the supramolecular synthons are entirely different, triphenylboroxine-4,4'dipyridyl supramolecular heterosynthon is formed along with an extended network of H-bonds among the assemblage of appropriate functional groups. The supramolecular structure appears like two different ladders running across horizontal and vertical axes (see Figure 6.28).
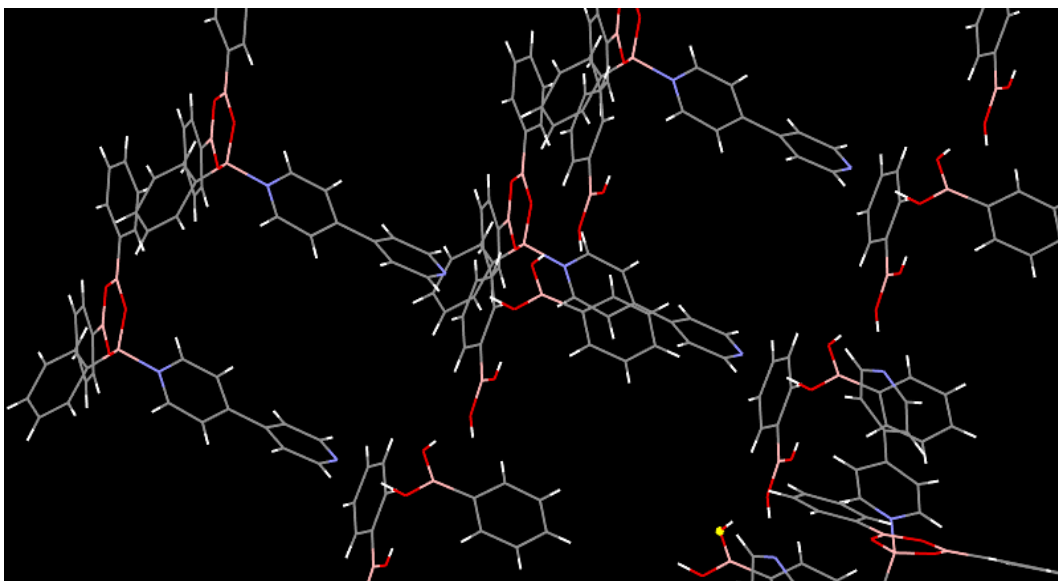
Figure 6.28: Supramolecular heterosynthon showing extended network of H-bonds corresponding to O−H---O and O-H---N interactions

The crystal structure is also in agreement with the IR spectral analysis. The vibrational analysis showed that the B-C stretching vibration displayed a doublet at 1104 and 1087 cm^{-1} which corresponds to the presence of triphenylboroxine. The band is weaker in phenylboronic acid with a disappearance of peaks at 1197 and 929 cm^{-1} which corresponds to B-OH in the spectra of phenylboronic anhydride (triphenylboroxine) – this further supports this work. Some characteristic modes for boroxine ring stretching, of boron and oxygen atoms, were observed. The symmetric stretching frequency of the boron atoms of the main ring were observed at 1281 and 1467cm^{-1}. The symmetric stretching frequency of the oxygen atoms of the main ring were observed at 824.5 cm^{-1}. These results indicate the formation of the tetracoordinate adduct of 2,4,6-triphenyl-1,3,5,2,4,6-trioxatriborinane.

It was observed that the B-O bond length (1.43-1.47 Å) remained in between the B-O single bond length (1.55 Å) and the B-O double bond (1.33 Å) of

215

boron, thereby enhancing the aromaticity of the molecule. Generally, the boron atoms in boroxines possess a higher Lewis acidity. Nevertheless, the x-ray structure analysis of boroxines provided evidence for the existence of a π-ring system. The structural data (B-O bond lengths and O-B-O bond angles) of the boroxine derivatives are also shown in the table. The bond angles increased toward 120^0 as the phenyl ring on boron pulls the lone pair electrons of the oxygen toward boron; thus resulting in an increase in molecular aromaticity.

6.4   Discussion

The study of multicomponent systems of phenylboronic acid and 4,4'-dipyridine and 4-phenylpyridine has been investigated using a mixture of both stoichiometrics and non-stoichiometrics, through the use of PXRD, IR and NMR. Despite the use of different solvents for the appearance of multicomponent systems, the infrared absorption spectroscopy established a number of imperative attributes that are linked specifically to the identification of strong O-H stretching which is involved with the formation of hydrogen bonding networks and the existence of all expected functional groups. For the phenylboronic acid and 4,4'-bipyridine multicomponent systems, boroxine ring formation was observed in the non-stoichiometric 1:2 products. As the solvents were not dried prior to their use, it is believed that the water molecule also contributed to the hydrogen bonded network.

The results obtained in this research study support the established work of Kua and Lovine[111]. In particular, the trimerisation of phenylboronic acids to

form boroxine rings is thermodynamically unfavourable, however the research also revealed that the formation of stable 1:1 adducts in the presence of pyridine is highly favourable, as compared to the 1:2 adducts. These two observations also support and agree with the experimental results presented.

In addition, this research identified that the substitution of π-electron-withdrawing groups in the para-position of the phenyl ring further destabilised the trimer with respect to its monomers; furthermore, the opposite was observed for the π-electron donors. To form the adduct, it was found that net electron withdrawing and electron-donating ability of the para-substituents is important in either stabilising or destabilising the boron that binds the amine.

This research also confirms that hydrogen bonding and π–π stacking play an important role in crystal packing, molecular recognition and the stability of the inclusion complex; however, it should be noted that they are weaker than the covalent force[45].

Although this current study focused predominantly on the pyridine ligands (4,4'-bipyridine and 4-phenylpyridine) with phenylboronic acid, it was observed that 4,4'-bipyridine (bpy) resulted in self-assembly because of its bifunctional and bidentate nature which was more vigilant in forming strong hydrogen bonded networks as compared to single N carrying 4,phenylpyridine where the phenyl group acted to block the functional group for hydrogen bonded networks.

However, ultimately, it is concluded that phenylboronic acid can organise into fascinating topological architectures in order to form co-crystals with nitrogen carrying ligands (4,4'-bipyridine and 4-phenylpyridine).

Chapter 7

7.0   Conclusions and Further Work

7.1   Conclusions

The main aim of this research was to investigate the multicomponent neutral molecular complexes that form a crystalline solid, as these are intrinsically less prone to polymorphism than individual components. For this purpose, a systematic approach for designing and rationalising multicomponents was made by firstly introducing the concept of supramolecular synthesis, whereby intermolecular interactions were acknowledged as being reliably able to bring together two distinct molecules in a process that is parallel to organic covalent synthesis. The multicomponent (co-crystal) formers in this study were phenylboronic acid, 4,4'-bipyridine, 4-phenylpyridine, nicotinamide, isonicotinamide, L/DL-malic acid and L/DL-phenyllactic acid that were used in different molar ratios of the starting material and the different solvents. The literature publicised demonstrated that isonicotinamide and nicotinamide were polymorphic in their unimolecular states[114,115], but they had N carrying molecules that were dimorphic in the following combinations: phenylboronic acid-4,4'-dipyridine;   phenylboronic acid-4-phenylpyridine; phenylboronic acid-nicotinamide;   phenylboronic   acid-isonicotinamide;   L-malic acid-nicotinamide; DL-malic acid-nicotinamide; L-phenyllactic acid-nicotinamide; and,   DL-phenyllactic   acid-isonicotinamide.   These   co-crystals   were assembled primarily using carboxylic acid and phenol hydrogen bond donors which encouraged hydrogen to bond to the pyridine N or amide carbonyl acceptors.   Conformational   differences   within   the   nicotinamide   and

isonicotinamide molecules led to different packing arrangements that used the same combination of hydrogen bonded interactions.

The research also exploited chiral dicarboxylic acid, racemic mixtures and amines so that they could be used as building blocks to constrain the acid-base interactions and encourage chain formation; the results of which were assessed to determine the effect of using chiral versus racemic building blocks to prepare a suitable crystalline form. For this purpose, powder diffraction data was used to determine the crystal structure. Similarly FT-IR analysis was conducted on the co-crystal systems to determine which vibrational modes were most affected by the formation and assembly of the supramolecular synthons, and to determine the magnitude of perturbation in the vibrational frequencies of the involved modes.

The HNMR study provided a sound overview about the stoichiometric ratios and the structure of the molecule. A slow evaporation method was used to maximise and grow enough crystal to allow for further study of the crystal structure by single crystal analysis. Most of the multicomponents showed new phase formations which were different from their starting material.

This study also identified hydrogen bonding and π–π stacking as playing important roles in crystal packing, molecular recognition and the stability of the inclusion complex; although, it is noteworthy that these forces are weaker than the covalent force. The multicomponent complex of phenylboronic acid and pyridine ligands (4,4'-bipyridine and 4-phenylpyridine) showed evidence of new phase formation. The results also revealed the self-assembly of 4,4'-

bipyridine (bpy) because of its bifunctional and bidentate nature which was clearly more vigilant in forming strong hydrogen bonded networks when compared to single N carrying 4-phenylpyridine. The co-crystal of phenylboronic acid and 4,4'-dipyridyl TA-I-54-2a (ratio 1:1) in the methanol solvent displayed the space group as $P2_1/c$, this illustrated that the formation of triphenylboroxine was an important aspect of this research as it studied the dynamic covalent chemistry. The phenylboronic acid molecule was bound to the triphenylboroxine ring oxygen through a pair of O–H$_{\text{(phenylboronic acid)}}$ --- O$_{\text{(boroxine)}}$ hydrogen bonds. The 4,4'-dipyridyl molecule also demonstrated interactions to another molecule of phenylboronic acid through a pair of N, with the ring carbons. However the supramolecular heterosynthon showed O-H---O and O-H---N interactions. With regards to this, the supramolecular structure visually resembled two different ladders running across horizontal and vertical axes.

The crystal structure of the same starting material for the different molar ratio of 2:1 in acetone as the solvent (TA-I-54-1c) showed the space group as C2. In this case, the conformation of BOH in boronic acid was observed as syn-syn; to illustrate, each 4,4'-dipyridyl ring was stacked parallel to the other 4,4'-dipyridyl ring – this may have been as a result of the π-π interactions of the two aromatic rings.

The crystal structure of the co-crystal of phenylboronic acid and 4-phenylpyridine (TA_I-56-2c) in ratio 1:1 in the acetone solution displayed the space group as $P2_1/c$. The 4-phenylpyridine interacted through phenyl rings indicating π-π interactions; the 4-phenylpyridine molecule also demonstrated

interactions with another molecule of cyclotrimeric phenylboroxine through a pair of N, with the ring carbons.

The co-crystal of phenylboronic acid and nicotinamide (TA-I-20-3a) displayed the geometry of the crystal as triclinic in the form of supramolecular assemblies which involved hydrogen bonds between the $B(OH)_2$ groups and the nicotinamide nitrogens and carboxamide group. Each dimeric phenylboronic acid ensemble was linked with the hydrogen bonds to the other nicotinamide molecules which provided an infinite array of layers. The phenylboronic acid molecule was bound to the two distinct molecules of nicotinamide through O–H---N–H(Nicotinamide). In addition, the phenylboronic acid molecule was bound to the other molecule of phenylboronic acid through a pair of O–H---O hydrogen bonds.

The system under investigation, using nicotinamide and isonicotinamide with DL- and L-malic acid demonstrated that usual carboxylic acid to amide hydrogen bonding subsisted – this was further alleviated by the additional hydrogen bonding from the amide-amide and carboxylic-carboxylic acid. The single crystal analysis of the DL-malic acid and nicotinamide (TA-1-17-3b) showed colourless blocks in the orthorhombic space group of $Pca2_1$, where the nicotinamide essentially bridged the two malic acids of the dimer which formed a carboxylate COH to pyridine nitrogen and amide nitrogen to the alcohol OH of the second malic acid. This complex network of interconnected dimer units was stabilised by aromatic π-π interactions between the nicotinamide – this was in addition to the hydrogen bonded systems.

The crystal structure of the co-crystal of L-phenyllactic acid and isonicotinamide (TA-I-52-1a) displayed the geometry of the crystal as triclinic. The packing revealed that the primary intermolecular interaction was the O-H---N hydrogen bond between the acid and the N-heterocyclic nitrogen atom as well as the amide-amide dimer and the OH---OH interaction; these were further stabilised with intermolecular C−H---O and C−H---π interactions. The supramolecular heterosynthon corresponded to O−H---N (heteroaryl) and N−H---O=C interactions, as well as O-H---O-H interactions.

The crystal structure of co-crystal DL-phenyllactic acid and isonicotinamide (TA-I-31-3c) displayed the geometry of the crystal as triclinic, where the isonicotinamide molecule was bound to the other molecule of isonicotinamide through C=O$_{(Isonicotinamide)}$---N–H$_{(isonicotinamide \ ')}$ and N–H---C=O. The isonicotinamide molecule was bound to one molecule of DL-phenyllactic acid through N$_{(pyridine \ ring \ )}$---O–H$_{carboxyl}$ hydrogen bonds. The nicotinamide molecule also showed interactions to another molecule of DL-phenyllactic acid through a pair of N$_{(pyridine \ ring)}$，with the ring carbons.

The use of different solvents (acetone, acetonitrile and methanol) did not indicate that the solvent molecules were directly involved in the bonding pattern of multicomponent complexes. However, slight changes in the PXRD pattern could be explained by the consideration of the competition of the solvent-solute interactions and the discrete acid-amide interactions which suggests that solvent selectivity may be worth considering; consequently, the detail provided by this research with regards to the solubility is likely to be of value with regards to explicit solvent-solute interactions which could be

considered to explain this difference. These results also indicated that solvents could play an important role in the selective growth of a desired molecular complex. Furthermore, this research confirmed that carboxylic acid and boronic acid could develop fascinating topological architectures by the formation of co-crystals with nitrogen carrying ligands (pyridine and amides).

Consequently, it is possible to conclude, from the above discussions, that all of the systems under investigation outlined the supramolecular structure where chiral and racemic forms of acids resulted in the formation of adducts for interactions with the given diamines. The overall stoichiometry of the supramolecular structures were very much similar, however they did exhibit different spacing groups.

7.2   Further Work

Despite the co-crystallisation techniques providing effective means to discover new solid state forms, further challenging aspects still need investigation with regards to the development of efficient co-crystal screening technologies; in particular:

Solid based techniques, such as neat grinding and liquid assisted grinding, should be applied to demonstrate a higher selectivity, as compared to solvent based approaches which would reveal the co-crystallisation potential of multiple molecular species.

The experimental results could be further compared with the theoretical calculation using a computational method.

The use of ^{13}CNMR analysis could provide further evidence with regards to crystal structures.

The unambiguous characterisation by 2D NMR could be completed in order to provide verification of the crystal structure.

Standard technology, such as DSC and thermogravimetric analysis, could help to "unveil" the relative stability of new solid state forms when compared to their individual component.

Aromatic solvents, such as benzene and toluene, could be used to investigate the π-π interaction of co-crystals with the solvent.

References

1   (a) Lehn, J.-M. *Angew. Chem., Int. Ed.*, **1990**, 29, 1304–1319. (b) Lehn, J.-M. *J. Chem. Sci.,* **1994**, 106, 915–922. (c) Lehn, J.-M. *Chem. Soc. Rev.,* **2007**, 36, 151–160.

2   Bathori, N.B., Lemmerer, A., Venter, G.A., Bourne, S.A., and Caira, M.R. Pharmaceutical Co-crystals with Isonicotinamide; Vitamin B3, Clofibric Acid, and Diclofenac; and Two Isonicotinamide Hydrates. *Crystal Growth and Design*, **2011**, 11, 75.

3   Schmidt, G.M. *J, Pure Appl. Chem.*, **1971**, 27, 647-647.

4   Desiraju, G. *The Design of Organic Solids, Crystal Engineering*, Elsevier, Amsterdam, **1989.**

5   Morissette, S.L., Almarsson, M.L., Peterson, J.F., Remenar, M.J., Read, A.V., Lemmo, S., Ellis, M.J. and Gardner, C.R. *Advanced Drug Delivery Reviews*, **2004**, 56, 275-300.

6   Stahly, G.P. *J. Crystal. Growth and Design*, **2009**, Vol. 9, 4212-4229.

7   Frisic, T. and Jones W. *J. Crystal Growth and Design*, **2009**, Volume 9, 1621-1637.

8   Almarsson, O., Zaworotko, M.J. *Chem Comm*, **2005**, 4601–460.

9   Sugiyama, T., Meng, J. and Matsuura, T. *Journal of Molecular Structure*, **2002**, 611(1-3), 53-64.

10   Aakeroy, C.B. and Desper, J. *Chemical Communications*, **2007**, 3936-3938.

11   Christer, B. and Aakeroy, A.M.B. *Angewandte Chemie International Edition*, **2001**, 40, 3240-3240.

12   Friscic, A. *Angewandte Chemie International Edition*, **2006**, 45 (45), 7546-7550.

13   Kumar. S., Biswas, P. and Kaul, I., *J. Phys. Chem. A,* **2011**, 115, 7461–7472.

14   Burley, S.K., Petsko, G.A. *Science,* **1985**, 229, 23.

15   Meyer, E.A., Castellano, R.K. and Diederich, F. *Angew. Chem., Int. Ed.*, **2003**, 42, 1210.

16   Desiraju, G.R. *Angew. Chem., Int. Ed.*, **1995**, 34, 2311.

17   Hong, B.H., Bae, S.C., Lee, C.-W., Jeong, S. and Kim, K.S., *Science*, *2001*, 294, 348.

18   Seaton. C., Parkin. A., Wilson. C.C. and Blagden. N. *Crystal Growth and Design*, **2009**, Vol. 9, No. 1, 47-56.

19   Helmenstine, A.M. *Vander Waals Forces Definition*, Available online from:

www.about.com.chemistry, accessed 20 April 2014.

[20]   Bryce, M.R. and Murphy, L.C. *Nature*, **1984**, 19, 119-126.

[21]   Hunter, C.A. and Sanders, J.K.M., *J. Am. Chem. Soc.*, **1990**, 112(14), 5525-5534.

[22]   Waters, M.L. *Current Opinion in Chemical Biology*, **2002**, 6 (6), 736-741.

[23]   Almarsson, O. and Zaworotko, M.J. *Chemical Communications*, **2004**, 1889-1896.

[24]   Desiraju, G.R. *Science*, **1997**, 278, 404-405.

[25]   (A) Etter, M.C. *Acc. Chem. Res.*, **1990**, 23, 120−126. (B) Etter, M., Macdonald C. and Bernstein, J.C. *J. Acta Crystallogr., Sect. B: Struct. Sci.,* **1990**, 46, 256-262. (C) Bernstein, J., Davis, R.E., Shimoni, L. and Chang, N.-L. *Angew. Chem., Int. Ed. Engl.* **1995**, 34, 1555−1573.

[26]   Lemmerer. A., Adsmond. D.A., Esterhuysen, C., Bernstein. J. *Crystal Growth Design*, **2013**, 13, 3935−3952.

[27]   Brittain, H.G. *Crystal Growth and Design*, **2009**, Vol. 9, No. 5, 2492.

[28]   Khan, M., Enkelmann, V. and Brunklaus, G. *J. Am. Chem. Soc.* **2010**, 132, 5254–5263.

[29]   Thalladi, V.R., Satish Goud, B. Hoy, V.J., Allen, F.H., Howard, J.A.K. and Desiraju, G.R. *Chemical Communications*, **1996**, 401–402, Abstract.

[30]   Simon. J. and Bassoul, P. *Design of Molecular Materials: Supramolecular Engineering*, **2000**, Wiley, VCH.

[31]   Aakero¨ Y.C.B., Beatty, A.M., Helfrich, B.A. and Nieuwenhuyzen, M. *Crystal Growth and Design*, **2003**, 3, 159.

[32]   Soai, K., Shibata, T., Morioka, H. and Choji, K. *Nature*, **1995**, 378, 767-768.

[33]   Noorduin, W.L. *J. Am. Chem. Soc.*, **2008**, 130, 1158-1159.

[34]   Holden, A. and Singer, P. *Crystal Growth and Design*, **2005**, 291

[35]   McBride, J.M. and Carter, R.L. *Angew. Chem. Int Ed.*, **1991**, 30, 293-295.

[36]   Frank, F.C. *Biochim. Biophys. Acta.,* **1953**, 11, 459-463.

[37]   Kondepudi, D.K., Kaufman, R.J. and Singh, N. *Science*, **1990**, 250, 975-977.

[38]   Viedma, C. *Phys. Rev. Lett.*, **2005**, 94.

[39]   Jacques, J. *The Molecule and it's Double*, McGraw-Hill Inc., New York, **1993.**

[40]   March, J. *Advanced Organic Chemistry* (3rd Ed.), John Wiley and Sons, New York, **1985**, 94-95.

41   Welch, C.J. **in** P.R. Brown and E. Grushka (Editors), *Advances in Chromatography*, Vol. 35, Marcel Dekker, Inc., New York, **1995**, p.172..

42   Ahuja, S. **in** S. Ahuja, "Chiral Separation by Liquid Chromatography", *American Chemical Society*, Washington, D.C., **1991**, Ch. 1: 1.

43   Eames, J. *Angew. Chem. Int. Ed.*, **2000**, 39, 885-888.

44   Kellogg, R.M., Nieuwenhuijzen, J.W. and Pouwer, K. *Grimbergen Synthesis*, **2003**, 10, 126-1638.

45   Korich, A.L. and Lovin, P.M. *Dalton Trans.*, **2010**, 39, 1423–1431.

46   Cote, A.P., Benin, A.I., Ockwig, N.W., O'Keeffe, M., Matzger, A.J. and Yaghi, O.M. *Science*, **2005**, 310, 1166-1170.

47   Yaghi. O, *Science*, **2005**, 1166-1170.

48   Campbell, N.L., Clowes, R., Ritchie, L.K. and Cooper, A.I. *Chem. Mater,* **2009**, 21, 204-206.

49   Wan, S., Guo, J., Kim, J., Ihee, H. and Jiang, D.L. *Angew. Chem., Int. Ed.*, **2009**, 48, 5439–5442.

50   Smith, B.R. and Sweet F. *J. of Colloid and Interface Science*, **1971**, Vol. 37 (3), 612-618.

51   Sohnel, O. "Some Factors", *J. Crystal Research and Technology*, **1981**, Vol. 16 (6), 651-654.

52   Sohnel, O. and Mullin, J. *J. of Crystal Growth and Design*, **1982**, Vol. 60 (2), 239-250.

53   Glynn, P.D. and Reardon E.J. *Amer. J. Sci.*, **1990**, 290, 164–201.

54   Frenkel, L.S.D. *J. Chem. Phys.*, **2004**, 120: 301L.

55   Karki, S., Friscic, T., Jones, W. and Motherwell, W.D.S. "Screening for Pharmaceutical Cocrystal Hydrates via Neat and Liquid-Assisted Grinding". *Mol. Pharmaceutics*, **2007**, 4 (3), 347−354.

56   Friscic, T., Trask, A.V., Jones, W. and Motherwell, W.D.S. "Screening for Inclusion Compounds and Systematic Construction of Three-Component Solids by Liquid-Assisted Grinding". *Angew. Chem., Int. Ed.*, **2006**, 45, 7546−7550.

57   Viertelhaus, S., Hilfiker, R., and Blatter, F. "Piracetam Co-Crystals with OH-Group Functionalized Carboxylic Acids". *Cryst. Growth Des.,* **2009**, 9 (5), 2220−2228.

58   Zhang, G.G.Z., Henry, R.F., Brochardt, T.B., and Lou, X. "Efficient Co-crystal Screening Using Solution-Mediated Phase Transformation". *J. Pharm. Sci,.* **2007**, 96 (5), 990−995.

59 Viertelhaus, S., Hilfiker, R. and Blatter, F. "Piracetam Co-Crystals with OH-Group Functionalized Carboxylic Acids". *Cryst. Growth Des.* **2009**, 9 (5), 2220−2228

60 Li,J., Bourne, S.A. and Mino, R. *Caira Chem. Commun.,* **2011**, 47, 1530–1532.

61 Mata, V.G. and Rodrigues, A.E. *Chromatogr A.*, **2001**, 23-40.

62 Renato, A., Chiarella, R.J. and Davey, *M.L. Peterson Journal of Pharmaceutical Sciences*, **2010**; 99, 4054-71.

63 Akalin, E. and Akyüz, S. *Vibrational Spectroscopy*, **2006**, 42, 333–340.

64 Wash, P.L., Maverick, E., Chiefari, J. and Lightner, D.A. "Acid-Amide Intermolecular Hydrogen Bonding", *J. Am. Chem. Soc.* **1997**, 119, 3802-3806.

65 Aakerö, Y.C.B. and Schultheiss, N. "Assembly of Molecular Solids via Non-Covalent Interactions", **in** D. Braga and F. Grepioni (Eds.) *Making Crystal Growth and Design,* Wiley-Vch: Weinheim, Germany, **2007**, 209-240.

66 McMahon, J.A., Bis, J.A., Vishweshar, P., Shattock, T.R., Mclaughlin, O.L. and Zaworotko, M.J.Z. "*Kristallogr.", Crystal Growth and Design,* **2005**, 220, 340−350.

67 Hamilton, W.C. and Ibers, J. A. *Hydrogen Bonding in Solids.* W. A. Benjamin, Inc. New York, **1968.**

68 Porter, W. Lii, E.S. and Matzger A.J. "Polymorphism In Carbamazepine Co-Crystals", *Crystal Growth and Design*, **2008**, 14-16.

69 Sheikh, A.Y, Rahim, S.A., Hammond, R.B. and Roberts, K.J.*Cryst Eng. Comm,* **2009**, 11, 501-509.

70 Hino, T., Ford, J.L. and Powell, M.W. *Therm. Acta*, **2001**, 374, 85−92.

71 (A) Miyaura, N. and Suzuki, A. *Chem. Rev.* **1995**, 95, 2457–2483. (B) Matteson, D.S. *Tetrahedron,* **1989**, 45, 1859–1885. (C) Hall, D.G. *Boronic Acids: Preparation, Applications in Organic Synthesis and Medicine,* **2005**, Wiley- VCH: Weinheim, Germany.

72 (A) Soloway, A.H., Tjarks, W., Barnum, B.A., Rong, R.-A., Barth, R.F., Codogni, I. M. and Wilson, J.G. *Chem. Rev.*, **1998**, 98, 1515–1562. (B) Yang, W., Gao, X. and Wang, B. *Med. Res. Rev.,* **2003**, 23, 346–36.

73 Desiraju, G. *Science*, **2011**, Vol. 54, No. 12, 1909–1919.

74 Pedireddi, V.R., Seetha Lekshmi, N. *Tetrahedron Lett*, **2004**, 45, 1903–1906.

75 Shimpi, M.R., Seetha Lekshmi, N. and Pedireddi, V.R. *Cryst Growth Des*, **2007**, 7: 1958–1963.

76 (A) Cote, A.P., Benin, A.I., Ockwig, N.W., O'Keeffe, M., Matzger, A.J. and Yaghi, O.M., *Science*, **2005**, 310, 1166–1170. (B) Cheney, M.L., Weyna, D.R., Shan, N., Hanna, M., Wojtas, L. and Zaworotko, M.J. *Crystal Growth and Design*, **2010**, 10 (10), 4401–4413.

77   Cheney, M.L., Shan, N., Healey, E.R., Hanna, M., Wojtas, L., Zaworotko, Sava, V., Song, S.and Sanachez-Ramos, J.R. *Crystal Growth and Design,* **2010**, 10, 394-405.

78   Wright, W.B. and King, G.S.D. *Acta Crystallogr.*, **1954**, 7, 283.

79   Miwa, Y., Mizuno, T., Tsuchida, K., Taga T. and Iwata, Y. "Acta Crystallogr.", *Sect. B: Struct. Sci.*, **1999**, 55, 78.

80   Akalin, E., Yilmaz, A. and Akyuz, S. *Journal of Molecular Structure,* **2005,** 744–747 881–886.

81   Barth, J.V., Constantini, G. and Kern, K. *Nature*, **2005**, 437, 671–679.

82   *International Tables for Crystallography*. Vol. A, Space Group Symmetry. **1983**, Springer.

83   Bhogala, B.R., Basavoju, S., Nangia A. *Cryst. Eng. Comm.,* **2005**, 7, 551.

84   Aakeroy C.B.; Beatty A.M.; Helfrich B.A.; Am J.; *Chem.Soc.* **2002**, 124, 14425.

85   Lemmerer, A. and Bernstein, J. *Cryst. Eng. Comm.,* **2010**, 12, 2029.

86   Vishweshwar, P. Nangia, A. and Lynch, V.M. *CSD REF CODE.*

87   (A) Sangster, J.J. *Phys. Chem.* Ref. Data, **1999**, 28 (4), 889. (B) Sekiguchi, K., Himuro, I., Horikoshi, I., Tsukada, T., Okamoto, T. and Yotsuyanagi, T. *Chem. Pharm. Bull.*, **1969**, 17, 191.

88   Schrader, B. *Infrared and Raman Atlas of Organic Compounds (2nd Ed.)*, **1989**, VCH: Weinheim.

89   Baranska, H., Kuduk-Jaworska, J., Szostak, R. and Romaniewska, A. *J. Raman Spectrosc.*, **2003**, 34: 68–76.

90   Van Loock, J.F.J., Van Havere, W. and Lenstra, A.T.H. *Bull. Soc. Chim. Belg.*, **1981**, 90, 161.

91   Wolfs, I. and Desseyn, H.O. *Appl. Spectrosc.*, **1996**, 50, 1000.

92   Navare, P.S. and MacDonald, J.C. "Investigation of Stability and Structure in Three Homochiral and Heterochiral Crystalline Forms of 3-Phenyllactic Acid". *Cryst. Growth Des.*, **2011**, 11, 2422–2428.

93   Bellamy, L.J. *The infra-red spectra of complex molecules* (3rd Ed.). Chapman and Hall: New York, **1975**.

94   (A) Burley, S.K. and Petsko, G.A. *Science*, **1985**, 229, 23. (B) Meyer, E.A., Castellano, R.K. and Diederich, F. *Angew. Chem., Int. Ed.,* **2003**, 42, 1210.

95   Aitipamula, S., Chow, P.S. and Tan, R.B.H., *Crystal Growth and Design,* **2010**, Vol. 10, 2229-2238.

96   Akalin E., Akyu¨z, S. and Mol, J. *Struct.*, **1999**, 482/483, 175.

97   Rodriguez-Cuamatzi, P., Luna-Garcı´a, R., Torres-Huerta, A., Bernal-Uruchurtu, M.I., Barba, V. and Ho¨pfl*, H. *Crystal Growth and Design,* **2009**, Vol. 9, No. 3, 1575.

98   Faniraannd, J.A. and Shurvell, H.F. "Infrared spectra of phenylboronic acid (normal and deuterated) and diphenylphenylboronate", *Canadian Journal of Chemistry*, 46, 2089, **1968**.

99   Chen, H., Lee, M., Lee, J., Kim, J.-H., Gal, Y.-S., Hwang, Y.-H., An, Y.G. and Koh, K. "Formation and Characterization of Self-Assembled Phenylboronic Acid Derivative Monolayers toward Developing Monosaccharide Sensing-Interface", *Sensors*, **2007**, 7, 1480-1495.

100 Akalin, E. and Akyu¨z, S. and Mol. J. *Struct.*, **2001**, 563/564, 579.

101 Pedireddi, V.R., Seetha Lekshmi, N., "Tetrahedron Lett.", Crystal Engineering, 2004, 45, 1903-2150.

102 (A) Desiraju, G.R. *Acc. Chem. Res.*, **1996**, 29, 441–449. (B) Steiner, T. *Chem. Commun.,* **1997**, 727–734. (C) Berger, I. and Egli, M*. Chem. Eur. J.*, **1997**, 3, 1400–1404. (D) Bodige, S.G.; Rogers, R.D. and Blackstock, S.C*. Chem. Commun.*, **1997**, 1669–1670. (E) Calhorda, M.J. *Chem. Commun.*, **2000**, 801–809. (F) Rahman, A.N.M.M., Bishop, R., Craig, D.C. and Scudder, M.L. *Eur. J. Org. Chem.*, **2003**, 72–81.

103 (A) Glo´wka, M.L., Martynowski, D., Kozlowska, K. *J. Mol. Struct.,* **1999**, 474, 81–89. (B) Nishio, M. *Crystal Growth and Design,* **2004**, 6, 130–158. (C) Meyer, E.A., Castellano, R.K. and Diederich, F. *Angew. Chem., Int. Ed.*, **2003**, 42, 1210–1250.

104 *Cambridge Structural Database*, Cambridge Crystallographic Data Centre, Version 5.25, **November 2003**, Cambridge, UK.

105 Mishra, B.K. and Sathyamurthy, N*. J. Phys. Chem. A.*, **2005**, 109, 6–8.

106 Kua, J., Fletcher, M.N. and Lovine, P.M. *J. Phys. Chem. A.*, **2006**, 110, 8158-8166.

107 (1a) Wakabayashi,S.; (1b) Sugihara,Y.; (1c) Takakura, K.; (1d) Murata, S.; (1e) Tomioka, H.; (1f) Ohnishi, S.; (1g) Tatsumi, K. "Synthesis, Structural Features and Stability in Solution", *J. Org. Chem.*, **1999**, 64, 6999-7008.

108 Sokolov, A.N. and MacGillivray, L.R. *Crystal Growth and Design,* **2006**, Vol. 6, No. 11, 2615-2624.

109 Sunil, V., Bhushan, S.S. and Gautam, D.R., *Science*, **2011**, Vol. 54 No. 12, 1909-1919.

110 (A) Braga, D., Polito, M., Bi, M., D'Addario, D., Tagliavini, E. and Sturba, L. *Organometallics,* **2003**, 22, 2142–2150. (B) Pedireddi,, V.R. and Seetha Lekshmi, N. *Tetrahedron Lett.*, **2004**, 45, 1903–1906. (C) Aakero¨y, C.B., Desper, J., Levin, B. and Salmon, D.J. *ACA Trans.*, **2004**, 39, 123–129. (D) Aakero¨y, C.B., Desper, J. and Levin, B. *Cryst. Eng. Comm.,* **2005**, 7, 102–107. (E) Dabrowski, M., Lulinski, S., Serwatowski, J. and Szczerbinska, M. *Acta Crystallogr.*, **2006**, 62, 702.

111 Kua, J. and Lovine, P.M. *J. Phys. Chem. A.*, **2005**, 109, 8938-8943.

[112] (A) Sugihara, Y., Miyatake, R,, Takakura, K. and Yano, S.J. *Chem. Soc., Chem. Commun.,* **1994**, 1925. (B) Sugihara, Y., Takakura, K., Murafuji, T., Miyatake, R., Nakasuji, K., Kato, M. and Yano, S. *J. Org. Chem.*, **1996**, 61, 6829.

[113] Murafuji, T., Mouri, R., Sugihara, Y., Takakura, K., Mikata, Y. and Yano, S. *Tetrahedron,* **1996**, 52, 13933.

[114] Vishweshwar, P., Nangia A. and Lynch, V.M. *Crystal Growth & Design*, **2003**, 3, 783.

[115] Aakeröy C.B. and Salmon, D.J. *Cryst. Eng. Comm.,* **2005**, 7, 439.

Appendices

Appendix A: Chapter 3

Table AA 3.1: PXRD data for samples TA-I-17-2a (1:1), TA-I-17-2b (1:2), TA-I-17-2c (2:1), in methanol

DL-Malic acid	Iso stnd	Iso EHOWIH	Iso EHOWIH01	Iso EHOWIH02	TA-I-17-2a	TA-I-17-2b	TA-I-17-2c
2-Theta °	2-Theta°	2-Theta °	2-Theta °	2-Theta °	2-Theta °	2-Theta °	2-Theta °
	17.842						8.567
					10.08		10.48
					13.41		13.81
				11.677			
14.25				14.625			
				16.09	16.05	16.51	16.34
				16.52	16.53	16.92	16.97
	17.84	17.859	17.84		17.25		17.67
	18.85	18.748	18.76	18.63	18.24	18.70	18.58
18.95					18.68	18.94	
	19.41	19.34	19.34	19.14	19.85		19.07
20.52		20.48	20.47	20.14	20.32		20.31

	20.87		20.99	20.75			
				20.98			
21.27		21.03		21.94	21.26		21.63
				22.21			
23.92	23.449	23.49	23.48	23.46		23.14	23.72
	24.454	24.38	24.39	24.60	24.16	24.73	24.50
24.91					24.83		
				25.40		25.279	25.011
	25.94			25.79			25.223
		26.09	26.06		26.33		
	26.64	26.93	26.89			26.787	26.64
27.09					27.11	27.12	27.44
27.92					27.72		
28.33	28.16	28.06	28.07	28.99	28.66		28.09
		29.94	29.92	29.78		29.734	29.07

			30.83	30.38	30.06		30.38
	30.00	30.88		30.75	30.99		
	30.95						
	31.29	31.19	31.16	31.40		31.343	31.38
32.91	32.46	32.48	32.45	32.53	32.59	32.439	32.23
33.11	33.33	33.26	33.48	33.49		33.304	33.38
	33.89	33.51	33.86				33.84
		33.86					
				34.99			
	35.41	35.66	35.61	35.52			
36.01	36.10	36.15	36.15		36.32		
	36.54	36.56	36.56				
37.44		37.83		37.28	37.14	37.63	37.13
37.80							37.64
	38.15	38.04	38.04	38.90	38.06		

	38.80					38.85	
	39.32	39.06	39.00				
		39.33	39.33				
40.48				40.50			
41.18	41.38	41.28	41.30				
		41.70					
42.19	42.24	42.04					
		42.81	42.75				
43.64	43.45	43.97	43.88				
44.48	44.93	44.90	44.91				
45.37		45.46		45.32			
45.37							
	46.81	46.15					
	47.78	47.14	47.74				
		47.75					

		48.09	48.05				
		48.53					
	49.493	49.46					

Table AA 3.2: PXRD data for samples TA-I-18-1a (1:1), TA-I-18-1b (1:2), TA-I-18-1c (2:1), in acetone

DL-Malic acid	Iso stnd	Iso EHOWIH	Iso EHOWIH01	Iso EHOWIH02	TA-I-18-1a	TA-I-18-1b	TA-I-18-1c
2-Theta °	2-Theta °	2-Theta °	2-Theta °	2-Theta °	2-Theta °	2-Theta °	2-Theta °
						7.319	
						8.796	
							10.45
				11.677			
					13.901		13.8
14.254				14.625		14.584	
				16.097			
				16.52	16.523	16.365	16.444
							16.838
	17.842	17.859	17.843		17.684	17.553	17.607
	18.855	18.748	18.766	18.626	18.671	18.538	
18.95						18.937	

242

	19.411	19.347	19.347	19.14	19.131		19.139
20.518	20.874	20.485	20.468	20.138	20.8		
			20.996	20.747			20.689
				20.988			
21.275		21.037		21.94	21.241	21.418	21.083
					21.664		21.633
				22.214		22.275	
						22.894	
23.927	23.449	23.498	23.48	23.457		23.75	
24.911	24.454	24.385	24.396	24.601	24.655	24.325	24.581
						24.904	
				25.403	25.306	25.152	25.367
	25.937			25.789	25.52	25.664	
	26.644	26.093	26.059		26.723	26.646	
		26.934	26.898		26.894		

27.094					27.572	27.968	27.454
27.92							
28.333	28.166	28.061	28.076	28.996	28.126	28.525	28.085
					28.32		
		29.937	29.925	29.781	29.131	29.754	29.008
			30.836	30.381	30.543		30.387
	30.007	30.882		30.752			
	30.945						
	31.29	31.198	31.163	31.404			
32.91	32.456	32.474	32.45	32.533			
33.111	33.324	33.26	33.485	33.492		33.17	
	33.895	33.51	33.864				
		33.856					
				34.992			34.128
	35.415	35.658	35.607	35.524		35.401	

36.014	36.105	36.156	36.154				36.016
	36.545	36.556	36.56				36.645
37.44		37.831		37.284		37.36	
37.806							
	38.154	38.042	38.041	38.903	38.342	38.294	38.163
	38.803						
	39.321	39.06	39.002		39.5		39.1
		39.331	39.336			39.317	39.339
40.48				40.503			
41.176	41.388	41.281	41.302				41.859
		41.702					
42.195	42.249	42.042					
		42.819	42.754				
43.635	43.456	43.97	43.883				
44.478	44.932	44.902	44.913				

45.372		45.463		45.323			
45.372							
	46.816	46.156					
	47.778	47.141	47.745				
		47.753					
		48.094	48.05				
		48.538					
	49.493	49.468					

Table AA 3.3: PXRD data for samples TA-I-18-3a (1:1), TA-I-18-3b (1:2), TA-I-18-3c (2:1), in acetonitrile

Malic acid	Iso stnd	Iso EHOWIH	Iso EHOWIH01	Iso EHOWIH02	TA-I-18-3a	TA-I-18-3b	TA-I-18-3c
2-Theta °	2-Theta °	2-Theta °	2-Theta °	2-Theta °	2-Theta °	2-Theta °	2-Theta °
						6.766	
					10.39		10.372
				11.677			
					13.759	13.476	13.733
14.254				14.625			
						15.147	
				16.097	16.397	16.882	16.362
				16.52	16.912		16.87
	17.842	17.859	17.843		17.555	17.997	17.525
	18.855	18.748	18.766	18.626			

18.95							
	19.411	19.347	19.347	19.14	19.102		19.064
20.518	20.874	20.485	20.468	20.138			
			20.996	20.747	20.63	20.302	
				20.988			20.598
21.275		21.037			21.122		
				21.94	21.592	21.994	21.568
				22.214	22.511	22.491	22.538
23.927	23.449	23.498	23.48	23.457	23.354	23.864	23.356
					23.894		
	24.454	24.385	24.396		24.46	24.196	24.506
24.911				24.601	24.643	24.704	
				25.403	25.4	25.54	
	25.937			25.789			

	26.644	26.093	26.059				26.035
		26.934	26.898				
27.094					27.426		27.394
27.92							
28.333	28.166	28.061	28.076		28.086	28.123	28.063
				28.996	28.485	28.421	28.97
		29.937	29.925	29.781	29.018		
			30.836	30.381	30.408		30.365
	30.007	30.882		30.752			
	30.945						
	31.29	31.198	31.163	31.404	31.452		31.211
	32.456	32.474	32.45	32.533		32.097	
32.91						32.661	
33.111	33.324	33.26	33.485	33.492	33.767		33.752
	33.895	33.51	33.864				

		33.856					
				34.992	34.078	34.095	34.003
	35.415	35.658	35.607	35.524	35.95		35.913
36.014	36.105	36.156	36.154		36.589	36.221	36.619
	36.545	36.556	36.56		36.589		
37.44		37.831		37.284		37.051	
37.806						37.683	
	38.154	38.042	38.041	38.903	38.125	38.291	38.093
	38.803			38.903	38.357	38.859	38.356
		39.06	39.002				
	39.321	39.331	39.336		39.21		39.269
40.48				40.503			
41.176	41.388	41.281	41.302				
		41.702					
42.195	42.249	42.042					

		42.819	42.754				
43.635	43.456	43.97	43.883				
44.478	44.932	44.902	44.913				
45.372		45.463		45.323			
45.372							
	46.816	46.156					
	47.778	47.141	47.745				
		47.753					
		48.094	48.05				
		48.538					
	49.493	49.468					

Table AA 3.4: PXRD data for samples TA-I-17-3a (1:1), TA-I-17-3b (1:2), TA-I-17-3c (2:1), in methanol

Malic acid	Nicotin-amide	Nicoam 01	Nicoam 02	Nicoam	TA-I-17-3a	TA-I-17-3b	TA-I-17-3c
2-Theta °	2-Theta °	2-Theta °	2-Theta °	2-Theta °	2-Theta °	2-Theta °	2-Theta °
					7.68	7.787	7.645
	11.67	11.328	11.301	11.296			
14.52		14.839	14.801	14.764		14.903	14.859
	15.115				15.398	15.465	15.335
					17.966	17.805	17.272
18.95					18.545	18.168	18.065
						18.487	
			19.061				
		19.551	19.52	19.495		19.592	19.292
	19.822	19.96	19.884	19.858			
20.518	20.19						20.047
							20.831

21.275					21.709		
	22.524	22.295	22.215	22.184	22.14	22.309	22.203
		22.784	22.697	22.68		22.716	
	23.03	23.167	23.348	23.347	23.17	23.271	23.24
23.927	23.646	23.868				23.986	23.504
24.91		24.75	24.701	24.662		24.563	24.463
			25.379	25.366		25.431	25.272
	25.707	25.871	25.823	25.819		25.925	
	26.114	26.395					
27.094	27.603		27.311	27.266		27.345	27.852
27.92		27.91			27.811	27.851	
			28.443	28.438			
28.33	28.72	28.905	28.861	28.845			28.766
		29.378					
	30.37	30.199	30.141	30.088			

		31.602				31.129	31.376
32.91	32.79	32.899	32.575	32.6			32.542
33.111		33.145					
		33.708	33.594			33.64	33.373
	34.61	34.442	34.412			34.713	
		35.153	35.764				
		35.83					
36.014	36.82		36.478	36.935			
			36.981				
37.44	37.212	37.082				37.085	37.466
37.806							
	38.93	38.802	38.666	38.64			
						39.144	
40.48			40.945				
41.17		41.06	41.466	41.475			

		41.724					
42.19							
43.63							
44.478							
45.37							
			46.593	46.627			
	47.9	47.744	47.307	47.692			
		48.001	47.705				
		48.62	48.809				

Table AA 3.5: PXRD data for samples TA-I-18-2a (1:1), TA-I-18-2b (1:2), TA-I-18-2c(2:1), in acetone

Malic acid	Nicotinamide	Nicoam 01	Nicoam 02	Nicoam	TA-I-18-2a	TA-I-18-2b	TA-I-18-2c
2-Theta °	2-Theta °	2-Theta °	2-Theta °	2-Theta °	2-Theta °	2-Theta °	2-Theta °
					7.881	7.833	7.728
	11.67	11.328	11.301	11.296			
14.52		14.839	14.801	14.764			14.872
	15.115				15.053	15.024	
					15.551	15.497	15.414
18.95					18.233	18.182	18.024
			19.061		19.396	19.385	19.275
		19.551	19.52	19.495			
	19.822	19.96	19.884	19.858			
20.518	20.19						
					20.951	20.943	20.81

21.275					21.644	21.614	21.465
	22.524	22.295	22.215	22.184	22.355	22.349	22.228
		22.784	22.697	22.68			
	23.03	23.167	23.348	23.347	23.325	23.337	23.234
23.927	23.646	23.868					
24.91		24.75	24.701	24.662	24.609	24.582	24.444
			25.379	25.366	25.449		25.341
	25.707	25.871	25.823	25.819	25.843	25.463	
	26.114	26.395			26.617	26.592	26.494
27.094	27.603		27.311	27.266	27.22	27.157	27.008
27.92		27.91				27.986	27.898
			28.443	28.438	28.008		
28.33	28.72	28.905	28.861	28.845	28.902	28.831	28.721
		29.378					
	30.37	30.199	30.141	30.088			

		31.602			31.46	31.474	
32.91	32.79	32.899	32.575	32.6			
33.111		33.145			33.24		33.185
		33.708	33.594		33.539	33.391	
	34.61	34.442	34.412				
		35.153	35.764				
		35.83					
36.014	36.82		36.478	36.935			
			36.981		37.731		
37.44	37.212						
37.806		37.082			37.731		
	38.93	38.802	38.666	38.64			
40.48			40.945				
41.17		41.06	41.466	41.475			

		41.724					
42.19							
43.63							
44.478							
45.37							
			46.593	46.627			
	47.9	47.744	47.307	47.692			
		48.001	47.705				
		48.62	48.809				

Table AA 3.6: PXRD data for samples TA-I-18-4a (1:1), TA-I-18-4b (1:2), TA-I-18-4c (2:1), in methanol

| DL-malic acid | Nicotin amide Std | NICOAM | NICOAM01 | NICOAM02 | TA-I-18-4a | TA-I-18-4b | TA-I-18-4c |
2-Theta °	2-Theta °	2-Theta °	2-Theta °	2-Theta °	2-Theta °	2-Theta °	2-Theta °
					7.83	7.717	7.794
	11.671	11.296	11.328	11.301			
					10.312		
14.254		14.764	14.839	14.801		14.905	14.994
	15.115				15.036	15.402	15.479
					15.505		
						16.71	16.753
						17.363	17.412
18.95					18.186	18.084	18.153
	19.822	19.041	19.137	19.061	19.09	19.015	19.049
		19.495	19.551	19.52	19.431	19.331	19.405
		19.858	19.96	19.884			

20.518	20.19				20.93	20.854	20.917
21.275					21.627	21.497	21.577
	22.524	22.184	22.295	22.215	22.365	22.285	22.347
		22.68	22.784	22.697		22.76	22.827
	23.031	23.347	23.167	23.348	23.328	23.276	23.334
23.927	23.646		23.868				
24.911		24.662	24.75	24.701	24.601	24.484	24.575
		25.366		25.379	25.443	25.335	25.399
	25.707	25.819	25.871	25.823		25.61	25.699
	26.114		26.395	26.601	26.603	26.487	26.569
27.094		27.266	27.017	27.311			27.05
27.92	27.603		27.91		27.966	27.895	27.952
28.333		28.438		28.443			
	28.724	28.845	28.905	28.861	28.904	28.771	28.859
	29.158		29.378	29.64		29.102	29.171

	30.375	30.088	30.199	30.141	30.209	30.072	30.191
	31.399	31.207	31.602	31.193	31.526	31.404	31.483
		32.6	32.388	32.575	32.209		32.143
32.91	32.798		32.899				
33.111			33.145			33.15	33.237
	33.892	33.557	33.708	33.594	33.377	33.404	33.489
	34.61	34.09, 34.37	34.442	34.05, 34.412	34.284	34.155	34.22
	34.743	34.758		34.763	34.75	34.623	34.652
			35.153				
		35.72	35.839	35.764			
36.014		36.494		36.478			
	36.82	36.935	36.808	36.981		36.852	36.85
37.44	37.212						
37.806			37.082		37.686	37.585	37.604
	38.935	38.64	38.802	38.666	38.515	38.42	38.477

			39.294			39.437	39.441
		39.567	39.702	39.612			
40.48		40.166	40.467	40.167	40.215	40.094	40.194
		40.914		40.945			
41.176	41.339	41.475	41.06	41.466			
	41.656	41.822	41.724	41.861			
42.195							
43.635	43.688	43.464			43.877		43.856
44.478		44.413					
45.372							
		46.627	46.539	46.593			
	47.9	47.312	47.137	47.307		47.47	47.527
		47.692	47.744	47.705			
			48.001	48.809			
			48.62				

	49.148		49.526				

Table AA 3.7: PXRD data for samples TA-I-22-2a (1:1), TA-I-22-2c (2:1), in methanol

L-Malic acid	Iso stnd	Iso EHOWIH	Iso EHOWIH01	Iso EHOWIH02	TA-I-22-2b	TA-I-22-2c
2-Theta °	2-Theta °	2-Theta °	2-Theta °	2-Theta °	2-Theta °	2-Theta °
7.558						
				11.677		11.995
				14.625		
					15.134	
				16.097		
				16.52	16.807	16.93
17.917	17.842	17.859	17.843		17.895	
	18.855	18.748	18.766	18.626		
19.375	19.411	19.347	19.347	19.14		

20.147	20.874	20.485	20.468	20.138		
20.809			20.996	20.747		
				20.988		
21.067		21.037				21.15
21.981				21.94	21.865	
22.405				22.214	22.442	
	23.449	23.498	23.48	23.457	23.813	23.891
24.443	24.454	24.385	24.396		24.219	
				24.601	24.634	
				25.403	25.495	25.478
	25.937			25.789		
26.008	26.644	26.093	26.059			

26.314						
		26.934	26.898			
27.045						
27.782					27.991	
	28.166	28.061	28.076		28.398	
				28.996		
29.487						
29.762		29.937	29.925	29.781		
30.324	30.007			30.381		
	30.945	30.882	30.836	30.752		
31.911	31.29	31.198	31.163	31.404		31.533
	32.456	32.474	32.45	32.533	32.802	

	33.324	33.26	33.485	33.492		
	33.895	33.51	33.864		33.991	
		33.856				
34.106						
				34.992		
35.496	35.415	35.658	35.607	35.524		35.039
35.81						
	36.105	36.156	36.154			36.081
	36.545	36.556	36.56			
37.09						37.191
37.779		37.831		37.284	37.562	
38.4	38.154	38.042	38.041			38.284
	38.803			38.903	38.844	
		39.06	39.002			

39.477	39.321	39.331	39.336			39.379
40.014						
40.742				40.503		
	41.388	41.281	41.302			
41.575		41.702				
42.219	42.249	42.042				
		42.819	42.754			
47.871	43.456	43.97	43.883			
	44.932	44.902	44.913			
		45.463		45.323		
	46.816	46.156				
		47.141				
47.871	47.778	47.753	47.745			
		48.094	48.05			

		48.538				
	49.493	49.468				

Table AA 3.8: PXRD data for samples TA-I-22-3a (1:1), TA-I-22-3b (1:2), TA-I-22-3c (2:1), in acetone

L-Malic acid	Iso stnd	Iso EHOWIH	Iso EHOWIH01	Iso EHOWIH02	TA-I-22-3a	TA-I-22-3b	TA-I-22-3c
2-Theta °	2-Theta °	2-Theta °	2-Theta °	2-Theta °	2-Theta °	2-Theta °	
6.71					6.717	6.681	
				11.677			
						13.406	
				14.625			
					15.156	15.156	
				16.097			
				16.52	16.806	16.791	
17.917	17.842	17.859	17.843		17.898	17.893	
	18.855	18.748	18.766	18.626			
19.375	19.411	19.347	19.347	19.14			
20.147	20.874	20.485	20.468	20.138	20.171	20.128	

20.809			20.996	20.747			
				20.988			
21.067		21.037					
21.981				21.94	21.873	21.859	
22.405				22.214	22.444	22.432	
	23.449	23.498	23.48	23.457			
					23.837	23.822	
24.443	24.454	24.385	24.396		24.232	24.225	
				24.601	24.613	24.593	
				25.403	25.484	25.477	
	25.937			25.789			
26.008	26.644	26.093	26.059				
26.314							
		26.934	26.898				

27.045							
27.782						27.999	
	28.166	28.061	28.076		28.017	28.367	
				28.996	28.384		
29.487							
29.762		29.937	29.925	29.781			
30.324	30.007			30.381			
	30.945	30.882	30.836	30.752			
31.911	31.29	31.198	31.163	31.404			
	32.456	32.474	32.45	32.533	32.058	32.052	
						32.834	
	33.324	33.26	33.485	33.492			
	33.895	33.51	33.864		33.987	33.967	

		33.856					
34.106							
				34.992			
35.496	35.415	35.658	35.607	35.524			
35.81							
	36.105	36.156	36.154				
	36.545	36.556	36.56				
37.09							
37.779		37.831		37.284	37.565	37.536	
38.4	38.154	38.042	38.041				
	38.803			38.903	38.851	38.829	
		39.06	39.002		39.156	39.149	
39.477	39.321	39.331	39.336				
40.014							

40.742				40.503			
	41.388	41.281	41.302				
41.575		41.702					
42.219	42.249	42.042					
		42.819	42.754				
47.871	43.456	43.97	43.883				
	44.932	44.902	44.913				
		45.463		45.323			
	46.816	46.156					
		47.141					
47.871	47.778	47.753	47.745				
		48.094	48.05				
		48.538					
	49.493	49.468					

Table AA 3.9: PXRD data for samples TA-I-22-4a (1:1), TA-I-22-4b (1:2), TA-I-22-4c (2:1), in acetonitrile

L-Malic acid	Iso stnd	Iso EHOWIH	Iso EHOWIH01	Iso EHOWIH02	TA-I-22-4a	TA-I-22-4b	TA-I-22-4c
2-Theta °	2-Theta °	2-Theta °	2-Theta °	2-Theta °	2-Theta °	2-Theta °	2-Theta °
6.717					6.637		
					9.21		
					10.545		
				11.677		11.688	
					12.436		
					13.101		
					13.592		
				14.625			
					15.241		15.112
				16.097	16.373		
				16.52		16.65	16.695

					17.182		
17.917	17.842	17.859	17.843		17.43		17.834
					18.315		
	18.855	18.748	18.766	18.626			
					18.6		
19.375	19.411	19.347	19.347	19.14	19.065		
					19.637		
20.147	20.874	20.485	20.468	20.138	20.252		
20.809			20.996	20.747		20.953	20.908
				20.988			
21.067		21.037			21.235		
21.981				21.94	21.858	21.979	21.842
22.405				22.214			22.395

	23.449	23.498	23.48	23.457	23.228	23.55	23.777
24.443	24.454	24.385	24.396		24.335		24.275
				24.601	24.87		24.515
				25.403		25.203	25.246
	25.937			25.789			25.463
26.008	26.644	26.093	26.059		26.27	26.654	26.876
26.314							
		26.934	26.898				
27.045					27.506	27.498	
27.782							27.991
	28.166	28.061	28.076				28.326
				28.996			
29.487							

29.762		29.937	29.925	29.781	29.626	29.365	
30.324	30.007			30.381		30.30	
	30.945	30.882	30.836	30.752			
31.911	31.29	31.198	31.163	31.404		31.23	
	32.456	32.474	32.45	32.533			
	33.324	33.26	33.485	33.492			
	33.895	33.51	33.864			33.976	33.967
		33.856					
34.106							
				34.992		34.653	34.886
35.496	35.415	35.658	35.607	35.524		35.553	
35.81							35.841
	36.105	36.156	36.154			36.222	
	36.545	36.556	36.56				

37.09						37.084	37.012
37.779		37.831		37.284			37.532
38.4	38.154	38.042	38.041			38.023	
	38.803			38.903			38.87
		39.06	39.002			39.003	39.17
39.477	39.321	39.331	39.336				
40.014							
40.742				40.503			40.767
	41.388	41.281	41.302				
41.575		41.702					
42.219	42.249	42.042					
		42.819	42.754				
47.871	43.456	43.97	43.883				
	44.932	44.902	44.913				

		45.463		45.323			
	46.816	46.156					
		47.141					
47.871	47.778	47.753	47.745				
		48.094	48.05				
		48.538					
	49.493	49.468					

Table AA 3.10: PXRD data for samples TA-I-23-2a (1:1), TA-I-23-2b (1:2), TA-I-23-2c (2:1), in acetone

L-Malic acid	Nicotinamide Std	NICOAM	NICOAM01	NICOAM02	TA-I-23-2a	TA-I-23-2b	TA-I-23-2c
2-Theta °	2-Theta °	2-Theta °	2-Theta °	2-Theta °		2-Theta °	2-Theta °
6.717						8.597	
	11.671	11.296	11.328	11.301			
		14.764	14.839	14.801	14.39	14.629	
	15.115						
					18.99	18.509	
17.917							
19.375		19.041	19.137	19.061			
	19.822	19.495	19.551	19.52		19.705	19.425
		19.858	19.96	19.884			
20.147	20.19						
20.809							
21.067					21.08		21.097

21.981						21.455	21.491
22.405	22.524	22.184	22.295	22.215			
		22.68	22.784	22.697			22.975
	23.031	23.347	23.167	23.348			
	23.646		23.868				
						24.076	24.01
24.44						24.41	
		24.662	24.75	24.701		24.912	
		25.366		25.379	25.20	25.447	
	25.707	25.819	25.871	25.823	25.98		25.849
26.008	26.114			26.601			
26.314			26.395			26.217	
27.045		27.266	27.017	27.311			
27.782	27.603		27.91		27.74	27.982	
		28.438		28.443			28.212

	28.724	28.845	28.905	28.861	28.89		
29.487	29.158		29.378				29.145
29.762				29.64		29.109	
30.324	30.375	30.088	30.199	30.141			
31.911	31.399	31.207	31.602	31.193		31.659	
		32.6	32.388	32.575			
	32.798		32.899			32.649	
			33.145				
	33.892	33.557	33.708	33.594			
34.106	34.61	34.09, 34.37	34.442	34.05, 34.412			
	34.743	34.758		34.763			
35.496			35.153				
35.81		35.72	35.839	35.764			35.284
		36.494		36.478			
	36.82	36.935	36.808	36.981			

37.09	37.212		37.082				
37.779						37.305	
38.4	38.935	38.64	38.802	38.666		38.098	
			39.294				
39.477		39.567	39.702	39.612			
40.014		40.166	40.467	40.167			

Table AA 3.11: PXRD data for samples TA-I-22-3a (1:1), TA-I-22-3b (1:2), TA-I-22-3c (2:1), in acetone

L-Malic acid	Nicotinamide Std	NICOAM	NICOAM01	NICOAM02	TA-I-24-1a	TA-I-24-1b	TA-I-24-1c
2-Theta °	2-Theta °	2-Theta °	2-Theta °	2-Theta °	2-Theta °	2-Theta °	2-Theta °
6.717							
	11.671	11.296	11.328	11.301			
						12.232	
		14.764	14.839	14.801		14.371	
	15.115						
					17.327	17.32	
17.91					17.923		
					18.963	18.984	18.913
19.375		19.041	19.137	19.061			
	19.822	19.495	19.551	19.52		19.453	
		19.858	19.96	19.884			

20.147	20.19				20.154	20.16	20.586
20.809					20.638	20.633	20.996
21.067					21.058	21.081	
21.981							
22.405	22.524	22.184	22.295	22.215	22.24	22.193	22.145
		22.68	22.784	22.697	22.54	22.549	22.476
	23.031	23.347	23.167	23.348	23.571	23.576	23.509
	23.646		23.868				
24.443							
		24.662	24.75	24.701		24.646	
		25.366		25.379		25.255	25.368
	25.707	25.819	25.871	25.823	25.424	25.953	
26.008	26.114			26.601			
26.314			26.395		26.471	26.481	26.421

27.045		27.266	27.017	27.311			
27.782	27.603		27.91		27.721	27.746	27.673
		28.438		28.443		28.701	
	28.724	28.845	28.905	28.861	28.657	28.88	28.595
29.487	29.158		29.378		29.289	29.315	29.237
29.762				29.64			
30.324	30.375	30.088	30.199	30.141		30.141	
31.911	31.399	31.207	31.602	31.193	31.277	31.295	31.238
		32.6	32.388	32.575			
	32.798		32.899				
			33.145		33.257	33.276	33.199
	33.892	33.557	33.708	33.594		33.837	
34.106	34.61	34.09, 34.37	34.442	34.05, 34.412			
	34.743	34.758		34.763	34.857	34.857	34.79

35.496			35.153				
35.81		35.72	35.839	35.764	35.999	35.996	
		36.494		36.478			36.973
	36.82	36.935	36.808	36.981			
37.09	37.212		37.082		37.037	37.058	
37.779						37.914	
38.4	38.935	38.64	38.802	38.666		38.696	
			39.294				
39.477		39.567	39.702	39.612			
40.014		40.166	40.467	40.167	40.262	40.27	
40.742		40.914		40.945			
41.575	41.339	41.475	41.06	41.466			
	41.656	41.822	41.724	41.861			

Table AA 3.12: PXRD data for samples TA-I-23-3a (1:1), TA-I-23-3c (2:1), in methanol

L-Malic acid	Nicotinamide Std	NICOAM	NICOAM01	NICOAM02	TA-I-23-3a	TA-I-23-3c
2-Theta °	2-Theta °	2-Theta °	2-Theta °	2-Theta °	2-Theta °	2-Theta °
6.717						
					7.47	
	11.671	11.296	11.328			
		14.764	14.839			
	15.115					
17.917					17.62	
					18.25	
19.375		19.041	19.137		19.27	19.25
	19.822	19.495	19.551			
		19.858	19.96			
20.147	20.19				20.02	

20.809					20.91	20.89
21.067					21.33	21.31
21.981						
22.405	22.524	22.184	22.295		22.42	
		22.68	22.784		22.82	22.67
	23.031	23.347	23.167			
	23.646		23.868		23.89	23.79
24.443						
		24.662	24.75		24.72	
		25.366				
	25.707	25.819	25.871		25.71	25.68
26.008	26.114				26.76	
26.314			26.395			
27.045		27.266	27.017		27.05	

27.782	27.603		27.91			
		28.438			28.01	28.03
	28.724	28.845	28.905		28.95	28.93
29.487	29.158		29.378			
29.762					29.56	
30.324	30.375	30.088	30.199		30.17	
	31.399	31.207			31.02	
31.911			31.602		31.57	
		32.6	32.388			
	32.798		32.899			
			33.145			
	33.892	33.557	33.708		33.50	
34.106	34.61	34.09, 34.37	34.442	412	34.06	
	34.743	34.758				

35.496			35.153		35.12	
35.81		35.72	35.839			
		36.494			36.11	
	36.82	36.935	36.808		36.82	
37.09	37.212		37.082		37.28	
37.779					37.67	
					38.33	
38.4	38.935	38.64	38.802		38.95	
			39.294		39.37	
39.477		39.567	39.702			
40.014		40.166	40.467			
40.742		40.914				
41.575	41.339	41.475	41.06			
	41.656	41.822	41.724			

293

Table AA 3.13: FT-IR assignments for samples TA-I-18-1a (1:1), TA-I-18-1b (1:2), TA-I-18-1c (2:1), and its starting materials in acetone

Isonicotinamide	DL-Malic acid	TA-I-18-1a	TA-I-18-1b	TA-I-18-1c	Assignment
(cm-1)	(cm-1)	(cm-1)	(cm-1)	(cm-1)	
	3445 s	3488		3400	_(OH) of CHOH
3370, 3186		3386, 3204	3388	3389	ú NH2 (100), ú NH2 (100)
3076, 3064, 3053, 3041		3099	3102		ú CH (99), ú CH (100)
	3030 s, br		3089		_(OH) of COOH hydrogen bond mode _s(CH2)
	2911 sh	2926	2985, 2978	2925	ú CH2
	2624 m, br				Combinations H2 bond mode,dimer
	1739 vvs, 1716 vvs, 1690 vvs	1712	1680	1716	(C= O) of dimeric COOH out-of-phase
1667			1636	1636	ú CO
1624, 1596		1616	1616		δNH2 , ú ring +δCCH , ú ring
1552		1551	1557	1557	ú ring

1496				1457	δCCH +ύ ring
1410		1414	1413	1414	δCCH +ύ ring
	1442 s-m				_(C–O) Cυ(OH) of COOH, (acid II)
	1410 s-m				υ(CH2_scis
1395		1397	1397		ύ CN + δCC , δCCH+δCCO
	1385 w				υ(CH) of CHOH
	1359 m.-w		1308		δ(CH2) SCIS, δ(CH2)wag
	1290 s, d				υ(OH) C_(C–O) of COOH(acid III)
	1277 sh				υ(CH2)twist,(OH), (C–O)
	1267 sh			1263	δ(CH) of CHOD
1265		1262			ū ring
1228			1249		δCCH +ύ ring
	1219 m			1222	δ(CH2)
	1185 s				δ(CH2) twist, δ(CH2)scis

1148		1157			ring+CCH+CN+CC
1122					CCH+ ring
	1103 s	1110			(CH2)SCIS, ū(C-O),δ(OH)
1085					δ CCH +ύ ring
1063		1056		1055	NH2 rock +ύCN
	1033 w	1023		1023	ύ(C–C), (CH)
994			980		Ring
969		963		965	CH
	968 m				(C–C), υ(C-O)tors (acid IV)
955					ū CH
	951m				δ(OD)+ υ(C-O)of COOD(acidIII)
	885m,	882			δ(C-O), (C-CH2), (C-H)
875					ᵞCH
853					ᵞCH+ᵞ CC +ᵞCO
	825vvw				δ(C-O), (C-CH2), (C-H)

	790 vw	796		796	δ(CH2)
778					γring +γco
755				751	δ ring + úcc + úring
	750 vw	751	746		O-C=Odef.coupled with OH
	724 vvw				Def
708					ring + CO
	667 m	677			υ(C–H), υ(C–CH2),
669					ring+ring
629					δ CCO + ú ring
542					NH2 twist + ring + CC

S=strong, v=very, m=medium, w=week, sh=shoulder, as=antisymmetric, symsymmetric, i.p=in-plane

Table AA 3.14: FT-IR assignment of TA-I-18-2(a) (b) (c) for DL-malic acid and isonicotinamide and products of crystallisation (1:1), (1:2) and (2:1)

Assignment is made using the literature [16,22]

Isonicotinamide	DL-Malic acid	TA-I-18-3a 1:1	TA-I-18-3b 1:2	TA-I-18-3c 2:1	Assignment
(cm^{-1})	(cm^{-1})	$cm^{-1})$	(cm^{-1})	(cm^{-1})	
	3445 s	3491	3460	3490	_(OH) of CHOH
3370, 3186		3383,3203, 3203	3386, 3166	3383, 3204	ú NH2 (100), ú NH2 (100)
3076, 3064, 3053, 3041		3096,		3096	ú CH (99), ú CH (100)
	3030 s, br				_(OH) of COOH hydrogen bond mode _s(CH2)
	2911 sh	2894	2836	2895	ú CH2
	2624 m, br	2772	2782	2771	Combinations H2 bond mode dimer
		2462	2469	2463	
	1739 vvs, 1716 vvs, 1690 vvs	1714	1693, 1693	1716, 1684	(C= O) of dimeric COOH out-of-phase
1667					ú CO

1624, 1596		1588		1587	δNH2 , ύ ring +δCCH , ύ ring
1552		1547	1550	1547	ύ ring
1496					δCCH +ύ ring
1410		1416		1416	δCCH +ύ ring
	1442 s-m				_(C–O) Cυ(OH) of COOH, (acid II)
	1410 s-m				υ(CH2_scis)
1395			1339		ύ CN + δCC , δCCH+δCCO
	1385 w				υ(CH) of CHOH
	1359 m.-w		1323		δ(CH2) SCIS, δ(CH2)wag
	1290 s, d				υ(OH) C_(C–O) of COOH(acid III)
	1277 sh				υ(CH2)twist,(OH), (C–O)
	1267 sh				δ(CH) of CHOD
1265				1262	ū ring
1228		1220	1239	1220	δCCH +ύ ring
	1219 m				δ(CH2)

	1185 s		1168	1168	δ(CH2) twist, δ(CH2)scis
1148					ring+ CCH+CN+CC
1122					CCH+ ring
	1103 s	1107		1108	(CH2)SCIS
1085			1092		δ CCH +ú ring
1063			1053	1046	NH2 rock +úCN
	1033 w	1028	1028	1028	ú(C–C), (CH)
994					Ring
969		962		965	CH
	968 m				(C–C), υ(C-O)tors (acid IV)
955					ū CH
	951m		947		δ(OD)+ υ(C-O)of COOD(acid)
	885m,	893	860	894	δ(C-O), (C-CH2), (C-H)
875					ᵞCH
853		854		853	ᵞCH+ᵞ CC +ᵞCO

	825vvw		808		δ(C-O), (C-CH2), (C-H)
	790 vw	798		798	δ(CH2)
778					γring +γco
755		759	752	760	δ ring (30)+ úcc(17)+ úring
	750 vw				O-C=Odef.coupled with OH
	724 vvw				Def
708					ring + CO
	667 m	675	669	676	υ(C–H), υ(C–CH2),
669					ring+ring
629					δ CCO + ú ring
542					NH2 twist + ring + CC

S=strong, v=very, m=medium, w=week, sh=shoulder, as=antisymmetric, symsymmetric, i.p=in-plane

Table AA 3.15: FT-IR assignments for samples TA-I-18-2a (1:1), TA-I-18-2b (1:2), TA-I-18-2c (2:1), and its starting materials in acetone

Assignment is made using the literature. [16,22]

Nicotinamide FT-IR (cm^{-1})	DL-Malic acid FT-IR (cm^{-1})	TA-I-18-2a FT-IR (cm^{-1})	TA-I-18-2b FT-IR (cm^{-1})	TA-I-18-2c FT-IR (cm^{-1})	Assignment
	3445 s	3408	3475, 3400	3475, 3404	_(OH) of CHOH
3366, 3167		3207	3220	3343, 3220	ú NH2 (100), ú NH2 (100)
	3030 s, br	3079			_(OH) of COOH hydrogen bond mode _s(CH2_
	2911 sh		2983, 2930	2931	ú CH2
		2897, 2833	2850	2852	
2782, 2316			2767	2761	ú CH (99), ú CH (100)
	2624 m, br				Combinations H2 bond mode,dimer
		2480	2480	2486	
	1739 vvs, 1716 vvs, 1690 vvs		1717	1722	(C= O) of dimeric COOH out-of-phase
1962		1919	1921	1922	

1680		1695	1681	1676	ú CO
1483, 1618		1602	1615	1615	CN amide Stretch
		1562	1575	1575	
1341					CH ip bend
1410					δCCH +ú ring
	1442 s-m	1443		1425	_(C–O) Cυ(OH) of COOH, (acid II)
	1410 s-m	1408	1417		υ(CH2_scis
1395			1399	1399	ú CN + δCC , δCCH+δCCO
	1385 w				υ(CH) of CHOH
	1359 m.-w	1308		1369	δ(CH2) SCIS, δ(CH2)wag
	1290 s, d	1281	1299	1299	υ(OH) C_(C–O) of COOH(acid III)
	1277 sh				υ(CH2)twist,(OH), (C–O)
	1267 sh		1240	1243	δ(CH) of CHOD
1230		1232	1224	1222	CC stretch
1200					CH ip bend

	1219 m				δ(CH2)
	1185 s	1178	1192	1192	δ(CH2) twist, δ(CH2)scis
1154		1147			CC strech
1122					CH ip bend
	1103 s	1105	1108	1108	(CH2)SCIS, ū(C-O),δ(OH)
1027		1046	1044	1044	NH2 rock
1063					NH2 rock +úCN
	1033 w			1005	ú(C–C), (CH)
972		991			CH op bend
936					CH op bend
	968 m		943	943	(C–C), υ(C-O)tors (acid IV)
	951m	951		902	δ(OD)+ υ(C-O)of COOD(acidIII)
	885m,	882	897, 860		δ(C-O), (C-CH2), (C-H)
827					CH op bend
853		841			Vvw

	825vvw		831	831	δ(C-O), (C-CH2), (C-H)
	790 vw	794	798	796	δ(CH2)
777					γring + ring def
	750 vw	751		752	O-C=Odef.coupled with OH
	724 vvw				Def
702		704	702		Ring op. Bend γ ring
	667 m				υ(C–H), υ(C–CH2),

Table AA 3.16: FT-IR assignments for samples TA-I-18-4a (1:1), TA-I-18-4b (1:2), TA-I-18-4c (2:1), and its starting materials in acetonitrile

Assignment is made using the literature. [16,22]

Nicotinamide	DL-Malic acid	TA-I-18-4a	TA-I-18-4b	TA-I-18-4c	Assignment
FT-IR (cm^{-1})	FT-IR (cm^{-1})	FT-IR (cm^{-1})	FT-IR (cm^{-1})	FT-IR (cm^{-1})	
	3445 s	34454	3445	3446	_(OH) of CHOH
3366, 3167		3361,3300	3361,3300	3364,3301	ú NH2 (100), ú NH2 (100)
2782, 2316					ú CH (99), ú CH (100)
	3030 s, br	3114	3112	3114	_(OH) of COOH hydrogen bond mode _s(CH2_
	2911 sh	2913	2913	2913	ú CH2
		2831		2832	
	2624 m, br	2683	2684	2683	Combinations H2 bond mode,dimer
		2156	2155	2155	
		1822	1818	1819	
	1739 vvs, 1716 vvs, 1690 vvs	1695	1695	1696	(C= O) of dimeric COOH out-of-phase

1680		1641	1640	1640	ú CO
		1591	1591	1591	
1483, 1618		1491	1492	1492	CN amide Stretch
1341					CH ip bend
1410		1411	1411	1411	δCCH +ú ring
	1442 s-m				_(C–O) Cυ(OH) of COOH, (acid II)
	1410 s-m				υ(CH2_scis
1395					ú CN + δCC , δCCH+δCCO
	1385 w	1385	1385	1385	υ(CH) of CHOH
	1359 m.-w	1331	1333	1333	δ(CH2) SCIS, δ(CH2)wag
	1290 s, d				υ(OH) C_(C–O) of COOH(acid III)
	1277 sh				υ(CH2)twist,(OH), (C–O)
	1267 sh	1269	1268	1268	δ(CH) of CHOD
1230		1234	1233	1233	CC strech

307

1200		1207	1207	1207	CH ip bend
	1219 m				δ(CH2)
	1185 s				δ(CH2) twist, δ(CH2)scis
1154		1136	1136	1137	CC strech
1122					CH ip bend
	1103 s				(CH2)SCIS, ū(C-O),δ(OH)
1027					NH2 rock
1063		1065	1067	1066	NH2 rock +úCN
	1033 w	1019	1020	1021	ú(C–C), (CH)
972					CH op bend
936					CH op bend
	968 m				(C–C), υ(C-O)tors (acid IV)
	951m	951	952	953	δ(OD)+ υ(C-O)of COOD(acidIII)
	885m,	856	859	859	δ(C-O), (C-CH2), (C-H)
827					CH op bend

853					Vvw
	825vvw				δ(C-O), (C-CH2), (C-H)
	790 vw				δ(CH2)
777					γring + ring def
	750 vw				O-C=Odef.coupled with OH
	724 vvw		732		Def
702					Ring op. Bend γ ring
	667 m	672		672	υ(C–H), υ(C–CH2),

Table AA 3.17: FT-IR assignments for samples TA-I-23-2a (1:1), TA-I-23-2b (1:2), TA-I-23-2c (2:1), and its starting materials in acetone

Nicotinamide FT-IR(cm-1)	L-Malic acid FT-IR (cm-1)	TA-I-23-2a FT-IR (cm-1)	TA-I-23-2b FT-IR (cm-1)	TA-I-23-2c FT-IR (cm-1)	Assignment
	3537 vs, br		3446	3407	_(OH) of CHOH
3366, 3167		3206, 3109, 3075	3207, 3058	3206	ú NH2 (100), ú NH2 (100)
2782, 2316					ú CH (99), ú CH (100)
		2996, 2966	2987	2996, 2967	
	3393 sh		3380		_(OH) of COOH hydrogen bond mode _s(CH2_
	2670 sh				ú (OD) of CHOD
		1924			
	1721 vs	1716		1717	(C= O) of dimeric COOH out-of-phase
1680		1609	1677	1682	ú CO
		1566		1566	
1483, 1618		1444,1401	1613, 1484	1443	CN amide Stretch

	1413 s-m		1424		u(CH)2_scis
1410					δCCH +ú ring
1395		1362	1396	1362	ú CN + δCC , δCCH+δCCO
1341		1308	1339, 1313	1308	CH ip bend
	1288 m	1270	1262	1271	(OD)+(C-O)of COOD
1230		1244		1244	CC stretch
	1224 m				δ(CH2)
1200		1213	1204	1213	CH ip bend
	1186 m	1169	1171	1170	δ(CH2) twist, δ(CH2)scis
1154		1148	1131	1148	CC stretch
1122					CH ip bend
1063		1098	1079	1098	NH2 rock +úCN
	1036 w	1049	1049	1048	ú(C–C), (CH)
1027			1040		NH2 rock

311

	1107 s			1013	(CH2)SCIS, ῡ(C-O),δ(OH)
972			965	992	CH op bend
936			945	950	CH op bend
	899 vw	891	831		δ(C-O), (C-CH2), (C-H)
827					CH op bend
853		846		846	Vvw
777			761	781	γring + ring def
	757 vw	741		741	δ(CH2)
702					Ring op. Bend γ ring
	660 m	686	691	696	υ(C–H), υ(C–CH2),

Table AA 3.18: FT-IR assignments for samples TA-I-24-1a (1:1), TA-I-24-1b (1:2), TA-I-24-1c (2:1), and its starting materials in acetonitrile

Nicotinamide FT-IR(cm-1)	L-Malic acid FT-IR (cm^{-1})	TA-I-24-1a FT-IR (cm^{-1})	TA-I-24-1b FT-IR (cm^{-1})	TA-I-24-1c FT-IR (cm^{-1})	Assignment
	3537 vs, br	3405		3406	_(OH) of CHOH
3366, 3167		3206, 3072	3380, 3206	3206, 3072	ú NH2 (100), ú NH2 (100)
		2964	2964	2992, 2965	
		2855	2853	2856	
2782, 2316			2515		ú CH (99), ú CH (100)
	3393 sh				_(OH) of COOH hydrogen bond mode _s(CH2_
	2670 sh				ú (OD) of CHOD
		1918	1917	1918	
	1721 vs	1713		1714	(C= O) of dimeric COOH out-of-phase
1680		1677	1677	1678	ú CO

1483, 1618		1607, 1563	1604, 1563	1601, 1563	CN amide Stretch
	1413 s-m	1446	1444	1446	υ(CH)2_scis
1410		1404	1400	1404	δCCH +ύ ring
1395					ύ CN + δCC , δCCH+δCCO
1341		1307	1307	1307	CH ip bend
					ύ CN + δCC , δCCH+δCCO
	1288 m	1275	1275	1275	(OD)+(C-O)of COOD
1230					CC strech
	1224 m	1212	1211	1212	δ(CH2)
1200					CH ip bend
	1186 m	1167	1167	1167	δ(CH2) twist, δ(CH2)scis
1154					CC strech
1122					CH ip bend
	1107 s				(CH2)SCIS, ū(C-O),δ(OH)

1063		1098	1098	1097	NH2 rock +úCN
	1036 w				ú(C–C), (CH)
1027		1047	1047	1047	NH2 rock
972		991	990	991	CH op bend
936		958	955	958	CH op bend
	899 vw				δ(C-O), (C-CH2), (C-H)
827		846			CH op bend
853		886	880	871	Vvw
777		796		786	γring + ring def
	757 vw	741	743		δ(CH2)
702					Ring op. Bend γ ring
	660 m	691	690	691	υ(C–H), υ(C–CH2),

Table AA 3.19: IR-FT assignments for samples TA-I-23-2a (1:1), TA-I-23-2b (1:2), TA-I-23-2c (2:1), and its starting materials in acetone

Nicotinamide FT-IR(cm-1)	L-Malic acid FT-IR (cm^{-1})	TA-I-23-2a FT-IR (cm^{-1})	TA-I-23-2b FT-IR (cm^{-1})	TA-I-23-2c FT-IR (cm^{-1})	Assignment
	3537 vs, br		3446	3407	_(OH) of CHOH
3366, 3167		3206, 3109, 3075	3207, 3058	3206	ú NH2 (100), ú NH2 (100)
2782, 2316					ú CH (99), ú CH (100)
		2996, 2966	2987	2996, 2967	
	3393 sh		3380		_(OH) of COOH hydrogen bond mode _s(CH2_
	2670 sh				ú (OD) of CHOD
		1924			
	1721 vs	1716		1717	(C= O) of dimeric COOH out-of-phase
1680		1609	1677	1682	ú CO
		1566		1566	

1483, 1618		1444,1401	1613, 1484	1443	CN amide Stretch
	1413 s-m		1424		u(CH)2_scis
1410					δCCH +ú ring
1395		1362	1396	1362	ú CN + δCC , δCCH+δCCO
1341		1308	1339, 1313	1308	CH ip bend
	1288 m	1270	1262	1271	(OD)+(C-O)of COOD
1230		1244		1244	CC stretch
	1224 m				δ(CH2)
1200		1213	1204	1213	CH ip bend
	1186 m	1169	1171	1170	δ(CH2) twist, δ(CH2)scis
1154		1148	1131	1148	CC stretch
1122					CH ip bend
1063		1098	1079	1098	NH2 rock +úCN
	1036 w	1049	1049	1048	ú(C–C), (CH)

1027			1040		NH2 rock
	1107 s			1013	(CH2)SCIS, ῡ(C-O),δ(OH)
972			965	992	CH op bend
936			945	950	CH op bend
	899 vw	891	831		δ(C-O), (C-CH2), (C-H)
827					CH op bend
853		846		846	Vvw
777			761	781	γring + ring def
	757 vw	741		741	δ(CH2)
702					Ring op. Bend γ ring
	660 m	686	691	696	υ(C–H), υ(C–CH2),

318

Table AA 3.20: FT-IR assignments for samples TA-I-24-1a (1:1), TA-I-24-1b (1:2), TA-I-24-1c (2:1), and its starting materials in acetonitrile

Nicotinamide FT-IR(cm-1)	L-Malic acid FT-IR (cm^{-1})	TA-I-24-1a FT-IR (cm^{-1})	TA-I-24-1b FT-IR (cm^{-1})	TA-I-24-1c FT-IR (cm^{-1})	Assignment
	3537 vs, br	3405		3406	_(OH) of CHOH
3366, 3167		3206, 3072	3380, 3206	3206, 3072	ú NH2 (100), ú NH2 (100)
		2964	2964	2992, 2965	
		2855	2853	2856	
2782, 2316			2515		ú CH (99), ú CH (100)
	3393 sh				_(OH) of COOH hydrogen bond mode _s(CH2_
	2670 sh				ú (OD) of CHOD
		1918	1917	1918	
	1721 vs	1713		1714	(C= O) of dimeric COOH out-of-phase
1680		1677	1677	1678	ú CO

1483, 1618		1607, 1563	1604, 1563	1601, 1563	CN amide Stretch
	1413 s-m	1446	1444	1446	υ(CH)2_scis
1410		1404	1400	1404	δCCH +ύ ring
1395					ύ CN + δCC , δCCH+δCCO
1341		1307	1307	1307	CH ip bend
					ύ CN + δCC , δCCH+δCCO
	1288 m	1275	1275	1275	(OD)+(C-O)of COOD
1230					CC strech
	1224 m	1212	1211	1212	δ(CH2)
1200					CH ip bend
	1186 m	1167	1167	1167	δ(CH2) twist, δ(CH2)scis
1154					CC strech
1122					CH ip bend
	1107 s				(CH2)SCIS, ū(C-O),δ(OH)

1063		1098	1098	1097	NH2 rock +úCN
	1036 w				ú(C–C), (CH)
1027		1047	1047	1047	NH2 rock
972		991	990	991	CH op bend
936		958	955	958	CH op bend
	899 vw				δ(C-O), (C-CH2), (C-H)
827		846			CH op bend
853		886	880	871	Vvw
777		796		786	γring + ring def
	757 vw	741	743		δ(CH2)
702					Ring op. Bend γ ring
	660 m	691	690	691	υ(C–H), υ(C–CH2),

NMR ANALYSIS

Figure AA 3.1: 1HNMR TA-I-17-2b 1:2 ratio using (CD3) 2OD as solvent. 1HNMR 400MHz ((CD3)2OD-d6): δ = 8.70(dd, 2H), 7.77(dd, 2H), 4.5 (dd, 1H), 2.6(dd, 1H), 2.8(dd, 1H)
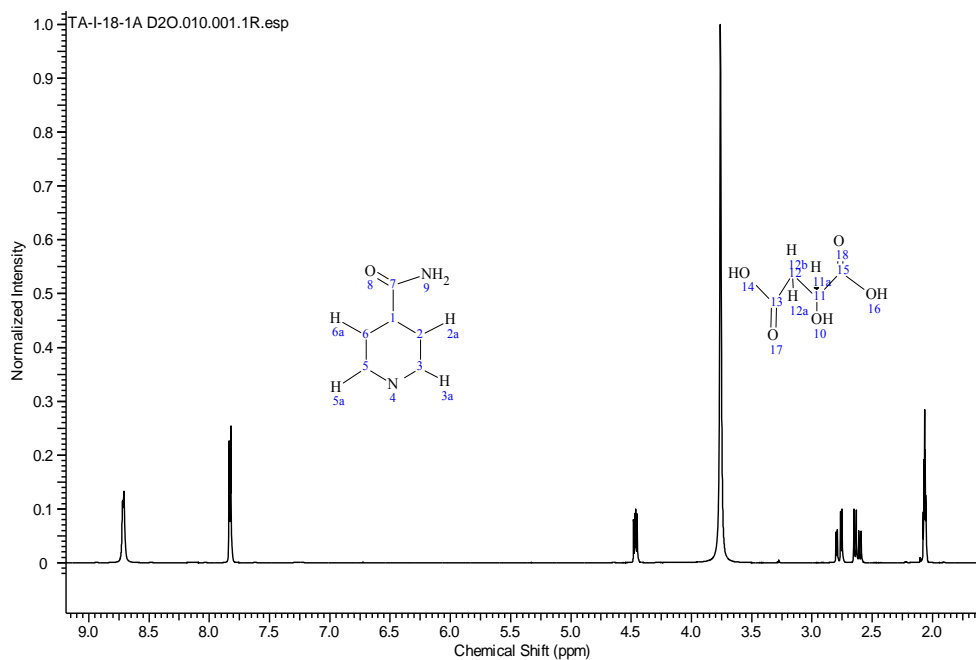
Figure AA 3.2: 1HNMR of malic acid and isonicotinamid product (from 1:1 starting ratio) using (CD$_3$)$_2$CO as solvent. 1HNMR 400MH

322
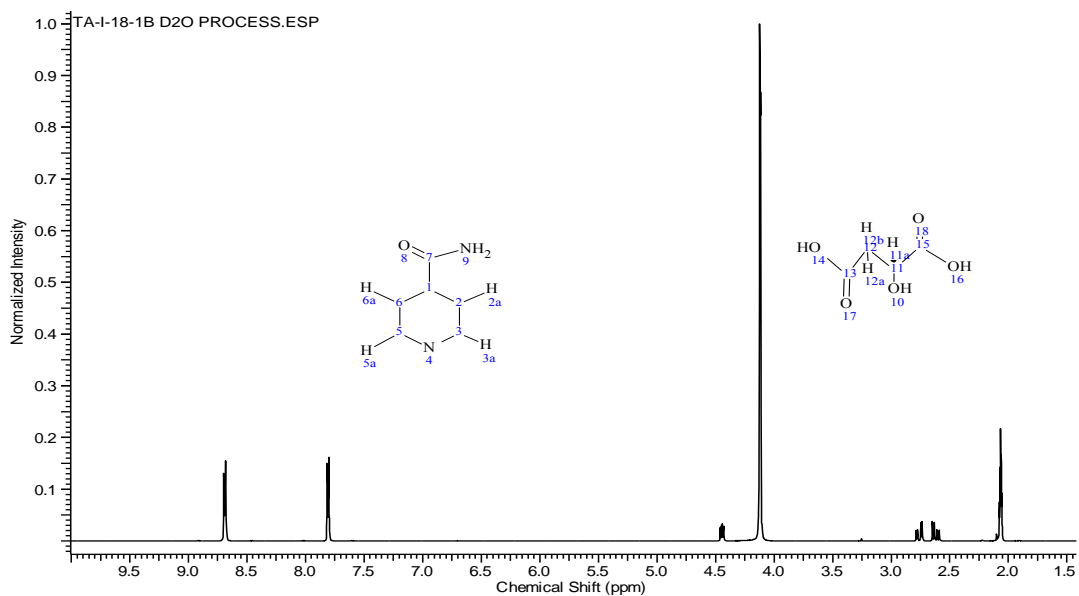
Figure AA 3.3: 1HNMR of malic acid and isonicotinamid product (from 1:2 starting ratio) using (CD$_3$)$_2$CO as solvent. 1HNMR 400MH
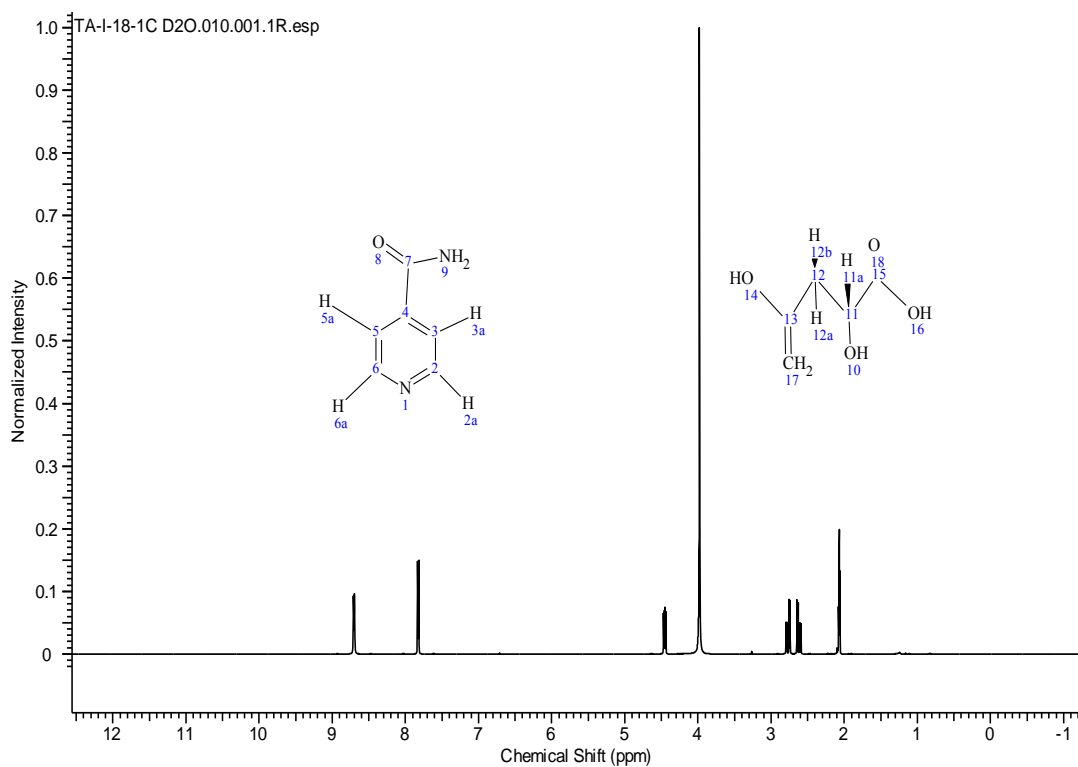
Figure AA 3.4: 1HNMR of malic acid and isonicotinamide product (from 2:1 starting ratio) using (CD$_3$)$_2$CO as solvent. 1HNMR 400M

323
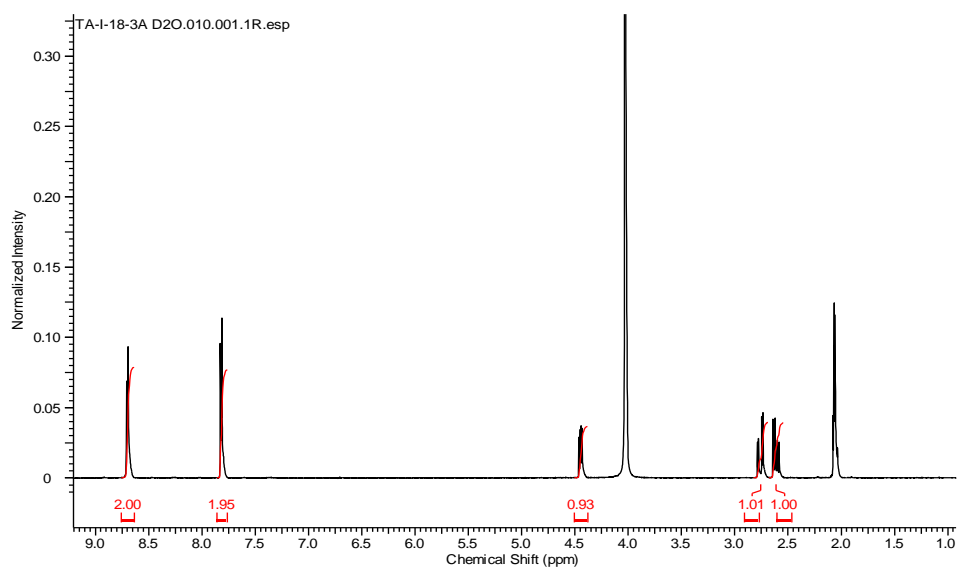
Figure AA 3.5: 1HNMR of DL-malic acid and isonicotinamide (from 1:1 starting ratio) using acetone-d6 as solvent. 1HNMR 400MH ((CD$_3$)$_3$OD-d$_6$): δ = 8.70(dd, 2H), 7.77(dd, 2H), 4.5 (dd, 1H), 2.6 (dd, 1H), 2.8 (dd, 1H)
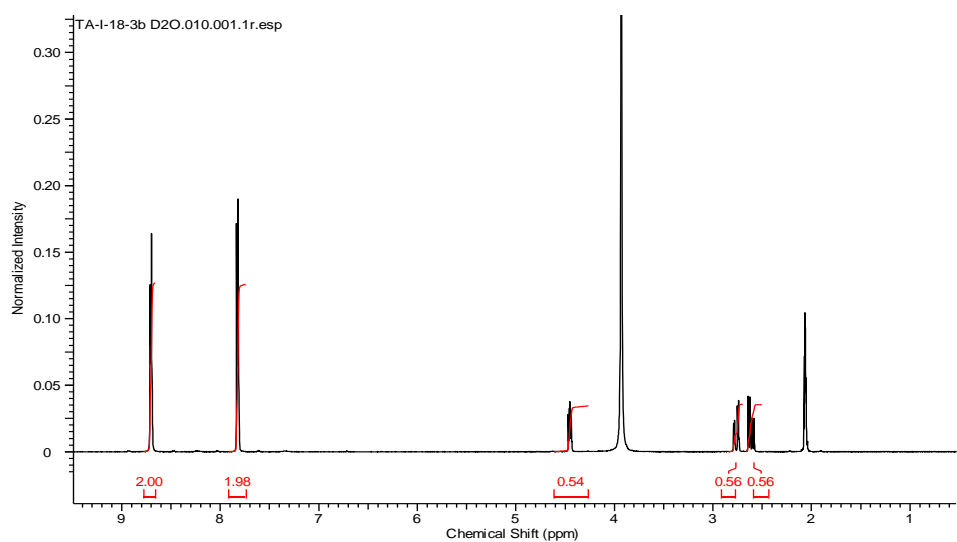
Figure AA 3.6: 1HNMR of DL-malic acid and isonicotinamide (from 1:2 starting ratio) using acetone-d6 as solvent. 1HNMR 400MH ((CD$_3$)$_3$OD-d$_6$): δ = 8.70(dd, 2H), 7.77(dd, 2H), 4.5 (dd, 1H), 2.6(dd, 1H), 2.8(dd, 1H)
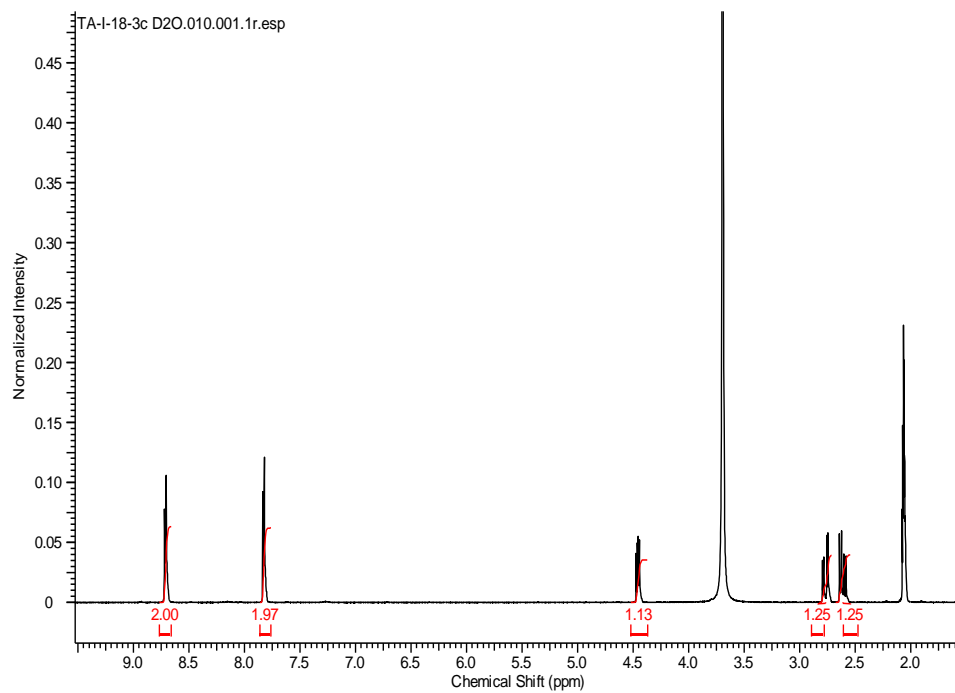
Figure AA 3.7: 1HNMR of DL-malic acid and isonicotinamide (from 2:1 starting ratio) using acetone-d6 as solvent. 1HNMP 400MH ((ΨΔ₃)₃OΔ-δ₆):¨δ = 8.70(δδ, 2H), 7.77(δδ, 2H), 4.5 (δδ, 1H), 2.6(δδ, 1H), 2.8(δδ, 1H)

Appendix B: Chapter 4

Table AB 4.1: PXRD data for samples TA-I-52-1a (1:1), TA-I-52-1b (1:2), in acetone

L-phenyllactic acid	Iso stnd	Iso EHOWIH	Iso EHOWIH01	Iso EHOWIH02	TA-I-52-1a	TA-I-52-1B
2-Theta °	2-Theta °	2-Theta °	2-Theta °	2-Theta °	2-Theta °	2-Theta °
10.28					7.63	7.77
11.698					10.05	10.23
14.668					11.815	15.303
15.911				11.677	15.159	17.913
18.2					15.71	18.244
18.762					17.735	18.665
19.119					18.534	20.342
19.805				14.625	20.191	23.025
20.2					23	23.194
20.611				16.097	23.981	24.157
20.945				16.52	25.291	25.44

21.644					28.69	28.773
23.128	17.842	17.859	17.843		30.571	30.24
24.105					35.971	30.752
26.255	18.855	18.748	18.766	18.626		37.678
27.785						
29.666	19.411	19.347	19.347	19.14		
30.305	20.874	20.485	20.468	20.138		
30.927			20.996	20.747		
31.98				20.988		
33.34		21.037				
33.534				21.94		
33.913				22.214		
35.314						
35.946	23.449	23.498	23.48	23.457		
36.49						

36.942	24.454	24.385	24.396			
37.674				24.601		
38.706				25.403		
39.761	25.937			25.789		
	26.644	26.093	26.059			
		26.934	26.898			
	28.166	28.061	28.076			
				28.996		
		29.937	29.925	29.781		
			30.836	30.381		
	30.007	30.882		30.752		
	30.945					

	31.29	31.198	31.163	31.404		
	32.456	32.474	32.45	32.533		
	33.324	33.26	33.485	33.492		
	33.895	33.51	33.864			
		33.856				
				34.992		
	35.415	35.658	35.607	35.524		
	36.105	36.156	36.154			
	36.545	36.556	36.56			
		37.831		37.284		
	38.154	38.042	38.041	38.903		
	38.803			38.903		
		39.06	39.002			

330

39.321	39.331	39.336			
			40.503		
41.388	41.281	41.302			
	41.702				
42.249	42.042				
	42.819	42.754			
43.456	43.97	43.883			
44.932	44.902	44.913			
	45.463		45.323		
46.816	46.156				
47.778	47.141	47.745			
	47.753				
	48.094	48.05			

		48.538				
	49.493	49.468				

Table AB 4.2: PXRD data for samples TA-I-53-3a (1:1), TA-I-53-3b (1:2), in methanol

L-phenyllactic acid	Nicotinamide Std	NICOAM	NICOAM01	NICOAM02	TA-I-53-3a	TA-I-53-3b
2-Theta°	2-Theta°	2-Theta°	2-Theta°	2-Theta°	2-Theta°	2-Theta°
10.28					18.005	5.16
11.698	11.671	11.296	11.328	11.301	20.26	14.883
14.668					25.561	17.641
15.911		14.764	14.839	14.801	27.212	19.85
18.2	15.115					22.28
20.611						25.189
20.945						25.798
21.644						27.322
23.128						37.023
24.105	19.822	19.041	19.137	19.061		38.737
26.255		19.495	19.551	19.52		

27.785		19.858	19.96	19.884		
29.666	20.19					
30.305						
30.927	22.524	22.184	22.295	22.215		
31.98		22.68	22.784	22.697		
33.34	23.031	23.347	23.167	23.348		
33.534	23.646		23.868			
33.913		24.662	24.75	24.701		
35.314		25.366		25.379		
35.946	25.707	25.819	25.871	25.823		
36.49	26.114		26.395	26.601		
36.942		27.266	27.017	27.311		
37.674	27.603		27.91			
38.706		28.438		28.443		
	28.724	28.845	28.905	28.861		

	29.158		29.378	29.64		
	30.375	30.088	30.199	30.141		
	31.399	31.207	31.602	31.193		
		32.6	32.388	32.575		
	32.798		32.899			
			33.145			
	33.892	33.557	33.708	33.594		
	34.61	34.09, 34.37	34.442	34.05, 34.412		
	34.743	34.758		34.763		
			35.153			
		35.72	35.839	35.764		
		36.494		36.478		
	36.82	36.935	36.808	36.981		
	37.212					
			37.082			

	38.935	38.64	38.802	38.666	
			39.294		
		39.567	39.702	39.612	
		40.166	40.467	40.167	
		40.914		40.945	
	41.339	41.475	41.06	41.466	
	41.656	41.822	41.724	41.861	
	43.688	43.464			
		44.413			
		46.627	46.539	46.593	
	47.9	47.312	47.137	47.307	
		47.692	47.744	47.705	
			48.001	48.809	

			48.62			
	49.148		49.526			
	38.154	38.042	38.041			
	38.803			38.903		
		39.06	39.002			
	39.321	39.331	39.336			
				40.503		
	41.388	41.281	41.302			
		41.702				
	42.249	42.042				
		42.819	42.754			
	43.456	43.97	43.883			
	44.932	44.902	44.913			
		45.463		45.323		

	46.816	46.156				
		47.141				
	47.778	47.753	47.745			
		48.094	48.05			
		48.538				
	49.493	49.468				

Table AB 4.3: PXRD data for samples TA-I-53-4a (1:1), TA-I-53-4b (1:2), TA-I-52-2c (2:1), in acetonitrile

L-phenyllactic acid	Nicotinamide Std	NICOAM	NICOAM01	NICOAM02	TA-I-53-4a	TA-I-53-4b
2-Theta °	2-Theta °	2-Theta °	2-Theta °	2-Theta °	2-Theta °	2-Theta °
10.28					14.841	25.77
11.698	11.671	11.296	11.328	11.301	15.412	25.016
14.668					22.253	34.438
15.911		14.764	14.839	14.801	22.842	30.256
18.2	15.115				27.723	
20.611					37.01	
20.945					39.101	
21.644						
23.128						
24.105	19.822	19.041	19.137	19.061		
26.255		19.495	19.551	19.52		

27.785		19.858	19.96	19.884		
29.666	20.19					
30.305						
30.927	22.524	22.184	22.295	22.215		
31.98		22.68	22.784	22.697		
33.34	23.031	23.347	23.167	23.348		
33.534	23.646		23.868			
33.913		24.662	24.75	24.701		
35.314		25.366		25.379		
35.946	25.707	25.819	25.871	25.823		
36.49	26.114		26.395	26.601		
36.942		27.266	27.017	27.311		
37.674	27.603		27.91			
38.706		28.438		28.443		
	28.724	28.845	28.905	28.861		

29.158		29.378	29.64		
30.375	30.088	30.199	30.141		
31.399	31.207	31.602	31.193		
	32.6	32.388	32.575		
32.798		32.899			
		33.145			
33.892	33.557	33.708	33.594		
34.61	34.09, 34.37	34.442	34.05, 34.412		
34.743	34.758		34.763		
		35.153			
	35.72	35.839	35.764		
	36.494		36.478		
36.82	36.935	36.808	36.981		
37.212					
		37.082			

341

	38.935	38.64	38.802	38.666		
			39.294			
		39.567	39.702	39.612		
		40.166	40.467	40.167		
		40.914		40.945		
	41.339	41.475	41.06	41.466		
	41.656	41.822	41.724	41.861		
	43.688	43.464				
		44.413				
		46.627	46.539	46.593		
	47.9	47.312	47.137	47.307		
		47.692	47.744	47.705		
			48.001	48.809		

			48.62			
	49.148		49.526			
	38.154	38.042	38.041			
	38.803			38.903		
		39.06	39.002			
	39.321	39.331	39.336			
				40.503		
	41.388	41.281	41.302			
		41.702				
	42.249	42.042				
		42.819	42.754			
	43.456	43.97	43.883			
	44.932	44.902	44.913			
		45.463		45.323		

	46.816	46.156				
		47.141				
	47.778	47.753	47.745			
		48.094	48.05			
		48.538				
	49.493	49.468				

Table AB 4.4: PXRD data for samples TA-I-31-1a (1:1), TA-I-31-1b (1:2), TA-I-31-1c (2:1), in acetone

DL-Phenyllactic acid	Iso stnd	EHOWIH	EHOWIH01	EHOWIH02	TA-I-31-1a	TA-I-31-1b	TA-I-31-1c
2-Theta°	2-Theta°	2-Theta °	2-Theta °	2-Theta °	2-Theta °	2-Theta °	2-Theta °
8.328					8.089	8.015	8.028
10.939						10.222	
				11.677			
13.183							
14.88				14.625			
15.044							
					15.894		15.719
16.24							
16.443				16.097			
16.68				16.52			

	17.842	17.859	17.843		17.81	17.801	17.72
18.54	18.855	18.748	18.766	18.626			18.666
18.737					18.899		
19.354	19.411	19.347	19.347	19.14			19.339
		20.485	20.468	20.138			
20.333	20.874		20.996	20.747			
20.541				20.988			20.499
		21.037					
21.848				21.94			
22.481				22.214			
						23.009	
23.405	23.449	23.498	23.48	23.457	23.719	23.783	23.56
					23.9		23.796

24.174	24.454	24.385	24.396			24.475	
24.78				24.601	24.618		24.522
25.52				25.403	25.567	25.391	25.476
25.763	25.937			25.789			
		26.093	26.059				26.172
26.358	26.644						
		26.934	26.898				
27.547							
27.813							
28.58	28.166	28.061	28.076				
28.99				28.996	28.759	28.583	28.716
29.174							
29.94		29.937	29.925	29.781			
30.151	30.007			30.381	30.463		
30.784	30.945	30.882	30.836	30.752			30.624

31.241	31.29	31.198	31.163	31.404			31.393
					31.462	31.493	
32.781	32.456	32.474	32.45	32.533			
	33.324	33.26					
		33.51	33.485	33.492			
33.04	33.895	33.856	33.864				
34.137							
34.53							34.484
				34.992			
35.764	35.415	35.658	35.607	35.524			
	36.105	36.156	36.154				

36.724	36.545	36.556	36.56				
37.396				37.284			
37.902		37.831			37.984		
	38.154	38.042	38.041				
	38.803			38.903			
39.087		39.06	39.002		39.184		
39.557	39.321	39.331	39.336				
				40.503			
	41.388	41.281	41.302				
		41.702					
	42.249	42.042					
		42.819	42.754				
	43.456	43.97	43.883				

44.932	44.902	44.913				
	45.463		45.323			
	46.156					
46.816						
	47.141					
47.778	47.753	47.745				
	48.094	48.05				
	48.538					
49.493	49.468					

Table AB 4.5: PXRD data for samples TA-I-31-2a (1:1), TA-I-31-2b (1:2), TA-I-31-2c (2:1), in methanol

DL-Phenyllactic acid	Iso Stnd	Iso EHOWIH	Iso EHOWIH01	Iso EHOWIH02	TA-I-31-2a	TA-I-31-2b	TA-I-31-2c
2-Theta°	2-Theta°	2-Theta°	2-Theta °	2-Theta °	2-Theta °	2-Theta °	2-Theta °
8.328					8.119	8.11	8.158
10.939					10.283		
				11.677			
							12.279
13.183							
14.88				14.625			
15.044							15.09
						15.979	15.964
16.24							

16.443				16.097	16.003		
16.68				16.52			
							17.04
	17.842	17.859	17.843		17.857	17.833	17.883
18.54	18.855	18.748	18.766	18.626			
18.737					18.968	18.889	
19.354	19.411	19.347	19.347	19.14			19.493
		20.485	20.468	20.138			
20.333	20.874		20.996	20.747			20.718
20.541				20.988			
		21.037					
21.848				21.94			21.666
22.481				22.214			
							22.824

						23.249	
23.405	23.449	23.498	23.48	23.457		23.62	23.963
					23.908	23.893	
24.174	24.454	24.385	24.396				
24.78				24.601	24.621	24.698	24.629
25.52				25.403	25.59	25.617	25.641
25.763	25.937			25.789			
	26.644	26.093	26.059				
26.358					26.367		
		26.934	26.898			26.638	
27.547							
27.813							
28.58	28.166	28.061	28.076				
28.99				28.996	28.832	28.862	28.889
29.174							

29.94		29.937	29.925	29.781			
30.151	30.007			30.381			
30.784	30.945	30.882	30.836	30.752	30.684		
31.241	31.29	31.198	31.163	31.404	31.438	31.512	
					32.065		
32.781	32.456	32.474	32.45	32.533			32.646
	33.324	33.26					
		33.51	33.485	33.492			
33.04	33.895	33.856	33.864		33.684		
34.137							
34.53							34.777
				34.992			

35.764	35.415	35.658	35.607	35.524			
	36.105	36.156	36.154				
36.724	36.545	36.556	36.56			36.636	
37.396				37.284			
37.902		37.831					
	38.154	38.042	38.041		38.233		
	38.803			38.903		38.884	
39.087		39.06	39.002				
39.557	39.321	39.331	39.336				39.459
				40.503			
	41.388	41.281	41.302				
		41.702					
	42.249	42.042					

		42.819	42.754				
	43.456	43.97	43.883				
	44.932	44.902	44.913				
		45.463		45.323			
		46.156					
	46.816						
		47.141					
	47.778	47.753	47.745				
		48.094	48.05				
		48.538					
	49.493	49.468					

Table AB 4.6: PXRD data for samples TA-I-31-3a (1:1), TA-I-31-3b (1:2), TA-I-31-3c (2:1), in acetonitrile

DL-Phenyllactic acid	Iso stnd	EHOWIH	EHOWIH01	EHOWIH02	TA-I-31-3a	TA-I-31-3b	TA-I-31-3c
2-Theta°	2-Theta°	2-Theta °	2-Theta °	2-Theta °	2-Theta °	2-Theta °	2-Theta °
8.328							
10.939							
						11.249	
				11.677			
13.183							
14.88				14.625			
15.044							
16.24							
16.443				16.097			

16.68				16.52			
					17.497	17.468	17.537
	17.842	17.859	17.843				
18.54	18.855	18.748	18.766	18.626			
18.737							
19.354	19.411	19.347	19.347	19.14			
		20.485	20.468	20.138			
20.333	20.874		20.996	20.747			
20.541				20.988			
		21.037					
21.848				21.94			
22.481				22.214		22.046	
					22.871	22.833	22.874
23.405	23.449	23.498	23.48	23.457	23.308	23.329	23.346

24.174	24.454	24.385	24.396			24.25	
24.78				24.601			
25.52				25.403	25.234	25.17	25.125
25.763	25.937			25.789			
	26.644	26.093	26.059				
26.358		26.934	26.898				
27.547							
27.813							
28.58	28.166	28.061	28.076		28.352	28.387	28.365
28.99				28.996			
29.174							
29.94		29.937	29.925	29.781			
30.151	30.007			30.381			

30.784	30.945	30.882	30.836	30.752			
31.241	31.29	31.198	31.163	31.404			
32.781	32.456	32.474	32.45	32.533			
	33.324	33.26					
		33.51	33.485	33.492			
33.04	33.895	33.856	33.864				
34.137							
34.53						34.663	
				34.992			
35.764	35.415	35.658	35.607	35.524			
	36.105	36.156	36.154				
36.724	36.545	36.556	36.56			36.543	

37.396				37.284		
37.902		37.831				
	38.154	38.042	38.041			
	38.803			38.903		
39.087		39.06	39.002			
39.557	39.321	39.331	39.336			
				40.503		
	41.388	41.281	41.302			
		41.702				
	42.249	42.042				
		42.819	42.754			
	43.456	43.97	43.883			
	44.932	44.902	44.913			

		45.463		45.323			
		46.156					
	46.816						
		47.141					
	47.778	47.753	47.745				
		48.094	48.05				
		48.538					
	49.493	49.468					

Table AB 4.7: PXRD data for samples TA-I-32-2a (1:1), TA-I-32-2b (1:2), TA-I-32-2c (2:1), in acetone

DL-Phenyllactic acid	Nicotinamide Std	NICOAM	NICOAM01	NICOAM02	TA-I-32-2a	TA-I-32-2b	TA-I-32-2c
2-Theta °	2-Theta °	2-Theta °	2-Theta °	2-Theta °	2-Theta °	2-Theta °	2-Theta °
							5.914
						7.989	
8.328					8.157		8.277
						8.995	
					9.77	9.827	9.871
10.939							
	11.671	11.296	11.328	11.301			
						12.107	12.881
13.183						13.284	
					14.436		
14.88		14.764	14.839	14.801		14.693	

15.044	15.115						
16.24							16.428
16.443					16.321	16.411	
16.68					16.826		16.977
						17.405	
							17.795
18.54					18.126	18.136	18.471
18.737					18.697	18.504	
						18.857	18.672
19.354		19.041	19.137	19.061			
		19.495	19.551	19.52			
	19.822	19.858	19.96	19.884	19.711	19.726	19.77
20.333	20.19						
20.541							20.9
					21.054		21.114

21.848					21.678	21.633	
22.481	22.524	22.184	22.295	22.215	22.364	22.388	
		22.68	22.784	22.697	22.967	22.987	
23.405	23.031	23.347	23.167	23.348	23.464		23.281
	23.646		23.868		23.828		
24.174							24.003
24.78		24.662	24.75	24.701	24.87	24.939	24.929
25.52		25.366		25.379			
25.763	25.707	25.819	25.871	25.823			
	26.114			26.601			26.513
26.358			26.395			26.744	
27.547		27.266	27.017	27.311			
27.813	27.603		27.91			27.928	
28.58		28.438		28.443	28.039		28.251
28.99	28.724	28.845	28.905	28.861	28.822		

29.174	29.158		29.378				
29.94				29.64			
30.151	30.375	30.088	30.199	30.141		30.032	
30.784							
31.241	31.399	31.207	31.602	31.193	31.017	31.134	
		32.6	32.388	32.575			
32.781	32.798		32.899				
33.04			33.145		33.12		
	33.892	33.557	33.708	33.594	33.399	33.623	
34.137		34.09,		34.05,			
34.53	34.61	34.37	34.442	34.412			
	34.743	34.758		34.763			
			35.153				
35.764		35.72	35.839	35.764			
		36.494		36.478			

36.724	36.82	36.935	36.808	36.981		36.796	
37.396	37.212		37.082			37.426	37.685
37.902							
	38.935	38.64	38.802	38.666			
39.087			39.294				
39.557		39.567	39.702	39.612			
		40.166	40.467	40.167			
		40.914		40.945			
	41.339	41.475	41.06	41.466			
	41.656	41.822	41.724	41.861			
	43.688	43.464					
		44.413					
		46.627	46.539	46.593			

47.9	47.312	47.137	47.307			
	47.692	47.744	47.705			
		48.001	48.809			
		48.62				
49.148		49.526				
38.154	38.042	38.041				
38.803			38.903			
	39.06	39.002				
39.321	39.331	39.336				
			40.503			
41.388	41.281	41.302				
	41.702					
42.249	42.042					
	42.819	42.754				

	43.456	43.97	43.883				
	44.932	44.902	44.913				
		45.463		45.323			
	46.816	46.156					
		47.141					
	47.778	47.753	47.745				
		48.094	48.05				
		48.538					
	49.493	49.468					

Table AB 4.8: PXRD data for samples TA-I-32-3a (1:1), TA-I-32-3b (1:2), TA-I-32-3c (2:1), in methanol

DL-Phenyllactic acid	Nicotinamide Std	NICOAM	NICOAM01	NICOAM02	TA-I-32-3a	TA-I-32-3b	TA-I-32-3c
2-Theta°	2-Theta°	2-Theta°	2-Theta°	2-Theta°	2-Theta°	2-Theta°	2-Theta°
8.328					8.348		
						9.731	
					10.203		
10.939							
	11.671	11.296	11.328	11.301			11.613
					12.477		
						12.029	
13.183							
14.88		14.764	14.839	14.801			
15.044	15.115						15.085

16.24							
						16.318	
16.443							
16.68							
					16.774		
						17.314	
					17.79		
						18.053	
18.54					18.498		
18.737							
							19.289
19.354		19.041	19.137	19.061			
		19.495	19.551	19.52			
						19.639	
	19.822	19.858	19.96	19.884			19.733

					20.098		20.034
20.333	20.19						
20.541							
						21.557	
21.848							
					22.021		
		22.184		22.215			
22.481			22.295			22.305	22.34
	22.524						22.496
		22.68	22.784	22.697	22.75		
						22.921	
23.405	23.031		23.167				
		23.347		23.348	23.353		
	23.646		23.868				

24.174							
24.78		24.662	24.75	24.701		24.844	
							24.917
					25.08		
25.52		25.366		25.379	25.31		
25.763	25.707	25.819	25.871	25.823			25.994
	26.114			26.601			
26.358			26.395				
		27.266	27.017	27.311			
27.547							27.563
27.813	27.603		27.91			27.842	
					28.311		
28.58		28.438		28.443			
							28.645

28.99	28.724	28.845	28.905	28.861			
29.174	29.158		29.378				
29.94				29.64			
30.151	30.375	30.088	30.199	30.141	30.378		
30.784							
31.241		31.207	31.602	31.193			
	31.399				31.46		
		32.6	32.388	32.575			
32.781	32.798		32.899				
33.04			33.145				
							30.426
		33.557	33.708	33.594			
	33.892				33.93		33.882
34.137		34.09,		34.05,			
34.53	34.61	34.37	34.442	34.412			

374

	34.743	34.758		34.763			34.712
			35.153				
35.764		35.72	35.839	35.764			
		36.494		36.478			
36.724	36.82	36.935	36.808	36.981		36.708	
37.396	37.212		37.082		37.178		37.194
37.902					37.814		
	38.935	38.64	38.802	38.666			38.90
39.087			39.294				
39.557		39.567	39.702	39.612			
		40.166	40.467	40.167			
		40.914		40.945			
	41.339	41.475	41.06	41.466			
	41.656	41.822	41.724	41.861			

43.688	43.464					
	44.413					
	46.627	46.539	46.593			
47.9	47.312	47.137	47.307			
	47.692	47.744	47.705			
		48.001	48.809			
		48.62				
49.148		49.526				
38.154	38.042	38.041				
38.803			38.903			
	39.06	39.002				
39.321	39.331	39.336				

				40.503		
	41.388	41.281	41.302			
		41.702				
	42.249	42.042				
		42.819	42.754			
	43.456	43.97	43.883			
	44.932	44.902	44.913			
		45.463		45.323		
	46.816	46.156				
		47.141				
	47.778	47.753	47.745			
		48.094	48.05			
		48.538				
	49.493	49.468				

Table AB 4.9: PXRD data for samples TA-I-32-4a (1:1), TA-I-32-4b (1:2), TA-I-32-4c (2:1), in acetonitrile

DL-Phenyllactic acid	Nicotinamide Std	NICOAM	NICOAM01	NICOAM02	TA-I-32-4a	TA-I-32-4b	TA-I-32-4c
2-Theta °	2-Theta °	2-Theta °	2-Theta °	2-Theta °	2-Theta °	2-Theta °	2-Theta °
					6.024		6.326
8.328						8.481	
							10.178
					9.891		9.242
						10.285	10.178
10.939							
	11.671	11.296	11.328	11.301			11.888
						12.588	
13.183							13.31
							13.673

14.88		14.764	14.839	14.801			
15.044	15.115						
16.24							
16.443							
16.68					16.549		
						16.881	16.821
					17.098		
					17.89	17.838	17.406
							18.166
18.54							
18.737					18.69	18.608	18.981
19.354		19.041	19.137	19.061			
		19.495	19.551	19.52			
	19.822	19.858	19.96	19.884	19.812		

							20.063
20.333	20.19					20.192	
20.541							
					21.144		21.362
21.848							
							21.6
						22.106	
22.481	22.524	22.184	22.295	22.215	22.595	22.831	
		22.68	22.784	22.697			
23.405	23.031	23.347	23.167	23.348			
	23.646		23.868		23.515	23.466	23.723
24.174							
24.78		24.662	24.75	24.701			24.571
					25.088		

25.52		25.366		25.379		25.348	
25.763	25.707	25.819	25.871	25.823			
	26.114			26.601			
26.358			26.395				
					26.938		26.901
27.547		27.266	27.017	27.311			27.164
27.813	27.603		27.91				
					28.27	28.329	
28.58		28.438		28.443			28.625
28.99	28.724	28.845	28.905	28.861			
29.174	29.158		29.378				
29.94				29.64			
30.151	30.375	30.088	30.199	30.141			
30.784							
31.241	31.399	31.207	31.602	31.193			

		32.6	32.388	32.575			
32.781	32.798		32.899				
33.04			33.145				33.338
	33.892	33.557	33.708	33.594			
34.137		34.09,		34.05,		34.02	
34.53	34.61	34.37	34.442	34.412			
	34.743	34.758		34.763			
			35.153				
35.764		35.72	35.839	35.764			
		36.494		36.478			
36.724	36.82	36.935	36.808	36.981			
37.396	37.212		37.082			37.222	
37.902						37.898	
	38.935	38.64	38.802	38.666			
39.087			39.294				

39.557		39.567	39.702	39.612			
		40.166	40.467	40.167			
		40.914		40.945			
	41.339	41.475	41.06	41.466			
	41.656	41.822	41.724	41.861			
	43.688	43.464					
		44.413					
		46.627	46.539	46.593			
	47.9	47.312	47.137	47.307			
		47.692	47.744	47.705			
			48.001	48.809			
			48.62				
	49.148		49.526				

383

38.154	38.042	38.041				
38.803			38.903			
	39.06	39.002				
39.321	39.331	39.336				
			40.503			
41.388	41.281	41.302				
	41.702					
42.249	42.042					
	42.819	42.754				
43.456	43.97	43.883				
44.932	44.902	44.913				
	45.463		45.323			
46.816	46.156					

		47.141					
	47.778	47.753	47.745				
		48.094	48.05				
		48.538					
	49.493	49.468					

Appendix C: Chapter 5

Table AC 5.1: PXRD data for samples TA-I-19-3a (1:1), TA-I-19-3b (1:2), TA-I-19-3c (2:1), in methanol

Phenylboronic Acid	Isostnd	EHOWIH	EHOWIH01	EHOWIH02	TA-I-19-3a	TA-19-3b	TA-I-19-3c
2-Theta°	2-Theta°	2-Theta°	2-Theta°	2-Theta°	2-Theta°	2-Theta°	2-Theta°
							7.903
9.94					9.236	9.261	9.429
						10.398	
						10.883	
						11.368	11.528
				11.677		11.993	
12.05							
12.86						12.926	
13.84						13.934	
				14.625		14.468	14.592
15.27					15.406	15.383	

							15.79
				16.097		16.48	
16.62				16.52	16.81	16.802	
17.31							17.046
	17.842	17.859	17.843		17.565	17.768	17.558,
18.26					18.494		
18.72	18.855	18.748	18.766	18.626		18.663	18.72
	19.411	19.347	19.347	19.14	19.428	19.298	
						19.973	19.744
20.88	20.874	20.485	20.468	20.138	20.6	20.16	
			20.996	20.747		20.712	
				20.988			
21.17		21.037			21.168	21.542	21.43
				21.94			21.665

22.00				22.214	22.244	22.28	22.244
							22.67
					23.007	23.16	23.102
	23.449	23.498	23.48	23.457	23.317	23.456	23.406
						23.786	23.56
24.01							
24.39	24.454	24.385	24.396				
				24.601		24.571	
						24.919	24.98
25.74				25.403	25.83	25.472	25.493
	25.937			25.789			25.78
26.02		26.09	26.06			26.22	26.13
	26.64	26.93	26.89				
					27.44		
					27.75	27.74	27.75

					27.96		
	28.16	28.06	28.07			28.12	28.20
28.48					28.49		
				28.99	28.76	28.885	28.72
					29.14	29.22	29.10
		29.94	29.92	29.78		29.69	
			30.83	30.38			
	30.00	30.88		30.75			
	30.94						
31.07		31.19	31.16				
31.72	31.29			31.40			31.73
	32.45	32.47	32.45	32.53			
	33.32	33.26	33.48	33.49			
33.61	33.89	33.51	33.86				

		33.85					
					34.34		
							35.10
				34.992			
	35.41	35.66	35.60	35.52	35.40		35.67
	36.10	36.15	36.15			36.071	36.13
	36.54	36.55	36.56				36.71
		37.83		37.28	37.52		
					37.90		
	38.15	38.04	38.04				38.11
38.98	38.80			38.90			
		39.06	39.00				
39.62	39.32	39.33	39.33				39.75
40.21				40.50		40.523	
40.31							

	41.38	41.28	41.30				41.08
		41.70					
	42.25	42.04					42.11
		42.82	42.75				
	43.45	43.97	43.88				
	44.93	44.90	44.91				
		45.46		45.32			45.07
							45.76
	46.82	46.15					
	47.77	47.14	47.74				47.31
		47.753					
		48.094	48.05				
		48.538					48.564
	49.493	49.468					

Table AC 5.2: PXRD data for samples TA-I-19-2a (1:1), TA-I-19-2b (1:2), TA-I-19-2c (2:1), in acetonitrile

Phenylboronic Acid	IsoStnd	EHOWIH	EHOWIH01	EHOWIH02	TA-I-19-2a	TA-I-19-2b	TA-I-19-2c
2-Theta°	2-Theta°	2-Theta °	2-Theta °	2-Theta°	2-Theta°	2-Theta°	2-Theta°
9.94						9.558	
				11.67			11.57
12.05							12.10
12.86							12.49
13.84							
				14.62			
15.27							
					15.96	15.91	
				16.09			
16.62				16.52			16.99

17.31					17.26	17.32	
	17.84	17.86	17.84		17.86	17.79	
18.26					18.25		
18.72	18.85	18.75	18.76	18.63			
						18.51	18.90
	19.41	19.35	19.34	19.14		19.42	
						19.80	
20.88	20.87	20.48	20.46	20.14			
			20.99	20.75			20.87
				20.98		20.89	
21.17		21.04			21.46		
				21.94	21.68	21.74	
22.00				22.21			22.09
					23.12		
	23.45	23.49	23.48	23.46	23.41	23.54	

					23.65	23.72	23.61
24.01					24.14		24.16
24.39	24.45	24.38	24.39				
				24.60			24.79
				25.40			25.13
25.74	25.94			25.79			
26.02	26.644	26.093	26.059			26.02	
		26.934	26.898				
	28.166	28.061	28.076		28.34	28.27	28.46
28.48				28.99	28.909		
						29.16	
					29.442	29.44	29.38
		29.937	29.925	29.78			29.85
		30.836	30.38				
	30.007					30.055	

	30.945	30.882		30.752			
31.07						31.045	
						31.48	
31.72	31.29	31.198	31.163	31.40	31.94	31.92	
	32.456	32.474	32.45	32.53			
	33.324	33.26	33.485	33.49			
33.61	33.895	33.51	33.864				
		33.856					
			34.99	34.998	34.86		
	35.415	35.658	35.607	35.524			
	36.105	36.156	36.154		36.042	36.10	
	36.545	36.556	36.56				
	37.831		37.284				

	38.154	38.042	38.041		38.157	38.129	
38.98	38.803			38.903			
		39.06	39.00				
39.62	39.32	39.33	39.33		39.93		
40.21				40.503			
40.31							
	41.38	41.28	41.30		41.37		
		41.70					
	42.25	42.04					
		42.82	42.75				
	43.45	43.97	43.88				
	44.93	44.90	44.91				
		45.463		45.323	45.45		
		46.15					
	46.81						

		47.141			47.53		
	47.78	47.753	47.74				
		48.094	48.05				
		48.538					

Table AC 5.3 PXRD data for samples TA-I-20-2a (1:1), TA-I-20-2b (1:2), TA-I-20-2c (2:1), in acetone

Phenylboronic acid	Nicotinamide	Nicoam1	Nicoam2	Nicoam	TA-I-20-2a	TA-I-20-2b	TA-I-20-2c
2-Theta°	2-Theta°	2-Theta°	2-Theta°	2-Theta°	2-Theta°	2-Theta°	2-Theta°
							5.183
							6.532
					7.812	7.793	7.101
							8.102
							8.519
							8.923
9.94					9.222	9.232	9.529
							10.396
	11.67	11.328	11.301	11.296			11.508
12.05					12.28		12.444
12.86							

							13.006
13.84							13.783
		14.839	14.801	14.764	14.529	14.51	14.509
15.27	15.115				15.48		15.852
					15.99		
16.62						16.016	16.295
							16.546
17.31					17.773		17.111
18.26							18.163
18.72					18.737	18.79	
			19.061				19.04
		19.551	19.52	19.495			19.518
	19.822	19.96	19.884	19.858	19.966		19.863
	20.19					20.048	20.282

20.88					20.872	20.913	
21.17							21.173
						21.949	21.803
22	22.524	22.295	22.215	22.184	22.034		
		22.784	22.697	22.68			
	23.03	23.167	23.348	23.347	23.213	23.303	23.228
	23.646	23.868					23.647
24.01							
24.39		24.75	24.701	24.662			24.334
							24.839
			25.379	25.366		25.175	
25.74	25.707	25.871	25.823	25.819	25.685	25.67	
26.02	26.114	26.395			26.378		26.062
	27.603		27.311	27.266	26.777	26.99	26.662

							27.066
		27.91			27.924	27.927	
			28.443	28.438			28.082
28.48	28.72	28.905	28.861	28.845			28.3
		29.378					29.566
	30.37	30.199	30.141	30.088	30.053	30.067	
31.07							
31.72		31.602					
	32.79	32.899	32.575	32.6			
		33.145					
33.61		33.708	33.594				
	34.61	34.442	34.412				
		35.153	35.764				
		35.83					

			36.478			36.312	
	36.82		36.981	36.935			
	37.212	37.082					
38.98	38.93	38.802	38.666	38.64			
39.62							
40.21			40.945				
		41.06	41.466	41.475			
		41.724					
46.31			46.593	46.627			

	47.9	47.744	47.307	47.692			
		48.001	47.705				
		48.62	48.809				

Table AC 5.4: PXRD data for samples TA-I-20-3a (1:1), TA-I-20-3b (1:2), TA-I-20-3c (2:1), in methanol

Phenylboronic acid	Nicotinamide	Nicoam1	Nicoam2	Nicoam	TA-I-20-3a	TA-I-20-3b	TA-I-20-3c
2-Theta°	2-Theta°	2-Theta°	2-Theta°	2-Theta°	2-Theta°	2-Theta°	2-Theta °
							6.549
					7.417		
9.94					9.285	9.591	9.122
					10.951		10.465
	11.67	11.328	11.301	11.296		11.295	
12.05							12.07
12.86							12.349
							13.02
13.84							13.526
		14.839	14.801	14.764	14.229	14.906	
15.27	15.115						15.171

16.62					16.008	16.374	16.266
							17.081
17.31							17.358
18.26					18.052		18.241
18.72					18.786		18.51
			19.061		19.232	19.099	
		19.551	19.52	19.495		19.57	19.545
	19.822	19.96	19.884	19.858			
	20.19						20.168
20.88					20.704		
					20.93		
21.17						21.256	21.177
							21.794
22	22.524	22.295	22.215	22.184	22.148	22.375	

		22.784	22.697	22.68	22.778		
	23.03	23.167	23.348	23.347	23.307		23.128
	23.646	23.868				23.609	
24.01							24.255
24.39		24.75	24.701	24.662		24.762	24.767
			25.379	25.366	25.205	25.506	
25.74	25.707	25.871	25.823	25.819		25.944	
26.02	26.114	26.395			26.638		26.188
	27.603		27.311	27.266	27.407	27.425	27.425
		27.91			27.999		
			28.443	28.438		28.316	
28.48	28.72	28.905	28.861	28.845			28.921
		29.378			29.688	29.984	
	30.37	30.199	30.141	30.088	30.12	30.456	

31.07						
31.72		31.602				
	32.79	32.899	32.575	32.6	32.577	32.944
		33.145				
33.61		33.708	33.594		33.722	
						34.039
	34.61	34.442	34.412			
		35.153	35.764			
		35.83				
	36.82		36.478	36.935		
			36.981			
	37.212	37.082				
					38.243	38.54
38.98	38.93	38.802	38.666	38.64		

39.62							
40.21			40.945				
		41.06	41.466	41.475			
		41.724			41.61		
46.31			46.593	46.627			
	47.9	47.744	47.307	47.692			
		48.001	47.705				
		48.62	48.809				

Table AC 5.5: PXRD data for samples TA-I-20-4a (1:1), TA-I-20-4b (1:2), TA-I-20-4c (2:1), in acetonitrile

Phenyl-boronic acid	Nicotinamide	Nicoam1	Nicoam2	Nicoam	TA-I-20-4a	TA-I-20-4b	TA-I-20-4c
2-Theta °	2-Theta °	2-Theta °	2-Theta °	2-Theta °	2-Theta °	2-Theta °	2-Theta °
							7.799
						8.201	
						8.457	
9.94							9.66
	11.67	11.328	11.301	11.296		11.956	11.185
12.05							12.202
12.86							
13.84							13.44
		14.839	14.801	14.764		14.798	14.564
15.27	15.115						15.614

16.62						16.26	16.322
17.31							17.843
18.26							
18.72						18.548	
			19.061				19.336
		19.551	19.52	19.495			19.45
	19.822	19.96	19.884	19.858			
	20.19						20.003
20.88						20.545	
21.17							
							21.906
22	22.524	22.295	22.215	22.184			
		22.784	22.697	22.68			
	23.03	23.167	23.348	23.347		23.487	23.016

	23.646	23.868					
24.01							24.003
24.39		24.75	24.701	24.662		24.408	
							25.17
			25.379	25.366		25.437	25.611
25.74	25.707	25.871	25.823	25.819			
26.02						26.086	
	26.114	26.395				26.739	26.325
						27.017	27.049
			27.311	27.266		27.361	
	27.603	27.91					27.992
			28.443	28.438			
28.48	28.72	28.905	28.861	28.845			
		29.378					29.824

	30.37	30.199	30.141	30.088		
31.07						
31.72		31.602				
	32.79	32.899	32.575	32.6		32.295
		33.145				
33.61		33.708	33.594			
	34.61	34.442	34.412			
		35.153	35.764			
		35.83				
			36.478			
	36.82		36.981	36.935		36.678
	37.212	37.082				
38.98	38.93	38.802	38.666	38.64		38.428

39.62							
40.21			40.945				40.55
		41.06	41.466	41.475			
		41.724					
46.31			46.593	46.627			
	47.9	47.744	47.307	47.692			
		48.001	47.705				
		48.62	48.809				

Appendix D: Chapter 6

Table AD 6.1: PXRD data for samples TA-I-54-1a (1:1), TA-I-54-1b (1:2), TA-I-54-1c (2:1), in acetone

Phenylboronic acid	4,4'-bipyridine	TA-I-54-1a	TA-I-54-1b	TA-I-54-1c
2-Theta °	2-Theta °	2-Theta °	2-Theta °	2-Theta °
				9.33
9.94	9.94			9.99
			11.25	
12.05		12.04	12.02	
	12.36			
12.86	13.03	13.18	13.17	
13.84				
15.27				15.46
				16.14
16.62				16.88
17.31	17.50, 17.67			
18.26	18.31		18.12	
18.72				18.51
	19.36			
		19.68	19.58	19.99
	20.13	20.16	20.12	
20.88	20.82			
21.17			21.27	21.23
	21.59			
22.00	22.37			
	22.98			22.83
				23.58

24.01		24.15	24.17	
24.39				
	25.03			
25.74	25.78	25.54	25.44	25.54
26.02	26.24		26.19	
		26.46	26.42	26.46
		27.32	27.17	
	27.81			
28.48			28.74	
	29.12	29.35	29.32	29.33
	30.38			
31.07	30.68		31.05	
31.72	31.92			
	32.40			
33.61	33.60	33.46	33.44	
	35.24			
			36.01	
		37.12	37.08	
			38.27	
38.98			38.52	
39.62				
40.21				
46.31				

Table AD 6.2: PXRD data for samples TA-I-54-2a (1:1), TA-I-54-2b (1:2), TA-I-54-2c (2:1), in methanol

Phenylboronic acid	4,4'-bipyridine	TA-I-54-2a	TA-I-54-2b	TA-I-54-2c
2-Theta °	2-Theta °	2-Theta °	2-Theta °	2-Theta °
		5.74		5.72
		7.42		
				8.19
				9.37
9.94	9.94	10.26		10.14
		10.80		
		11.28	11.14, 11.33	11.31
12.05		12.10	12.04	12.00
	12.36	12.40		12.61
12.86	13.03	13.01	13.00, 13.24	13.26
13.84		14.33		13.96
		14.62		14.67
15.27		15.13		15.60
		16.10		
16.62		16.54		16.61
			17.03	17.09
17.31	17.50, 17.67	17.45		17.42
18.26	18.31	18.23	18.28	18.15
18.72		18.72		18.75
	19.36	19.24	19.26	19.02
		19.68	19.58	19.76
	20.13	20.23	20.21	20.12
20.88	20.82			
21.17		21.54	21.49	21.46

	21.59			
22.00	22.37	22.21		22.28
			22.67	22.66
	22.98	22.85		
		23.60		23.48
24.01		24.06	24.33	24.00
24.39		24.62		24.23
	25.03			
25.74	25.78	25.53	25.56	25.56
26.02	26.24		26.32	26.31
		26.48	26.51	26.58
		27.32	27.12	27.16
	27.81	27.84	27.54	
28.48		28.26		
	29.12	29.33	29.41	29.41
		29.68	29.99	
	30.38	30.30		
	30.68	30.81	30.74	30.87
31.07		31.00	30.92	
			31.30	31.22
31.72	31.92	31.66		
	32.40	32.56	32.12	32.58
33.61	33.60	33.50	33.54	33.60
		34.61		34.16
	35.24			
		35.90		

		36.40		
		37.05	37.13	37.16
		38.34	38.46	38.23
38.98		38.53		38.59
39.62				
40.21				
46.31				

Table AD 6.3: PXRD data for samples TA-I-55-1a (1:1), TA-I-55-1b (1:2), TA-I-55-1c (2:1), in acetonitrile

Phenylboronic acid	4,4'-bipyridine	TA-I-55-1a	TA-I-55-1b	TA-I-55-1c
2-Theta °	2-Theta °	2-Theta °	2-Theta °	2-Theta °
				5.621
				9.06
9.94	9.94			
				10.40
		11.34	11.40	11.11, 11.64
12.05		12.11	12.18	
	12.36			12.29
12.86	13.03	13.25	13.37	12.88
13.84				
			14.71	14.03, 14.61
15.27				15.36
16.62				16.36
17.31	17.50, 17.67			17.12, 17.35
18.26	18.31	18.23	18.27	
18.72				18.66
	19.36			19.22
		19.74	19.83	
	20.13	20.23	20.29	20.23
20.88	20.82			20.58
21.17				21.28
	21.59	21.61	21.74	21.70
22.00	22.37			
	22.98	23.25	23.33	23.04,23.52
24.01				

24.39			24.41	24.38
	25.03			25.22
25.74	25.78	25.59	25.67	
26.02	26.24			26.30
		26.53	26.54	26.63,26.80
		27.32	27.32	27.52
	27.81			
28.48				28.55
	29.12	29.41	29.41	29.12
				29.78
	30.38			
31.07	30.68	31.18	31.27	30.79
31.72	31.92			31.89
	32.40			32.38
		32.80	32.85	
33.61	33.60		33.62	33.21
	35.24			
		37.15	37.21	
		38.36	38.42	
38.98			38.80	
39.62				39.25
40.21				
46.31				

Table AD 6.4: FT-IR assignments for samples TA-I-55-1a (1:1), TA-I-55-1b (1:2), TA-I-55-1c (2:1), and its starting materials in acetonitrile)

Assignment is made using the literature.[36]

Phenylboronic acid	4,4'-bipyridine	TAI-55-1a 1:1	TAI-55-1b 1:2	TAI-55-1c 2:1	Assignment [36]
cm-1	cm-1	cm-1	cm-1	cm-1	cm-1
	3429	3429	3429	3437	O-H, stretch
3273 3081 3024	3025 2927 2895	3044	3044	3075 3052	Csp2-H stretch
2419	2362				
1964 1896	1942 1868	1932			
	1654	1665	1665	1665	C=N stretch
1604	1647	1619		1624,1602	C=C stretch
1572	1592	1594	1594	1543	C=C stretch
	1540	1531	1531		C=C stretch
1499	1488	1483,1447	1483,1447	1493,1443	C=C stretch
1439	1406	1417		1413	B-O asym. stretch
1350		1400,1376	1400,1376	1391	
1275		1341,1313	1341,1313	1343,1327	
1191	1218	1211	1212	1225, 1208,1198	C-O stretch
1161	1123	1125	1127	1124	C-O stretch
					C-O stretch
1095	1075	1073	1098	1069	C-O stretch
1072	1038	1066	1066	1051	B-C stretch

1029		1042	1042		
		1023	1023	1020	
1007		1001	1001	1001	
972	988	990	990	982	B-O sym. stretch
923		845	845		Csp2- H bending
	850	801	801	810	B-O sym. stretch
804	803	781			Boroxole ring
764	733	733	716	747	BO2 out- of - Plane

Table AD 6.5: PXRD data for samples TA-I-56-1a (1:1), TA-I-56-1b (1:2), TA-I-56-1c (2:1), in methanol

Phenylboronic acid	4-phenyl pyridine	TA-I-56-1a	TA-I-56-1b	TA-I-56-1c
2-Theta °	2-Theta °	2-Theta °	2-Theta °	2-Theta °
			7.94	
		8.02	8.15	8.01, 8.20
		8.99	8.95	
	9.37		9.73	
9.94		10.10		10.12
				11.09
		11.96		11.95
				11.54
12.05			12.02	
12.86				
		13.41	13.43	13.33
13.84				14.29
			14.80	
15.27				15.49
		15.88	15.51	15.96
16.62		16.57		16.62
				16.93
17.31		17.02	17.02	17.53
		17.51,1782	17.64	
18.26		18.25	18.17	18.17
18.72		18.53	18.49	18.50
	18.93	18.75	18.82	

	19.44	19.12	19.27	
		19.85	19.78	19.68
		20.14	20.04	19.96,20.16
20.88		20.71	20.75	20.69
21.17	21.16	21.12		21.12
		21.28	21.47	
22.00	22.20	22.03	22.06	22.04
			22.79	22.52
	22.83			22.82
	23.34	23.33	23.23	23.36
24.01		23.85	23.70	
24.39		24.53	24.05	23.97
		24.79		24.84
25.74				
26.02				26.40
	27.05		27.31	
	27.92	27.80	27.75	27.78
28.48	28.74	28.74	28.71	28.57
	29.17	29.56	29.52	
		29.96		
		30.18		30.33
	30.71	30.71		
31.07				31.18
31.72		31.67		
				32.16

33.61	33.96	33.65		33.59
	34.66	34.79	34.13	
			34.96	
		35.08		
		35.79		
	36.38	35.96		36.02
				37.91
38.98	38.86		39.24	
39.62				39.38
40.21				
46.31				

Table AD 6.6: PXRD data for samples TA-I-56-2a (1:1), TA-I-56-2b (1:2), TA-I-56-2c (2:1), in acetone

Phenylboronic acid	4-phenyl pyridine	TA-I-56-2a	TA-I-56-2b	TA-I-56-2c
2-Thet°	2-Theta °	2-Theta °	2-Theta °	2-Theta °
		5.83		
		6.88		
		7.76		7.75
		8.02		8.00
				8.83
		9.08	9.788	9.56,9.94
9.94		10.14	10.61	
				11.54
12.05		11.97		11.81
	12.36	12.77	12.72	
12.86	13.03	13.26		13.09
13.84		13.95		14.29
		14.59		
15.27		15.34		15.64
		15.88		
16.62		16.87	16.66	16.44
				16.94
17.31	17.50, 17.67	17.53		17.53
		17.95	17.80	17.76
18.26	18.31	18.21		18.14
18.72		18.51	18.68	18.58
	19.36	19.36	18.94	19.02
		19.61	19.72	19.46

	20.13		20.00	20.56
20.88	20.82	20.89	20.68	20.74
21.17		21.15		21.19
	21.59		21.50	21.88
22.00	22.37	22.05	22.04	
		22.34	22.25	22.64
	22.98	22.72	23.00	23.19
		23.24	23.52	23.83
24.01		23.89	23.75	
24.39		24.62		24.61
	25.03	24.89	25.09	24.90
25.74	25.78	25.39	25.83	25.41
26.02	26.24	25.62	26.20	26.17
		26.21	26.29	
		27.32		27.16
	27.81	27.79	27.78	27.71
28.48		28.61		28.55
	29.12	29.49	29.32	
			29.87	29.71
	30.38			30.00
	30.68		30.57	
31.07				31.16
				31.55
31.72	31.92			
	32.40	32.99	32.37	32.78
			33.13	
33.61	33.60	33.65		33.56

		34.79		
	35.24			35.12
		35.08	35.83	35.89
		35.79	36.82	
				37.20
			38.31	
38.98			38.91	38.73
39.62				
40.21				
46.31				

Table AD 6.7: PXRD data for samples TA-I-56-3a (1:1), TA-I-56-3b (1:2), TA-I-56-3c (2:1), in acetone

Phenylboronic acid	4-phenyl pyridine	TA-I-56-3a	TA-I-56-3b	TA-I-56-3c
2-Theta °	2-Theta °	2-Theta °	2-Theta °	2-Theta °
		7.96		
			8.16	8.06
		9.06	9.20	9.05
9.94		9.70	9.68	9.68
		10.13	9.89	10.13
		11.87		
12.05			12.11	12.05
	12.36	12.94		
12.86	13.03			12.96
		13.35		13.48
13.84				14.28
			15.01	
15.27		15.45		
				15.83
16.62		16.96		16.64
17.31	17.50, 17.67	17.49	17.06	17.13
		17.77	17.75	17.84
18.26	18.31	18.22	18.38	18.24
18.72		18.68		18.58
		18.99		
	19.36	19.30	19.30	19.20
		19.78	19.48	19.69

			19.90	19.88
	20.13			20.14
20.88	20.82	20.74	20.90	20.77
21.17		21.21		21.23
	21.59	21.41	21.47	
22.00	22.37	22.10	22.14	22.12
			22.61	22.74
	22.98	22.90		
		23.28	23.35	23.25
24.01		23.81	23.85	
24.39				23.92
	25.03	25.08	25.13	24.69
25.74	25.78			25.78
26.02	26.24		26.41	26.56
		26.43	26.73	
	27.81	27.75	27.96	27.74
28.48		28.24	28.71	28.76
		28.62	28.39	
	29.12	29.42	29.58	
		29.77		29.60
	30.38		30.93	29.99
	30.68			30.83
31.07				
31.72	31.92			
	32.40			
33.61	33.60			33.38
	35.24		35.14	

			36.10	36.07
38.98				
39.62		39.09		
40.21				
46.31				

Table AD 6.8: FT-IR assignments for samples TA-I-56-3a (1:1), TA-I-56-3b (1:2), TA-I-56-3c (2:1), and its starting materials in Acetonitrile

Assignment is made using the literature.[36]

Phenylboronic acid	4-phenyl pyridine	TAI-56-3a	TAI-56-3b	TAI-56-3c	Assignment [36]
cm^{-1}	cm^{-1}	cm^{-1}	cm^{-1}	cm^{-1}	cm^{-1}
	3436	3436	3447	3533	O-H, stretch
3273, 3081 3024	3058	3074 2924	2920	3074 3053 3032	C_{sp2}-H stretch
2419		2348			
1964	1958				
1894					
			1749	1710,1692	
	1667	1630	1629	1665,1630	C=N stretch
1604		1601	1601	1601	C=C stretch
1572	1587	1550	1550	1573	C=C stretch
	1543		1544,1507	1551,1513	C=C stretch
1499	1482	1485	1481	1486	C=C stretch
1439	1446	1444	1441	1450,1444	B-O asym. stretch
	1409		1406	1403	
1350	1340,1333	1345,1329	1339,1329	1345,1330	
1275, 1191	1232 1189	1281 1200	1281,1258 1199	1281,1256	C-O stretch
1161	1162	1175		1200,1175	C-O stretch
1095	1103	1124		1125	C-O stretch
1072	1072	1084		1085	C-O stretch
1029	1041	1069,1029			B-C stretch

1007	1002				
972	986				B-O sym. stretch
923	917	846	852	851,846	C_{sp2}- H bending
803	830	826	848		B-O sym. stretch
764	761	779	720	702	Boroxole ring
697, 857	740	702, 679	665	675	BO_2 out- of – Plane